



NTNU – Trondheim
Norwegian University of
Science and Technology

Alginate Microcapsules for Cell Therapy

Effect of capsule composition on complement
activation, cytokine secretion, and protein
adsorption in a whole blood model

Mathias Pontus Andreas Ørning

Chemical Engineering and Biotechnology

Submission date: June 2012

Supervisor: Gudmund Skjåk-Bræk, IBT

Co-supervisor: Anne Mari Rokstad, IKM

Norwegian University of Science and Technology
Department of Biotechnology

Preface

This master thesis is a part of the master degree program Industrial Chemistry and Biotechnology at the Norwegian University of Science and Technology. It is the result of laboratory work carried out at the Department of Cancer Research and Molecular Medicine during the spring semester 2012.

I would deeply like to thank my supervisor, Researcher Anne Mari Rokstad, for introducing me to the world of alginate microcapsules and biocompatibility. You have triggered my interest in biomaterials through your great passion for the field. I am very thankful for having been offered the opportunity to work and write my thesis in your lab group. A thank you is also directed to Professor Asbjørn M. Nilsen for forwarding my inquiry into available thesis topics to Anne Mari. I would like to thank Senior Engineers Bjørg Steinkjer and Liv Ryan for training and guidance, and also Senior Engineer Kjartan W. Egeberg for help using the confocal microscope. In addition, I would like to thank Professor Gudmund Skjåk-Bræk for being my supervisor at the Department of Biotechnology. And finally, a thank you goes out to my family as well as my fellow class mates and lab students.

Abstract

Encapsulation of pancreatic islets in alginate microbeads and microcapsules show great promise for the treatment of Type 1 diabetes mellitus. Significant progress has been made in developing a biocompatible capsule that allows sufficient exchange of nutrients and products with the encapsulated cells, while at the same time maintaining a barrier to immune cells and preventing rejection of the transplanted cells. However, a truly biocompatible capsule has, as yet, not been developed, and implanted capsules often trigger low levels of inflammation leading to fibrosis, diminished insulin secretion, and sometimes death of the encapsulated cells.

A lepirudin-based human whole blood model was used to demonstrate the inflammatory potential of a set of different alginate microcapsules and microbeads. This was performed to elucidate the effect of different capsule and bead parameters, such as the effect of a hollow versus solid inner core, polycation type, polycation concentration, alginate type, and capsule and bead diameter. Complement activation after incubation of capsules in whole blood was measured as sTCC generation. In addition, the secretion of chemokines, inflammatory cytokines, anti-inflammatory cytokines, and growth factors was analyzed by ELISA and Bio-plex. Leukocyte activation as measured by CD11b expression was detected using flow cytometry. Finally, Confocal Laser Scanning Microscopy (CLSM) was used in order to screen for a set of plasma proteins and observe what proteins adsorbed to the capsule surface.

TAM alginate microbeads did not trigger complement activation, secretion of cytokines, or up-regulation of CD11b expression, and thus appeared to have a minimal inflammatory potential. In addition, the protein adsorption assay showed no apparent protein surface deposition on the microbeads after 6 hours of incubation in plasma of the proteins screened for (complement protein C3, complement regulatory proteins factor H, factor I, C1 inhibitor, and vitronectin, as well as coagulation cascade proteins fibrinogen, plasminogen, and HMWK).

Solid alginate APA microcapsules containing poly-L-lysine (PLL), on the other hand, showed an increase in complement component sTCC levels, in chemokine levels (IL-8, MCP-1, and MIP-1 α), in inflammatory cytokine levels (IL-6, IL-1 β , and TNF α), in anti-inflammatory cytokine levels (IL-1RA and IL-10), and in growth factors levels (PDGF, HGF, and VEGF), as well as a decrease in cytokine IP-10 levels. In addition, the capsules also stimulated leukocyte activation by up-regulating the expression of CD11b. The solid APA microcapsules showed heavy C3 adsorption, coupled with vitronectin and factor H surface deposition, indicating increased complement activity on these capsules.

Hollow APA microcapsules with PLL triggered a rapid and strong sTCC response, as well as significantly increased secretion of the chemokine MCP-1. At the same time, a significant decrease in secretion of chemokines (IL-8 and MIP-1 α) and inflammatory cytokines (IL-1 β and

TNF α), as well as a decrease in secretion of growth factor VEGF, and cytokine MIF, and an increase in cytokine IP-10 was observed. All these cytokine levels except the chemokine MCP-1 and the complement complex sTCC suggested reduced inflammatory potential for hollow APA capsules. It was proposed that these capsules adsorbed the anaphylatoxins C3a and C5a, thus preventing the complement mediated activation of leukocytes. No increased surface adsorption of C3 was detected on hollow APA capsules compared to solid APA capsules. Conversely, the C3 adsorption was higher on solid APA capsules, thereby not reflecting the increased sTCC generation seen for hollow APA capsules. One explanation for this might be that the hollow capsules secreted some soluble molecule capable of triggering sTCC generation.

No apparent change in inflammatory potential could be observed by exchanging the polycation PLL with PLO (poly-L-ornithine), except for abolishing the strong sTCC response observed for hollow APA capsules with PLL as well as lowering the MCP-1 response. It was suggested that this observation could be the result of PLO reducing the permeability of the capsules, thus preventing the diffusion of the hypothesized soluble trigger of sTCC.

Increased sTCC was detected with increasing PLL concentration in High G alginate APA capsules. The same could not be observed for High M alginate capsules, however, the chemokine IL-8 and the inflammatory cytokines IL-1 β and TNF α increased with increasing PLL concentration, suggesting increased inflammation with increasing PLL concentration. No change in inflammatory potential could be detected with varying alginate microbead diameter. Nor could any change in inflammatory potential be observed by the addition of HEPES in the gelling solution.

TAM alginate microbeads appear to have the lowest inflammatory potential of the capsules tested, and are therefore the most suited for *in vivo* application from an inflammatory aspect, as demonstrated by the whole blood assay. A recent study in Type 1 diabetes patients however showed increased fibrosis when encapsulating human islet cells in barium alginate microbeads [61]. Further studies where incubation of TAM microbeads with isolated monocytes are co-cultured with fibroblasts could further elucidate the mechanisms of fibrosis on the microbeads. In addition, continued screening of protein adsorption on the bead surface should be performed.

Sammendrag

Innkapsling og transplantering av Langerhansk øyvev i alginat-mikrokapsler viser potensiale innenfor behandling av Diabetes Mellitus type 1. Fremsteg har blitt gjort innenfor utviklingen av kapsler som er biokompatible og som tillater tilstrekkelig diffusjon av næringsstoffer og celleprodukter inn og ut av kapslene, samtidig som kapslene fungerer som en barriere mot pasientens immunceller og forhindrer frastøting av implantatet. Men fullstendig biokompatible kapsler har enda ikke blitt utviklet, og kapsler trigger ofte lav inflammasjon som kan føre til overvekst på kapslene, minsket insulin sekresjon, og i visse tilfeller også celledød.

En lepirudin-basert fullblodsmodell ble brukt til å teste forskjellige alginat-kapsler og deres inflammatoriske potensiale. Dette ble utført i et forsøk på å kaste lys over forskjellige kapselparametere slik som løselig eller fast kjerne, polykation type, polykation konsentrasjon, alginat type og kapsel diameter, og hvilken effekt disse parameterene har på inflammasjon. Komplement-aktivering ble målt som sTCC-dannelse etter inkubering av kapsler i fullblod. I tillegg ble sekresjon av chemokiner, cytokiner, og vekst faktorer målt ved hjelp av ELISA og Bio-plex. Leukocyt-aktivering ble målt som CD11b-ekspresjon ved hjelp av flow cytometri. Tilslutt ble et konfokal laser scanning mikroskop tatt i bruk til å studere deponering av plasma-proteiner på overflaten av kapslene.

TAM-alginatkuler aktiverte hverken komplement, sekresjon av cytokiner eller oppregulering av CD11b, og hadde derfor et tilsynelatende lavt inflammatorisk potensiale. I tillegg ble det ikke oppdaget noe protein-adsorpsjon på disse kapslene etter 6 timers inkubering i plasma (komplementprotein C3, de regulatoriske komplementproteinene factor H, factor I, C1 inhibitor og vitronectin, så vell som koagulasjonsproteinene fibrinogen, plasminogen og HMWK)

APA-kapsler med fast kjerne inneholdende poly-L-lysine (PLL) viste derimot økt komplementaktivering (sTCC), i tillegg til økte chemokine-verdier (IL-8, MCP-1, and MIP-1 α), cytokineverdier (IL-1 β , IL-6, TNF α , IL-1RA og IL-10) og vekstfaktorer (PDGF, HGF og VEGF). Det ble også påvist en nedgang i IP-10 verdier, oppregulering av CD11b, så vell som C3, vitronectin og factor H overflatedeponering, noe som indikerte økt komplementaktivitet.

APA-kapsler med løselig kjerne inneholdende PLL viste en rask og høy sTCC-respons, og signifikant økning i MCP-1 sekresjon. Men samtidig viste de signifikant minskning i chemokiner (IL-8 and MIP-1 α) og inflammatoriske cytokiner (IL-1 β and TNF α), vekstfaktor VEGF og cytokin MIF, samt en økning i cytokin IP-10. Alle disse nivåene unntatt MCP-1 og sTCC indikerte et redusert inflammatorisk potensiale for APA-kapsler med løselig kjerne. Det ble foreslått at kapslene adsorberte anafylatoksinene C3a og C5a, og dermed forhindret komplementmediert aktivering av de hvite blodcellene. Ingen økt C3-deponering kunne observeres for APA-kapsler med løselig kjerne sammenlignet med fast kjerne. Isteden var det kapslene med fast kjerne som

viste høyest C3-deponering. Dette samsvarte ikke med de forhøyede sTCC nivåene observert for kapslene med løselig kjerne, og det ble foreslått at et løselig stoff diffunderte ut av disse kapslene og trigget sTCC dannelse.

Ved å bytte ut PLL med PLO (poly-L-ornithine) i kapsler med løselig kjerne, ble den forhøyede sTCC- og MCP-1 responsen for disse kapslene senket. Ellers påvirket ikke PLO kapslens cytokin-profil nevneverdig. Det ble foreslått at PLO kunne redusere permeabiliteten til kapslene og på den måten forhindre diffunderingen av eventuelle stoffer ut av kapslene som kunne føre til sTCC-dannelse.

Økte sTCC-nivåer ble observert i takt med økende PLL-konsentrasjon i kapsler med høy-G alginat. Det samme kunne ikke observeres i kapsler med høy-M alginat. Man kunne derimot se økte IL-8, IL-1 β og TNF α -nivåer, noe som likevel tydet på økt inflammatorisk potensiale i tråd med økende PLL-konsentrasjon. Ingen forandring i inflammatorisk potensiale kunne observeres med varierende kapseldiameter. Det virket heller ikke som om tilsetningen av HEPES i gelingsløsningen påvirket dette.

TAM-alginatkuler viste seg å stimulere inflammasjon i minst grad av de kapslene som ble testet her i fullblodsmodellen. Det kan derfor virke som om disse kapslene er best egnet til *in vivo* bruk, ut fra et inflammatorisk synspunkt. Men i en studie hvor Diabetes type 1 pasienter ble behandlet med øyvev innkapslet i barium-alginatkuler [61], ble det påvist overvekst på kulene og svekket sekresjon av insulin. Muligheter for videre studier kan derfor inkludere inkubering av TAM-kuler med isolerte monocytter og fibroblaster for å studere mekanismene bak overvekst nøyere. I tillegg bør det fortsettes med protein-adsorpsjonsstudier hvor flere plasmaproteiner screenes, og hvor kapslene inkuberes over en lenger periode.

Contents

1	INTRODUCTION	1
1.1	Encapsulation	1
1.1.1	Encapsulation of cells for treatment of Type 1 diabetes	1
1.1.2	Immunoisolation of cell transplants	2
1.2	Alginate	3
1.2.1	Composition	4
1.2.2	Alginate gels	5
1.3	Alginate microcapsules	5
1.3.1	Formation of alginate beads and capsules	5
1.3.2	Capsule types	6
1.4	Biocompatibility and inflammation	8
1.4.1	The complement system	8
1.4.2	Hemostasis	16
1.4.3	Inflammatory response following microcapsule implantation	18
1.4.4	Biocompatibility of alginate microcapsules in vivo	22
1.4.5	Towards increased biocompatibility	23
1.5	Aims	24
2	MATERIALS AND METHODS	26
2.1	Formation of alginate microcapsules	26
2.1.1	Alginate solution	26
2.1.2	Gelling solution	26
2.1.3	Bead preparation	27
2.2	Whole blood assay	28
2.3	Flow cytometry	29
2.4	ELISA	29
2.4.1	IL-8	30
2.4.2	TNF- α	30
2.4.3	sTCC	31
2.5	Bio-plex	31
2.6	Protein adsorption assay	33
2.7	Statistical methods	34
3	RESULTS	35
3.1	Capsule diameters	35
3.2	C3 and fibrinogen depositions on the capsule surface	35
3.3	Complement activation and leukocyte response	40
3.3.1	TCC response	40
3.3.2	IL-8 response	44

3.3.3	Leukocyte activation as measure by CD11b expression	44
3.3.4	Chemokines	46
3.3.5	Inflammatory cytokines	47
3.3.6	Anti-inflammatory cytokines	49
3.3.7	Growth factors	50
3.3.8	MIF, IP-10, IFN- γ , and RANTES	52
3.3.9	Statistical analysis	54
3.4	Leukocyte response towards TAM capsules	58
3.4.1	Chemokines	58
3.4.2	Inflammatory cytokines	58
3.4.3	Anti-inflammatory cytokines	58
3.4.4	Growth factors	58
3.4.5	MIF, IP-10, IFN- γ and RANTES	66
3.5	Regulatory complement protein and coagulation cascade protein deposition on capsule surface	66
3.6	Effect of lepirudin on protein adsorption	73
4	DISCUSSION	77
4.1	The whole blood model for evaluating biocompatibility	77
4.2	Capsule parameters	78
4.2.1	Polycation	78
4.2.2	Alginate type	79
4.2.3	TAM capsules	79
4.3	Complement activation	80
4.4	Cytokine secretion and CD11b expression	81
4.4.1	TAM beads vs APA capsules	81
4.4.2	Effect of a soluble core	82
4.4.3	PLL vs PLO	82
4.4.4	Effect of PLL concentration	83
4.4.5	Effect of alginate composition	84
4.4.6	Effect of capsule size	85
4.4.7	Effect of HEPES	86
4.5	Cytokine response to TAM beads	86
4.6	Protein adsorption on alginate microcapsules	86
4.7	Coagulation and the effect of lepirudin	87
4.8	Comparisons to in vivo biocompatibility studies	88
4.9	Future perspectives	88
5	CONCLUSION	90
A	Materials and instruments	101

B Individual donors	104
C ELISA data	106
C.1 IL-8 1 h	106
C.2 IL-8 4 h	107
C.3 sTCC 1 h	107
C.4 sTCC 4 h	108
D Bio-plex data	109
D.1 MIP-1 α	109
D.2 MCP-1	110
D.3 MIF	111
D.4 IP-10	112
D.5 IL-1 β	113
D.6 TNF- α	114
D.7 IL-6	115
D.8 IL-1RA	116
D.9 IL-10	117
D.10 PDGF-BB	118
D.11 HGF	119
D.12 VEGF	120
D.13 IFN- γ	121
D.14 RANTES	122
E Flow cytometer data	123
F Statistical analysis	124
F.1 IL-8 1h	125
F.2 IL-8 4h	126
F.3 sTCC 1h	127
F.4 sTCC 4h	128
F.5 MIP-1 α	129
F.6 MCP-1	130
F.7 MIF	131
F.8 IP-10	132
F.9 IL-1 β	133
F.10 TNF- α	134
F.11 IL-6	135
F.12 IL-1RA	136
F.13 IL-10	137
F.14 PDGF	138

F.15 HGF	139
F.16 VEGF	140
F.17 IFN- γ	141
F.18 RANTES	142

1 INTRODUCTION

1.1 Encapsulation

Encapsulation of biologically active materials to protect and allow for controlled administration of chemicals, drugs, proteins, vaccines, and food additives, is a well-established method. Living cells may also be encapsulated, either for use in industry, agriculture, or cell therapy. Materials that have been utilized for cell encapsulation include alginate, collagen, gelatin, chitosan, and agarose. Although there are many applications of encapsulation for cell therapy, one of the most studied systems, and perhaps also the most promising, is the encapsulation of insulin producing cells into alginate capsules for transplantation and treatment of Type 1 diabetes.

1.1.1 Encapsulation of cells for treatment of Type 1 diabetes

The main goal of cell encapsulation in cell therapy is to overcome the problem of graft rejection. As all transplanted cells are recognized as foreign, patients having undergone a transplantation, be it a whole organ transplant or just individual cells, need to be on a lifelong regime of immunosuppressive drugs to prevent or minimize the rejection of transplant by the host immune system. As these drugs suppress and limit the immune system, the patient will be more susceptible to infections as well as having an increased risk of tumor development [1].

By encapsulating cells in a biomaterial such as alginate, the aim is to mask the cells from the body's immune system but still allow for products and substrates to pass through. In the case of encapsulation of insulin producing islets, the capsule must permit insulin and glucose to pass through the capsule, allowing normal regulation of the patient's blood glucose. If successful, this technique would remove the need of immunosuppression and be a major step toward a functional cure for Type 1 diabetes.

Type 1 diabetes is an autoimmune disease where the immune system targets and destroys the insulin-producing beta cells of the pancreas. This leads to a shortage of insulin in the blood which subsequently results in increased blood glucose. Complications include cardiovascular disease, and damage to the nerve system, the retina, and the kidneys, if the disease is poorly managed [2]. If left untreated the disease will result in death. The current therapy of choice is treatment with insulin where daily injections must be administered indefinitely. Transplantation of islets of Langerhans or a whole pancreas has been successful in normalizing blood glucose levels, however, because Type 1 diabetes is an autoimmune disease, the host immune system will continue to target and destroy the transplanted beta cells even if a close donor match is found with limited graft rejection. A strict immunosuppression regime is therefore required. In addition, as many as 3 million people in U.S.A may have Type 1 diabetes [3], a number that way exceeds the supply of human pancreases.

1.1.2 Immunoisolation of cell transplants

The human immune system is programmed to distinguish self from non-self. This allows it to recognize pathogens that have infected the body, as well as deal with self-cells that have deviated from their original role and purpose, such as cancer cells. This defense, which is crucial for survival in an environment where the body continuously is bombarded with pathogenic microbes trying to invade our body, is at the same time what makes it so difficult to transplant organs and cells into the body. Even when the transplant donor is a close match, e.g. a relative, small differences in the molecules coating the cells can result in the host immune system reacting to the transplant and rejecting the graft. Lifelong immunosuppression must be administered along with its numerous side effects. Sometimes these side effects might even outweigh the benefits of the transplant itself. And for the case of using organs or cells from other animals (xenografts) as opposed to from humans (allografts) the complications are even greater.

The transplantation of a graft from a donor that is not closely related to the patient will result in rejection. This happens mainly because of differences between host and graft MHC molecules that are positioned on the surface of the cells. These molecules are meant to help the immune system detect infections. Immune cells (T-cells) can, however, detect differences between the MHC molecules present on host cells, and those on graft cells. If this happens and the T-cells subsequently become activated, a highly specific attack will be initiated towards the graft cells presenting the foreign MHC molecules. MHC matching between donor and host is therefore performed for whole organ transplantation so as to minimize the likelihood of rejection.

However, even with a close MHC match, rejection might still occur. MHC is an abbreviation of major histocompatibility complex, and differences here is the major reason for incompatibility between host and donor. There are also minor histocompatibility antigens that differ between members of the same species. These antigens are proteins that are expressed and secreted by the graft, taken up by host cells and presented on MHC molecules on the surface of antigen presenting cells. As they differ from the proteins of the host, immune cells will recognize them as foreign and target the cells expressing them, i.e. the graft cells. The immune cells will believe the graft cells are infected and start killing them, thereby rejecting the graft.

Immunoisolation of the graft, e.g. by encapsulating the graft cells in alginate microcapsules, prevents the direct contact between graft cells and host immune cells. No T-cells can thereby attach to graft cells and recognize the different MHC molecules present. Alginate microcapsules are however porous and proteins might leak out of the capsules. Immunoisolation can therefore prevent the direct targeting of the graft cells, but may still indirectly activate the host immune system, see figure 1.1. Cytotoxic T-cells, a major participant in graft rejection, requires direct contact with the target cell and thus may be prevented from attacking the graft. The release of cytokines and the productions of antibodies might be harder to counteract. Molecules secreted

by immune cells such as IL-1 β , TNF- α , and IFN- γ , and antibodies, as well as complement components, are all small enough that they might diffuse into the capsule and target the graft cells. This might in turn damage the cells and result in lysis. Still, a big part of an immune attack involves the direct contact of immune cells which may be eliminated by encapsulating the cells in alginate microcapsules.

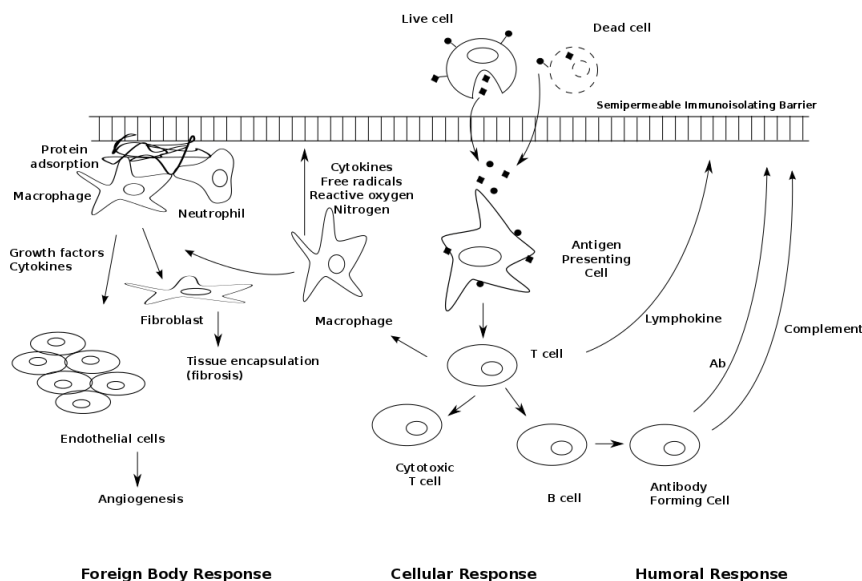


Figure 1.1: An overview of possible responses aimed toward encapsulated cells. Adapted from [4].

1.2 Alginate

Alginate is a biopolymer widely used in industry mainly for its stabilizing and viscosifying abilities as well as for retaining water and forming gels [5]. More recently alginate has been implemented in medical applications such as dressings in surgery and wound management [6]. In addition, because of its abundance, biocompatibility, and biodegradability properties, alginates are regarded as the most suitable biomaterial for cell microencapsulation. This work focus on the encapsulation of cells for transplantation into patients.

To date all commercially available alginate is produced from algae, where its main function is conferring strength and flexibility to the algal tissue. It exists as a gel containing Na⁺, Ca²⁺, Mg²⁺, Sr²⁺, and Ba²⁺ ions, and is located in the intercellular matrix of the algae. Alginate is also produced by certain bacterial strains, however microbial fermentation is thus far not economically favorable mainly due to the low cost of cultivating seaweeds in under-water farms [7].

1.2.1 Composition

Alginate is a biopolymer produced by brown seaweeds and by the Gram-negative bacteria *Pseudomonas* and *Azotobacter*, and is made up of 1-4-linked α -L-guluronic acid (G) and β -D-mannuronic acid (M) as shown in figure 1.2. These sugar acids are distributed in blocks of continuous M-residues, G-residues, or as alternating MG-residues. High resolution ^1H - and ^{13}C -nuclear magnetic resonance spectroscopy (NMR) can be used to determine the composition and sequence parameters of the alginate polymer.

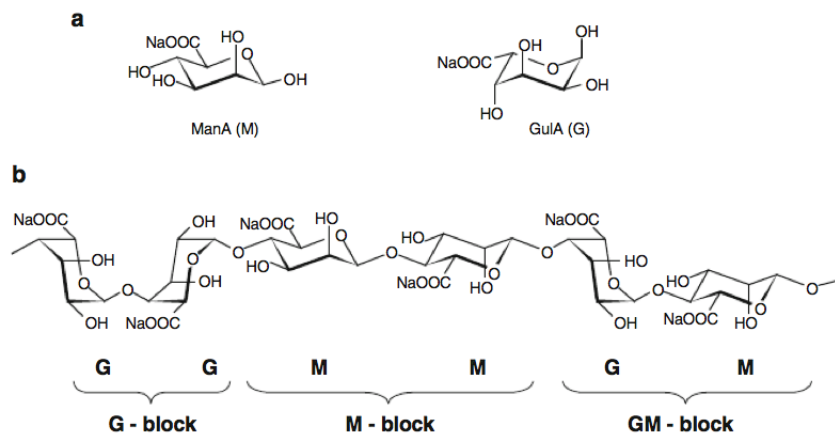


Figure 1.2: Composition of sodium alginate [5]. **a** The ${}^4\text{C}_1$ conformation of β -D-mannuronic acid (M) and ${}^1\text{C}_4$ conformation of α -L-guluronic acid (G). **b** Ring conformation of the different blocks in alginate.

The composition of alginate varies widely depending on the source of the alginate. For alginate produced by algae the fraction of G-residues (F_G) can vary in the range of 0.20 to 0.85 [8]. Alginates isolated from *Macrocystis pyrifera* are characterized by a lower content of G-blocks ($F_G=0.4$) while, in general, high contents of G are found in alginates from *Laminaria hyperborea* algae ($F_G=0.6$) [9]. Caution should be exercised here as alginate from *M. pyrifera* is frequently mentioned in encapsulation literature as high-M alginate to distinguish it from the *L. hyperborea* alginate. Nevertheless, the M fraction is not as high as the M rich alginate (86-99.9% M-blocks) also going under the name high-M alginate seen to stimulate cytokine production in monocytes [10]. Alginates produced by the bacterial strains *Azotobacter* and *Pseudomonas* often show increased variability in the composition of the polymer, with *Pseudomonas* species lacking G-blocks [11]. The biggest difference between algal and bacterial alginates is, however, the capability of bacteria to add *O*-acetylations on C-2 and/or C-3 on mannuronic acid residues, affecting the swelling and water-binding properties of the alginate gel [11, 12].

The stabilizing and viscosifying abilities as well as the properties of retaining water and forming gels, for which alginate is widely used, are dependent on the composition of the biopolymer

with different combinations of the monomers M and G giving the polymer different physical properties. For example, the formation of gels depends on G-repeats interacting with divalent cations (e.g. Ca^{2+} or Ba^{2+}) in the solution, making the gel strength dependent on the amount and length of G-blocks present [7].

1.2.2 Alginate gels

Alginate forms a gel by binding to divalent cations, a process that is highly specific with an affinity for the ions depending on the composition of the alginate. The process of gelation is explained by the egg-box model [13]. Repeats of G-residues create cavities which function as binding sites for ions, allowing a lateral association of the polymer chains, see figure 1.3. This co-operative binding gives the gel a rigidity depending on the gelling ion which decreases in the order of $\text{Ba}^{2+} > \text{Sr}^{2+} > \text{Ca}^{2+} > \text{Mg}^{2+}$. This appears also to be the cationic selectivity for G-blocks while M- and MG-blocks are almost without selectivity [14]. Thus the main structural feature contributing to gel-formation is the length of these G-blocks [15], giving alginate gels with a high M content ($F_G=0.4$) such as alginate from *M. pyrifera* lower strength and stability as compared to those made from high G alginates ($F_G=0.6$) such as *L. hyperborea* alginate [16].

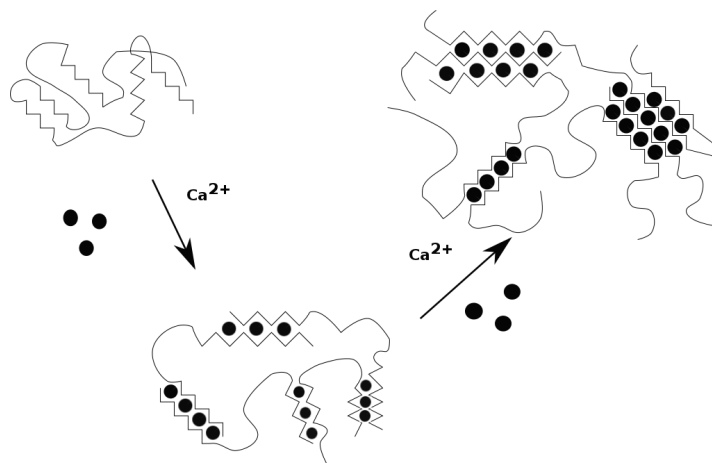


Figure 1.3: The egg-box model. Lateral association of chains by chelation of divalent cations. Figure adapted from [17]. Zigzag regions represent blocks of G-residues.

1.3 Alginate microcapsules

1.3.1 Formation of alginate beads and capsules

Alginate beads are formed by dripping an alginate solution into a mixture containing divalent cations causing the polymer to cross-link and form a gel, see figure 1.4. This happens rapidly and irreversibly, and the alginate bead will have a shape and property depending on the composition of the alginate as well as the gelling solution. The usual choice of gelling ion is Ca^{2+} because of its selective binding to G-blocks and non-toxicity. Ba^{2+} is also commonly used because of

its potential to stabilize the bead even further, however, as Ba^{2+} is toxic to the human body, lower concentrations are used to prevent leakage of ions out of the bead. Usually Ba^{2+} is only used for alginate beads (where gelled alginate is the only component) while alginate-polycation-alginate (APA) microcapsules consists of a stabilizing polycation layer outside of the alginate core making the use of Ba^{2+} redundant.

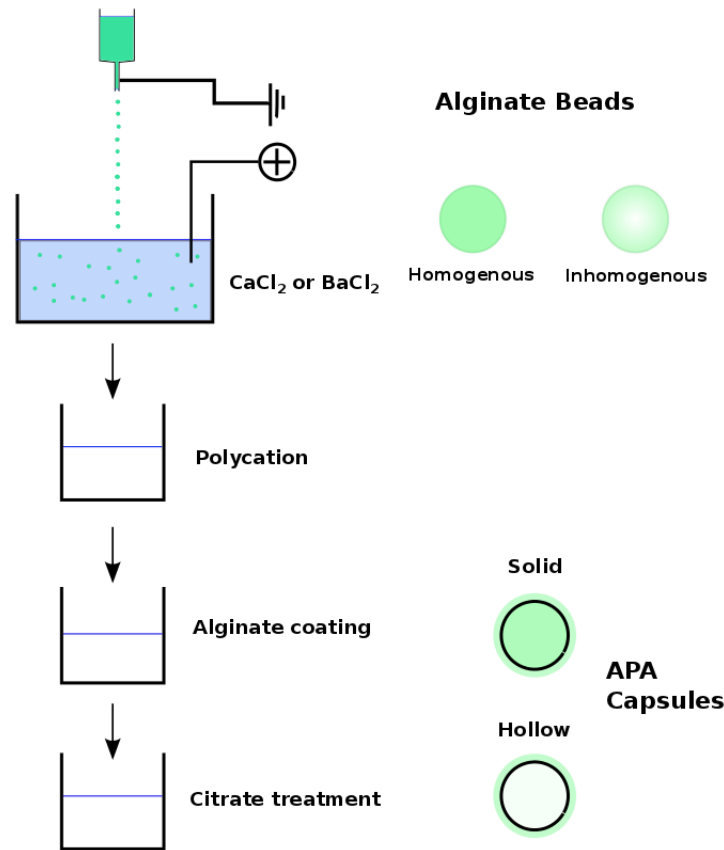


Figure 1.4: Capsule formation by dripping an alginate solution into a gelling bath. Depending on the gelling solution we will get either homogenous or in-homogenous alginate capsules. These can be further given a polycation layer and coated with a new alginate solution to create alginate-polycation-alginate (APA) capsules. If these capsules are then treated with citrate, the inner core will be liquefied and the capsules will be termed hollow. For encapsulation of cells, the alginate solution in the first step will be mixed with a cell suspension. Figure adapted from [4]

1.3.2 Capsule types

The first step in the encapsulation process is the formation of an alginate bead, as described in section 1.3.1. Two types of alginate beads can be made depending on the gelling conditions, homogenic and inhomogenic beads. The difference lies in the distribution of the polymer throughout the bead, with inhomogenic beads being characterized by a higher concentration

of alginate towards the surface of the bead than in the center. Homogenic beads, in contrast, formed in the presence of non-gelling cations such as sodium or magnesium, will have an even distribution of alginate throughout the bead. If only the gelling ion is present in the gelling solution it will rapidly and almost irreversibly bind to the alginate polymer thereby causing it to gel, creating a gelling zone which moves towards the center of the bead. The alginate will in turn move towards the gelling zone creating a lower concentration of alginate in the center. However, the presence of non-gelling ions, e.g. sodium, will slow down this diffusion of the alginate towards the gelling zone, thus allowing a more evenly distribution of the polymer throughout the bead as the polymer gels [18].

The polymer distribution in the capsule is an important factor to consider when encapsulating cells. Inhomogeneous alginate beads have a lower porosity at the surface due to the higher polymer concentration here [10], and will also exhibit a higher resistance towards swelling [18]. The porosity of the beads determines the permeability, a crucial factor for allowing nutrients to diffuse into and products out of the bead containing cells. At the same time the alginate capsule is supposed to function as an immunobarrier preventing not only immune cells from entering the capsule, but also molecules such as certain, but not all, cytokines, immunoglobulins and proteins of the complement system. All capsules made in this work were inhomogenous capsules.

Choice of alginate type is also an important factor, as this influences the stability of the alginate bead, as well as having an effect on the biocompatibility of the bead, as mentioned in section 1.2.2. The first capsules made by Lim and Sum for the treatment of Type 1 diabetes [19] had a poly-L-lysine (PLL) coating around the bead, see figure 1.4, which main function was to confer a stabilizing effect so that the capsules did not break after being implanted. As it has been shown repeatedly that the PLL layer is immunostimulating [20], an additional coating layer of alginate is required, shielding the polycation layer from the immune system. The alginate composition also plays a part here as medium G alginates ($F_G=0.4-0.6$) result in increased longevity of these capsules and less over-growth, as compared to high G alginates [21]. This was shown to be due to an inadequate binding of high G alginate to PLL, and not a response to the alginate itself, as capsules without PLL did not elicit the same fibrotic response. Progress in the choice of alginate, as well as choice of gelling conditions, has also furthered the potential of alginate beads. Alginate beads have now been made that withstand prolonged incubation *in vivo* [22]. This was performed using inhomogenous, intermediate G alginate beads, gelled in the presence of CaCl_2 with a small concentration of BaCl_2 . Nevertheless, because of discrepancies in the methods used by the different research groups over the last couple of decades, a truly biocompatible alginate microcapsule that sustains prolonged survival of the encapsulated cells has not yet been identified. This work attempts to get a better overview of the many different parameters involved in capsule formation, and how they affect the biocompatibility of the capsules.

1.4 Biocompatibility and inflammation

A new definition of biocompatibility was recently put forth. Here, biocompatibility is defined as “the ability of a material to locally trigger and guide non-fibrotic wound healing, reconstruction and tissue integration” [23]. This was a response to what was generally observed for implants previously considered to be biocompatible, an observation termed the foreign body response (FBR). FBR refers to the envelopment of an implant into a thin, tough collagen capsule (fibrosis) which is nonadherent to the implant, with little vascularity in the collagen capsule, but with macrophages and foreign body giant cells attached to the surface of the implant [24]. Evidence suggests this is due to low-levels of inflammation triggered by the implant, which persists indefinitely [23]. The isolation of the implant prevents it from efficiently performing its purpose, whether it be sensing body metabolites, controlled drug delivery, or electric recording of nerve cells, to name a few [23].

In today’s medicine it is increasingly common to make use of implanted foreign materials to treat patients, be it with prostheses, dialysis membranes, catheters, stents, or other medical devices. As most of these materials come in contact with blood, interactions between the biomaterial and the defense system in our blood may initiate responses ranging from systemic inflammation to thrombosis. There are two reasons why our bodies react to these implanted materials [25]. One is that they are recognized as foreign and thereby potentially dangerous, and the other is that they lack the regulatory molecules present on our own cells preventing an immunologic attack. The only truly biocompatible surface is the intact endothelial cell layer lining the blood vessels [26]. When this surface is disrupted, or when foreign materials (biomaterials or microorganisms) are introduced into the blood stream, the complement system and the coagulation cascade becomes activated so as to remove the foreign material or clot and seal the disrupted area [27]. Because of tight crosstalk between these two systems as well as with the other cells in the blood (platelets, leukocytes) and the cells lining the blood vessel (endothelial cells), activation of one part may lead to a combined response of the whole defense system [28]. It is therefore important to minimize the activation of the complement system and the coagulation cascade upon contact with the biomaterial, in order to reduce the side effects as much as possible.

1.4.1 The complement system

The complement system is a part of the innate immune system and is made up of a large number of different plasma proteins that interact with each other to help fight infection by opsonizing pathogens (induces phagocytosis of the pathogens) and inducing inflammatory responses. The innate immune system is a primary protection against pathogens that prevents the body from being overwhelmed by the vast number of microorganisms that we regularly come in contact with. Only when the innate defense is bypassed is an adaptive immune response required.

The complement system is made up of an intricate network of more than 30 different plasma proteins, with many of them being proteases that are activated only after cleavage [27]. These proteins compose a cascade where the cleavage and activation of a small number of proteins will be able to cleave and activate a large number of downstream proteins resulting in a disproportionately large complement response. The three main consequences of complement activation are the opsonization of pathogens, the recruitment of inflammatory and immunocompetent cells, and the direct killing of pathogens [27].

There are three distinct pathways through which complement can be activated at the surface of a pathogen: the classical pathway (CP), the lectin pathway (LP) and the alternative pathway (AP) [27], see Figure 1.5. However, these three pathways all converge in cleavage and activation of complement component C3 into C3a and C3b. C3b is deposited on the surface of the pathogen promoting phagocytosis, and, together with other complement components, is able to cleave downstream proteins allowing the cascade to propagate. The end product of the cascade is the terminal complement complex (TCC), sometimes also called the membrane attack complex (MAC), which inserts into the membrane of the pathogen leading to the eventual destruction of the pathogen. Furthermore, at each step in the cascade a complement component is cleaved into a bigger part acting as a protease, and a smaller part acting as an anaphylatoxin. These anaphylatoxins help recruit immune cells to the site by inducing adhesion molecules in the endothelial cells lining the blood vessels, as well as inducing inflammation, smooth muscle contraction, and increased vascular permeability.

The classical pathway

The first protein of the classical pathway is the C1 protein, composed of the subunits C1q, C1r and C1s [27]. C1 links the adaptive humoral immune response to the complement system by binding to antibodies complexed with antigens. In addition, C1 can also trigger the complement activation in the absence of antibodies as it can bind to surfaces of certain pathogens. Binding of C1q to the surface of a pathogen or the constant region of an antibody, will lead to a conformational change in the C1 complex. This is followed by C1r cleaving C1s thus exposing a serine protease able to cleave two other proteins in the complement cascade, C4 and C2. As C4 and C2 are cleaved by the active C1 protein, two small components will diffuse away, C2b and C4a, while the larger C2a and C4b will attach to the surface of the pathogen and form the C3 convertase C4b2a. The chronological order of this event is C4 being cleaved by C1 with the subsequent attachment of C4b to the surface of the pathogen. C4b then binds C2 which enables C1 to cleave C2 into C2b and a. The C3 convertase C4b2a will then cleave and deposit large amounts of C3b on the pathogen surface.

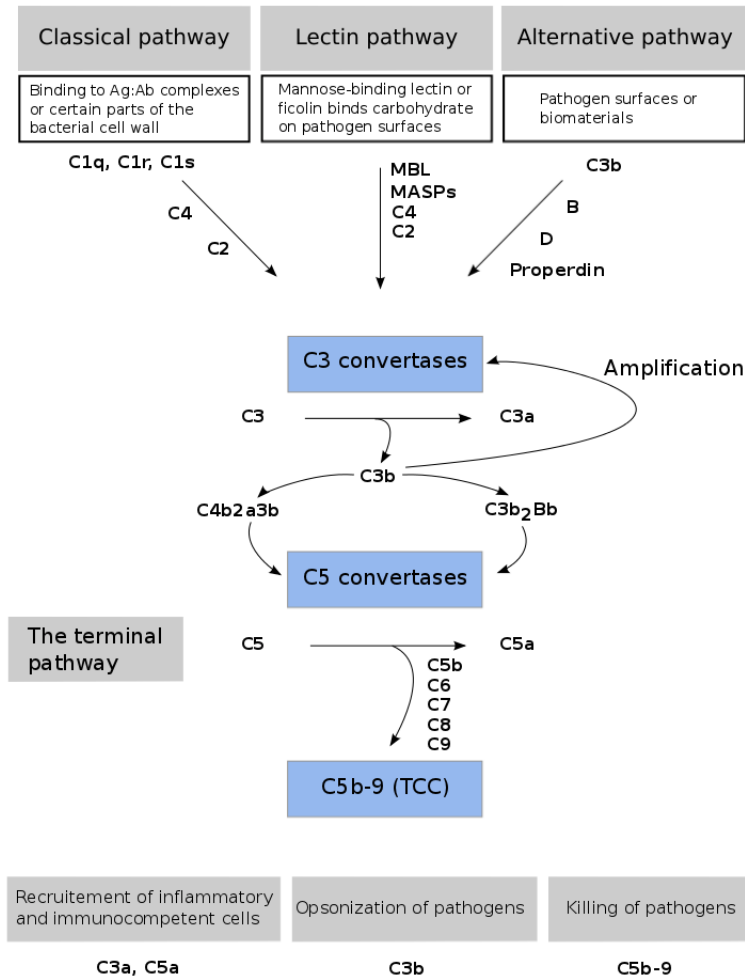


Figure 1.5: The complement cascade. Adapted and modified from [27]

The lectin pathway

Instead of C1q binding to pathogen surfaces or antigen antibody complexes, the LP makes use of a mannose-binding lectin (MBL) or a ficolin which binds directly to mannose residues present on many pathogens [27]. Mannose is also present on the body's own cells, but then it is covered by other sugar groups such as sialic acid. MBL forms a complex with the two zymogens MASP-1 and MASP-2 in a similar fashion as in the C1 complex. Binding of MBL to a pathogen enables MASP-2 to cleave C4 and C2 forming the same C3 convertase as in the classical pathway.

The alternative pathway

The alternative pathway is the complement activation pathway most associated with activation upon contact with biomaterials [28]. The pathway is triggered directly by foreign surfaces which

do not provide sufficient down regulation of the C3 convertase. Host cells do not activate the alternative pathway because of the numerous regulatory proteins located on their membranes capable of controlling the cascade. The pathway can be activated in at least three different ways [27]. Either by a spontaneous formation of C3(H₂O) as shown in figure 1.6, by C3b deposited by the classical or the lectin pathway, or by the positive regulator properdin. The alternative pathway will function as an amplification loop helping the complement system to enhance an initially weak stimulus. It has been shown that from an initial specific activation of the CP, the AP is capable of contributing to more than 80 % of the C5a and the membrane attack complex C5b-9 formed [29].

C3 is abundant in plasma and C3b is produced constantly by spontaneous cleavage, also known as the “tick-over” process [27]. This process generates C3(H₂O) by spontaneous hydrolysis of the thioesterbond in C3. Once C3(H₂O) is generated it can bind to the plasma protein factor B, which will subsequently be allowed to be cleaved by a plasma protease called factor D. Just as for C2 and C4 the small part of factor B will diffuse away while the bigger Bb will remain bound to C3(H₂O). C3(H₂O)Bb will then function as a fluid phase C3 convertase creating C3b. If there is a pathogen surface close by C3b might bind to this surface through its exposed thioester group. Surface bound C3b is able to bind factor B which can then be cleaved to Bb by factor D just as was the case for C3(H₂O)-bound B. However, if no surface is present C3b will rapidly become inactivated by hydrolysis of the thioester group. The surface bound C3bBb is the C3 convertase created by the alternative pathway, and will go on and cleave more C3 depositing more C3b on the pathogen surface.

The pathway might also be activated through deposition of C3b on the surface by CP and LP as described earlier. The C3b will bind factor B and will end up with the same C3 convertase as mentioned in the paragraph above. Thus the alternative pathway can be viewed as an amplification loop of the already activated classical or lectin pathways.

The positive regulatory plasma protein properdin, or factor P, is able to bind to the C3bBb C3 convertase increasing the stability up to 10 times [27]. Properdin might also bind directly to a pathogen surface. Surface bound properdin might then bind C3b which again binds factor B. Factor B then becomes cleaved by factor D creating the C3 convertase PC3bBb [30].

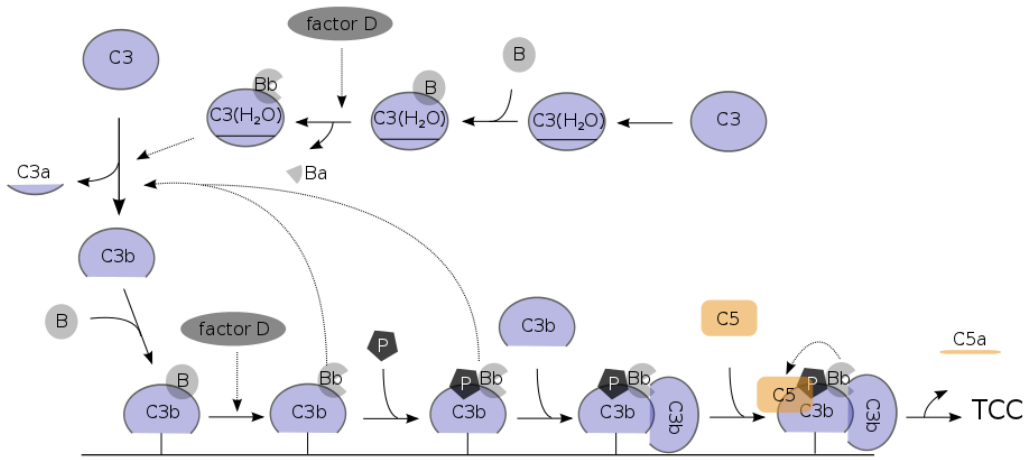


Figure 1.6: The alternative pathway depicted here as triggered by spontaneous hydrolysis of the thioester bond in C3, and attachment to a pathogen surface. This pathway may also be triggered by already present C3 convertases generated from the classical or lectin pathway, or by properdin binding directly to a pathogen surface. Adapted and modified from T.S. Jokiranta, Univ. of Helsinki

The terminal pathway

Once the C3 convertases have formed, huge amounts of C3b will become deposited on the surface of the pathogen [27]. As many as 1000 C3b molecules can attach to the surface of a pathogen due to a single C3 convertase, and C3 is the most abundant of all the complement proteins, circulating freely in the plasma at a concentration of 1.2 mg/ml [27]. As the C3 convertase cleaves C3, C3b will attach to the convertase complex creating either C4b2a3b or C3b₂Bb depending on which pathway initiated the cascade. When C3b attaches to the C3 convertase the complex will now be able to cleave C5 into C5a and C5b and is therefore called a C5 convertase. C5 binds to the C3b molecule and is cleaved by the protease activity of C2a or Bb. As C5b is generated it will facilitate the assembly of the membrane attack complex (or TCC) and its insertion into the cell membrane. This begins with C5b binding C6 and C7, creating a conformational change in the proteins exposing a hydrophobic site on C7 allowing the C5b67 complex to attach and insert into the lipid bilayer of the cell membrane. This again will allow C8 to bind to the complex and insert itself into the membrane as well. It all ends with 10 to 16 C9 molecules binding to the complex, inserting into the membrane and creating a pore spanning the lipid bilayer. This leads to the disruption of the proton gradient across the membrane, the penetration of lysozymes into the cell and finally the destruction of the pathogen.

Even though the complement cascade ends up with the membrane attack complex and the final destruction of the pathogen, an important function of complement is to facilitate the uptake and destruction of pathogens by phagocytic cells [27]. A major function of C3b is the opsonization of pathogens which occurs through binding of a C3b molecule to the receptor CR1 (also called CD35). CR1 is expressed on monocytes and neutrophils, and binding of C3b to

CR1 can lead to phagocytosis in the presence of other immune mediators such as for instance the anaphylatoxin C5a. The receptors CR2 (CD21), CR3 (CD11b) and CR4 (CD11c) all bind to inactivated forms of C3b that remain attached to the pathogen surface. CD11b can be expressed by both monocytes and granulocytes and is often used as a marker for activation of these cells. CD11b is known to be important for leukocyte adhesion and migration [27]. The anaphylatoxins (so named because of their potential to cause anaphylactic shock) C3a, C4a, and C5a all act on specific receptors on endothelial cells, mast cells, and phagocytes to produce inflammatory responses. They induce smooth muscle contraction and increase vascular permeability increasing blood flow and allowing leukocytes to reach areas of infection. C3a and C5a also induce expression of adhesion molecules. C3a and C5a activates mast cells and macrophages to produce $\text{TNF}\alpha$ and histamines contributing further to the inflammatory response. IL-8 (also called CXCL8) is another cytokine produced by among other monocytes when activated by the complement system [31]. IL8, which is also pro-inflammatory, will attract neutrophils to the site of inflammation.

Regulators of the complement system

As uncontrolled complement activation can cause extensive damage to cells, there needs to be a mechanism to protect host cells from the detrimental effects of an inappropriate complement response. The complement system is therefore tightly regulated at several steps of the cascade by proteins present both in the plasma and on host cell membranes.

As the complement activation is heavily dependent on the C3 convertase, most of these regulatory proteins interact with C3b to either prevent the formation of the convertase, or promote its dissociation. One such protein is the membrane bound, factor B antagonist, decay-accelerating factor (DAF), competing with and displacing Bb from C3b thus preventing the formation of the AP C3 convertase, see figure 1.7. Another membrane attached regulator is CR1, also capable of displacing Bb. Binding of C3b to CR1 can, as mentioned above, also lead to phagocytosis in the presence of other immune mediators. Yet another membrane bound regulator is the membrane cofactor of proteolysis (MCP) which do not displace Bb but acts as a cofactor for factor I. Two membrane bound regulators acting on a different part of the complement cascade than the ones above is protectin and vitronectin, which inhibits the binding of C9 to the C5b6-8 complex. The difference between protectin and vitronectin is that protectin is a membrane bound regulator on almost all tissues in the body as well as on circulating cells [32], while vitronectin is a multifunctional, soluble, plasma protein with other functions as well [33].

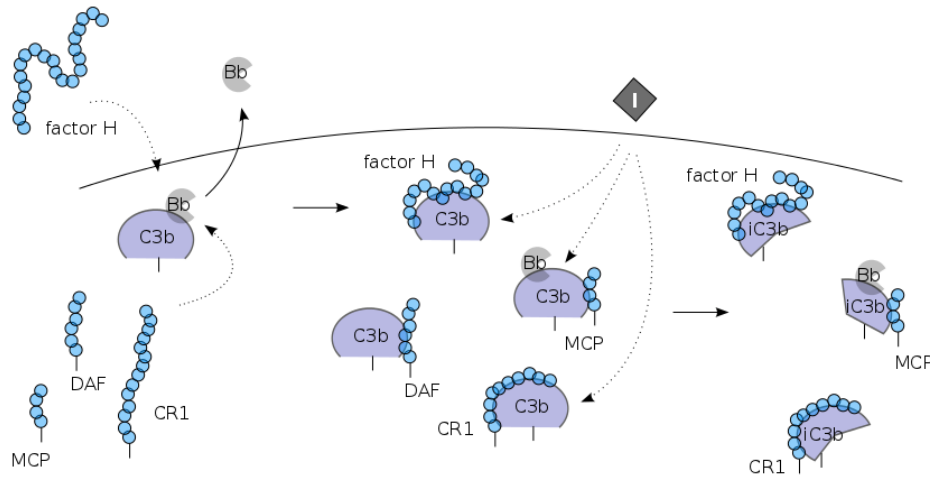


Figure 1.7: Complement regulation of C3b. Factor H, DAF, CR1, and MCP bind to C3b and inhibit the formation of a C5 convertase by either displacing Bb, or by acting as a cofactor for factor I, cleaving C3b into inactive iC3b. Adapted and modified from [27].

Factor I is a soluble protein capable of cleaving and inactivating both soluble and membrane bound C3b and C4b in the presence of a cofactor, for instance MCP [34]. Factor I circulates in plasma in an active form, but is able to cleave C3b or C4b only when they are bound to a cofactor protein. Both C3b and C4b will then be cleaved into iC3b and iC4b. iC3b will be further cleaved into C3dg while iC4b will be cleaved into C4c and C4d, and thus permanently inactivated.

The C3b molecule is not only affected by membrane attached regulators. The circulating factor H for instance, the most important fluid phase regulator of the AP, is also capable of binding to C3b and displacing Bb. Factor I will then attach to the factor H:C3b complex and be able to cleave C3b. Other soluble plasma circulating regulators include the C4b-binding protein (C4BP), the major fluid phase regulator of the CP and LP. C4BP works in a similar way for the CP C3 convertase as the soluble factor H does for the AP C3 convertase, namely by displacing C2a. C4BP bound C4b can then be inactivated by factor I, just as for factor H bound C3b.

Another soluble regulator of the complement system is the inhibitor of C1 (C1i). C1i acts on an upstream part of the cascade by binding to the active enzyme complex C1r:C1s. This causes C1r:C1s to dissociate from C1q and thereby dissolving the C1 protein and preventing further cleavage of C4 and C2. A summary of these regulators can be found in table 1.1

Table 1.1: Regulatory proteins of the complement system [27]

Name	Role in the regulation of complement activation	Localization
C1 inhibitor (C1i)	Binds to activated C1, dissociating C1r and C1s from C1q. Also functions as a cofactor for factor I	Circulating in plasma
C4-binding protein (C4BP)	Binds to C4b displacing C2a, and cofactor for factor I	Circulating in plasma
Complement receptor 1 (CR1, CD35)	Binds C3b or C4b and displaces C2a and Bb respectively. Also cofactor for factor I	Mainly on surfaces of erythrocytes and leukocytes
Factor H	Binds C3b displacing Bb, and a cofactor for factor I	Circulating in plasma
Factor I	Serine protease that cleaves C3b and C4b bound to a cofactor	Circulating in plasma
Decay-accelerating factor (DAF, CD55)	Binds C3b and C4b and displaces C2a and Bb respectively	Found on most cells in the body
Membrane cofactor protein (MCP, CD46)	Cofactor for factor I	Found on most cells in the body
Protectin (CD59)	Prevents formation of membrane attack complex	Circulating in plasma
Vitronectin	Prevents formation of membrane attack complex	Found in almost all tissues in the body, and on all circulating cells [32]

The complement system can be seen as in a continuous struggle between the regulatory proteins preventing the body’s own cells from being attacked, and the complement proteins binding to pathogens and keeping the body clear of infections. The presence of regulatory proteins on the cell membranes determines if the cell will become targeted by the complement cascade or not. Complement regulators such as DAF and MCP effectively compete with factor B for binding to C3b attached to the surface of cells. On host cells these regulatory proteins will “win” over factor B and prevent the complement from triggering. On pathogen surfaces, as well as on biomaterials, lacking regulatory proteins, factor B will effectively bind to C3b and result in complement activation. Nevertheless, the presence of regulators is not always exclusive for host cells. Some bacteria, viruses, and parasites express proteins that recruit regulators of complement which protects them during an infection. One example is the M-protein of *Streptococcus pyogenes* which binds among others the regulator C4BP, aiding the bacteria in its fight against the body’s immune system [35].

1.4.2 Hemostasis

Hemostasis describes the process of solidifying blood in order to prevent excessive bleeding, for instance in the case of vascular injury. This happens by vasoconstriction, the formation of a platelet plug, and the final activation of the coagulation system resulting in the formation of a fibrin clot. It is not only vascular injury that results in hemostasis however, the presence of biomaterials might also induce this response. For example cardiovascular devices are associated with numerous complications due to bioincompatibility of the material coming in contact with blood. The risk of thrombotic complications appears to be varying between 2 % and 10 % depending on the device [28]. These complications may result in fatality, in addition to high costs associated with follow-up intervention.

The anticoagulant and antithrombotic properties associated with the endothelium layer making up the blood vessels, prevents the blood from coagulating as it flows through the body. An inserted medical device does not have the properties of the endothelium and will therefore trigger interactions between the blood and the biomaterial, resulting in protein adsorption, the activation of the complement and the coagulation cascade, and the adhesion of cells. All these interactions are highly interconnected and it therefore requires that they are all considered when discussing biocompatibility.

The coagulation system is a complex cascade composing several proteolytic reactions which result in the formation of a fibrin plug. The cascade involves a number of zymogens, similar to that of the complement cascade, that are all sequentially activated into enzymes capable of cleaving and activating the next zymogen in the cascade. Initiation of the coagulation occurs either by the exposure of tissue factor (TF), or by surface-mediated contact activation. TF is present in the connective tissue that surrounds the blood vessels and will be exposed in the case of vascular injury [36]. TF may also be expressed on endothelial cells as well as circulating monocytes [37, 38]. The two pathways converge into a common pathway resulting in the formation of a stable fibrin clot upon cleavage of fibrinogen into fibrin by thrombin, and the subsequent cross-linking of the fibrin fibers by factor XIIIa, see figure 1.8.

For activation through the contact activation pathway, also called the intrinsic pathway, factor XII has to come in contact with a negatively charged surface to become activated. As there are not many negatively charged surfaces inside the body, the importance of this pathway to normal blood coagulation is uncertain. Also, no observable bleeding disorders are seen in patients that do not have factor XII [39]. Some hematology textbooks therefore omit the intrinsic pathway along with factor XII, and rather begin with tissue factor and the factor VIIa-TF complex. Nonetheless, activation of the intrinsic pathway has been detected in the presence of artificial surfaces [40, 41]. It is also important to keep in mind that the coagulation cascade consists of several feedback loops, see figure 1.8. Activated thrombin will for instance interact

1.4.3 Inflammatory response following microcapsule implantation

As alginate microcapsules are meant to exchange nutrients and products with their environment, they will come in contact with different bodily fluids depending on where they are inserted. This might, in addition to causing injury during the implantation procedure itself, induce complement activation and trigger the coagulation cascade, promote the activation and adhesion of leukocytes resulting in inflammation, as well as cause fibrous over-growth on the capsules. The first thing that happens when a biomaterial comes in contact with blood, is the adsorption of plasma proteins such as albumin, IgG, and the complement proteins C1, C3, and C4 [25] on the surface of the material, see figure 1.9. Some proteins are known to adopt a new conformation when they are adsorbed to a surface as for instance is the case for C3 [44] and IgG [45]. Both these proteins, and especially when having an altered shape [26], may induce activation of the complement system. In addition, adsorbed factor XII is reported to trigger contact activation [46], and adsorbed fibrinogen may bind to and activate platelets [47]. Once the complement component C3b is made and bound to this initial layer of plasma proteins, the alternative pathway amplification loop can be initiated. Formation of anaphylatoxins will recruit and activate leukocytes which will then induce an inflammatory response. During the implantation of the microcapsules, the injury to vascularized connective tissue might further promote the adsorption of proteins on the capsule surface through initiation of inflammatory responses and thrombus formation [48].

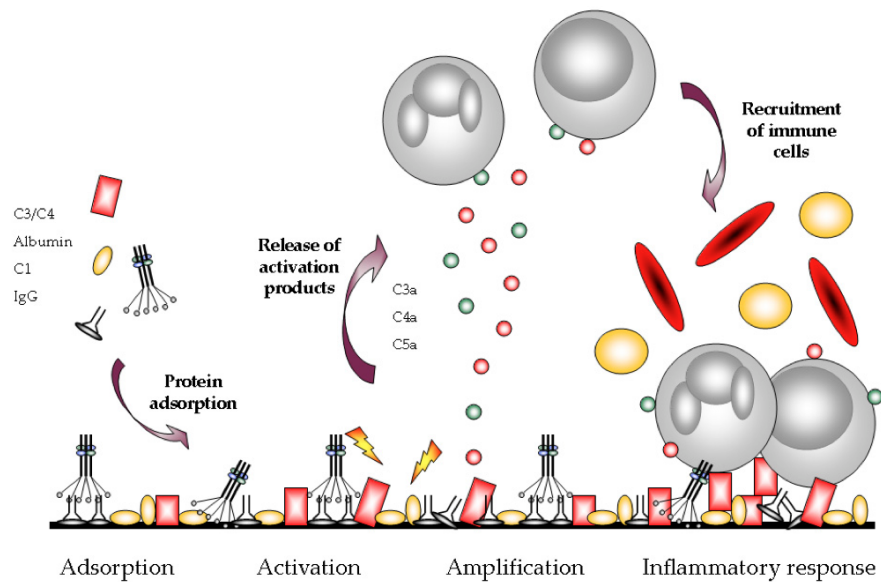


Figure 1.9: An illustration of protein adsorption, complement activation and leukocyte recruitment on a biomaterial surface. Plasma proteins will be adsorbed on the surface of the biomaterial triggering a conformational change in some of the proteins. This change will facilitate the activation of the complement system, leading to the release of the anaphylatoxins C3a, C4a, and C5a, and the subsequent recruitment and activation of leukocytes inducing inflammation. Adapted from [25]

If factor XII is part of this initial protein layer, then alginate microcapsules might theoretically trigger the intrinsic coagulation pathway. Moderate amounts of factor XII have been observed on other biomaterials such as vascular grafts and hemodialysers, however not in its activated form [49, 50, 51]. As mentioned before, activation of the intrinsic pathway has been detected in the presence of artificial surfaces. But because patients with factor XII deficiency show similar levels of thrombin as do normal patients during a cardiopulmonary bypass [52], it is uncertain how much the activation of the intrinsic pathway contributes towards the activation of coagulation by biomaterials. Monocytes, recruited by complement activation, coming in contact with the biomaterial surface, might be triggered to express tissue factor. It is therefore possible that the extrinsic pathway rather than the intrinsic pathway is what contributes to activation of the coagulation. The role of leukocytes in biomaterial induced coagulation has previously been emphasized in experiments showing low levels of thrombin-antithrombin complex-formation in plasma, while higher in whole blood upon contact with a biomaterial [53].

Inflammation following the initial blood to material interaction will occur. The degree of inflammation depends on the extent of injury during the implantation, the implantation site, as well as the composition, conformation, and concentration of protein adsorbed on the surface [48]. Because of the capsule size, and the fact that they are implanted in the peritoneal cavity, minimal injury to surrounding tissue is achieved. Attachment of neutrophils and monocytes to the protein layer, as shown in figure 1.9, may trigger the secretion of chemokines such as IL-8 and MCP-1 (monocyte chemotactic protein 1, not to be confused with the complement regulatory protein MCP) [27]. IL-8 and MCP-1 attracts other cells by acting on leukocytes rolling along the endothelial cells lining the blood vessels, and up-regulating certain adhesion molecules on the leukocytes allowing them to attach and cross the blood vessel wall by squeezing between the cells [27]. In addition, if the capsules trigger the coagulation cascade or the complement cascade, components of these cascades will act as chemokines as well, as mentioned previously for the complement system. The molecules IL-8 and MCP-1 will not only recruit leukocytes, but will also activate them [27]. Activated leukocytes, in particular the monocytes, will start secreting more chemokines, as well as different inflammatory cytokines that is supposed to help contain the assumed infection. Among the cytokines are $\text{TNF}\alpha$ which activates the endothelium and increases the vascular permeability of the blood vessels facilitating the migration of leukocytes out of the blood stream, in addition to antibodies and complement proteins [27]. It also relaxes the smooth muscle cells lining the blood vessel, increasing the diameter, and thus causing increased blood flow to the site of inflammation. The complement proteins C5a, C3a, and C4a, have a similar influence on the blood vessels. Platelet adhesion to the protein layer, as well as clot formation, will also release chemoattractants such as $\text{TGF-}\beta$, PDGF, and IL-1 that can direct leukocytes to the capsules [48]. Monocytes will start developing into macrophages and begin secreting even more cytokines. Secreted molecules include chemokines such as IL-8, MCP-1, and MIP-1 α , and inflammatory cytokines such as $\text{TNF}\alpha$, IL-1 β , and IL-6, as well as a group of other molecules, see table 1.2. $\text{TNF}\alpha$, IL-1 β , and IL-6 have a wide spectrum of biologi-

cal activities including raising body temperature and inducing synthesis of acute-phase proteins [27], and are therefore well suited for measuring inflammation *in vitro*.

As monocytes adhere to the capsules and start developing into macrophages, their natural function is to phagocytize pathogens and cell debris [27]. When they are unable to do so, for particles larger than 10 μm , they start developing into foreign body giant cells [48]. This inability to phagocytize the alginate microcapsules, a process called frustrated phagocytosis, might lead to the release of mediators of degradation such as reactive oxygen intermediates, degrading enzymes, and acids damaging the capsules.

Macrophages may also secrete fibroblast growth stimulating factors and factors promoting angiogenesis [54], see figure 1.10. As the stimulation of fibroblasts has been shown to correlate with the *in vivo* fibrosis [55], macrophages may therefore affect the formation of over-growth on alginate microcapsules. Over-growth prevents proper nutrient and oxygen diffusion to the encapsulated cells leading to loss of cell viability and functionality [56], and should be minimized as much as possible. Capsules therefore have to be as inert towards leukocyte activation as possible, with minimal complement activation and triggering of the coagulation cascade. This is again linked with the composition, conformation, and concentration of proteins adsorbed on the surface of the capsules. A list of potentially important proteins screened for in this work is shown in table 1.3.

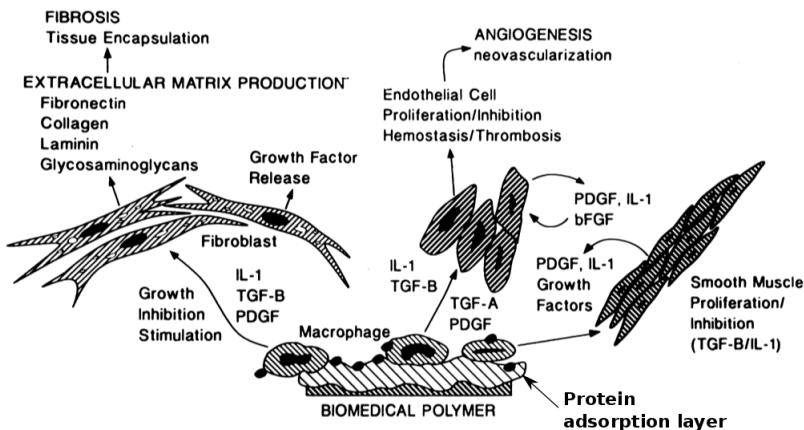


Figure 1.10: Fibrosis and angiogenesis stimulation by macrophages attached to an implanted biomaterial. The biomaterial is for our purposes alginate microcapsules. Adapted and modified from [56]

Table 1.2: Cytokines involved in inflammatory responses [25, 27].

Chemokine	Produced by	Target cells	Major effects
IL-8	Monocytes, macrophages, epithelial and endothelial cells	Neutrophils, naive T cells, fibroblasts	Mobilizes, activates and degranulates neutrophils. Angiogenesis
MIP-1 α	Monocytes, T cells, platelets and fibroblasts	Monocytes, NK cells, T cells and dendritic cells	Antiviral defense, induction of synthesis of pro-inflammatory cytokines
MCP-1	Monocytes, macrophages, and fibroblasts	Monocytes, NK cells, T cells and dendritic cells	Recruits monocytes and activates macrophages
Inflammatory Cytokine			
IL-1 β	Macrophages, epithelial cells	Macrophage and T cells	Cell activation and fever, pro-inflammatory
TNF α	Macrophages, NK cells, T cells		Pro-inflammatory. Promotes endothelial activation
IL-6	T cells, macrophages, and endothelial cells	T and B cells	T and B cell growth and differentiation. Acute phase protein production, fever
Anti-inflammatory Cytokine			
IL-1RA	Monocytes, macrophages, and neutrophils		Anti-inflammatory. IL-1 receptor antagonist
IL-10	Monocytes	Macrophages, lymphocytes	Potent suppressant of macrophage functions
Growth Factors			
PDGF	Platelets and other cells including eosinophils	Smooth muscle cells and fibroblasts	Important for vasculogenesis, angiogenesis, and cell division
HGF	Mesenchymal stem cells	Epithelial and endothelial cells	Regulates cell growth, cell motility, and morphogenesis
VEGF	Mast cells, platelets and neutrophils	Endothelial cells	Important for vasculogenesis and angiogenesis. Stimulates monocytes and macrophages
Other			
MIF	T cells, pituitary cells	Macrophages	Inhibits macrophage migration, stimulates macrophage activation
IP-10	Monocytes, endothelial cells and fibroblasts	Monocytes, NK cells and resting T cells	Immunostimulant, antiangiogenic, inhibited secretion by iC3b and C4b
IFN- γ	Leukocytes, dendritic cells	Macrophages, lymphocytes	Pro-inflammatory, antiviral, increased MCH class I expression
RANTES	T cells, endothelium, and platelets	Monocytes, NK cells, T cells and dendritic cells	Activates T cells, chronic inflammation

Table 1.3: Plasma proteins screened for in this work.

Proteins of the complement system [27]	Function
C1-inhibitor	Binds to activated C1, dissociating C1r and C1s from C1q. Also functions as a cofactor for factor I
C3	Part of the complement cascade by acting as a C5 convertase
Factor H	Binds C3b displacing Bb, and a cofactor for factor I
Factor I	Serine protease that cleaves C3b and C4b bound to a cofactor
Vitronectin	Prevents formation of membrane attack complex
Proteins of the coagulation cascade	
Fibrinogen	Cleaved into fibrin by thrombin. Cross-linked fibrin forms blood clot. Also mediate phagocyte binding to implant surfaces [48]
High molecular weight kininogen	Part of the contact activation pathway of the coagulation cascade. Cofactor of factor XI activation [28]
Plasminogen	Enzyme involved in hemostasis by degrading fibrin clots

1.4.4 Biocompatibility of alginate microcapsules in vivo

Alginate microcapsules have proven its potential in some animal models, while having had less success in others. They have been tested numerous times *in vivo*, with a varied outcome. The use of different animal models, variable sites of implantation, the state the cells are in when encapsulated, and compatibility between host and implanted cells, all affect the outcome of the experiment. In addition, because of a many times poor description of the alginate composition, and the use of different encapsulation protocols, it is often difficult to compare the results of the many experiments performed.

Successful implantation of encapsulated islet cells has clearly been easier to achieve in smaller animals than in larger ones. Lim and Sum reported in 1980 the first successful reversal of diabetes in Wistar rats for up to 3 weeks [19]. This was achieved by implanting islet isografts (from a genetically identical rat) enclosed within alginate microcapsules. The capsules were hollow alginate-poly-L-lysine capsules with an outer coating of polyethyleneimine. In 2001, Duvivier Kali et al. managed to reverse diabetes for up to 350 days for syngenic (identical) and allogenic (from the same species) transplantation in BALB/c and NOD mice by using barium alginate

beads [57]. More recently, human islet cells have also been encapsulated and tested *in vivo*. In 2008, human islet cells encapsulated in $\text{Ca}^{2+}/\text{Ba}^{2+}$ beads were transplanted into diabetic nude mice, resulting in insulin independence until the end of the study (260-329 days after transplantation) [22]. The capsules were then extracted and observed free of overgrowth and containing viable islets. Since nude mice, that lack a thymus and therefore have an inhibited immune system, was used, no immunosuppression was necessary. This might be the reason for the low over-growth observed on these capsules.

Experiments have also been performed in larger animals. In 1993, Soon Shiong et al. successfully managed to transplant islet allografts into diabetic dogs with and without immunosuppression [58]. Insulin independence was observed for up to 172 days. In 2005, R. B. Elliott et al. went one step further and transplanted piglet islets, encapsulated in APA capsules, into nondiabetic cynomolgus monkeys [59]. It was shown that after 8 weeks the piglet islets were healthy, however they did not evaluate the insulin production of the cells. Recently, there has also been experiments in humans where human islet cells were transplanted into patients with type 1 diabetes [60]. Cells were encapsulated in alginate-PLO capsules which were shown to preserve islet function without immunosuppression throughout the course of the trial (3 years). The grafts did not elicit any immune response, but the low number of islets transplanted per patient has limited the success of the trial as insulin independence was only achieved transiently in one of the patients. Additionally, in one of the patients a fibrotic lump was excised 5 years post implantation, consisting of capsules without any viable islet cells inside. Another study performed in 2009 with human islets encapsulated in barium beads, showed prolonged detection of C-peptide (used as an insulin production marker) in only one of four patients [61]. In addition, after 16 months capsules recovered were surrounded by fibrous tissue and contained necrotic islets. However, no major side effects or infection occurred, indicating the safety of the procedure.

1.4.5 Towards increased biocompatibility

Despite of intense research over several decades, there still do not exist a truly biocompatible material. Many different approaches are being put forward in order to increase the biocompatibility of a material, one being to modify the material itself. Chemical structure, including hydrophobicity and charge, as well as the surface properties such as topography and roughness of a material will greatly influence the biocompatibility [62]. In the case of alginate microcapsules, this is reflected in the composition of the alginate. Before Soon Shiong et al. managed to transplant islet cells into diabetic dogs, researchers had experienced difficulties with the larger animal model because of a high proliferation of fibroblasts stemming from IL-1, IL-6, and $\text{TNF}\alpha$ production [58]. This was discovered to be because of the low F_G alginate that was used in the early encapsulation experiments. The high M content (86-99.9 % M) stimulated the cytokine production as well as giving the capsules a weak integrity. Coating the capsules with

a stabilizing polycation layer was therefore necessary. Different types of layers that have been tested include poly-L-Lysine (PLL), poly-L-ornithine (PLO), and poly(methylene-co-guanidine) (PMCG). Evidence suggests that these coating layers are in various degrees immunostimulating with PLL perhaps the most [20]. A more recently proposed idea is to use a polymer that consists of zwitterions that give the coating an equal number of positive and negative surface charges, in an attempt to mimic the excellent resistance to protein adsorption and hemocompatibility of the zwitterionic phosphorylcholine group of cell membranes [63].

Another approach, perhaps more focused on solid biomaterials such as stents and catheters, could be to attach complement regulators to the surface of the biomaterial, or use surface coatings that might recruit these proteins. Factor H has previously been attached to biomaterial surfaces resulting in decreased activation of the complement system [64]. More inert surfaces has also successfully been obtained by immobilizing heparin and heparin-conjugates onto the biomaterials [65], which is thought to selectively bind certain regulatory proteins such as factor H and C1i [66, 67], as well as reduce adsorption of proteins undergoing surface-induced denaturation [68]. One might consider inhibiting the coagulation cascade using thrombin inhibitors such as lepirudin [69], or inhibit the activation of platelets by using platelet inhibitors such as aspirin [70]. However, the applicability of these approaches towards alginate microcapsules might be more limited.

1.5 Aims

The aim of the present study was to investigate the biocompatibility of a set of different alginate microcapsules. This was to be performed by incubating the capsules in whole blood, and then analyzing the activation of leukocytes, and production of cytokines and complement components. The capsule parameters that were investigated was:

- Polycation concentration
- Polycation type
- Alginate type
- Capsule type
- Capsule size
- Gelling conditions

High cytokine and complement responses *in vitro* could indicate increased risk of inflammatory responses and over-growth on capsules *in vivo*, limiting the efficacy of the encapsulated cells.

It was also sought to investigate if the lower complement responses towards TAM-capsules, as seen earlier compared to APA and also saline control, might be the result of adsorption of

complement inhibitors on the bead surface. Plasma-incubated capsules were therefore tagged with different fluorescent labeled antibodies towards complement and coagulation cascade components, and analyzed in a confocal laser scanning microscope.

2 MATERIALS AND METHODS

2.1 Formation of alginate microcapsules

Alginate-polycation-alginate (APA) with a hollow core, APA with a solid core, and TAM-capsules were made with varying alginate type and needle size, as well as with different polycation type and increasing concentration.

2.1.1 Alginate solution

Two types of ultrapure High-G sodium alginate from FMC BioPolymer AS (Novamatrix, Norway) and one ultrapure High-M sodium alginate, see table 2.1, was used throughout this study. The protein contents were less than 0.3% for all alginates as specified by the manufacturer, and endotoxin levels $\leq 100\text{EU/g}$. UP-LVG* is similar to UP-LVG but of a new batch, as the GMP license had expired on the original UP-LVG alginate. As batch variation might occur, this new alginate was included in the whole blood assay.

Table 2.1: Alginate solutions

Name	Algae	Batch	M_w [g/mol]	F_G	F_{GG}	$N_{G \geq 1}$
UP-LVG	<i>Laminaria hyperborea</i>	FP-603-04	75-200	0.67	0.55	12
UP-LVG*	<i>Laminaria hyperborea</i>	BP-1108-01	75-200	0.67	0.55	12
UP-100M	<i>Macrocystis pyrifera</i>	FP-209-02		0.44		

Ultra-pure alginate (1.8 g) was dissolved overnight in sterile, endotoxin free, non-pyrogenic, water (50 ml, B. Braun, Melsungen, Germany) with agitation. D-mannitol (50 ml, 0.6 M, BDH Anala R., VWR International Ltd, Pool, England) was added to the alginate solution creating an alginate concentration of 1.8 %. The pH of the solution was adjusted to between 7.2 and 7.4 with sterile NaOH and HCl. Finally, the alginate solution was filtered with a 0.2 μm filter to sterilize it, and kept refrigerated.

2.1.2 Gelling solution

The gelling solution was made by dissolving analytical grade $\text{CaCl}_2 \cdot 2\text{H}_2\text{O}$ (50 mM, Merck, Darmstadt, Germany), D-mannitol (0.15 M, HPLC degree, BDH Anala R., VWR International Ltd, Pool, England), and HEPES (10 mM, Sigma-Aldrich, St. Louis, MO, USA) over night in sterile, endotoxin free water. For the preparation of TAM capsules the gelling solution was added analytical grade BaCl_2 (1 mM, Merck, Darmstadt, Germany). The solution was then pH-calibrated to lie inside the physiological range of 7.3-7.4, using sterile NaOH and HCl. Lastly, the solution was filtered with a 0.2 μm filter to sterilize it, and then kept refrigerated.

2.1.3 Bead preparation

Ca-alginate capsules were made by dripping an alginate solution into the gelling solution described in section 2.1.2. For TAM-capsules 1 mM BaCl₂ was added to the gelling solution. A syringe containing alginate (1.8 %, 5 ml) was mounted on an infusion pump and connected to a needle through a thin, plastic tube. The needle was attached in a bead generator apparatus [71], and placed approximately 2 cm above the gelling bath which was continuously agitated using a magnetic stirrer. The droplet size was controlled using the high-voltage electrostatic bead generator (7 kV, 10 ml/h) and by using different needle sizes (0.25 mm, 0.35 mm, and 0.40 mm), that resulted in capsules with a diameter of between 400 and 700 µm depending on the method, the alginate type and the polycation concentration. The first capsule set was made using 4 needles attached in a multi-head scaffold, the second set was made using a single needle. All capsules were made with a flow of 10 ml/h, except TAM capsules made with 0.25 mm needle, 0.35 mm needle, and 0.40 mm needle, which were made using a flow of 6 ml/h, 8 ml/h, and 8 ml/h, respectively, see section 3.1. The beads were incubated in gelling solution for 10 minutes after the last alginate droplet was observed. The beads were then washed once with washing solution (sterile 0.9 % NaCl, 30 ml, B. Braun, Melsungen, Germany). For TAM-capsules, the beads were kept refrigerated in washing solution (12 ml).

For the preparation of APA capsules, the washed beads were placed in a polycation bath (25 ml) on agitation for 10 minutes. The polycation type and concentration was varied between poly-l-lysine (PLL Hydrochloride, Sigma-Aldrich Corp., St. Louis, MO, USA) and poly-l-ornithine (PLO Hydrobromide, Sigma-Aldrich Corp., St. Louis, MO, USA) at concentrations of 0.05 %, 0.1 %, and 0.14 %. After 10 minutes incubation in the polycation solution, the beads were washed once with washing solution before being placed in an alginate coating bath (0.1 % M. pyr alginate, 10 ml) on agitation for 10 minutes. The capsules, now APA with a solid core, were washed once with washing solution before being either stored in washing solution (12 ml), or treated with a analytical grade citrate solution (55 mM Na-citrate tribasic dihydrate, 20 ml, Merck, Darmstadt, Germany) on agitation for 10 minutes. Citrate-treated capsules, now APA hollow, had a soluble core which was observed in increased sedimentation time. The beads were then washed once with washing solution before being stored in the fridge in washing solution (12 ml).

The capsules were diluted to a workable concentration before being tested in the whole blood assay. They were also washed in order to remove any residual protein content that might have been still present. The alginate capsules stored in washing solution (12 ml) was aliquoted by suspending the capsule mixture, and transferring 1 ml of the mixture into 10 sterile eppendorf tubes. Residual capsules were divided over the eppendorf tubes, and an equal capsule volume was confirmed visually. The eppendorf tubes now had an approximate concentration of 0.5 ml beads in a total of 1.2 ml NaCl (sterile, 0.9 %). Each eppendorf tube was then washed twice

in washing solution before being diluted in a total of 5.5 ml NaCl (sterile, 0.9 %). Aliquots of 500 μ l solution was divided into 10 sterile NUNC polypropylene tubes. The supernatant (400 μ l) was removed leaving approximately 45.45 μ l capsules in a total volume of 100 μ l NaCl.

2.2 Whole blood assay

The whole blood model allows testing of microcapsules *in vitro*, using blood that still contains an intact complement cascade [31]. A potential indicator of the ability of the capsules to trigger inflammatory reactions is the activation of the complement cascade, as the level of complement activation often goes hand in hand with the properties of the biomaterial surface. Whole blood contains all the potential cellular and fluid phase mediators of inflammation, and is therefore ideal for studying the biocompatibility of the microcapsules *in vitro*. By using the highly specific thrombin inhibitor lepirudin, the blood is anti-coagulated while still avoiding complement and leukocyte activation. However, to minimize the activation by the tubes themselves, low activating polypropylene tubes had to be used.

Whole blood from voluntary donors was collected in polypropylene tubes (4.5 ml NUNC, Roskilde, Denmark) using BD vacutainer tops (Belliver Industrial Estate, Plymouth, UK) with added lepirudin (2.5 mg/ml, 80 μ l, Celgene Europe, Boudry, Switzerland). Approximately 4 ml of blood was collected per tube, giving a final lepirudin concentration of 0.05 mg/ml lepirudin. Dulbecco's PBS (100 μ l, with Mg^{2+} and Ca^{2+} , Sigma-Aldrich, St. Louis, MO, USA) was added to NUNC tubes containing capsules (45.45 μ l in a total volume of 100 μ l NaCl) and NUNC tubes containing negative and positive controls. Negative controls were T_0 and Saline containing sterile NaCl (100 μ l, 0.9 %), while positive controls contained Zymosan A (20 μ g/ml, Sigma-Aldrich, St. Louis, MO, USA, Z-4250) or LPS (2 μ g/ml, Invivogen, *E.coli* 0111-B4) in sterile NaCl. All tubes were pre-heated to 37°C before anti-coagulated blood (500 μ l) was added to each vial, carefully avoiding blood contamination of the screw cap. T_0 was immediately added EDTA (14 μ l, 10 mM final concentration), while other samples were incubated for 60 and 240 minutes in an incubator (37°C) under continuous rotation, prior to adding EDTA. EDTA (ethylenediaminetetraacetic acid) acts by chelating calcium and thereby stops the complement activation as many of the steps in the complement cascade are calcium-dependent. After the complement reaction had been stopped, the samples were centrifuged (3000 rpm, 15 minutes) and the plasma was stored in the freezer (-20°C) for later cytokine analysis.

The use of human whole blood for basal experiments was approved by the Regional Ethic Committee (REK) at NTNU in Norway. The experiments were performed in accordance with their guidelines.

2.3 Flow cytometry

Flow cytometry (FCM) was used to measure leukocyte activation upon incubation of whole blood with alginate capsules. FCM is a widely used technique for counting and examining cells. It works by passing a stream of sample solution through a laser and detecting side and forward scatter of the light, as well as any fluorescence. This permits close examination of each cell as it passes through the laser. Forward scatter correlates with the volume of the cell, while side scatter correlates with the granularity, making it possible to distinguish certain cell types from each other depending on size and inner complexity. Using fluorescent labeled markers one can further discriminate between different cells of interest. Fluorophore-conjugated antibody towards the membrane protein CD11b was used to detect the activation of monocytes and granulocytes as this protein gets up-regulated when the cells are activated. The membrane protein CD14, a coreceptor for TLR4 recognition of LPS [27], is found predominantly on monocytes and macrophages, and fluorophore-conjugated antibody towards CD14 was therefore used to gate for monocytes.

Expression of CD11b was measured in whole blood after one hour incubation with the capsules. Blood (50 μ l) was taken from the samples and fixed with PFA (1 %, 50 μ l, Sigma-Aldrich, St. Louis, MO, USA). Fixated blood (25 μ l) was then added an antibody mix (5 μ l) containing PE anti-CD11b (BD Biosciences, USA) and FITC anti-CD14 (BD Biosciences, USA) in equal amounts, and incubated dark for 15 minutes. Samples were transferred to flow-vials and added EasyLyse erythrocyte lysis buffer (500 μ l, Dako Cytomation, Glostrup, Denmark), followed by incubation for 15 minutes. CD11b expression on granulocytes and monocytes was then measured on flow cytometer by detecting CD11b⁺ cells. Monocytes and granulocytes were distinguished by side scatter and CD14 detection, as monocytes express more CD14, and granulocytes, containing granules, have a higher side scatter. Red blood cells were removed by addition of erythrocyte lysis buffer.

2.4 ELISA

Enzyme-linked immunosorbent assay (ELISA) was performed on plasma from whole blood assays. ELISA is a powerful assay used to detect the presence of an antigen in a sample, and was in this work used to detect the cytokines IL-8 and TNF- α , as well as the complement component TCC. Antigen specific antibodies are allowed to attach to a plastic multiwell plate before the sample plasma is added, see figure 2.1. Any antigen present in the plasma sample will bind to the high affinity antibodies coating the plate. Unbound antigen is then washed away. Finally, a labeled detection antibody that recognizes a different epitope to the coating antibody, is added, and bound antigen is detected. Here, the detection antibody was conjugated to biotin. Streptavidin-conjugated horse radish peroxidase (HRP) was then linked to the biotin antibody, before 3,3',5,5'-tetramethylbenzidine (TMB) was added. HRP is, in the presence of H₂O₂, able to oxidize TMB into its corresponding diimine resulting in the solution taking on a blue color

which can be detected by a spectrophotometer.

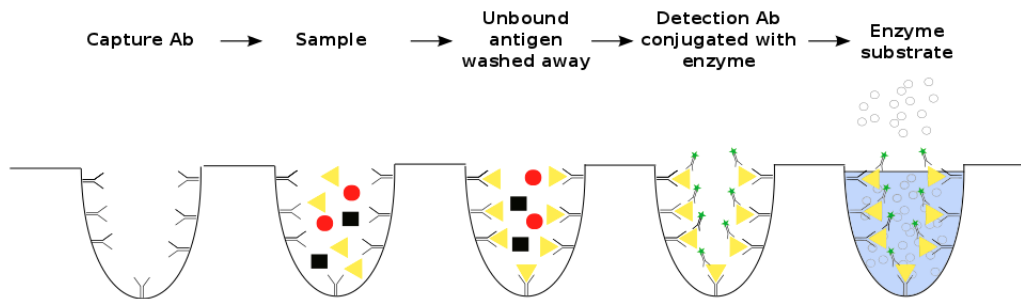


Figure 2.1: Principle of sandwich ELISA.

2.4.1 IL-8

IL-8 specific capture antibody (4.0 $\mu\text{g}/\text{ml}$ in PBS, 50 $\mu\text{l}/\text{well}$, R&D Systems, USA) was added to NUNC 96-well microplate and left to incubate over night at room temperature. The plate was then washed three times (275 μl PBST/well), before being blocked with BSA (1 % BSA in PBS, 200 $\mu\text{l}/\text{well}$, R&D Systems, USA) for one hour at room temperature. The plate was then washed as before, and samples were loaded. For samples incubated for one hour, capsules along with negative controls were diluted 1:4 in reagent diluent (0.1 % BSA and 0.05 % Tween 20 in tris-buffered saline). Positive controls were diluted 1:10 and 1:20. For samples incubated for four hours, T_0 was diluted 1:4, saline and TAM-capsules were diluted 1:8, APA-capsules were diluted 1:16, and positive controls were diluted 1:20 and 1:40 in reagent diluent. IL-8 standard was diluted to 2000 pg/ml in reagent diluent, and further serially diluted 1:2 in seven wells on the plate. All samples (50 $\mu\text{l}/\text{well}$) were loaded in triplicates. The plate was then left to incubate for two hours at room temperature, washed as before, and IL-8 specific detection Ab (20 ng/ml , 50 $\mu\text{l}/\text{well}$, R&D Systems, USA) was added. After two hours of incubation on bench at room temperature, the plate was washed again, and streptavidin-HRP (diluted 1:200 in reagent diluent, R&D Systems, USA) was added and left dark for 20 minutes. The plate was washed a final time as before, and TMB substrate reagent A and B (R&D Systems, USA) was mixed in equal amounts, and added to the plate. The plate was left dark for 20 minutes as the coloring reaction was taking place, and then H_2SO_4 (2 M, 50 $\mu\text{l}/\text{well}$, R&D Systems, USA) was added and the optical density determined at 450 nm using a spectrophotometer. Wavelength correction was set to 570 nm.

2.4.2 TNF- α

TNF- α ELISA (Human TNF- α DuoSet ELISA kit, R&D Systems, USA) was performed similarly to IL-8 described above. TNF- α specific capture Ab (4.0 $\mu\text{g}/\text{ml}$ in PBS, 50 $\mu\text{l}/\text{well}$) was added to NUNC 96-well microplate and left over night. The plate was washed as for IL-8 (three times, 275 μl PBST/well) and blocked with reagent diluent (1 % BSA in PBS, 200 $\mu\text{l}/\text{well}$). After one

hour the plate was washed and samples were added. Samples were diluted 1:2 in reagent diluent except for the positive controls which were diluted 1:10 and 1:20. Standard was diluted to 2000 pg/ml and further 1:2 serially diluted on the plate. All samples were loaded in triplicates, and incubated for two hours. The plate was then washed and TNF- α specific detection Ab was added (250 ng/ml, 50 μ l/well). After a two hour incubation and a new washing step, streptavidin-HRP (diluted 1:200 in reagent diluent, 50 μ l/well) was added. The plate was left dark for 20 minutes, washed, and equal amounts of TMB substrate A and B (50 μ l/well) was added. The reaction was stopped with H₂SO₄ (2 M, 50 μ l/well) and absorbance was detected at 450 nm along with wavelength correction at 570 nm.

2.4.3 sTCC

sTCC ELISA, developed by Mollnes et al. [72], was performed similarly to IL-8 and TNF- α , but with other incubation times, and with a specific streptavidin-HRP. The reagent diluent was added EDTA to avoid further activation.

TCC specific capture Ab (α E11 specific for C9, AntiBodyShop, Gentofte, Denmark) diluted 1:1000 in PBS was added to NUNC 96-well ELISA plates and incubated (overnight, 4°C). Plates were then washed (three times, 275 μ l PBST/well) using a 96-well plate washer. Blocking solution (0.1 % BSA in PBS, 200 μ l/well) was added and plates were incubated for a minimum of one hour at room temperature. This was followed by another washing step, before samples were diluted in reagent diluent (PBS with 0.2 % Tween 20 and 10 mM EDTA, 50 μ l/well) and loaded onto the plates. Plasma samples from one hour incubation was diluted 1:5 while plasma samples from four hour incubation was diluted 1:10, except for positive controls which were diluted 1:10 and 1:20 for one hour incubated plasma, and 1:20 and 1:40 for four hour incubated plasma. Standard (zymosan activated serum, 10 AU/ml) was serially diluted 1:2 on the plates. All samples were loaded in triplicates. After 1.5 hours incubation at room temperature, the plates were washed and detection Ab was added (diluted 1:5000, 50 μ l/well, Biotinylated Anti-human SC5b-9, Quidel, San Diego, USA), and incubated for 45 minutes at room temperature. Streptavidin-HRP (diluted 1:1000, 50 μ l/well) was added and the plates were left for 20 minutes covered in aluminum in order to avoid direct light. This was followed by a final washing step, TMB substrate was added (equal amounts of substrate A and substrate B, 50 μ l/well), and plates were covered anew. Approximately 20 minutes later the reaction was halted by adding H₂SO₄ (2 M, 50 μ l/well), and absorbance was detected at 450 nm with a wavelength correction set to 570 nm, using a spectrophotometer.

2.5 Bio-plex

The Bio-PlexTM Pro Assay (Bio-Rad Laboratories, Inc., Hercules, California, USA) was used to detect 15 different cytokines at once. It uses a principle not very different from a sandwich ELISA, but with magnetic beads covered with antibodies towards a specific cytokine instead of

using an antibody-covered plastic multiwell plate. The beads bind to the cytokine of interest through the covalently attached capture antibodies. After removing unbound protein, a biotinylated detection antibody is added which creates a sandwich complex, see figure 2.2. Finally, the addition of streptavidin-phycoerythrin (SA-PE) will allow quantification of the cytokine concentration by PE serving as a fluorescent indicator. As each type of bead has its own color code or spectral address, discrimination of the different beads is possible. Using a two laser flow cytometer, it is thus possible to detect which bead is present, and then quantify the presence of cytokine on the bead by determining the PE fluorescence. A red (635 nm) laser excites the fluorescent dyes within each bead, while a green (532 nm) laser excites PE.

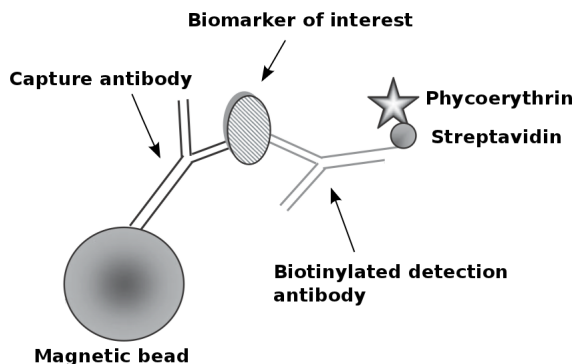


Figure 2.2: Bio-Plex sandwich immunoassay. The magnetic bead has a distinct color code which permits the direct determination of cytokine type. Phycoerythrin on the other hand allows for determination of the amount of cytokine present on the bead.

The xMAP Technology uses 5.6 micron polystyrene microspheres prepared in 96-wells Bio-Plex Pro flat bottom plates for magnetic based washing. The procedure using the Bio-plex kit (Bio-Rad Laboratories, Hercules, CA) is described in detail in the manufacturers instruction manual [73] and was performed accordingly, with the following exception: A volume of 25 μ l per well of beads, samples, standards and streptavidin-PE, was added. This was based on knowledge from previous experiments performed at the department of Cancer Research and Molecular Medicine, yielding satisfying results [74]. Plasma samples were prepared by diluting in Bio-Plex sample diluent (20 μ l plasma in 60 μ l sample diluent). Beads were read using the Bio-Plex 200 System. The concentration of 15 different cytokines was determined. The different cytokines are shown in table 2.2.

Table 2.2: Bio-Plex analyzed cytokines in plasma after whole blood assays

IL-1 β	IFN- γ	RANTES
IL-1ra	IP-10	TNF α
IL-6	MCP-1	VEGF
IL-8	MIP-1 α	HGF
IL-10	PDGF-BB	MIF

2.6 Protein adsorption assay

In order to understand what mechanisms are involved when the body responds to alginate microcapsules, it is important to know what proteins are adsorbed on the surface of the capsules. Do the capsules trigger the complement system? Are there inhibitory processes going on? And how does the coagulation cascade react to the capsules? To do this, capsules were incubated in either lepirudin conjugated plasma, or lepirudin conjugated whole blood. They were then washed (sterile 0.9 % NaCl, 500 μ l, B. Braun, Melsungen, Germany) and incubated with fluorochrome labeled antibody (50 μ g/ml, 37°C, 30 min, see table 2.3). Antibodies were first diluted to a 2x working solution in NaCl before 100 μ l was added to the capsules giving a final concentration of 50 μ g/ml. After incubation the capsules were washed once (sterile 0.9 % NaCl, 500 μ l) and stored in 200 μ l wash solution protected from light. In the case where a 2^o antibody was used, the capsules were washed (sterile 0.9 % NaCl, 500 μ l) after treatment with 1^o antibody, and incubated with 2^o antibody (10 μ g/ml, 37°C, 30 min, see table 2.3), before being washed again and stored in 200 μ l wash solution protected from light.

Table 2.3: Antibodies used in the protein adsorption assay

Antibody	Additional information	Company
α C3c	FITC labeled rabbit anti-human C3c	Dako
α Fibrinogen	FITC labeled rabbit anti-human fibrinogen	Dako
Neg. Control	FITC labeled rabbit anti-mouse IgG	Dako
α FactorH	Sheep anti-human factor H	The Binding Site
α Factor I	Sheep anti-human factor I	The Binding Site
α Plasminogen	Sheep anti-human plasminogen	The Binding Site
α Vitronectin	Sheep anti-human vitronectin	The Binding Site
α HMW Kininogen	Sheep anti-human HMW Kininogen	The Binding Site
α Fibrinogen	Sheep anti-human fibrinogen	The Binding Site
α C1 inactivator	Sheep anti-human C1-i	The Binding Site
Neg. Control	Sheep IgG	Sigma-Aldrich
2 ^o Ab	CF 633 labeled donkey anti-sheep IgG	Sigma-Aldrich

The capsules were then observed in a confocal laser scanning microscope (CLSM). For FITC labeled antibodies, a 488 nm Argon laser was used to excite the fluorochromes, for the CF 633 labeled antibodies a HeNe 633 nm laser was used. Microscope settings are shown in table 2.4. Pictures were taken as optical cross sections through the equator using both laser and differential interference contrast (DIC), as well as z-stack 3D projections of the surface using only laser.

Table 2.4: Setting for the CLSM in the protein adsorption assay.

Laser	Argon (488 nm), HeNe (633 nm)
Objectives	C-Apochromat 10x/0.45W, C-Apochromat 40x/1.2W
Beamsplitters	HFT 488, HFT 633
Filters	BP 505-530, LP 650
Pinholes	200 μ m

2.7 Statistical methods

The Wilcoxon signed-rank test was used to define statistical differences in cytokine response between the different capsules in the whole blood assay. It was assumed that the data was not normally distributed due to the low sample numbers ($n=5$). The Wilcoxon signed-rank test is a non-parametric, statistical hypothesis test that can be used when comparing two matched samples to assess whether their population means differ. As there are biological differences between each blood donor in the whole blood assay, this kind of paired difference test was preferred. In addition, the test does not assume normally distributed populations as it is non-parametric. The software SPSS Statistics (v. 20, IBM) was used for statistical calculations. Differences were considered significant at $P < 0.05$.

3 RESULTS

3.1 Capsule diameters

In order to study how different alginate microcapsule parameters such as size, alginate type, and polycation, affected the biocompatibility of the capsules, a set of 21 different capsules were made, and their diameter was measured, see table 3.1. The capsules were alginate beads, APA solid capsules, and APA hollow capsules.

Table 3.1: Overview of the different alginate capsules made and tested. TAM4 capsules were made with a new type of UP-LVG alginate marked with a *. The diameter is given as the mean of 20 capsules. Capsules were made with 4 needles and with a flow of 10 ml/h unless otherwise stated.

Capsule type	Alginate	Polycation	Polyation concentration (%)	Needle size (mm)	Additional comments	Capsule diameter (μm)	% CV
APA hollow	M. pyr	PLL	0.10	0.40		683.0	10.3
APA hollow	M. pyr	PLL	0.14	0.40		645.0	8.8
APA hollow	M. pyr	PLO	0.14	0.40		651.5	7.4
APA solid	M. pyr	PLL	0.05	0.40		647.0	13.1
APA solid	M. pyr	PLL	0.10	0.40		588.5	9.0
APA solid	UP-LVG	PLL	0.05	0.40		566.0	7.9
APA solid	UP-LVG	PLL	0.10	0.40		572.0	3.8
APA solid	UP-LVG	PLL	0.05	0.35		573.0	7.0
APA solid	UP-LVG	PLL	0.10	0.35		554.0	4.7
APA solid	UP-LVG	PLL	0.05	0.35	No HEPES	619.5	9.6
TAM	UP-LVG	-	-	0.40	No BaCl ₂	545.0	4.9
TAM	UP-LVG	-	-	0.40		502.0	8.3
TAM	M. pyr	-	-	0.40		513.0	8.0
TAM4	UP-LVG*	-	-	0.40		483.5	12.0
TAM	UP-LVG	-	-	0.35	No BaCl ₂	435.0	4.9
TAM	UP-LVG	-	-	0.35		422.5	8.2
TAM	M. pyr	-	-	0.35		377.0	8.1
TAM4	UP-LVG*	-	-	0.35		427.5	7.8
TAM	UP-LVG	-	-	0.25	Single needle 6 ml/h	342.5	4.0
TAM	UP-LVG	-	-	0.35	Single needle 8 ml/h	477	6.7
TAM	UP-LVG	-	-	0.40	Single needle 8 ml/h	588.5	2.5

3.2 C3 and fibrinogen depositions on the capsule surface

To get a first indication of complement activation, capsules were stained for C3 adsorption on the surface. As protein C3 plays a central part of the complement system, being the most abundant of the complement proteins [27], it is a good indicator of potential activation of the cascade. The detected C3c fragment of the C3 molecule is present both in the native C3 form,

as well as in the active C3b form. Detected C3 may therefore indicate adsorption of either native C3, or active C3 and C5 convertase (C3bBb and C3b₂Bb). One APA capsule (0.1 % PLL, UP-LVG, 0.4 mm) and one TAM bead (UP-LVG, 0.4 mm) was incubated in human lepirudin anti-coagulated plasma overnight, and stained with fluorescent labeled antibody towards C3c, see figure 3.2. Capsules were also stained with antibodies toward fibrinogen to get an indication of possible interaction and activation of the coagulation cascade. C3 adsorption was detected on the APA capsule, but not on the TAM bead. No fibrinogen adsorption was detected except for on collapsed and deformed APA capsules. These collapsed capsules did not represent the general capsule population, but, as there were always some collapsed capsules present, a picture was included to show the often increased protein adsorption seen on these capsules. The staining was specific for C3 and fibrinogen as demonstrated by the negative controls.

Additionally, capsules were incubated in both lepirudin anti-coagulated plasma and whole blood in order to determine if there were any differences in protein deposits on the surface of the capsules in the presence of cells, see figure 3.1. No difference in C3 and fibrinogen adsorption was detected.

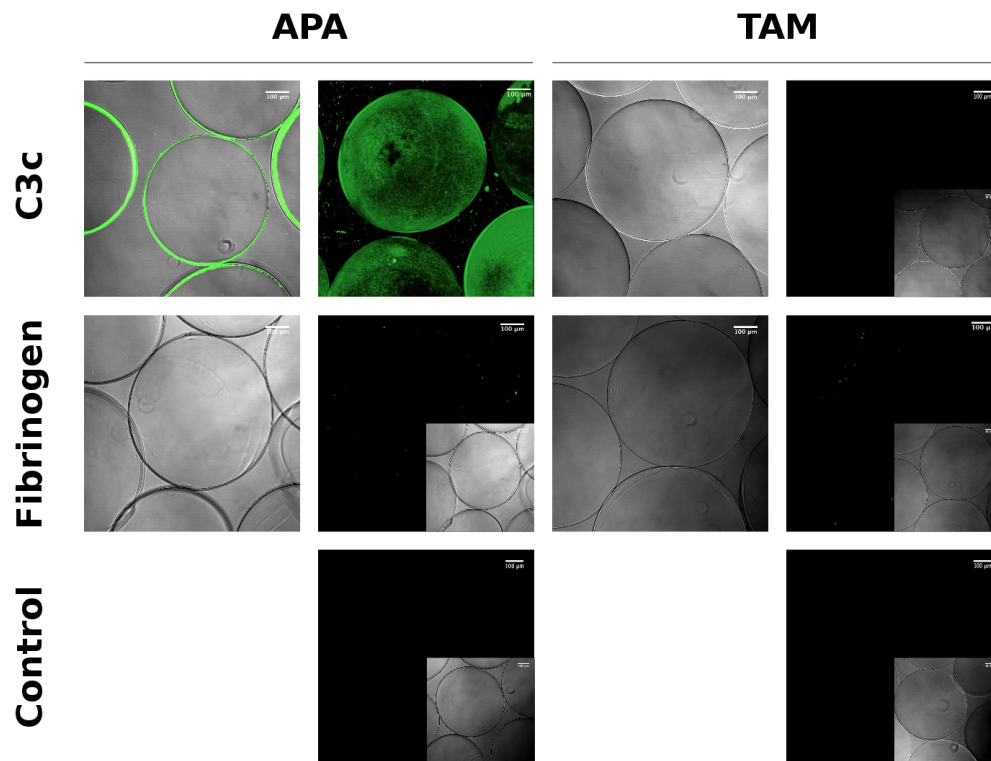


Figure 3.2: Protein adsorption on APA and TAM capsules after overnight incubation in plasma. Capsules were stained with FITC labeled rabbit α human C3c, rabbit α human fibrinogen, and rabbit α mouse IgG control antibody. Figures to the left and right of each column show optical sections through the equator and 3D projections, respectively.

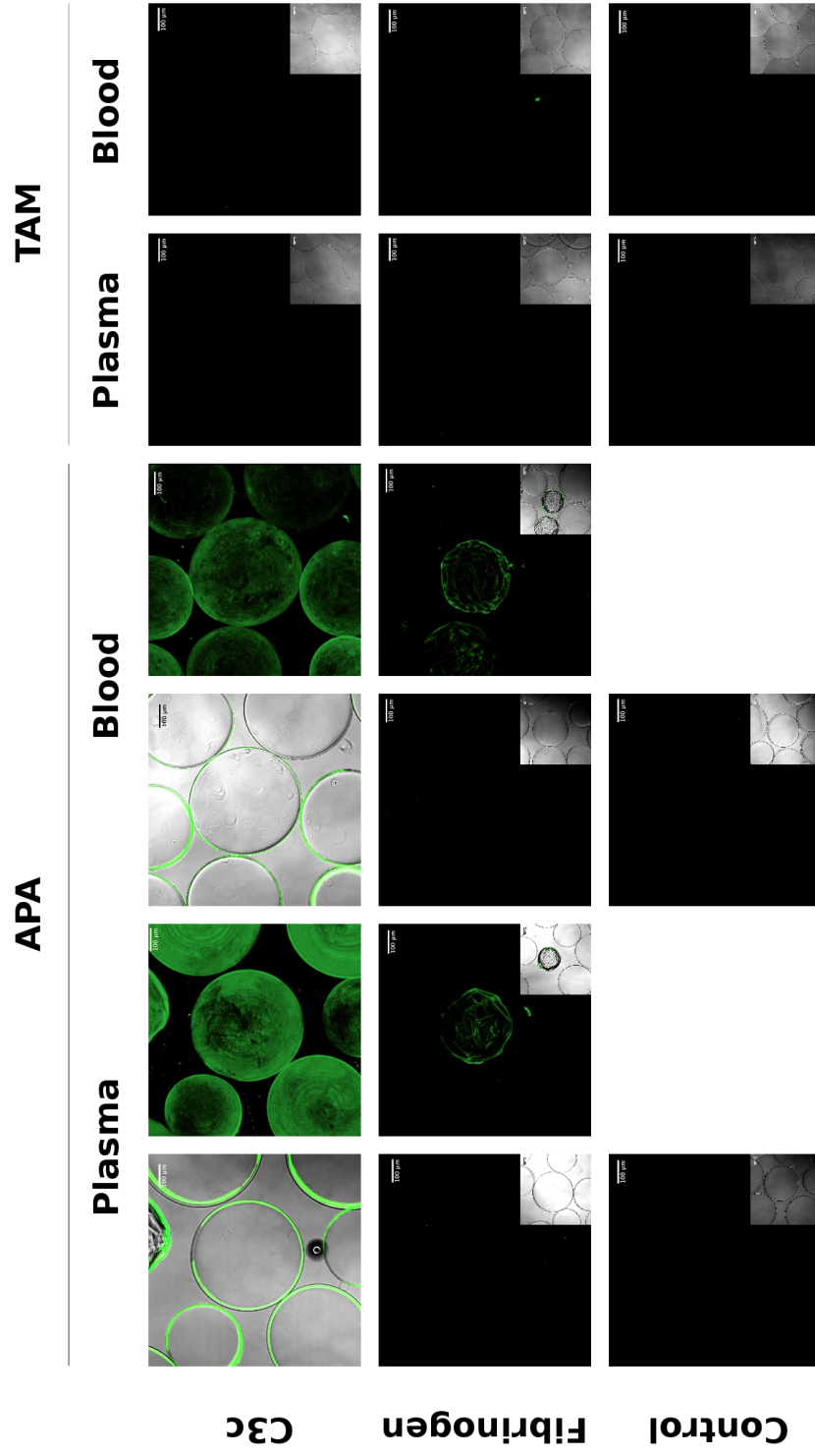
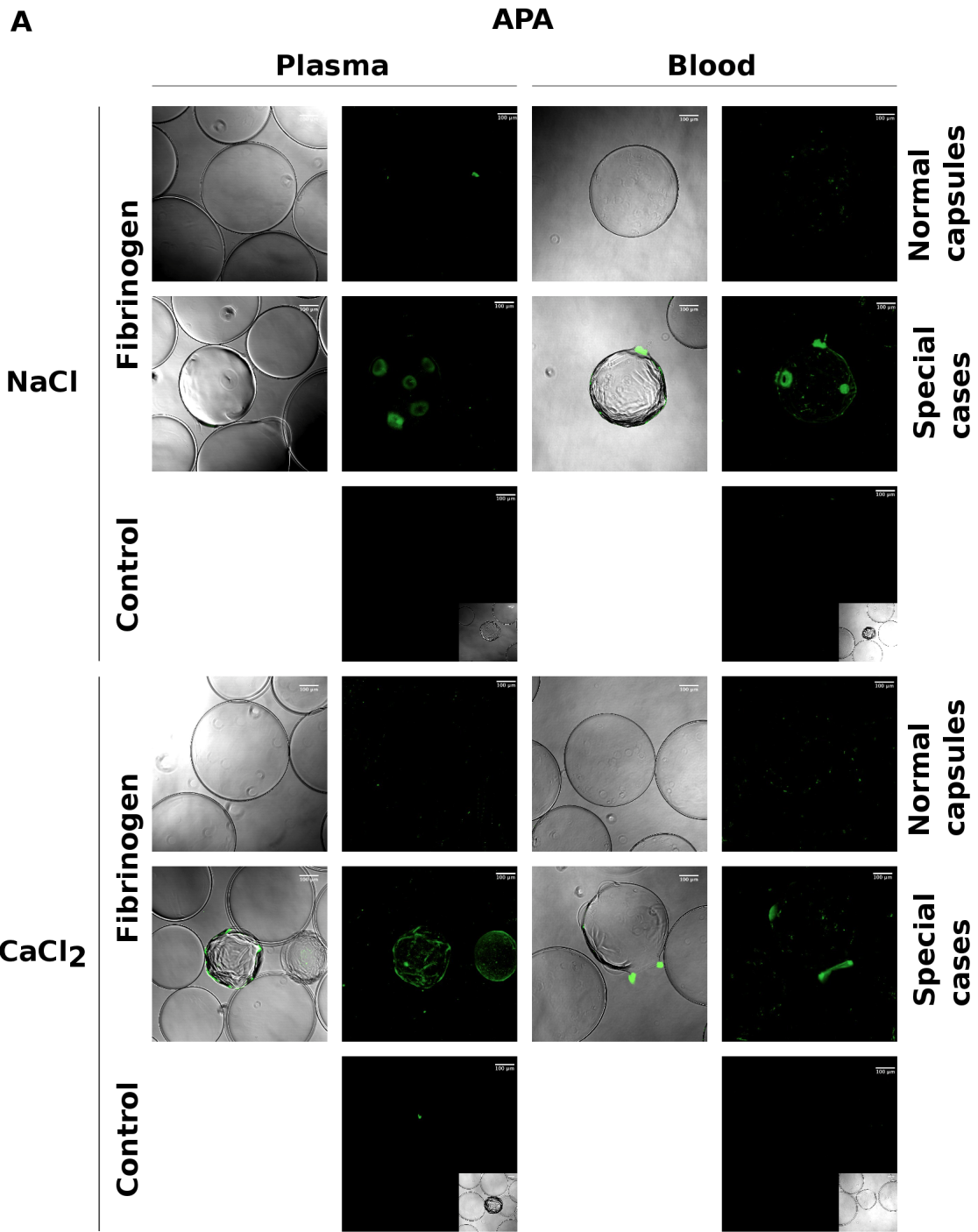


Figure 3.1: Protein adsorption on APA and TAM capsules after 6 hour incubation in plasma and in blood. Capsules were stained with FITC labeled rabbit anti-human C3c, rabbit anti-human fibrinogen, and rabbit anti-mouse IgG control antibody. Pictures are shown as either optical cross sections through the equator or 3D projections. Fibrinogen adsorption was only observed on shrunken and deformed APA capsules. However, no negative controls were included for these capsules, thus unspecific binding cannot be excluded.



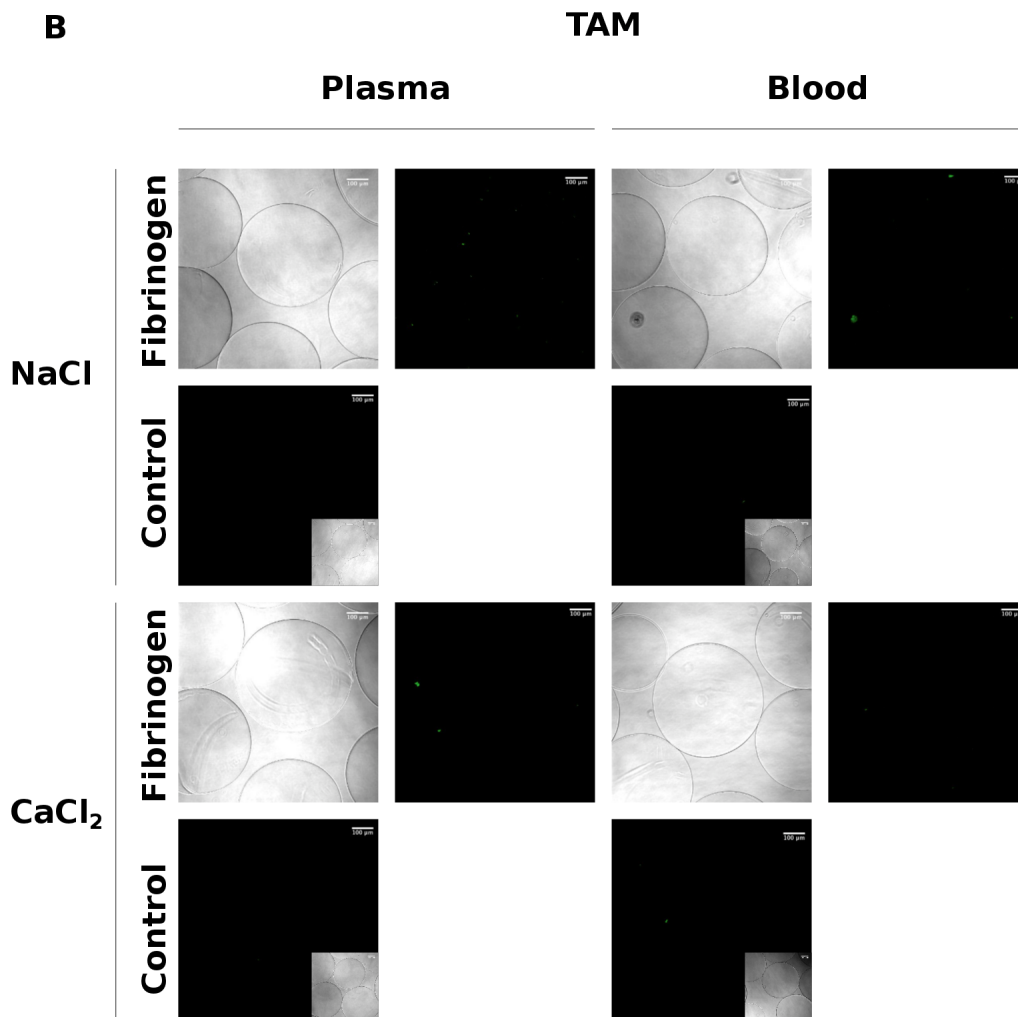


Figure 3.3: To determine if treatment with CaCl_2 would affect fibrinogen deposit, capsules washed in CaCl_2 and in NaCl were incubated for 6 hours in plasma and in blood. APA capsules are shown in figure A, while TAM capsules are shown in figure B. Capsules were stained with FITC labeled rabbit α human fibrinogen antibody, and rabbit α mouse IgG negative control antibody. Pictures of deformed capsules are shown for the APA capsules. These pictures do not represent the general capsule population, but are included as special cases. Only shrunk or damaged capsules display fibrinogen deposit with no apparent difference between CaCl_2 and NaCl treatment. Pictures are shown as optical sections through the equator and as 3D projections.

Finally, the effect on fibrinogen adsorption after treating the capsules with CaCl_2 are shown in figure 3.3. CaCl_2 treatment prevents the depletion of Ca^{2+} ions inside the capsule, and limits the ongoing dissolution of the polymer network, as Ca^{2+} ions are otherwise exchanged with Na^+ ions in the alginate polymer. But, as Ca^{2+} ions are involved in many of the steps in both the complement and the coagulation cascade, it was debated whether an increased presence of Ca^{2+} ions would affect the deposition of proteins on the capsule surface. No difference in fibrinogen adsorption between capsules stored in CaCl_2 and NaCl was observed.

3.3 Complement activation and leukocyte response

3.3.1 TCC response

Capsules were tested in the whole blood assay and incubated in lepirudin anti-coagulated whole blood for 1 hour and 4 hours. The plasma was obtained and analyzed for different cytokines as well as the terminal complement complex (sTCC). The formation of sTCC was measured after 1 hour and 4 hours, see figure 3.4. sTCC indicates activation of the complement cascade and is suggested to be the most sensitive and specific marker of complement activation. After 1 hour we could see a high increase in sTCC in APA hollow capsules, in some cases even as high as the positive control zymosan. These levels of sTCC was only observable for hollow APA with PLL, as the PLO capsule was at about the same level as the solid APA. After 4 hours we could still see a high response towards the hollow APA with PLL, but it would appear like the gap between hollow and solid APA was decreasing. An increase in PLL concentration resulted in a significant increase in sTCC levels, as shown in section 3.3.9. This corresponded with previous findings where PLL was observed to be sTCC stimulating and leukocyte activating [20]. TAM capsules showed a very low sTCC response which was also consistent with what has been observed earlier [20].

In order to see if the sTCC results could be reflected in C3 adsorption on the capsule surface, as well as to see how an increase in PLL concentration would affect the protein deposition, a set of different capsules was incubated in plasma for 4 hours. Moreover, the effect of replacing PLL with PLO was investigated, and if increasing TAM capsule size would affect the outcome. Figure 3.5 shows an increase in C3 adsorption with increasing PLL concentration. Pictures of 0.14 % PLO capsules should here be compared with pictures of 0.10 % PLL capsules, as 0.14 % PLO corresponded mole-wise to 0.10 % PLL with the PLO and PLL that was used in this work. The solid APA capsule appeared to have a much higher protein adsorption than did the hollow capsules. No adsorption could be seen on either TAM capsule. The high sTCC levels observed for hollow APA capsules with PLL could thus not be reflected in C3 adsorption on the capsule surface.

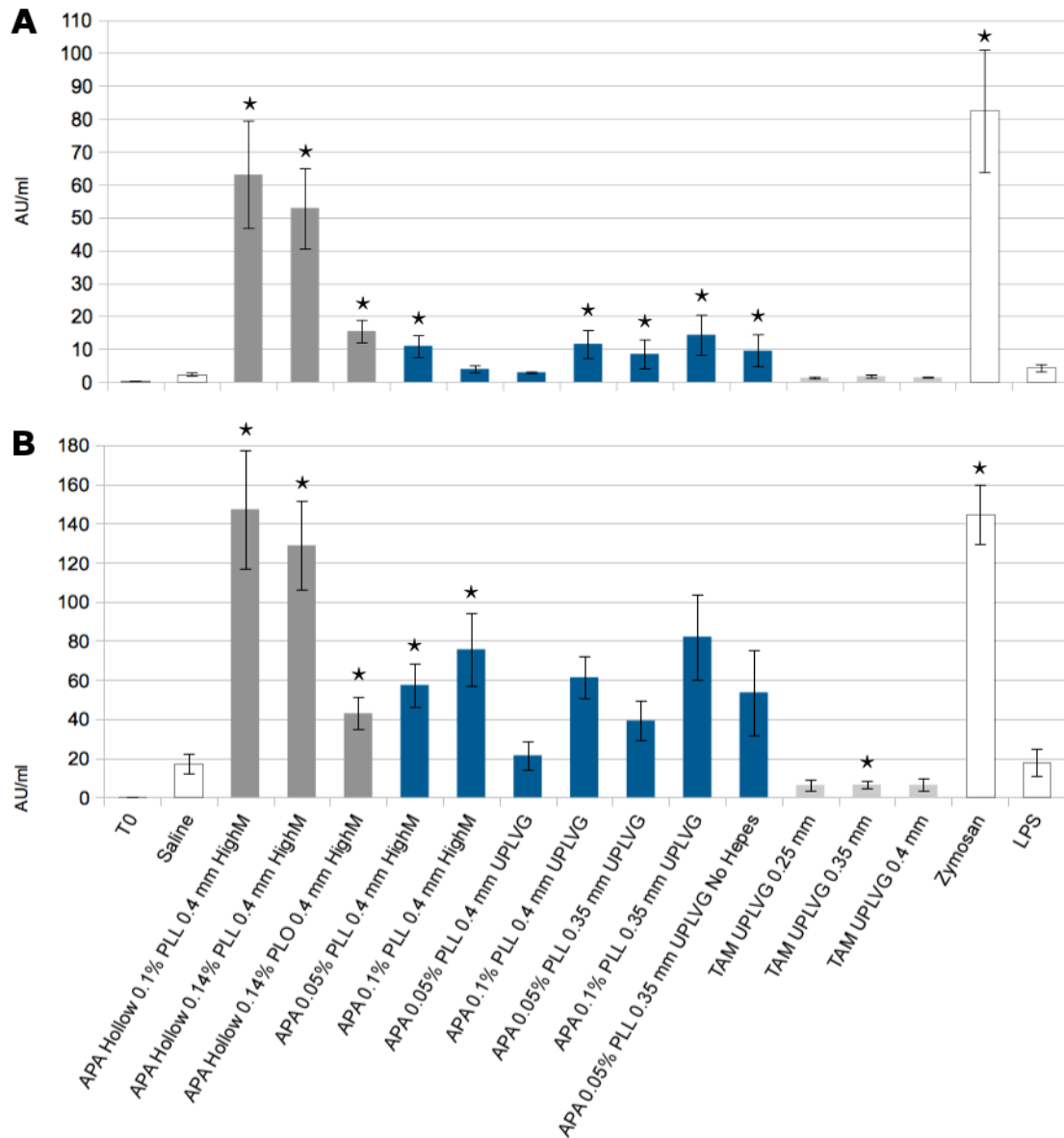
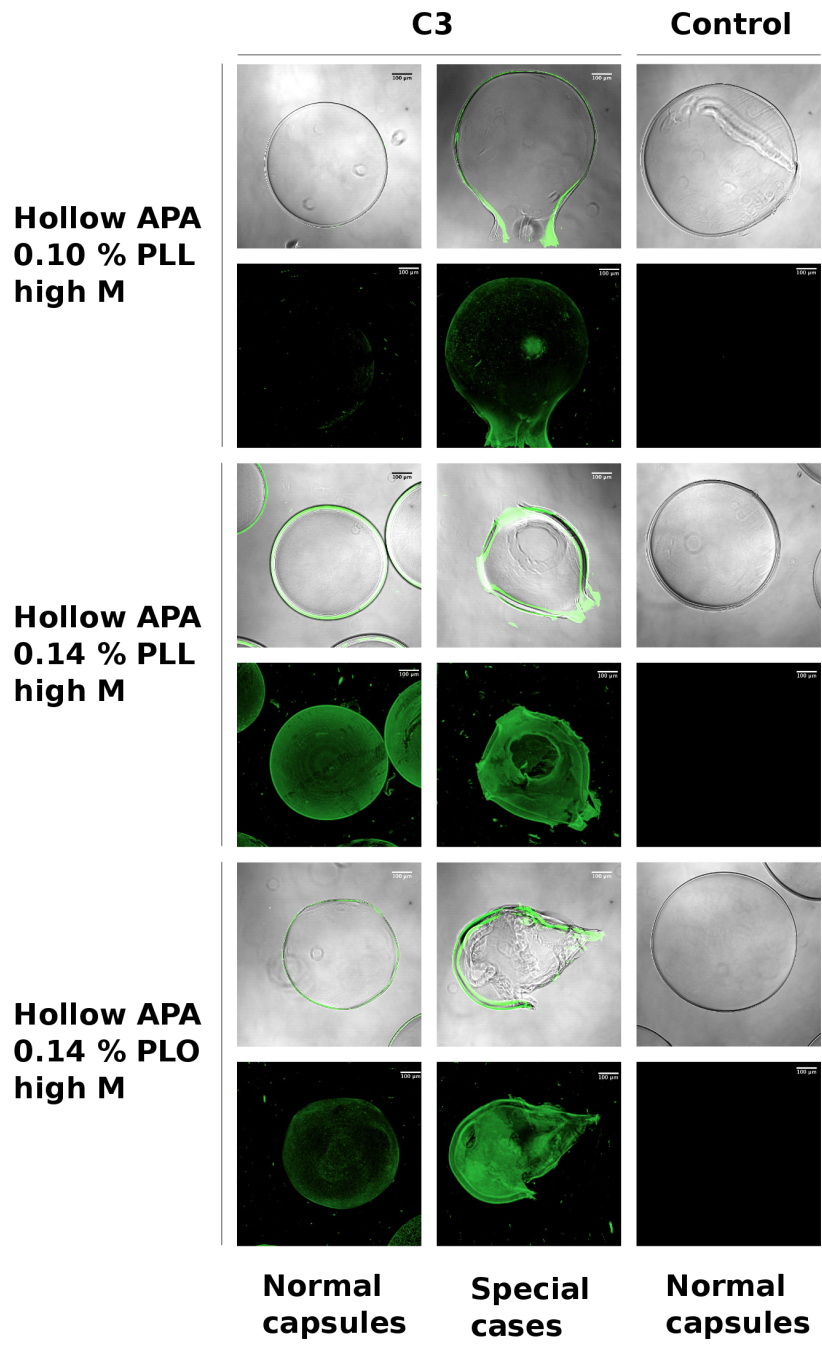


Figure 3.4: TCC after 1 hour (A) and 4 hours (B) incubation in whole blood. Data are expressed as means \pm SEM, $n = 5$ except for TAM UPLVG 0.25 mm and TAM UPLVG 0.4 mm, where $n = 4$. White bars are controls, grey bars are APA hollow capsules, blue bars APA solid, and light grey bars TAM capsules. Difference between saline and the other additives were considered statistically significant at $P < 0.05$ and marked with *. It should be noted that as the values of TAM UPLVG 0.25, 0.35, and 0.4 mm are similar, it is reasonable to assume that had $n = 5$ for TAM UPLVG 0.25 and 0.4 mm in B, they would also have been statistically significant towards saline.



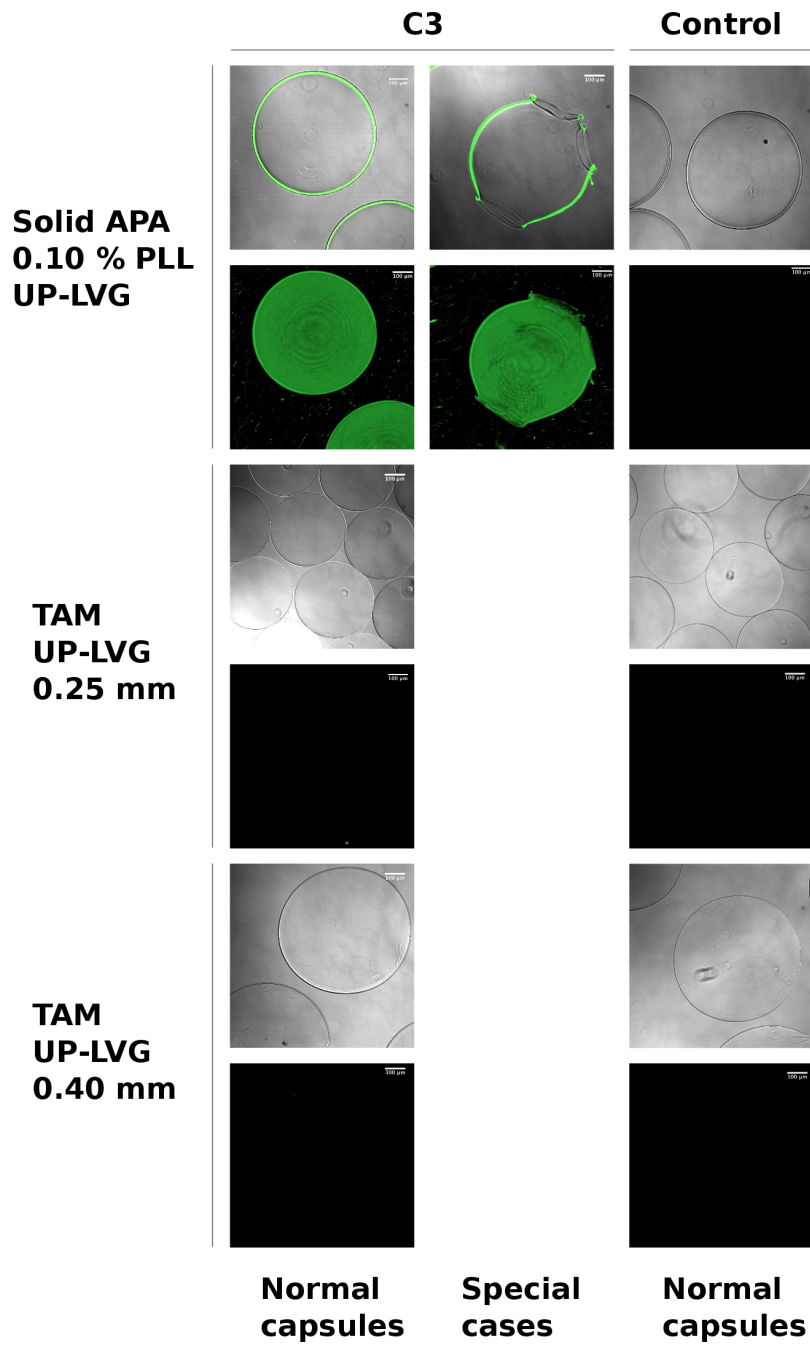


Figure 3.5: C3 adsorption on TAM capsules, and hollow and solid APA capsules, displayed as cross sections through the equator and as 3D projections. The same FITC labeled antibodies as described earlier were used. APA capsules were made with 0.40 mm needles. Pictures of the general capsule population are shown in the C3 left column, while broken capsules are shown in the C3 right column. The number of broken capsules was higher for 0.10 % PLL hollow APA than for 0.14 % PLL hollow APA

3.3.2 IL-8 response

The chemokine IL-8 was also measured after 1 hour and 4 hours, see figure 3.6. IL-8 is produced by macrophages, monocytes, epithelial cells and endothelial cells, but in the whole blood model monocytes are considered the main source of IL-8. IL-8 secretion is up-regulated when cells are activated, and functions as a pro-inflammatory molecule by inducing the chemotaxis of mainly neutrophil granulocytes to the site of inflammation. Figure 3.6A and B show the IL-8 response after 1 hour and 4 hours respectively. Significant difference between capsule and saline ($P < 0.05$) after 5 blood donors are shown. Because of a large deviation between different donors, especially after 1 hour incubation, it was not easy to see any clear-cut trends in the data, except that we could see a lower response for TAM capsules than APA capsules. In some cases the TAM capsules even gave a lower response than the saline control. After 4 hours, however, it appeared like the solid APA capsules gave a higher response than both hollow APA capsules and TAM capsules. In addition, the PLO capsule was the only APA capsule that was not significantly different from the saline control. In some donors, which was also observable in the mean after 1 hour, it appeared like increased PLL concentration gave an increased IL-8 response. However, in other donors the trend was the opposite.

3.3.3 Leukocyte activation as measure by CD11b expression

CD11b is an early activation marker of leukocytes, and is a receptor for inactivated C3b (iC3b). Expression of CD11b on granulocytes and monocytes was measured using flow cytometry 1 hour after addition of the capsules in the whole blood assay. Results from 3 donors are shown in figure 3.7. Individual donor comparisons of CD11b expression, sTCC generation, and IL-8 secretion are shown in appendix B. TAM capsules appeared to be less activating than APA, and in some cases also less activating than the saline negative control, which was in accordance with earlier observations [20]. However, not enough data was gathered to be able to say anything about the statistical significance of the differences. No difference between hollow APA and solid APA could be observed, but it looked like PLO capsules gave a slightly lower CD11b expression than PLL. Higher PLL concentration appeared to give a higher response for capsules with UPLVG (high G) alginate, and either no difference, or a lower response for increasing PLL concentration in capsules with high M alginate. This trend was also observed in sTCC levels after 1 hour. More data have to be gathered to be able to determine any significant difference between the capsules.

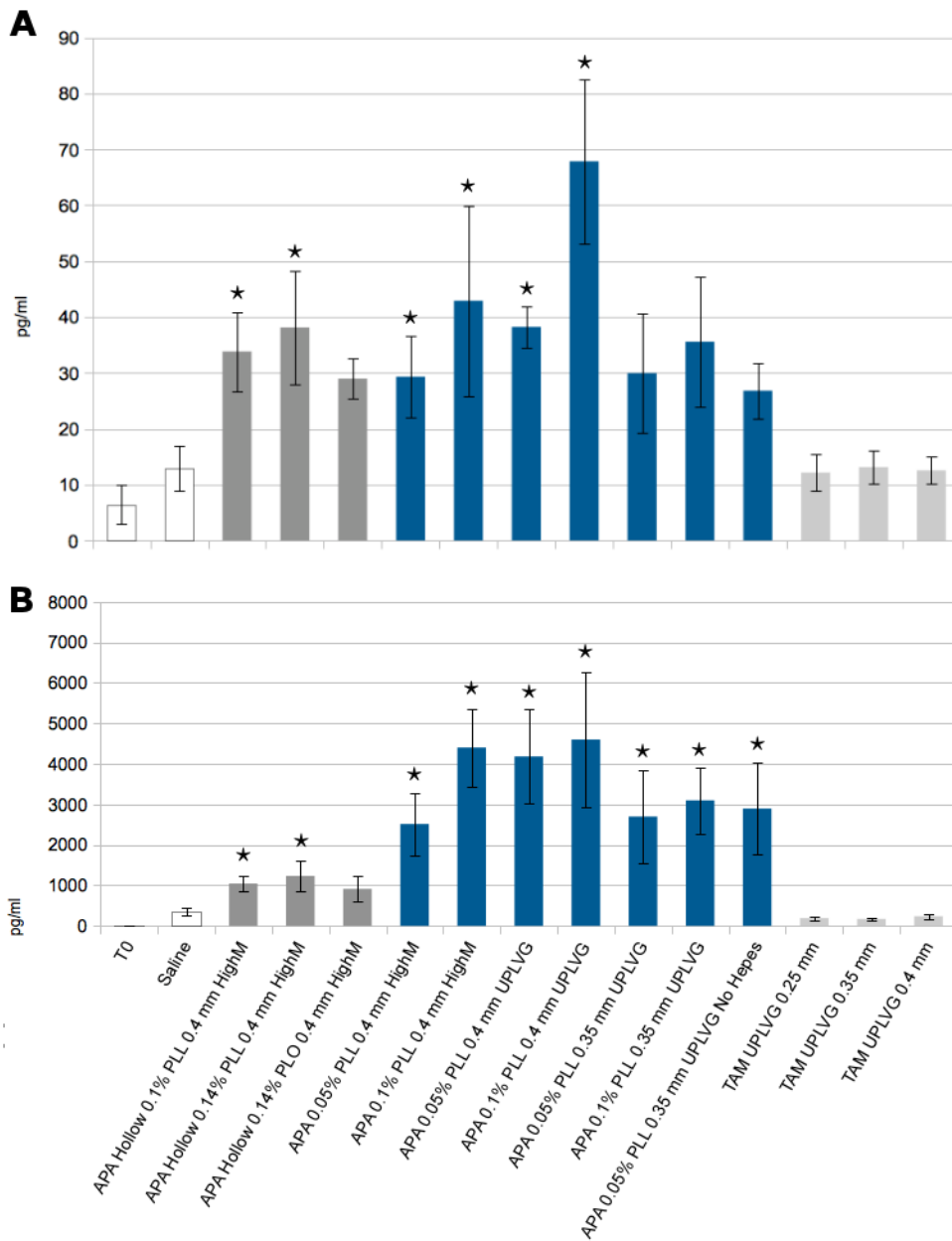


Figure 3.6: IL-8 after 1 hour (A) and 4 hours (B) incubation in whole blood. Data are expressed as means \pm SEM, $n = 5$ except for TAM UPLVG 0.25 mm and TAM UPLVG 0.4 mm, where $n = 4$. White bars are controls, grey bars are APA hollow capsules, blue bars APA solid, and light grey bars TAM capsules. Zymosan values for IL-8 after 1 and 4 hours are 349.8 ± 57.9 pg/ml and 9214.7 ± 1458.0 pg/ml respectively. Differences between saline and the other additives are considered statistically significant at $P < 0.05$ and marked with *.

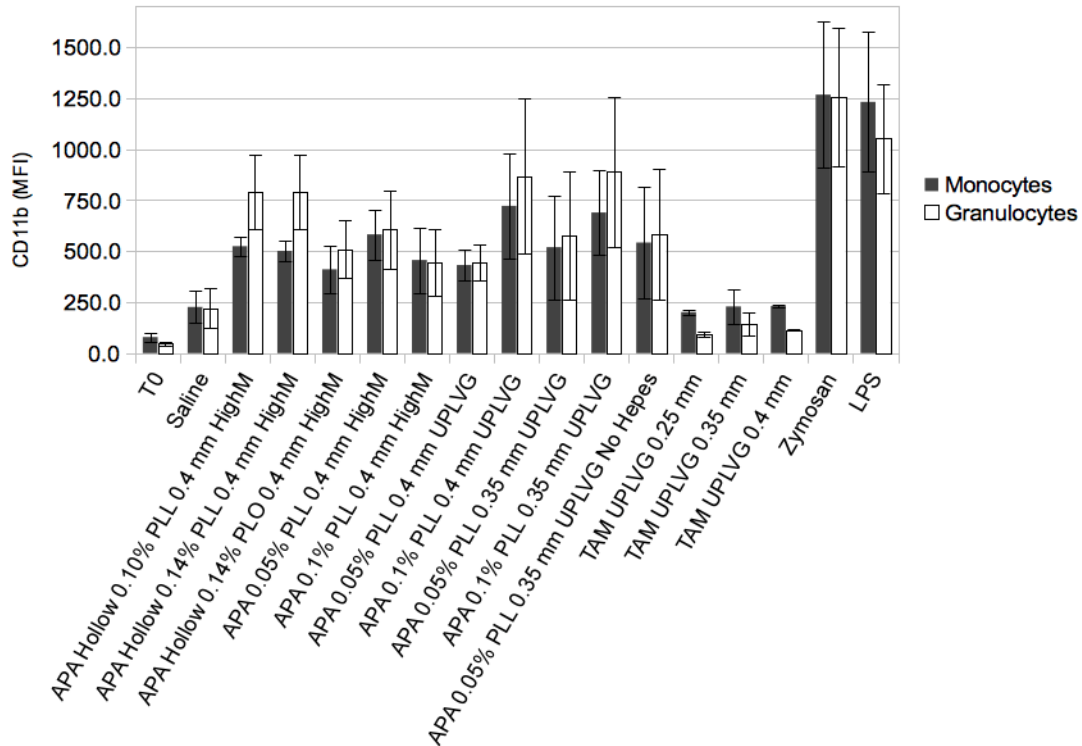


Figure 3.7: Leukocyte CD11b expression after 1 hour incubation in lepirudin anti-coagulated whole blood. Data is expressed as means \pm SEM, n = 3. CD11b expression was measured as median fluorescence intensity (MFI) on monocytes and granulocytes.

3.3.4 Chemokines

It was also screened for a set of different chemokines, cytokines, and growth factors, using a multiplex assay. This was only performed on whole blood after 4 hours incubation with capsules. A similar, although not as defined, picture as sTCC was observed for MCP-1, figure 3.8. Hollow APA capsules with PLL gave a stronger response than hollow APA capsules with PLO, and solid APA. Additionally, a lower response was observed for increasing PLL concentration for capsules with high M alginate, as was also observed in the up-regulation of CD11b. TAM capsules gave a weak response. MIP-1 α levels showed a clear increase for solid APA capsules with hollow APA capsules at the same level as TAM capsules, and only slightly higher than the saline control. These levels reflected the increased IL-8 response for solid APA capsules as shown earlier. For MIP-1 α , as was also the case for IL-8, it was hard to detect any effect of increasing PLL concentration, alginate type, or capsule diameter.

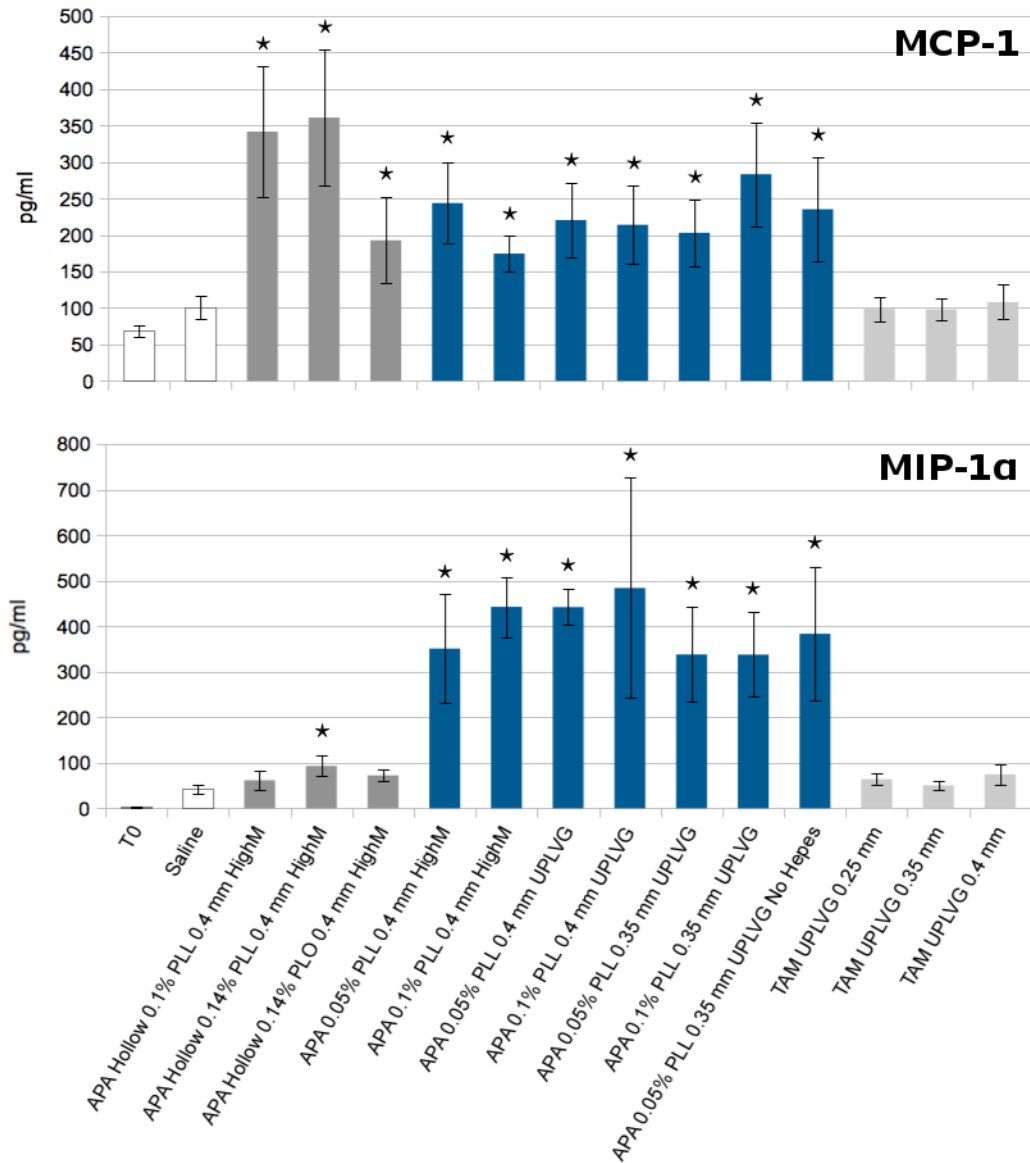


Figure 3.8: MCP-1 (A) and MIP-1 α (B) after 4 hours incubation in whole blood. Data are expressed as means \pm SEM, n = 5 except for TAM UPLVG 0.25 mm and TAM UPLVG 0.4 mm, where n = 4. White bars are controls, grey bars are APA hollow capsules, blue bars APA solid, and light grey bars TAM capsules. Zymosan values for MCP-1 and MIP-1 α are 229 \pm 54 pg/ml and 2986 \pm 345 pg/ml respectively. Difference between saline and the other additives are considered statistically significant at P<0.05 and marked with *.

3.3.5 Inflammatory cytokines

The inflammatory cytokine IL-6 showed a small increase in response to solid APA capsules, compared with the other capsule types, see figure 3.9. This increase was even more apparent in

IL-1 β and TNF α levels, figure 3.10. No apparent effect of PLL concentration, alginate type, or capsule diameter, could be observed. These cytokines, along with IL-6, are produced by among other the monocytes in the blood, and increased levels of these cytokines indicate an activation of the cells secreting them. However, it should be noted that all three cytokines showed a very low response compared to the positive control zymosan, which had cytokine levels several magnitudes higher than the other additives.

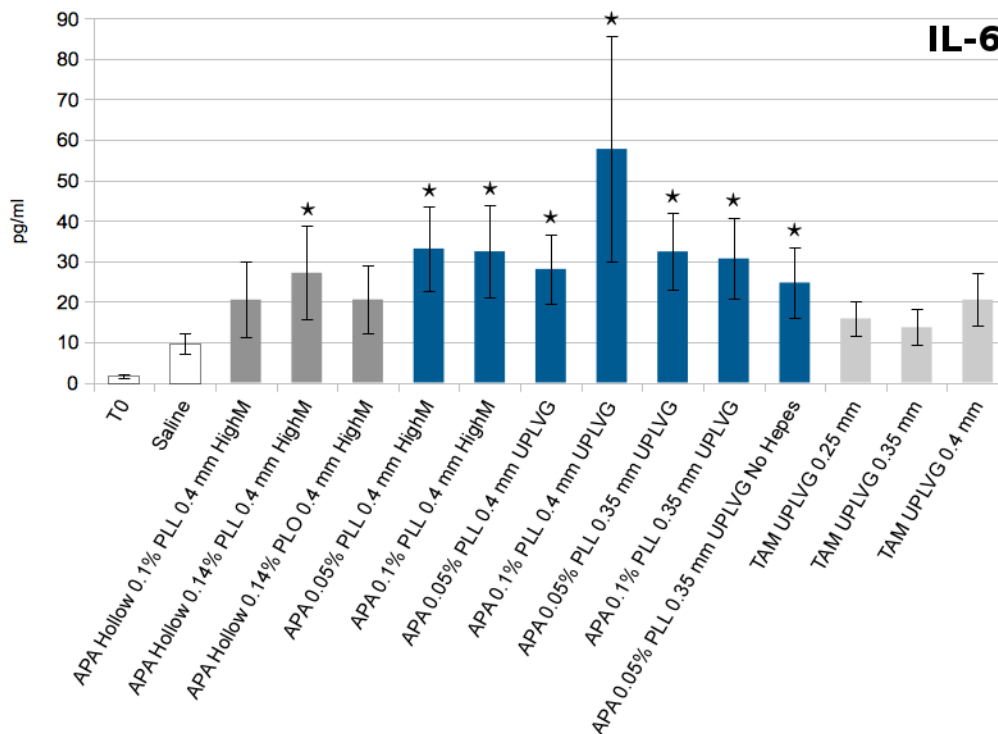


Figure 3.9: IL-6 after 4 hours incubation in whole blood. Data are expressed as means \pm SEM, $n = 5$ except for TAM UPLVG 0.25 mm and TAM UPLVG 0.4 mm, where $n = 4$. White bars are controls, grey bars are APA hollow capsules, blue bars APA solid, and light grey bars TAM capsules. Zymosan response is 9081 ± 1616 pg/ml. * $P < 0.05$.

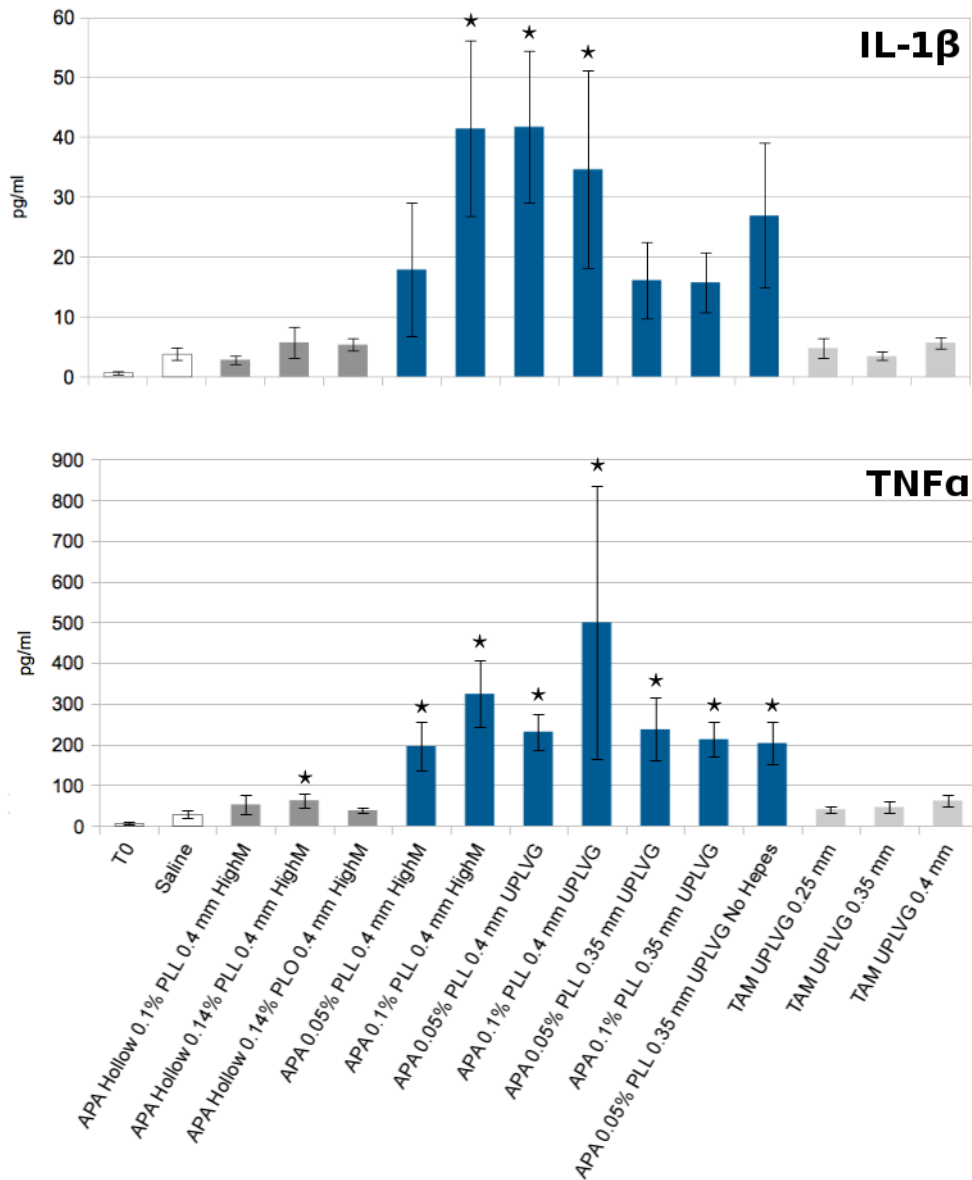


Figure 3.10: IL-1 β and TNF α after 4 hours incubation in whole blood. Data are expressed as means \pm SEM, n = 5 except for TAM UPLVG 0.25 mm and TAM UPLVG 0.4 mm, where n = 4. White bars are controls, grey bars are APA hollow capsules, blue bars APA solid, and light grey bars TAM capsules. Zymosan values for IL-1 β and TNF α are 1960 \pm 338 pg/ml and 12724 \pm 3036 pg/ml respectively. *P<0.05.

3.3.6 Anti-inflammatory cytokines

The anti-inflammatory cytokine IL-1RA showed a small increase for solid APA capsules, figure 3.11. No such increase could be observed for IL-10. Standard deviations were however quite big between the different donors.

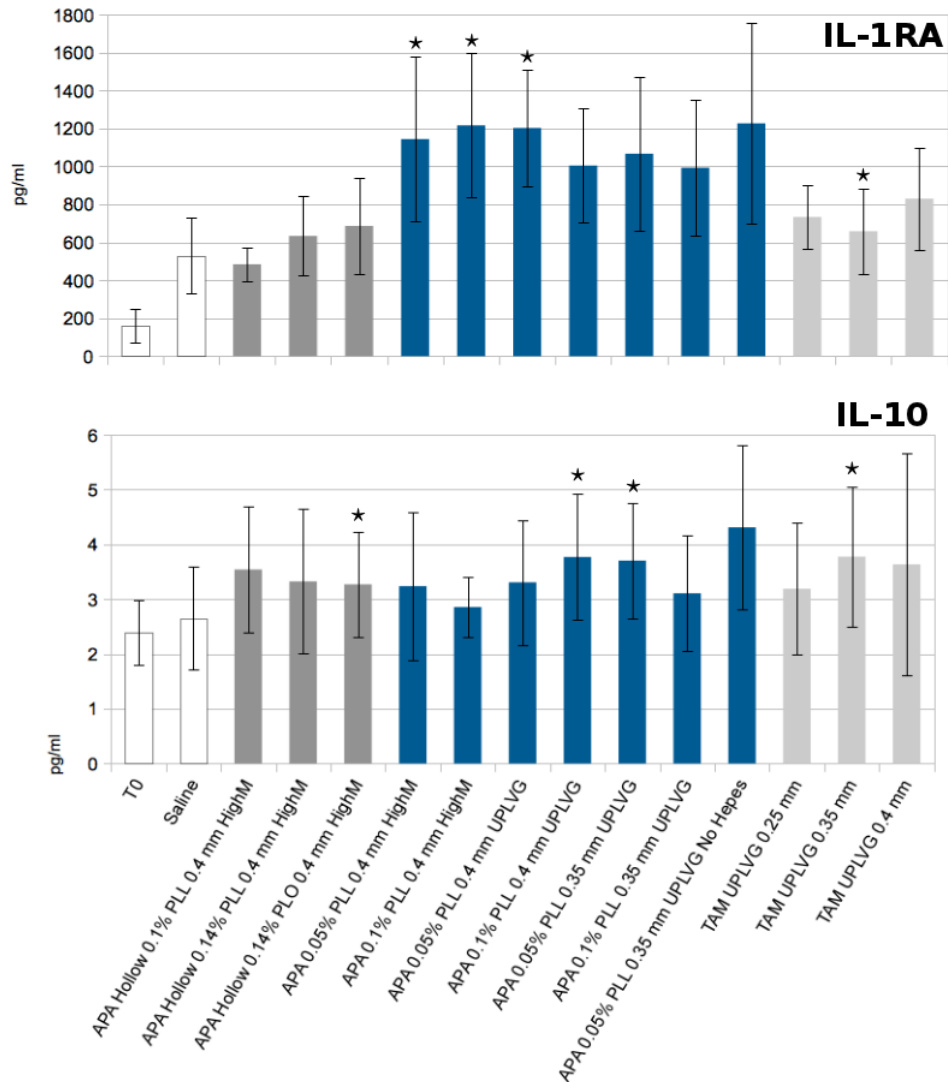


Figure 3.11: IL-1RA and IL-10 after 4 hours incubation in whole blood. Data are expressed as means \pm SEM, $n = 5$ except for TAM UPLVG 0.25 mm and TAM UPLVG 0.4 mm, where $n = 4$. White bars are controls, grey bars are APA hollow capsules, blue bars APA solid, and light grey bars TAM capsules. Zymosan values for IL-1RA and IL-10 are 1400 ± 473 pg/ml and 8.6 ± 1.3 pg/ml respectively. * $P < 0.05$.

3.3.7 Growth factors

As for the growth factors, a small increase in response to solid APA capsules and TAM capsules could be observed for PDGF-BB, figure 3.12. An increase in HGF levels in response to solid APA capsules was also observed, accompanied by a decrease in levels for TAM capsules below the saline control. VEGF levels showed yet again an increase in response towards solid capsules, with hollow APA capsules and TAM capsules at about the same level as the saline control, figure

3.13.

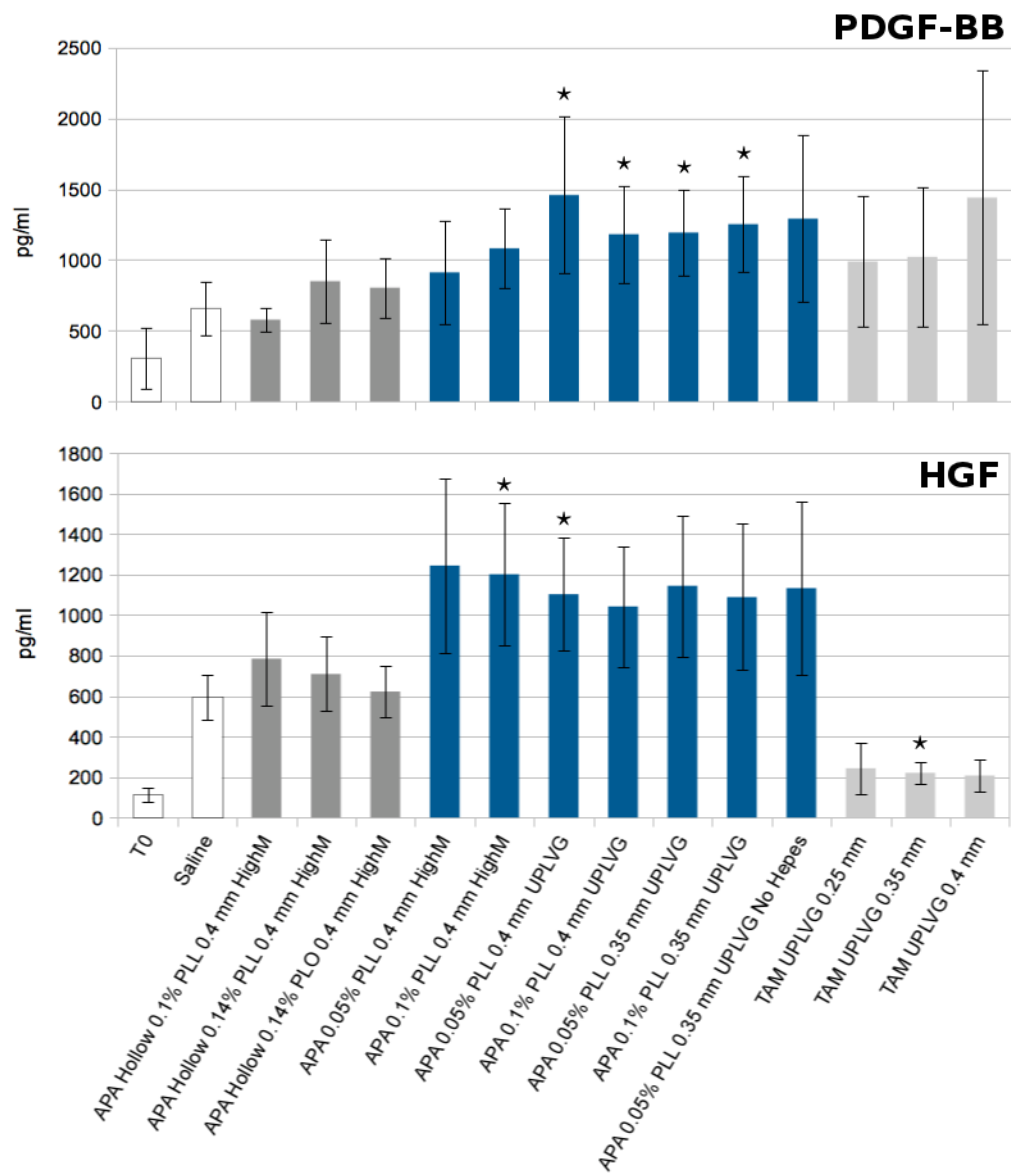


Figure 3.12: PDGF-BB and HGF after 4 hours incubation in whole blood. Data are expressed as means \pm SEM, $n = 5$ except for TAM UPLVG 0.25 mm and TAM UPLVG 0.4 mm, where $n = 4$. White bars are controls, grey bars are APA hollow capsules, blue bars APA solid, and light grey bars TAM capsules. Zymosan values for PDGF-BB and HGF are 1479 ± 416 pg/ml and 1246 ± 299 pg/ml respectively. * $P < 0.05$.

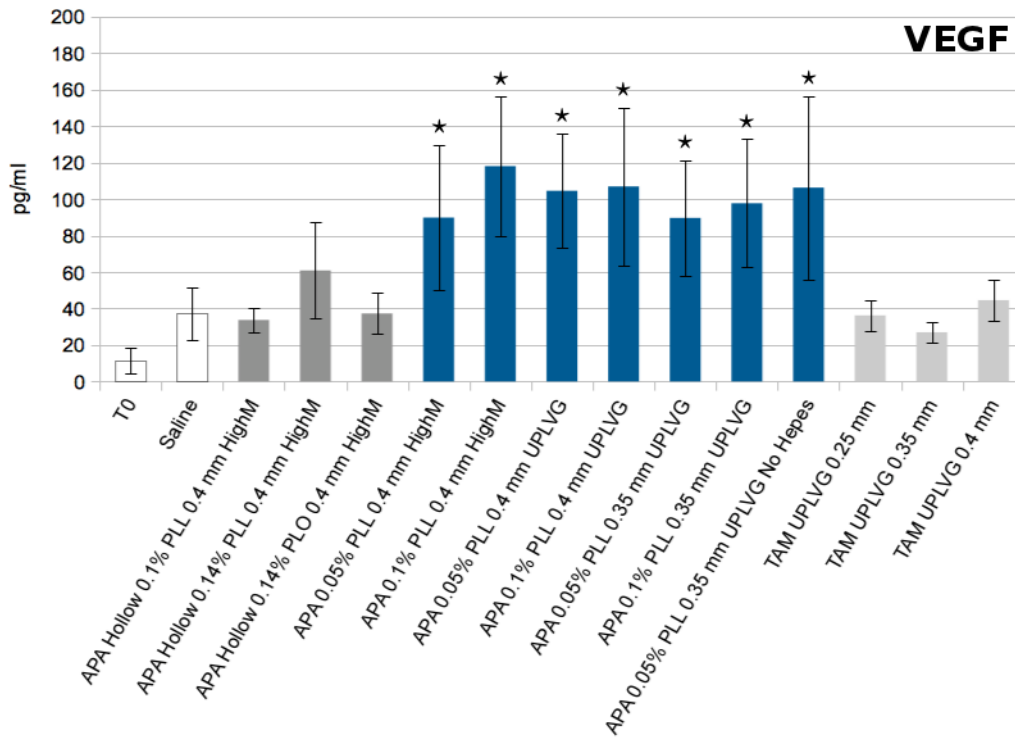


Figure 3.13: VEGF after 4 hours incubation in whole blood. Data are expressed as means \pm SEM, $n = 5$ except for TAM UPLVG 0.25 mm and TAM UPLVG 0.4 mm, where $n = 4$. White bars are controls, grey bars are APA hollow capsules, blue bars APA solid, and light grey bars TAM capsules. Zymosan value for VEGF is 55 ± 24 pg/ml. * $P < 0.05$.

3.3.8 MIF, IP-10, IFN- γ , and RANTES

MIF levels were higher for TAM capsules than seen before, at about the same level as APA capsules. IP-10 levels showed an opposite trend of what was seen for many of the other cytokines, with lower levels for solid APA, and higher levels for TAM capsules, figure 3.14. Lastly, IFN- γ and RANTES levels showed no apparent difference between additives and the saline control, figure 3.15.

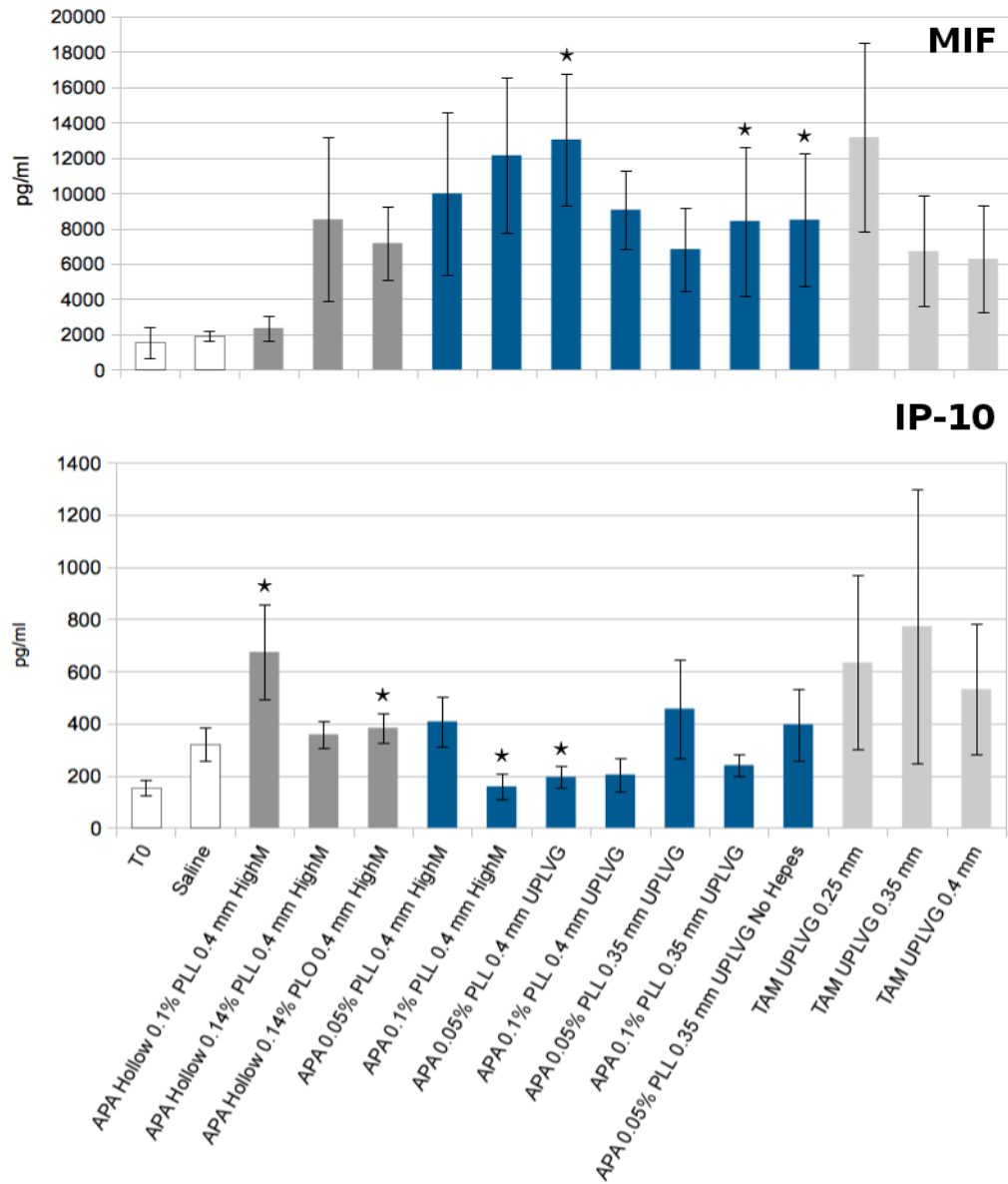


Figure 3.14: MIF and IP-10 after 4 hours incubation in whole blood. Data are expressed as means \pm SEM, $n = 5$ except for TAM UPLVG 0.25 mm and TAM UPLVG 0.4 mm, where $n = 4$. White bars are controls, grey bars are APA hollow capsules, blue bars APA solid, and light grey bars TAM capsules. Zymosan values for MIF and IP-10 are 6451 ± 2356 pg/ml and 1221 ± 157 pg/ml respectively. * $P < 0.05$.

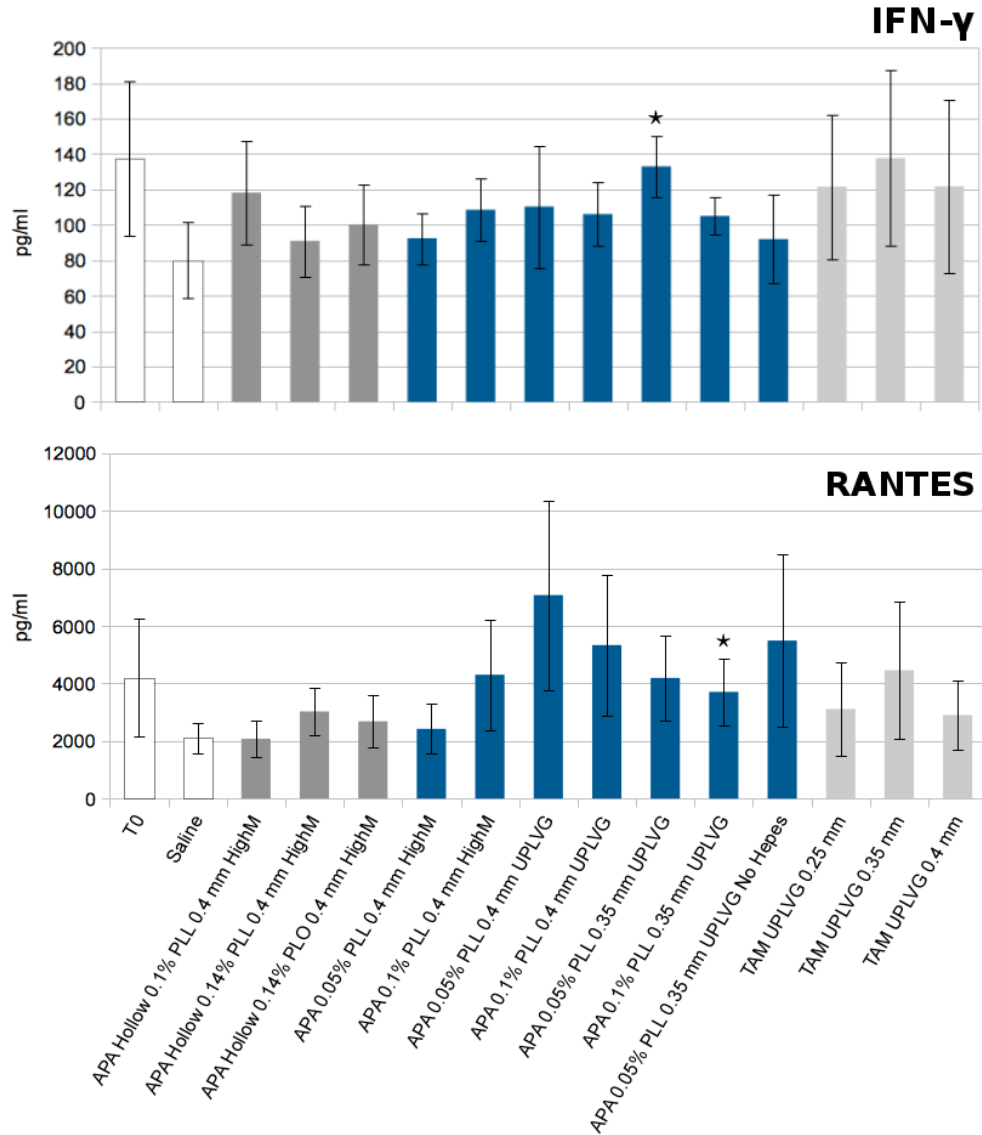


Figure 3.15: IFN- γ and RANTES after 4 hours incubation in whole blood. Data are expressed as means \pm SEM, n = 5 except for TAM UPLVG 0.25 mm and TAM UPLVG 0.4 mm, where n = 4. White bars are controls, grey bars are APA hollow capsules, blue bars APA solid, and light grey bars TAM capsules. Zymosan values for IFN- γ and RANTES are 140 ± 14 pg/ml and 7080 ± 2980 pg/ml respectively. *P<0.05.

3.3.9 Statistical analysis

Performing statistical analyses on the data showed no significant difference between the TAM capsules for any molecule measured, see table 3.2 and 3.3. Thus a change in capsule diameter between approximately 300 and 600 μ m did not affect the biocompatibility of the capsules, as measured by cytokine, chemokine, growth factor and sTCC levels. Comparing hollow and solid

APA capsules after 4 hours of incubation in whole blood, a significantly higher sTCC and MCP-1 response was seen for hollow capsules with PLL, while a significantly lower response was seen for the same capsules in chemokine levels (except MCP-1) and in inflammatory cytokine levels. No difference was seen in anti-inflammatory cytokines or growth factors except for VEGF which was also lower for hollow capsules. Looking at increasing PLL concentration, a higher response was detected in some cases but not all. Especially sTCC formation seemed to be affected by this, but also some chemokines and inflammatory cytokines gave a significant increase in response to higher concentration. Choice of polycation appeared to be of importance for sTCC and MCP-1 responses as a significantly lower response was detected for these molecules when PLO was used in the hollow capsules instead of PLL. A significant difference was also observed in IP-10 and IL-1 β levels for PLO versus PLL. Looking at alginate type, high M *M.pyr* alginate or high G UP-LVG alginate, differences in chemokine levels, cytokine levels, and growth factor levels could not be observed, with exceptions in IP-10, IL-8, and RANTES levels in some cases, see table 3.2 and 3.3. sTCC levels appeared to be lower for UP-LVG alginate when 0.05 % PLL was used, something that might be coupled with the increased stability conferred by the high G alginate. Finally, the addition of HEPES in the gelling solution did not significantly affect TCC, chemokine, cytokine, or growth factor responses.

Table 3.3: Significant differences between cytokine responses for the different capsules. All molecules were analyzed after 4 hours of incubation in whole blood.

	IL-1RA	IL-10	PDGF	HGF	VEGF	IFN- γ	RANTES
APA hollow, High M							
0.10 % PLL, 0.4 mm v	0.14 % PLL, 0.4 mm	No	No	No	No	No	No
APA hollow, High M							
0.10 % PLL, 0.4 mm v	0.14 % PLO, 0.4 mm	No	No	No	No	No	No
APA hollow, High M							
0.10 % PLL, 0.4 mm v	0.10 % PLL, 0.4 mm	No	No	No	Yes	No	No
APA solid, High M							
0.05 % PLL, 0.4 mm v	0.10 % PLL, 0.4 mm	No	No	No	Yes	No	No
APA solid, UP-LVG							
0.05 % PLL, 0.4 mm v	0.10 % PLL, 0.4 mm	Yes	No	No	No	No	No
APA solid, UP-LVG							
0.05 % PLL, 0.35 mm v	0.10 % PLL, 0.35 mm	No	Yes	No	No	No	No
APA solid, High M							
0.05 % PLL, 0.4 mm v	0.05 % PLL, 0.4 mm	No	No	No	No	No	Yes
APA solid, High M							
0.10 % PLL, 0.4 mm v	0.10 % PLL, 0.4 mm	No	No	No	No	No	No
APA solid, UP-LVG							
0.05 % PLL, 0.4 mm v	0.05 % PLL, 0.35 mm	No	No	No	No	No	No
APA solid, UP-LVG							
0.10 % PLL, 0.4 mm v	0.10 % PLL, 0.35 mm	No	No	No	No	No	No
APA solid, UP-LVG							
0.05 % PLL, 0.35 mm v	0.05 % PLL, 0.35 mm	No	No	No	No	No	No
APA solid, UP-LVG							
0.10 % PLL, 0.4 mm v	0.10 % PLL, 0.40 mm	No	No	No	No	No	No
APA solid, UP-LVG							
0.05 % PLL, 0.35 mm v	0.05 % PLL, 0.35 mm	No	No	No	No	No	No
TAM UP-LVG 0.25 mm v	TAM UP-LVG 0.35 mm	No	No	No	No	No	No
TAM UP-LVG 0.25 mm v	TAM UP-LVG 0.40 mm	No	No	No	No	No	No
TAM UP-LVG 0.35 mm v	TAM UP-LVG 0.40 mm	No	No	No	No	No	No

3.4 Leukocyte response towards TAM capsules

Alginate type, and the presence of BaCl_2 in the making of the TAM capsules was then investigated. Eight different TAM capsules were tested in 2 donors, together with two APA capsules, and the plasma was analyzed after 4 hours. The results of these 2 donors should be taken as no more than a preliminary indication of the biocompatibility of the different capsules. No statistical significance can be obtained from such a small data set.

3.4.1 Chemokines

It was analyzed for the same molecules on the different TAM capsules as on the first capsule set. The findings suggested a minimal stimulatory effect of the TAM capsules. MCP-1 levels showed an overall low response towards the different TAM capsules, with levels lower than APA capsules, and slightly lower than the saline control. Capsules gelled in the absence of BaCl_2 appeared to give a higher response than capsules gelled in with BaCl_2 . Also, capsules with the new type of UP-LVG alginate (UP-LVG*, TAM4 capsules) appeared to give a slightly lower response, however, since the levels were so close to the negative controls and it was only taken from two donors, no significant results could be concluded. Whole blood from more donors would have to be tested. For the chemokines MIP-1 α and IL-8 the picture was similar to what had been observed before, with overall low levels, slightly higher without BaCl_2 in the gelling solution, and a concomitant low response for UP-LVG* capsules, figures 3.17 and 3.18.

3.4.2 Inflammatory cytokines

As for the inflammatory cytokines, IL-1 β showed a lower response toward TAM capsules than the saline control, figure 3.19. TAM4 capsules appeared again to give a slightly lower response. For TNF α and IL-6, the detected levels were at or slightly higher than the saline control, figures 3.20 and 3.21.

3.4.3 Anti-inflammatory cytokines

The anti-inflammatory cytokines IL-1RA and IL-10 were at the same levels for TAM capsules as had been seen before, with yet again a somewhat lower response towards TAM4 capsules, showing a similar picture as for the inflammatory cytokines, see figures 3.22 and 3.23.

3.4.4 Growth factors

The growth factors PDGF-BB, HGF, and VEGF were also analyzed and are shown in figures 3.24, 3.25, and 3.26. The same trends could be observed here, as was seen for the other molecules.

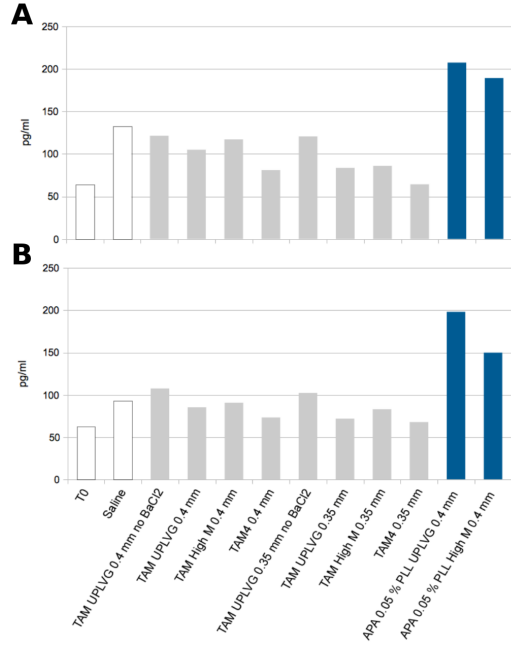


Figure 3.16: MCP-1 results after 4 hour incubation in whole blood for donor 1 (A) and donor 2 (B). Zymosan values are 119 pg/ml and 179 pg/ml for A and B respectively.

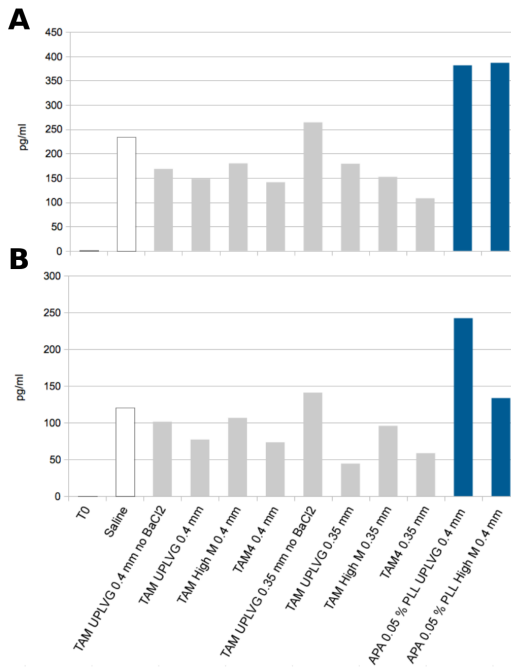


Figure 3.17: MIP-1α results after 4 hour incubation in whole blood for donor 1 (A) and donor 2 (B). Zymosan values are 2427 pg/ml and 2660 pg/ml for A and B respectively.

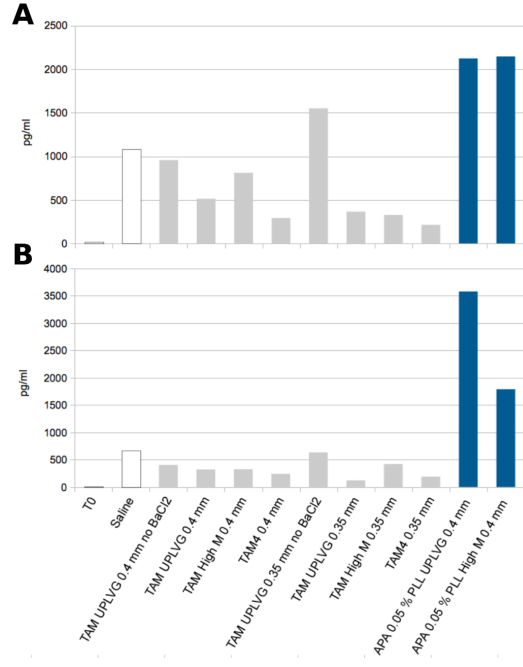


Figure 3.18: IL-8 results after 4 hour incubation in whole blood for donor 1 (A) and donor 2 (B). Zymosan values are 4879 pg/ml and 5843 pg/ml for A and B respectively.

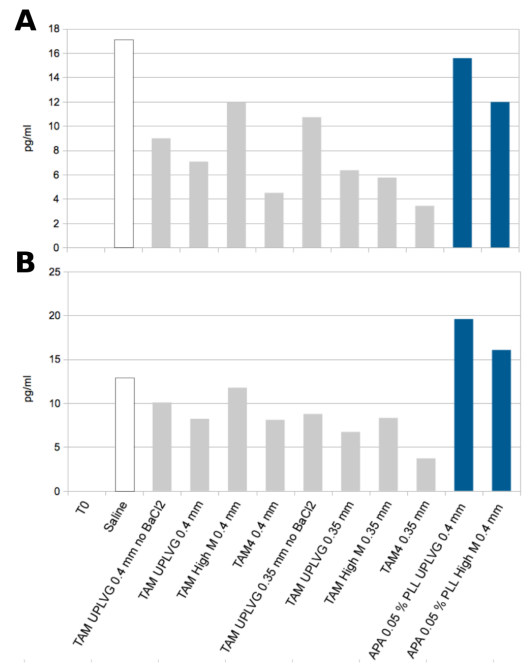


Figure 3.19: IL-1β results after 4 hour incubation in whole blood for donor 1 (A) and donor 2 (B). Zymosan values are 4315 pg/ml and 1173 pg/ml for A and B respectively.

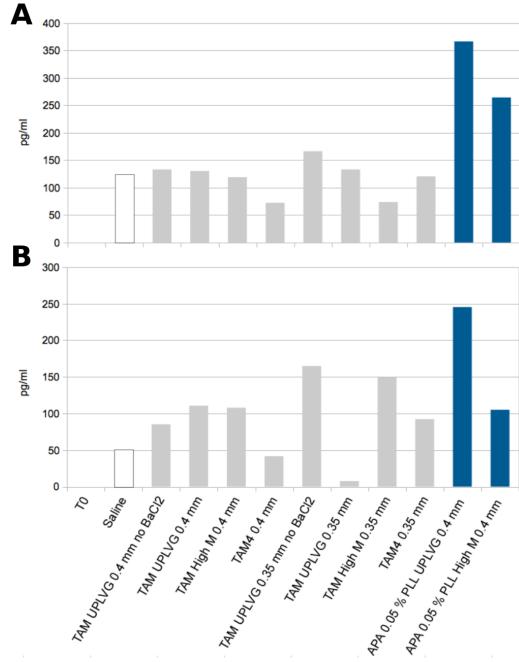


Figure 3.20: TNF α results after 4 hour incubation in whole blood for donor 1 (A) and donor 2 (B). Zymosan values are 31494 pg/ml and 7362 pg/ml for A and B respectively.

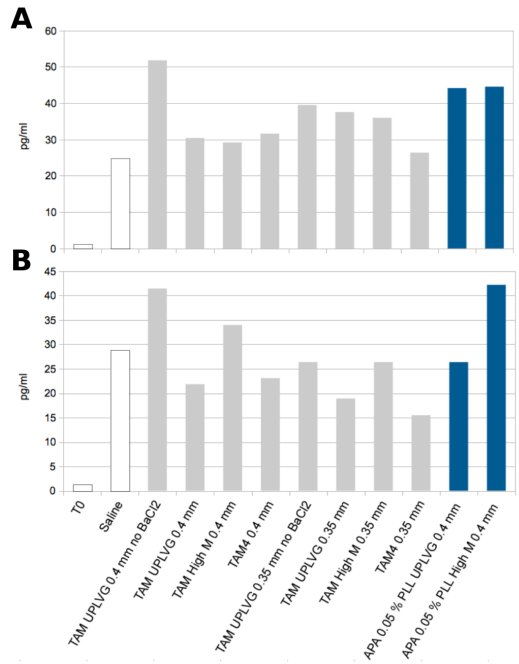


Figure 3.21: IL-6 results after 4 hour incubation in whole blood for donor 1 (A) and donor 2 (B). Zymosan values are 19255 pg/ml and 9976 pg/ml for A and B respectively.

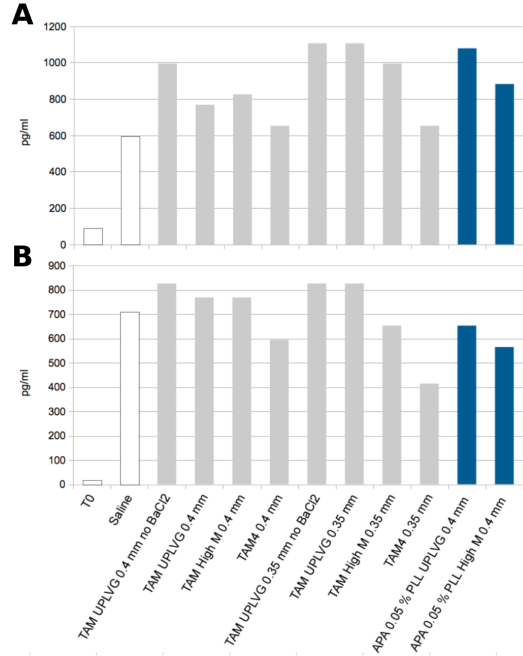


Figure 3.22: IL-1RA results after 4 hour incubation in whole blood for donor 1 (A) and donor 2 (B). Zymosan values are 938 pg/ml and 994 pg/ml for A and B respectively.

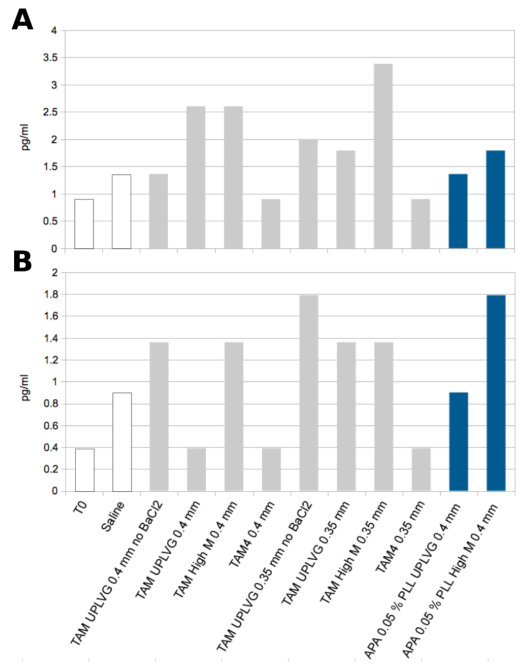


Figure 3.23: IL-10 results after 4 hour incubation in whole blood for donor 1 (A) and donor 2 (B). Zymosan values are 12.7 pg/ml and 8.4 pg/ml for A and B respectively.

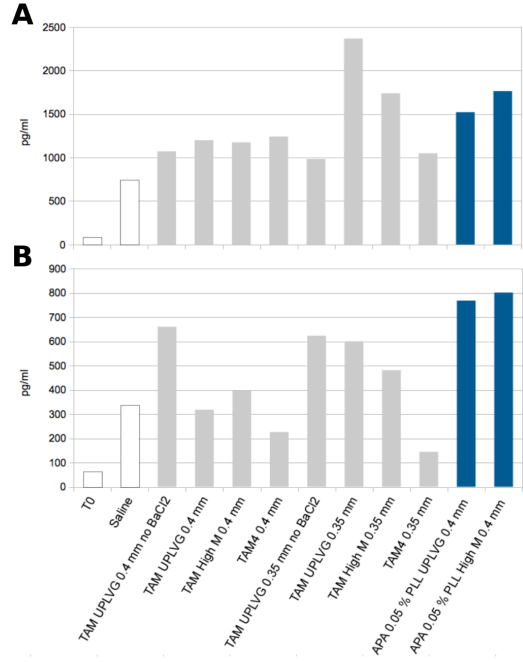


Figure 3.24: PDGF-BB results after 4 hour incubation in whole blood for donor 1 (A) and donor 2 (B). Zymosan values are 1901 pg/ml and 786 pg/ml for A and B respectively.

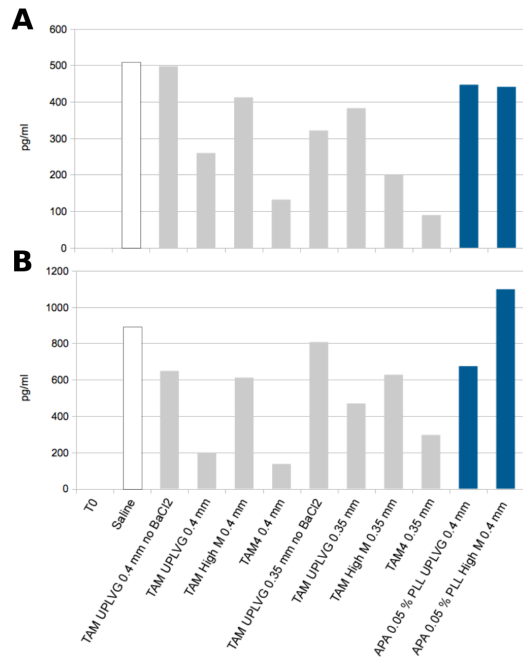


Figure 3.25: HGF results after 4 hour incubation in whole blood for donor 1 (A) and donor 2 (B). Zymosan values are 346.1 pg/ml and 913.9 pg/ml for A and B respectively.

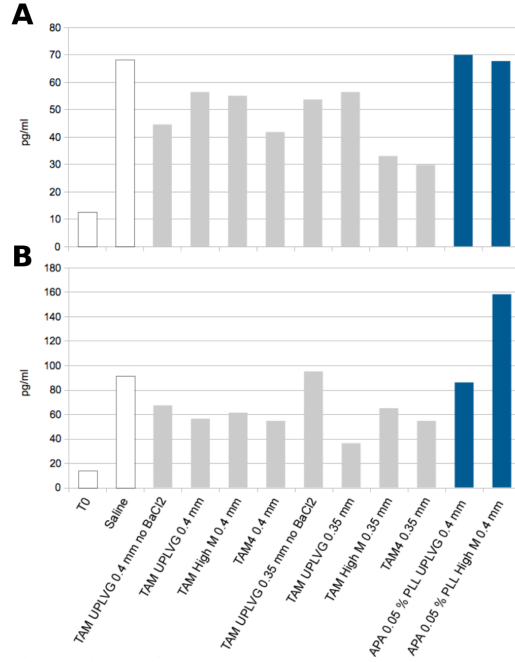


Figure 3.26: VEGF results after 4 hour incubation in whole blood for donor 1 (A) and donor 2 (B). Zymosan values are 73 pg/ml and 76 pg/ml for A and B respectively.

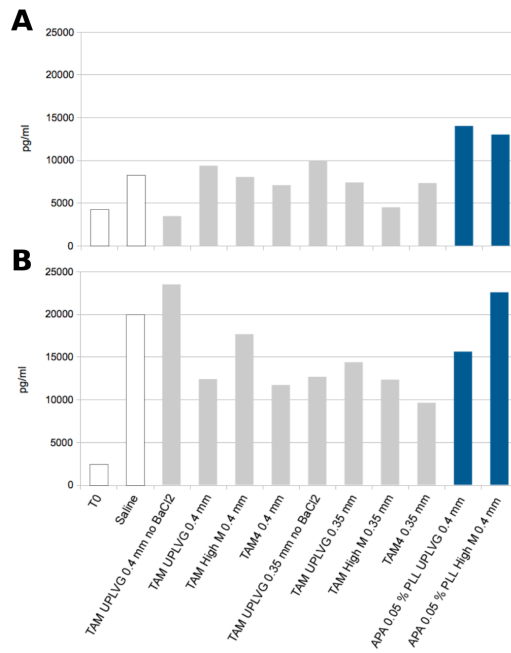


Figure 3.27: MIF results after 4 hour incubation in whole blood for donor 1 (A) and donor 2 (B). Zymosan values are 6889 pg/ml and 19193 pg/ml for A and B respectively.

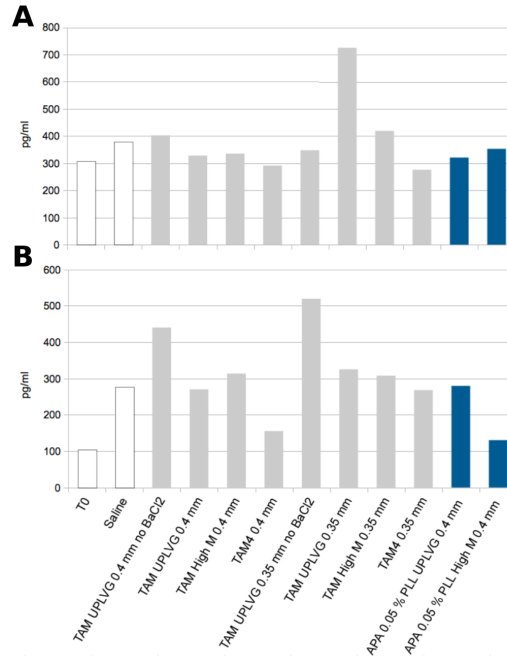


Figure 3.28: IP-10 results after 4 hour incubation in whole blood for donor 1 (A) and donor 2 (B). Zymosan values are 480 pg/ml and 1385 pg/ml for A and B respectively.

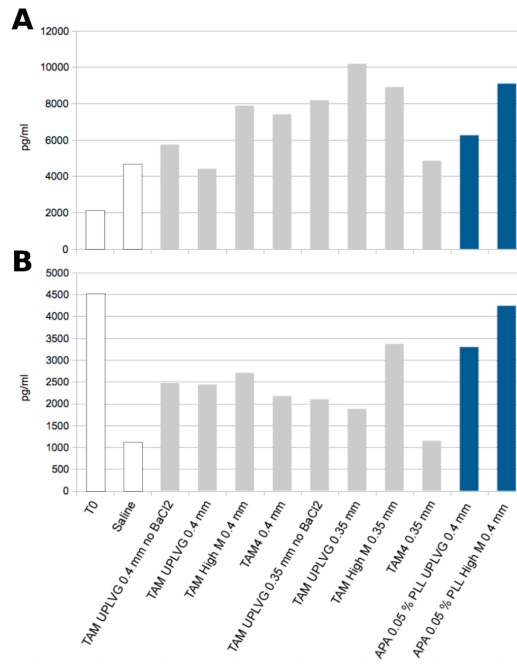


Figure 3.29: RANTES results after 4 hour incubation in whole blood for donor 1 (A) and donor 2 (B). Zymosan values are 18800 pg/ml and 14327 pg/ml for A and B respectively.

3.4.5 MIF, IP-10, IFN- γ and RANTES

For the molecule MIF, levels were at or below the saline control, figure 3.27. In most cases the TAM beads gave a lower response than APA capsules. No trend among the TAM beads could be observed, and changes in response most likely stemmed from donor variations. For IP-10, figure 3.28, the picture was similar to what had been observed before, with overall low levels, slightly higher without BaCl₂ in the gelling solution, and a concomitant low response for UP-LVG* capsules. Levels were here about the same as for APA capsules. For RANTES, figure 3.29, as was also the case for the first capsule set, it was harder to detect the same trends seen before. The secretion of RANTES seemed unaffected by the presence of capsules during the 4 hour incubation period. For the second donor we observed a very high T₀, possibly suggesting contamination of this vial.

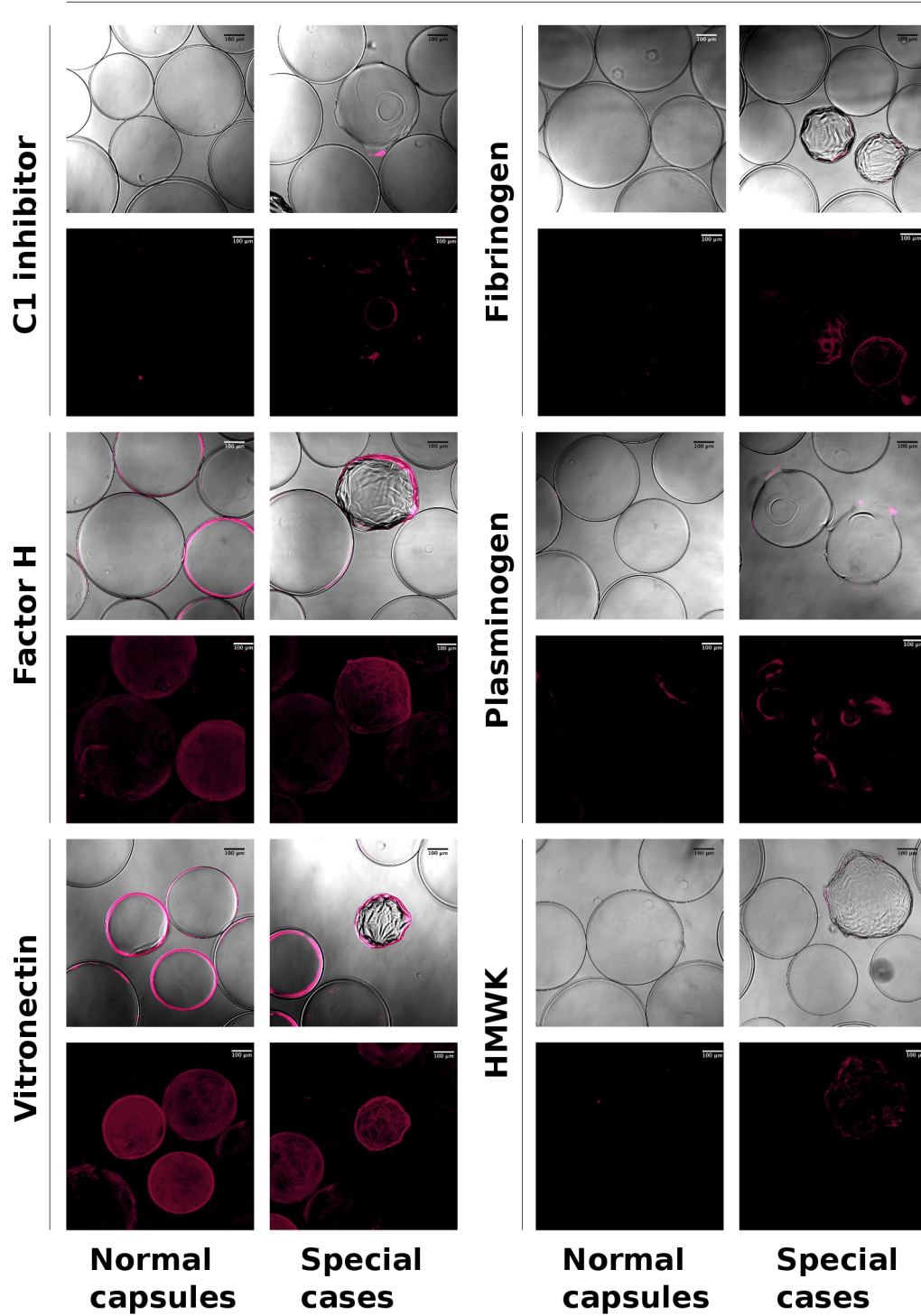
To sum up, it appears like the TAM capsules are minimally stimulating with responses at approximately the same level as the saline control. A general tendency towards an increased response to capsules without barium, and a slightly lower response for UP-LVG* alginate capsules, were seen, however, it cannot be excluded that these trends are a result of donor and procedure variations.

3.5 Regulatory complement protein and coagulation cascade protein deposition on capsule surface

In an attempt to get a better understanding of why TAM capsules triggered such a small cytokine response compared with APA capsules, TAM and APA capsules were stained for a set of inhibitory complement proteins, as well as some proteins involved in the coagulation cascade. TAM capsules (UP-LVG, 0.4 mm) and APA capsules (0.1 % PLL, UP-LVG, 0.4 mm) were incubated in plasma for 6 hours and overnight, and then stained with antibodies specific for the different proteins. High factor H adsorption along with vitronectin adsorption was seen on APA capsules, see figure 3.30. Also, collapsed APA capsules appeared to have a generally higher adsorption of proteins on their surface than did normal capsules. TAM capsules appeared more inert regarding protein deposition, as no protein adsorption was detected after 6 hours incubation, see figure 3.31. No marked increase in protein adsorption could be detected for APA capsules when incubating overnight. Deposition of vitronectin, plasminogen, fibrinogen, HMWK, and C1 inhibitor could be detected on a few TAM capsules when incubating overnight, although most capsules still appeared to be inert, see figure 3.33. Only plasminogen was adsorbed on a greater number of capsules. Nevertheless, an increase in adsorption was detected on TAM capsules when incubating overnight in plasma. Observation of protein adsorption after an even longer incubation period would be preferable, as capsules are destined to a much longer incubation period when implanted into patients.

6 h

APA



6 h

APA

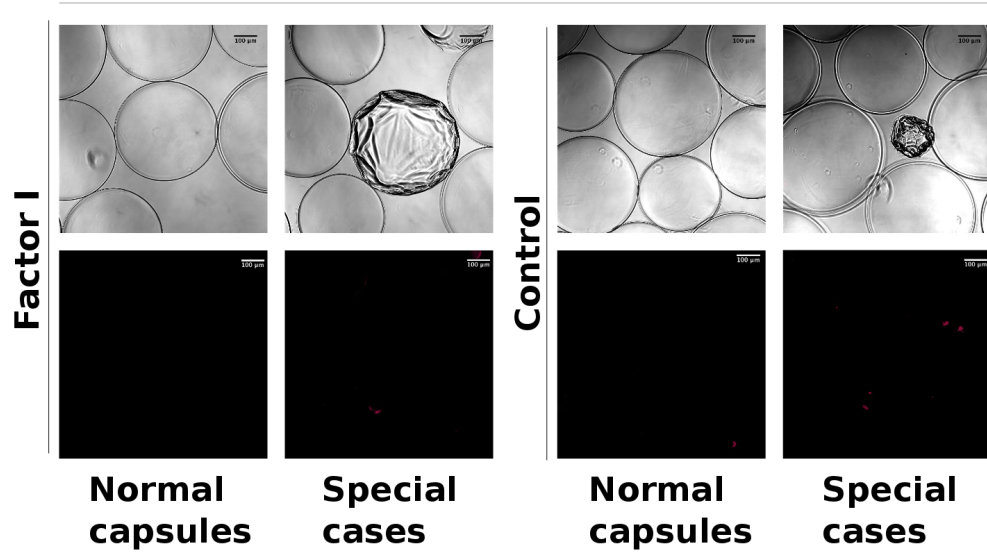


Figure 3.30: Adsorption of regulatory complement proteins and coagulation cascade proteins on APA capsules. Capsules were incubated for 6 hours in plasma, and stained with sheep anti-human protein antibodies, and sheep IgG negative control antibodies. Pictures of shrunk and deformed capsules were included as special cases as they did not represent the general capsule population. Pictures are displayed as cross sections through the equator and as 3D projections.

6 h

TAM

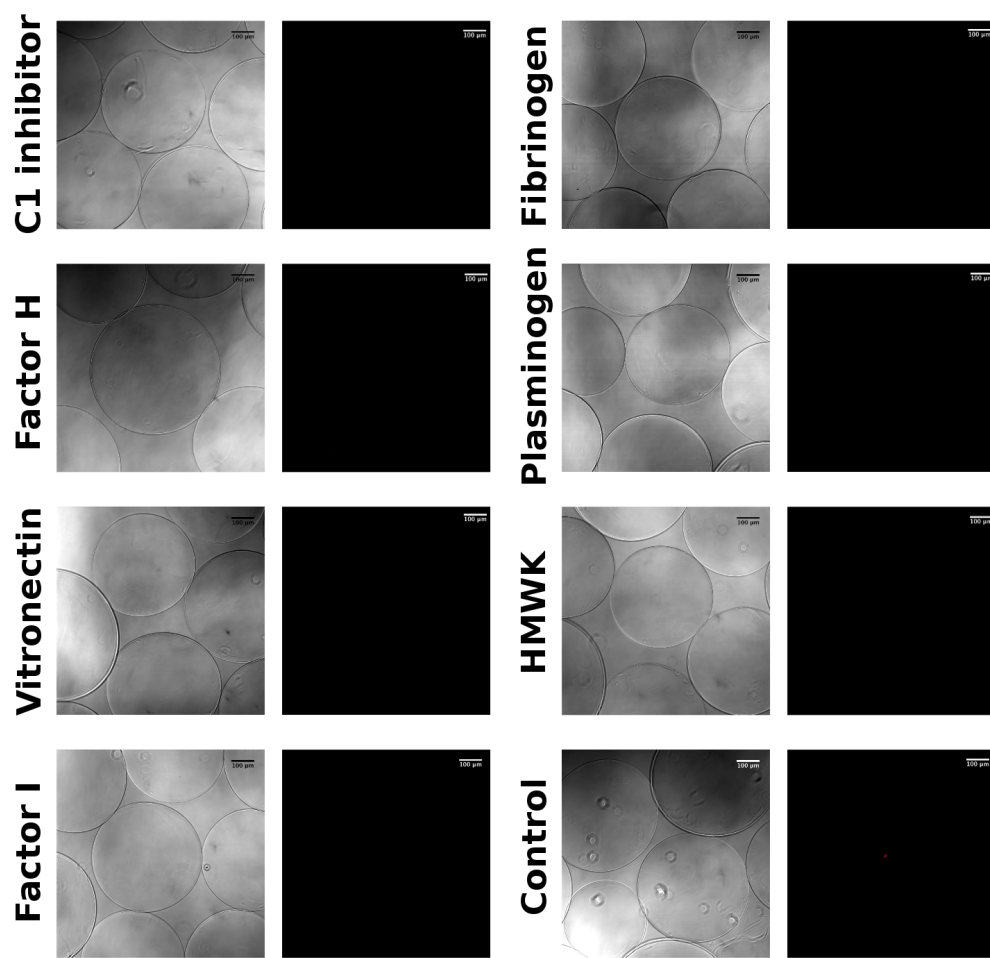
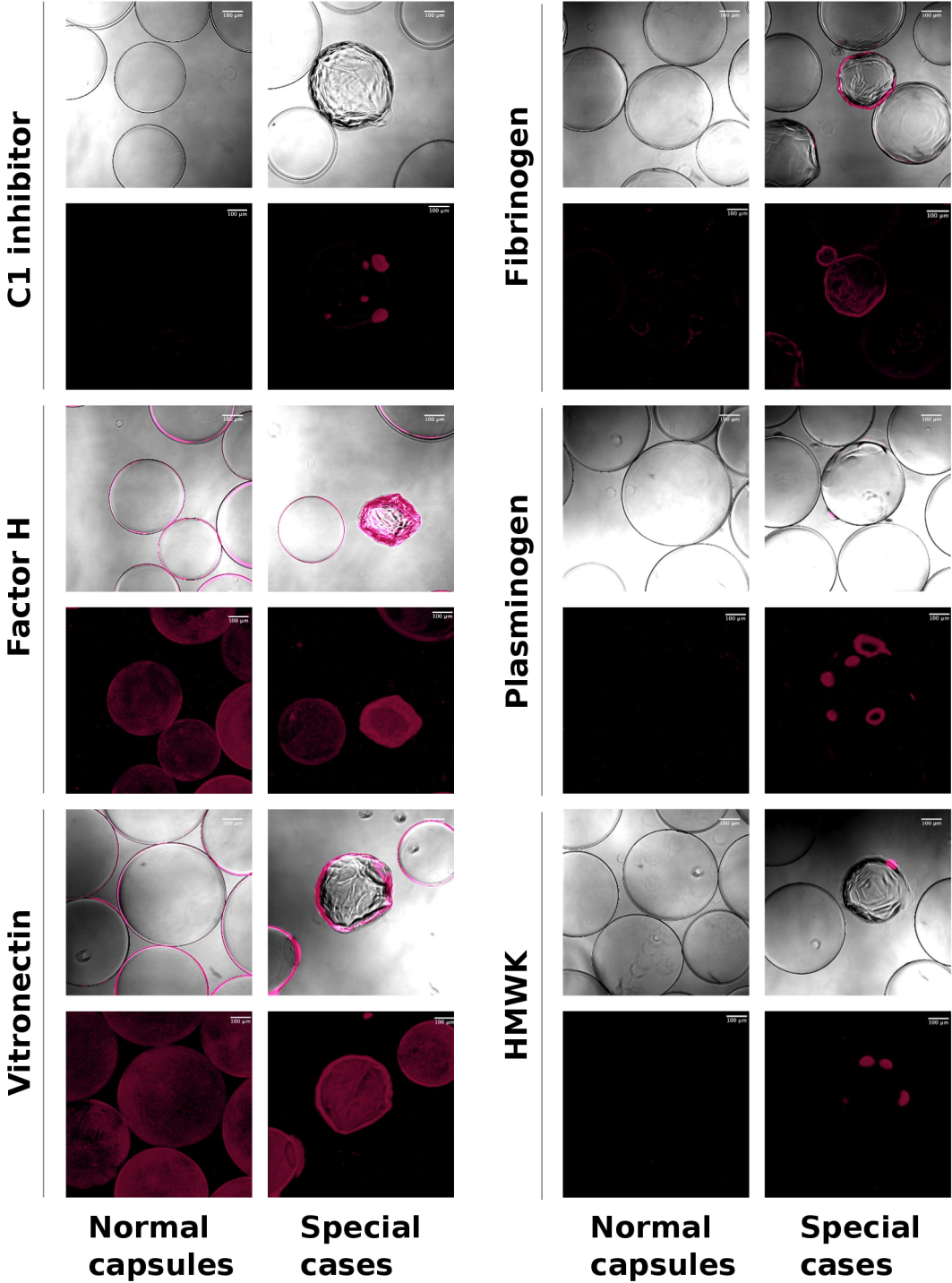


Figure 3.31: Adsorption of regulatory complement proteins and coagulation cascade proteins on TAM capsules. Capsules were incubated for 6 hours in plasma, and stained with sheep anti-human protein antibodies, and sheep IgG negative control antibodies. Pictures are displayed as cross sections through the equator and as 3D projections.

Over night

APA



Over night

APA

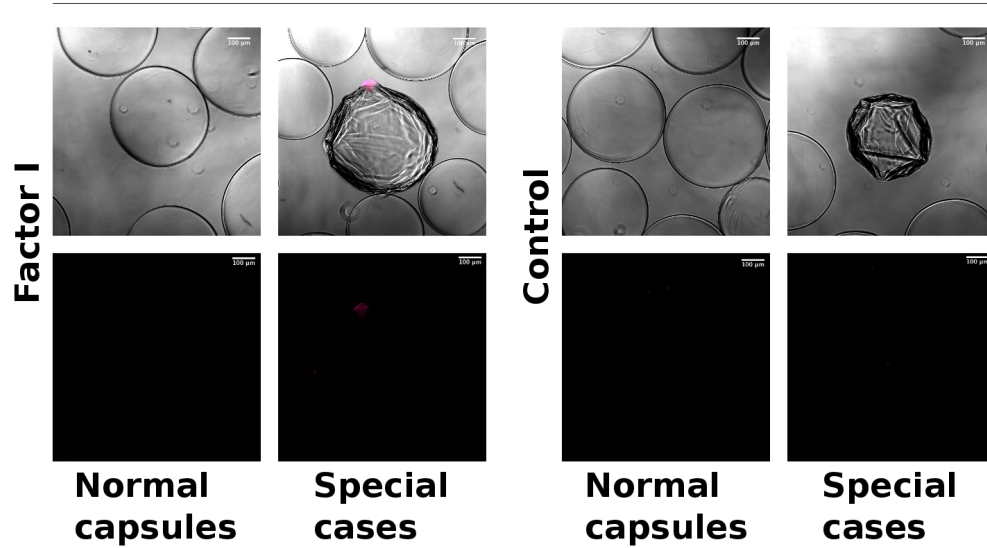
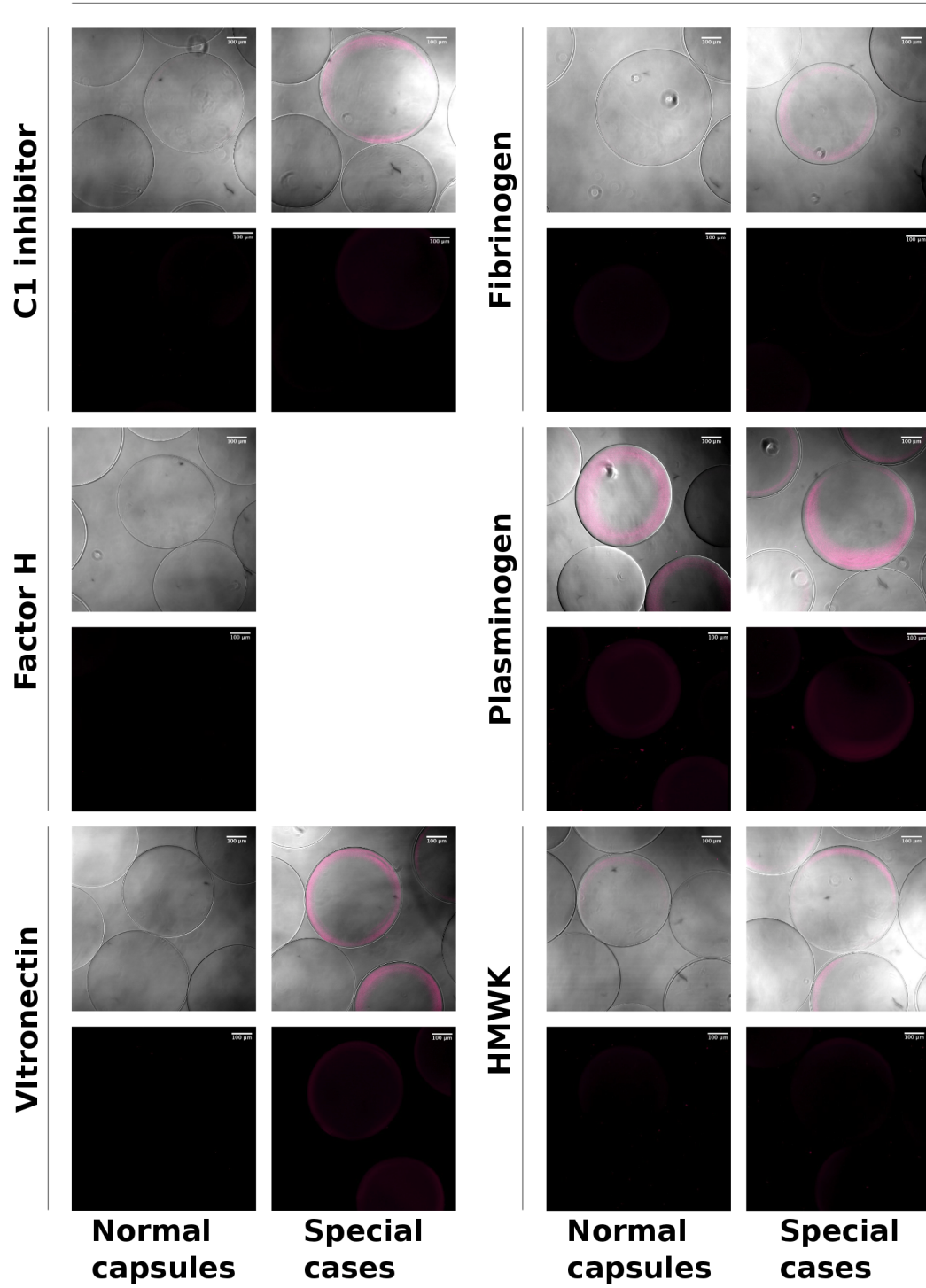


Figure 3.32: Adsorption of regulatory complement proteins and coagulation cascade proteins on APA capsules. Capsules were incubated overnight in plasma, and stained with sheep anti-human protein antibodies, and sheep IgG negative control antibodies. Pictures of shrunk and deformed capsules were included as special cases as they did not represent the general capsule population. Pictures are displayed as cross sections through the equator and as 3D projections.

Over night

TAM



Over night

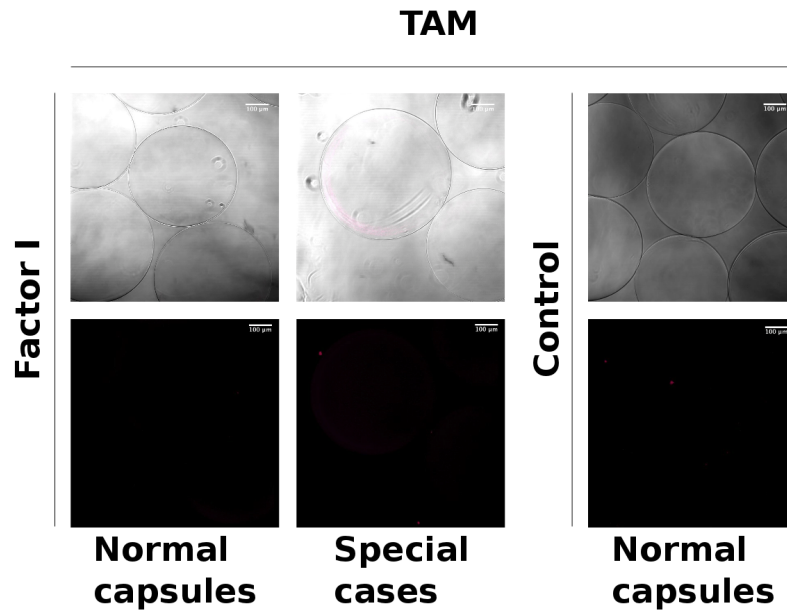


Figure 3.33: Adsorption of regulatory complement proteins and coagulation cascade proteins on TAM capsules. Capsules were incubated overnight in plasma, and stained with sheep anti-human protein antibodies, and sheep IgG negative control antibodies. Pictures of special cases are included where an increased adsorption was detected, but do not represent the general capsule population. Pictures are displayed as cross sections through the equator and as 3D projections.

3.6 Effect of lepirudin on protein adsorption

A concern was raised towards what affect the anti-coagulant lepirudin might have on adsorption of proteins on the capsules. As lepirudin is a direct thrombin inhibitor, it was debated whether it could affect the deposition of fibrinogen on the surface of the capsules. Capsules were therefore incubated in plasma anti-coagulated with different lepirudin concentrations. In the vial with no lepirudin added, the blood coagulated shortly after being extracted. Pictures of capsules incubated in plasma without lepirudin might therefore not give an accurate picture of protein adsorption on the capsules. The clotting process cleaves fibrinogen into fibrin, and cross links the molecule fibers. The concentration of soluble fibrinogen would therefore be diminished.

Fibrinogen

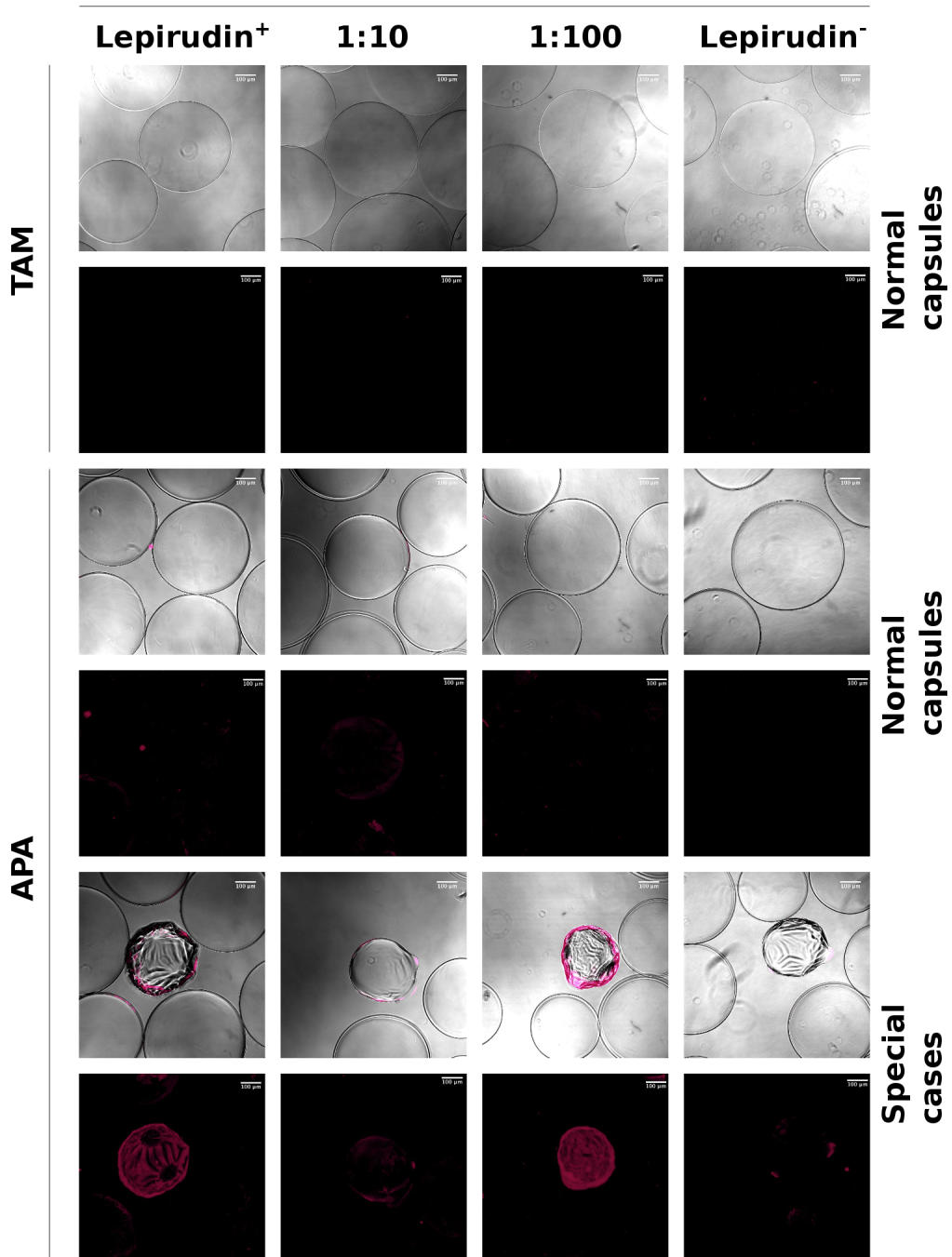


Figure 3.34: Adsorption of fibrinogen with different concentrations of the anti-coagulant lepirudin. Lepirudin positive samples were incubated in blood anticoagulated with 0.05 mg/ml lepirudin. Lepirudin negative samples were incubated in blood without anticoagulant. Capsules were incubated for 6 hours and stained with sheep anti-human fibrinogen antibodies, and sheep IgG negative control antibodies

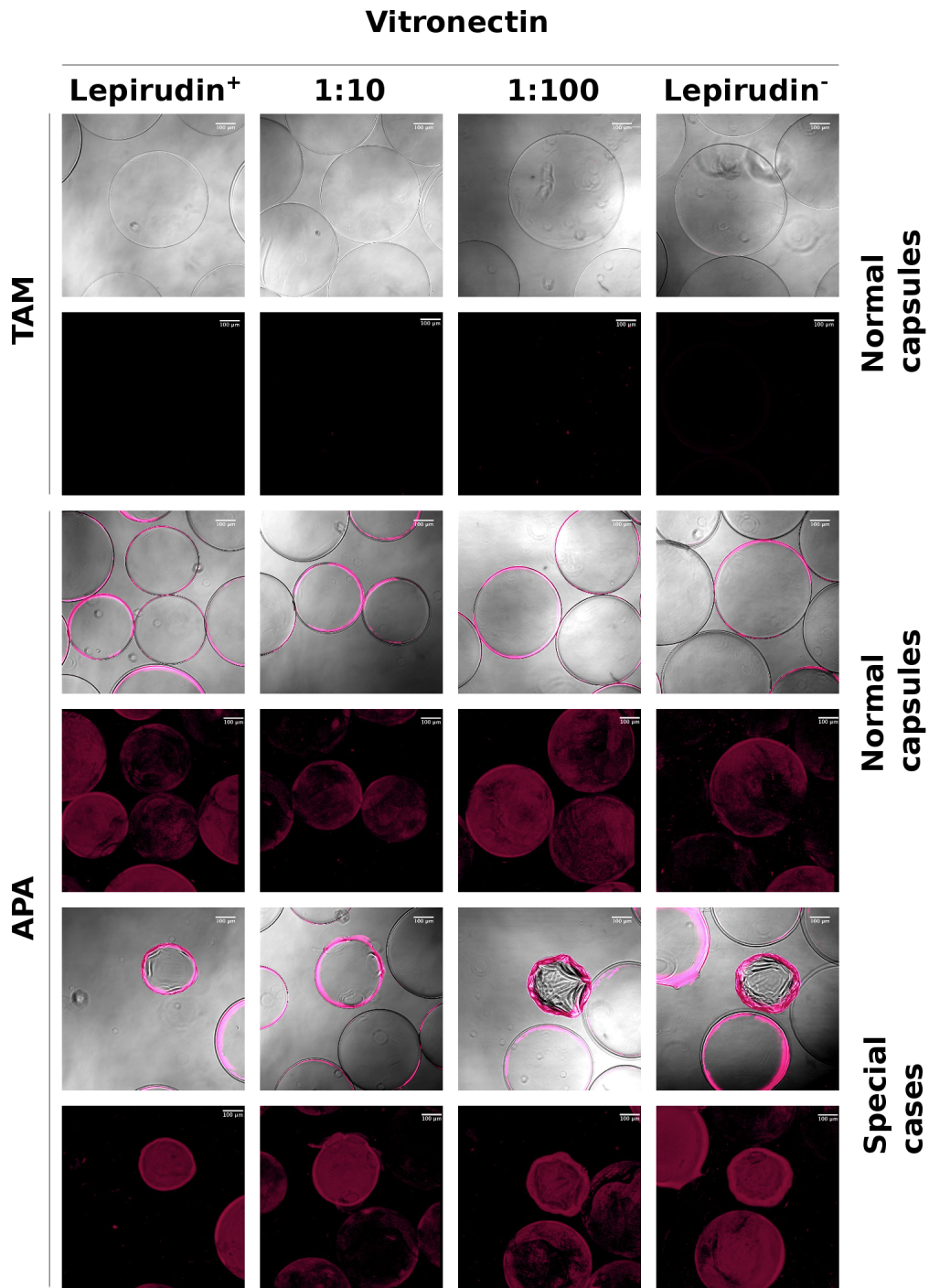


Figure 3.35: Adsorption of vitronectin with different concentrations of the anticoagulant lepirudin. Lepirudin positive samples were incubated in blood anticoagulated with 0.05 mg/ml lepirudin. Lepirudin negative samples were incubated in blood without anticoagulant. Capsules were incubated for 6 hours and stained with sheep anti-human vitronectin antibodies, and sheep IgG negative control antibodies

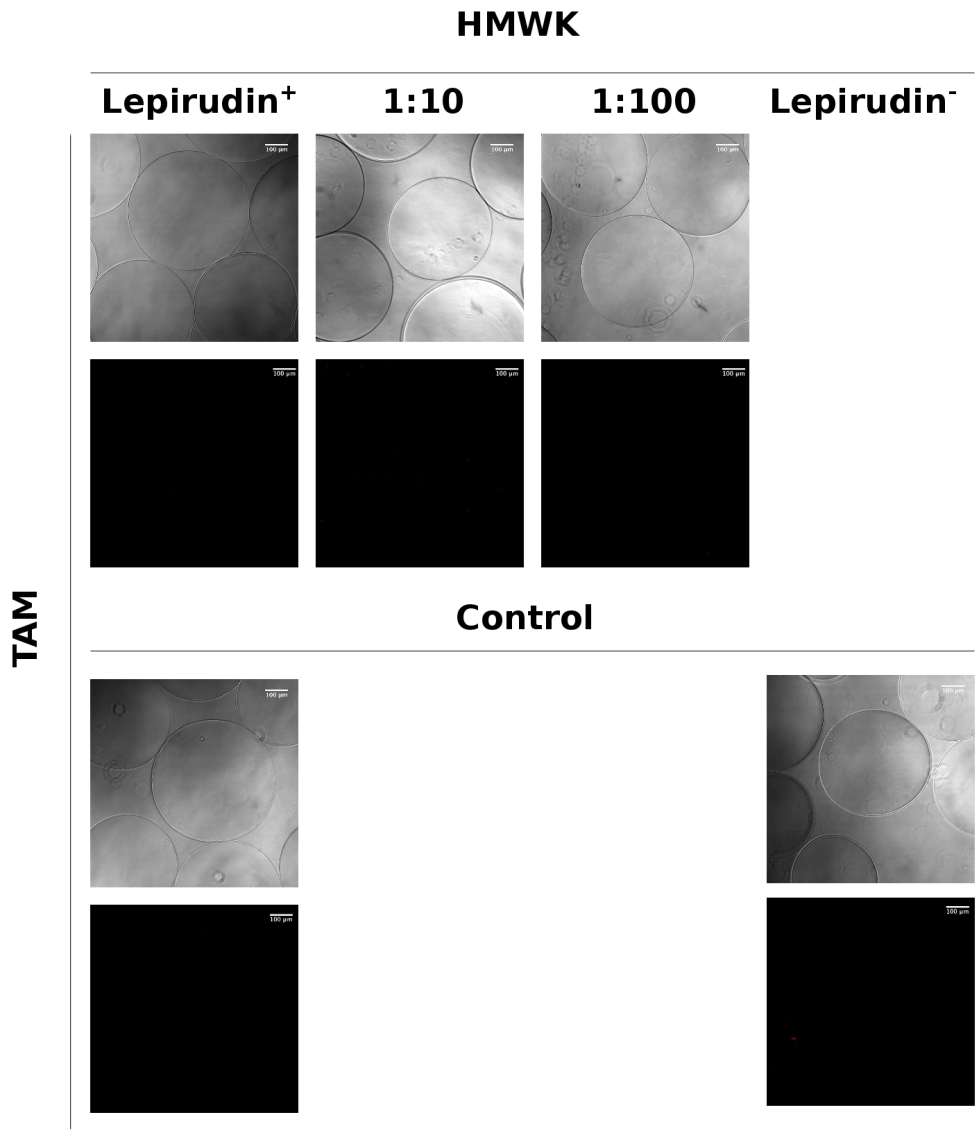


Figure 3.36: Adsorption of high molecular weight kinogen (HMWK) and negative control on TAM capsules after 6 hours incubation in plasma. Lepirudin positive samples were incubated in blood anticoagulated with 0.05 mg/ml lepirudin. Lepirudin negative samples were incubated in blood without anticoagulant. Capsules were stained with sheep anti-human HMWK antibodies, and sheep IgG negative control antibodies. Because of coagulation in the lepirudin negative sample, there was not enough plasma to test for HMWK adsorption. Negative controls are performed on TAM capsules at the two extremes, with and without lepirudin.

4 DISCUSSION

In this work, the biocompatibility of a set of different alginate microcapsules was studied in the whole blood model. Parameters such as capsule type, alginate type, polycation type, polycation concentration, and capsule size, were investigated. The goal was to increase our knowledge of the inflammatory mechanisms potentially involved upon implanting alginate capsules. Some of the questions raised included how the soluble inner core affects the immune response towards the capsules, how PLO compares with PLL as a stabilizing polycation layer, if the size of the capsule plays a role in the response, and why alginate beads incite a lower cytokine response than does the saline negative control.

4.1 The whole blood model for evaluating biocompatibility

The whole blood model represents a potent tool for unmasking the underlying mechanisms of biomaterial induced inflammation *in vitro*. This is based on previous studies where specific inhibition of proteins and receptors in whole blood has led to discoveries in the secretion of inflammatory mediators and how they are tied to complement activation [31, 75]. Using lepirudin-anticoagulated whole blood enables the study of how complement interacts in the inflammatory network, as lepirudin is a highly specific thrombin inhibitor that does not interfere with complement activation. The goal using the whole blood model was to reveal the inflammatory potential of different alginate microcapsules, and how changes in capsule composition affected this potential.

APA capsules, AP capsules, PMCG capsules, and TAM beads have previously been studied in the whole blood model [20]. The findings showed an increased sTCC response towards APA, AP, and PMCG, compared to TAM beads and saline negative control. Capsules here were made with 0.4 mm needles and 0.05 % PLL. Further analyzes on cytokine levels have shown decreased chemokine secretion and decreased inflammatory cytokine secretion towards TAM beads compared to APA, AP, and PMCG capsules [76]. Additionally, secretion of many of the cytokines has been observed to be complement dependent, as shown by addition of the C3 inhibitor compstatin.

It has also been demonstrated how polyvinyl chloride surfaces, cellulose ester or polyamide membranes induce a defined inflammatory response in whole blood [75, 77, 78]. Variability in the cytokine profiles of these materials has been observed, but increased levels of IL-8 have appeared in all cases. Increased IL-8 response also corresponded with complement activation in these studies, and might therefore be an important predictor of biomaterial tolerability. In this work, we observed a higher sTCC response, together with higher IL-8 levels, for the saline control compared to T0, which is consistent with activation of complement induced by the surface of the polypropylene vials used. The same could be seen in many of the other cytokine levels.

4.2 Capsule parameters

As it had been previously observed that changes in capsule parameters could appear to affect the inflammatory potential of alginate microcapsules [76], the aim of this work was to investigate different capsule compositions and preparation protocols in a controlled manner. The different parameters are shown in table 4.1.

Table 4.1: Capsule parameters investigated in this work
Parameter

Capsule type	TAM vs APA hollow vs solid APA
Polycation type	PLL vs PLO
Polycation concentration	0.05 %, 0.10 %, and 0.14 % PLL
Alginate type	High M vs High G
Capsule size	0.25 mm, 0.35 mm, and 0.40 mm needle size
Gelling conditions	With vs without BaCl ₂ in TAM gelling solution With vs without HEPES in gelling solution

4.2.1 Polycation

The first alginate microcapsules used to successfully encapsulate islet cells for the treatment of Type 1 diabetes in animals were APA microcapsules [19]. The use of a polycation layer in these capsules enabled them to withstand the harsh conditions involved in transplanting capsules into the peritoneal cavity without breaking and exposing the encapsulated cells to the host immune system. However, as the number of experiments has grown in the wake of this pioneering achievement, the polycation layer has generally come to be regarded as the main contributor of the bioincompatibility of capsules *in vivo* [17, 20, 79]. This could also be reflected in the triggering of leukocyte activation and cytokine production, as well as complement activation, in the whole blood assay performed in this work. Higher levels of the complement product sTCC, the chemokines IL-8, MCP-1, and MIP-1 α , the inflammatory cytokines TNF α and IL-1 β , as well as the growth factors HGF and VEGF were detected for APA capsules compared to TAM beads. Exchanging the commonly used PLL with PLO, as well as decreasing the concentration of PLL, might therefore present a way to decrease the inflammatory potential of the capsules, and was tested in this work.

4.2.2 Alginate type

The type of alginate has a major influence on the microcapsules. The earliest capsules used for cell encapsulation consisted of high M alginate (86-99.9 % M) which stimulated cytokine production [10]. Success had been achieved with these capsules in rats [19], but it was first when the immunostimulating effects of high M alginate was discovered, and capsules were made with alginate containing a higher fraction of G residues, that capsules started performing better in larger animals as well [58]. It is not only the immunostimulating properties of the alginate that has to be taken into account however. Stability of the alginate gel, pore size, and interaction with the coating layers are of importance. High G alginates tend to form stronger gels than High M alginates [16], because of the G-blocks having a greater affinity to cations. Conversely, High G ($F_G > 0.6$) alginates has been observed to perform worse in APA capsules than intermediate G alginate ($F_G = 0.4-0.6$) due to insufficient binding or complexing between alginate and the PLL coating [21]. Lastly, the size of the capsules has recently been an issue in the microcapsule community due to indications of over-growth correlating with capsule size [76].

4.2.3 TAM capsules

Improvements in alginate composition and gelling conditions have made it possible to omit the polycation layer and encapsulate cells directly in a bead consisting only of gelled alginate [22, 61]. The TAM beads used in this work were from an optimized alginate capsule design using high molecular weight alginate, with a high content of G, which, in combination with Ca^{2+} and a minimal concentration of Ba^{2+} , allows for very strong and stable microcapsules [80]. Also, the use of mannitol as osmolyte in both the alginate and in the gelling solution results in a higher concentration of alginate at the capsules surface than at the center [81]. All these factors improve the stability of the beads, making the polycation layer redundant. The fact that the TAM beads can be made in one step further tips the scale in their favor as this makes the encapsulation process easier with milder conditions for the cells. And, while comparing the beads to APA capsules, one also removes the presence of collapsed capsules that are always present, albeit at a very low number, in the APA capsule population. As shown in the protein adsorption assays in this work, these collapsed capsules have a higher protein deposition on their surface, and might therefore help further initiate a response.

There are however some draw backs with alginate beads. As only one defense barrier stands between the encapsulated cells and the host immune system, the stability of the gelled alginate is crucial. In addition, the beads will have a larger porosity than capsules with a polycation layer, allowing the diffusion of immunoglobulin G [82] and complement [83] into the cells. This might pose a problem as antibodies could be generated towards the encapsulated cells, diffuse into the capsules, bind to the cells, and possibly start a complement reaction. Conversely, an increased porosity might also to a greater extent allow secreted proteins from the encapsulated cells, or even residual protein from the alginate itself, to reach the host immune cells. This might

explain why there have been reported cases where hollow APA capsules with encapsulated tumor cells have performed better than TAM capsules [76]. The same picture was seen in a recent study with cynomolgus monkeys, where TAM capsules showed increased over-growth [76]. Still, microcapsules of similar permeability have previously been shown to protect grafts in mice [57], indicating no major problem of the bead porosity. In addition, the exposure of the negative surface charges present in the alginate polymer might stimulate coagulation cascade responses to a greater extent. This might also be a reason for the observed over-growth seen on capsules *in vivo* [76]. Negative surfaces are observed to adsorb factor XII of the coagulation system, which might then become activated and initiate the coagulation cascade. Use of a layer of zwitter ions coating the surface has been suggested, as these molecules, having an equal amount of positive and negative charges, tend to be particularly biocompatible, robust, and environmentally benign [84, 85].

4.3 Complement activation

The different alginate microcapsules were tested in the whole blood assay. The formation of sTCC indicates activation of complement as it is the final product of the complement cascade. It is suggested to be the most sensitive and specific marker of complement activation [20]. A rapid and strong response was detected for hollow APA capsules compared to solid APA capsules and TAM beads after 1 hour of incubation in whole blood. For some donors the hollow APA response was at the same level as the positive control zymosan. After 4 hours, the response was still high, at about the same level as zymosan, but it appeared like the gap between solid APA and hollow APA capsules was decreasing. This was further investigated to see if the same picture could be observed on the surface of the capsules. If the hollow capsules would elicit a strong sTCC response, then this should most likely also be detected on the capsule surface as an increase in C3 protein. When this could not be observed, it was debated whether some soluble molecule diffused out of the hollow APA capsules and triggered the sTCC response. A soluble PLL-alginate complex was suggested, which perhaps could trigger the spontaneous hydrolyzation of C3 into C3(H₂O), and the subsequent sTCC generation. But as the leukocyte CD11b expression, which is tightly linked to complement activation as it is a receptor for inactivated C3 and up-regulated by C5a [86], and also the IL-8 levels, could not reflect this strong increase in sTCC, it might indicate the presence of some molecule diffusing out of the hollow capsules and which is subsequently detected as sTCC by the complement detection method. Meaning that it is not actually linked to the complement cascade, but an assay mediated artifact. Still, this would then also have to explain the higher values of MCP-1 which were detected for the same hollow APA capsules. Perhaps the slow accumulation of C3 on the surface of the solid APA capsules is what is required for the cytokine stimulation. That the surface deposition of C3 facilitates the triggering of monocytes and granulocytes to secrete cytokines.

C3 inhibition studies might clarify if the observed sTCC response is a specific response to-

wards sTCC, or an assay mediated artifact. Addition of the C3-binding cyclic synthetic peptide compstatin would effectively inhibit the generation of C3a and sC5b-9 [87]. Still detectable sTCC would then be a confirmed artifact of the procedure. Interestingly, a similarly increased initial sTCC response has been detected for hollow PMCG capsules tested in the whole blood model [20]. These capsules have also been observed to have higher MCP-1 levels compared to solid APA capsules [76]. In that case both the sTCC and MCP-1 responses were confirmed to be of a complement nature [76].

A marked difference was observed in sTCC levels for hollow APA with PLO and with PLL. Hollow APA with PLO gave a response that was at about the same level as for solid APA capsules, while levels for hollow APA with PLL were much higher. This could indicate that, if the above assumption of a soluble artifact detectable as sTCC, or triggering sTCC, is valid, the PLO polycation might have reduced the permeability of the capsules in some way, preventing the diffusion of the compound out of the capsule. sTCC response towards TAM beads remained at or below the saline negative control at both 1 hour and 4 hours of incubation, with no detectable difference in capsule size.

PLL significantly affected complement activation. Increased PLL concentration in the APA capsules correlated with a significant increase in sTCC response for APA capsules having High-G alginate, after both 1 hour and 4 hours incubation. For capsules with High-M alginate the trend appeared to be the opposite. Here a significant decrease was observed for both hollow and solid APA with increasing PLL after 1 hour. The decrease for the solid APA capsule was also reflected in CD11b expression, further strengthening the results as CD11b is up-regulated by complement activation. After four hours, the solid APA capsule appeared to have changed into an increase in sTCC with an increase in PLL, but the difference was not significant. The apparent change in sTCC generation upon increasing PLL concentration between High G and High M alginate, especially after 1 hour, suggested a change in interaction between alginate and PLL depending on F_G , as will be discussed further in section 4.4.5.

4.4 Cytokine secretion and CD11b expression

4.4.1 TAM beads vs APA capsules

TAM beads outperformed solid APA capsules in regard to the majority of cytokine responses, in complement activation, and in CD11b expression. This was in concordance with comparisons between TAM and APA performed before [20]. Lower levels of the chemokines IL-8, MCP-1 and MIP-1 α , lower levels of the inflammatory cytokines TNF α and IL-1 β , lower levels of the growth factors HGF and VEGF, and lower levels of the complement complex sTCC was observed. In many cases the levels were at or below the saline negative control, suggesting activation from the incubation vials themselves to be the major part of any increase compared to initial blood values.

4.4.2 Effect of a soluble core

Hollow APA capsules along with solid APA capsules were tested in the whole blood assay to determine if there was any observable difference between the two types of capsules. As mentioned previously, the complement response showed significantly increased levels for hollow APA capsules compared to solid APA capsules and TAM beads. For some cytokines, however, the levels were significantly lower for APA capsules with a soluble core compared to APA capsules of the same composition but with a solid core. The chemokines IL-8 and MIP-1 α showed a significantly lower response towards hollow APA capsules compared to solid APA capsules after 4 hours of incubation, as did the pro-inflammatory cytokines TNF α and IL-1 β , the growth factor VEGF, and the cytokine MIF. The cytokine IP-10 showed a significantly higher response towards hollow APA capsules. All these responses indicated a lower degree of immune stimulation for capsules with hollow inner cores. Interestingly however, the chemokine MCP-1 for hollow capsules showed increased levels compared to solid capsules, reflecting the activating potential seen for sTCC. As mentioned before, increased MCP-1 and sTCC levels have been observed previously for hollow PMCG capsules [76, 20]. C3 inhibition with compstatin proved MCP-1 to be dependent on complement activation as levels decreased when compstatin was added [76].

If sTCC has been produced, then the anaphylatoxins C3a and C5a will also have been produced as these are split products in the complement cascade. C3a and C5a have been shown to induce NF κ B activation in human peripheral blood monocytes [88], and to up-regulate IL-8, IL-1 β and RANTES mRNA in human umbilical vein endothelial cells [89]. It is therefore reasonable to assume that the increased sTCC for APA solid capsules compared to TAM beads and saline controls are linked to the increased cytokine secretion seen for these capsules, through the anaphylatoxins C3a and C5a. This has also been confirmed through the addition of compstatin which lowered the secretion of many cytokines [76] in a recent, as yet unpublished, study. When it is in this study observed a strong sTCC response for hollow APA capsules, but then diminished cytokine secretion except for MCP-1 as compared to solid APA capsules, it could be proposed that the complement cascade split products C3a and C5a perhaps adsorb to these capsules to a greater degree than for solid APA capsules, thereby preventing C3a and C5a to reach the cells. This has also been seen for hollow PMCG capsules where C3a and C5a levels were significantly lower than the saline control [20]. Thus, the complement cascade is activated, but by sequestering the anaphylatoxins C3a and C5a further instigation of inflammatory responses might be prevented.

4.4.3 PLL vs PLO

For the discussion of polycation type, no significant change in levels of the chemokines IL-8, MIP-1 α , and MCP-1, nor in levels of the inflammatory cytokines TNF α and IL-6, the anti-inflammatory cytokines IL-1RA and IL-10, or the growth factors PDGF, HGF, and VEGF was observed by exchanging PLL with PLO. No change was detected in MIF, IFN- γ , or RANTES

levels either. A change was observed for sTCC as the levels of sTCC for hollow APA with PLO were about the same as for solid APA, while levels of sTCC for hollow APA with PLL were much higher. This could indicate that, as discussed earlier, the PLO polycation might have reduced the permeability of the capsules, preventing the diffusion of soluble molecules out of the capsule. Or that only the PLL-alginate complex, and not the PLO-alginate complex, was capable of triggering the sTCC response observed.

Also, a lower response was seen in IP-10, while a higher response was seen in IL-1 β , for capsules with PLO compared to PLL. The chemokine IP-10 is interesting in that increased IP-10 secretion has recently been shown to be affected by iC3b and C4b. By inhibiting IFN- β , iC3b and C4b inversely inhibit IP-10 secretion [90]. As the alternative pathway was previously found to be involved in the complement response towards activating alginate microcapsules [20], this would suggest iC3b to be the most likely cause for the detected lower values of IP-10 for APA solid capsules compared to TAM. In some cases IP-10 values for APA solid were even lower than the saline control. This had also been seen in a previous, as yet unpublished study [76]. The detected lower values of IP-10 for PLO compared to PLL would thus also suggest increased iC3b levels. Increased iC3b, the ligand for the receptor CD11b, could not be reflected in increased expression of CD11b. CD11b is shown to be up-regulated by C5a [86], and should thus be linked with complement activation. This could suggest that PLO stimulates the initiation of the complement cascade, but that the cascade then stops before the generation of the C5 convertase producing C5a. However, CD11b data are from 1 hour incubation while IP-10 data are from 4 hours, and might therefore not be completely comparable. To sum up, from the findings in this work, no improvement in biocompatibility can be observed by exchanging PLO with PLL. PLO capsules have been used in implantation experiments before, but have given no significantly better results than experiments with PLL [91, 92].

4.4.4 Effect of PLL concentration

PLL has been reported to trigger sTCC generation, as well as activation of leukocytes in whole blood [20]. In this work, an increase in PLL concentration was seen to affect mainly the sTCC response. For some capsules there was also a significant change in the chemokines IL-8, MCP-1, IP-10, the inflammatory cytokines IL-1 β , TNF α , the anti-inflammatory cytokines IL-1RA, IL-10, and the growth factor VEGF levels. For High M capsules, an increase in PLL from 0.05 % to 0.10 % gave an increase in IL-1 β and TNF α levels, as well as lower levels of IP-10. As discussed above, IP-10 has been shown to be inhibited by iC3b and C4b, and lower levels of IP-10 would suggest higher complement activation which could then result in activation of monocytes increasing the secretion of the inflammatory molecules IL-1 β and TNF α . IL-8 levels were also higher for the 0.10 % capsules, again pointing towards increased complement activation. Higher sTCC levels after 4 hours of incubation were observed for increasing PLL in this capsule type, however, the increase was not significant ($P < 0.05$). Furthermore, APA capsules with High G

not only showed higher sTCC levels with increasing PLL. An increase in MCP-1, as well as a decrease in IP-10, and a decrease in the anti-inflammatory molecules IL-1RA and IL-10 was also seen. This all leans towards an increased inflammatory response for High G alginate capsules with increasing PLL concentration.

There is however a structural benefit to having a higher concentration of polycation. This was seen when making the hollow APA capsules. Capsules with 0.05 % PLL were first made, but when treating these capsules with citrate the number of burst and deformed capsules was too high to be able to test them in the whole blood assay. When increasing the concentration to 0.10 % PLL, the number of burst capsules went considerably down, but was still higher than when using 0.14 % PLL hollow capsules.

4.4.5 Effect of alginate composition

A difference could be seen in 0.05 % PLL APA capsules with High M (*M. pyr*) versus High G (UP-LVG) alginate, in IL-8 levels, in TCC levels, in IP-10 levels, and in RANTES. An increase in IL-8 was seen for the High G capsule compared to the High M capsules, while a decrease was seen for the same capsule in TCC. An increase was seen in RANTES levels towards High G alginate, while a decrease was seen in IP-10 levels. As discussed earlier, IP-10 levels have recently been showed to correlate with iC3b and C4b generation [90]. This might suggest an increase in complement activation with High G alginate, however, this was not reflected in sTCC which decreased for High G alginate. Perhaps the complement cascade was initiated but then stopped before the final TCC molecule was generated. No difference in cytokine levels was observed for High M versus High G alginate in 0.10 % PLL APA capsules in this work.

As mentioned in section 4.3, there was a clear change in sTCC generation upon increasing PLL concentration between High G and High M alginate. For High M capsules, after 1 hour incubation, the sTCC response went down when increasing the PLL concentration. For High G capsules, after both 1 hour and 4 hours incubation, the sTCC response went up when increasing the PLL concentration. This suggested a change in interaction between alginate and PLL depending on F_G . As $F_G > 0.6$ alginate has been reported to bind PLL to a lesser extent than alginate with a lower F_G [21], perhaps switching to High G alginate allows more unbound PLL to leak out of the capsule and thereby result in a higher sTCC formation with higher capsule PLL concentration. This might also be the reason why we see a higher IL-8 response for High G compared to High M in the 0.05 % PLL capsule. High G alginates with $F_G > 0.6$ in APA capsules have been observed to perform worse than intermediate G alginates ($F_G = 0.4-0.6$) [21]. PLL binds to alginate by forming complexes with M-G sequences on the surface of the alginate beads [93]. Alginates with a lower fraction of M-G sequences might therefore bind insufficiently to the PLL layer, allowing uncomplexed PLL to leave the capsule and promote inflammation and over-growth [94, 95]. It might therefore be suggested that the increase in sTCC seen for

High G compared to High M capsules when increasing the PLL concentration is due to lower binding of PLL for High G alginate. And that the same effect could explain why we observe higher IL-8 levels, higher RANTES levels, and lower IP-10 levels for High G compared to High M alginate 0.05 % PLL capsules. That these increased levels are a consequence of insufficient binding, or complexing, to PLL, allowing some PLL to leak out of the capsule triggering the cytokine responses. However, we did observe lower levels of sTCC for the High G capsule compared to the High M capsule.

The lower levels of TCC for High G compared to High M in the 0.05 % PLL capsule might be linked with the overall shape and surface of the capsules as it was observed a higher capsule diameter for the High M capsule compared to the High G capsule. The size of the capsule and degree of swelling might be of importance as the swelling results in weaker and more permeable capsules that are more likely to break apart with time [96]. When increasing the PLL concentration to 0.10 % on APA capsules in this work, the difference in capsule diameter decreased probably due to the increase in the stabilizing polycation, and a significant difference between the two alginates was not observed in any cytokine, and only observed in TCC after 1 hour. Thus, increasing the PLL to 0.10 % removed all significant difference in cytokine and complement response levels between High M and High G capsules, when incubated for 4 hours. It might therefore also be proposed that the observed difference in complement response towards APA capsules with High M or High G alginate stems from the stabilizing effects of the High G alginate, and not from any increased immunogenicity of High M alginate. To be able to test this in a more thorough way, a soluble alginate assay should be performed, incubating soluble High M and High G alginate in different concentrations in whole blood.

To sum up, the results are very complex with many different factors involved and do not appear to point in one direction. More experiments would have to be performed to further deduce the individual contributions to the inflammatory potential of the PLL binding properties of the alginate, and its stabilizing effects.

4.4.6 Effect of capsule size

No difference in complement, cytokine, or CD11b response levels was seen with varying capsule diameter on TAM beads. A difference was seen for some APA capsules with varying diameter, but, as these capsules tended to swell more after preparation, it was harder to get a controlled comparison of their diameter, as can be seen from table 3.1. Significant differences in some of the cytokine levels here might be attributed to donor variations, which were quite big in some cases, especially for IL-8 values. It could also be that an increase in size for the APA capsules might have resulted in more adsorbed PLL on their surface which consequently might trigger a higher inflammatory response.

4.4.7 Effect of HEPES

The addition of HEPES in the gelling solution did not appear to affect the inflammatory potential of the capsules in regard to complement activation, cytokine secretion, or CD11b expression.

4.5 Cytokine response to TAM beads

As for the different TAM beads, the results only included data from two blood donors and any significant differences could not be concluded. The responses were in almost all cases at or slightly below the saline negative control, indicating that any increase in cytokine levels stemmed from the activating potential of the incubation vials themselves. It did, however, look like there was an increase in cytokine responses towards beads being gelled without BaCl₂. This might have been because of lower stability [80] resulting in a rougher bead surface and increased swelling, something that was also reflected in a slightly higher diameter for these beads. Another explanation might be that as barium further stabilizes the alginate gel, residual contaminants present in the alginate might to a greater extent leak out of the beads in the absence of barium. Residual contaminants such as proteins, endotoxins, and fucoidans, have been proven present even after purification, and might contribute to immunogenicity as well as altered functional properties of the alginate [97]. It did in any case not look like the presence of barium stimulated cytokine secretion. There also appeared to be quite good results for the TAM4 beads which contained the new type of High G alginate, as cytokine levels were in almost all cases slightly lower than beads with High M alginate. However, it is quite possible that as the response levels for the TAM beads were very low, any differences seen could solely be the result of assay variations or irregularities when preparing the beads.

4.6 Protein adsorption on alginate microcapsules

No differences could be observed in surface deposition of the proteins screened for in this work between plasma and whole blood. In addition, CaCl₂ treatment of capsules did not appear to affect fibrinogen adsorption. CaCl₂ treatment prevents the depletion of Ca²⁺ ions inside the capsule, and limits the ongoing dissolution of the polymer network. TAM beads appeared exceedingly inert when it came to deposition of proteins on the surface of the beads. After 6 hours incubation in whole blood and in plasma no complement C3 was found, indicating no initiation of the complement cascade. No fibrinogen or HMW kininogen was observed, which are proteins frequently seen to observe to biomaterials and might play a role in cell adhesion [24, 98]. Alongside this, no inhibitory protein (factor H, vitronectin, factor I, C1 inhibitor) adsorption was seen on TAM beads either. It was debated whether the observed TAM cytokine levels, which were often lower than the saline control, could be the result of regulatory proteins such as factor H binding to the bead surface and preventing the onset of the complement cascade. Lower than saline levels had previously also been observed for complement components in response to TAM beads [20]. This could not be supported by the protein adsorption findings

in this work. Instead, it was the APA capsules that displayed the greatest inhibitory effects as could be seen from heavy factor H and vitronectin adsorption. APA capsules also showed C3 surface adsorption. It might therefore be that the C3 presence in itself attracts the soluble regulatory proteins factor H and vitronectin, and that they are merely a side effect of the increased complement activity that is seen.

It was observed a slight increase in protein adsorption on TAM beads when letting the capsules incubate overnight. It would therefore have been interesting to allow capsules incubate over even longer periods of time before analyzing the protein deposition, as the capsules are supposed to stay inside the peritoneal cavity over much longer time than has been tested here, and protein adsorption might build up and contribute to the observed over-growth seen when explanting capsules in animal studies. The fact that the alginate polymer is negatively charged might affect the protein adsorption. Many of the proteins involved in initiation of the coagulation cascade are observed to bind to negatively charged surfaces [28, 99], and might be a reason for the increase over time of protein deposition seen here. For the APA capsules, the outer alginate layer is bound to the polycation layer, and this binding might result in neutralization of the negative charges, which might be why no increase over time is observed for the APA capsules. An increase in protein deposition on the capsule surface might allow cells to attach to the capsules and trigger inflammatory responses that lead to increased fibrosis, and thereby limit diffusion of nutrients and cell products across the capsule surface. Plasminogen adsorption on TAM surfaces was the protein that showed the most attachment when letting the capsules incubate overnight. Plasminogen is a protein involved in hemostasis as it, when cleaved into activated plasmin, is able to cleave cross-linked fibrin and break up any unwanted blood clots.

4.7 Coagulation and the effect of lepirudin

In order to minimize activation of the immune system from the vials itself, we used low activating polypropylene tubes. These are still somewhat activating as could be seen from the saline negative control used as a baseline for showing increased cytokine secretion, complement triggering, and leukocyte activation. Coagulation when the whole blood was incubated in polypropylene vials was prevented by addition of the anti-coagulant lepirudin. Lepirudin is a recombinant hirudin analog derived from yeast cells, and is a direct thrombin inhibitor. As it only binds thrombin, it should therefore not affect the complement cascade. It does, however, affect the coagulation cascade and might interfere with the deposit of fibrinogen/fibrin on the capsules as thrombin is upstream of fibrinogen in the coagulation cascade.

No effect of lepirudin could be seen on fibrinogen, vitronectin, and HMWK adsorption on capsules, with a decreasing concentration of lepirudin. For the lepirudin negative vial however, the blood started coagulating when incubated with capsules. It might therefore show a false picture of coagulation protein deposits as a lot of proteins will become cross-linked in the blood

clot, and thus might not bind to the capsule. An experiment should therefore be performed using another way of preventing coagulation in the test vials, for instance by coating the vials with heparin. This would prevent coagulation without the addition of lepirudin, but might also affect the complement cascade, as heparin is reported to recruit factor H as well as exerting a broad binding specificity for plasma proteins and activating various cells in the blood [100].

4.8 Comparisons to *in vivo* biocompatibility studies

The inflammatory potential observed for the different beads and capsules tested in this work, corresponds to some extent to what has been seen in *in vivo* studies previously. For instance, a marked decrease in chemokine, inflammatory cytokine, and sTCC responses was seen for TAM beads compared to APA capsules. This might be one reason why APA capsules repeatedly have shown a higher fibroblast over-growth than TAM beads in rodent models [57, 79, 95, 101]. Nevertheless, some researchers still think the addition of a permselective polycation layer such as PLL is required in larger animals to prevent the entrance of cytokines, Ig and complement [96]. In 2009, an attempt to implant human islet cells encapsulated in barium alginate capsules was made [61]. Prolonged detection of C-peptide (used as an indicator of insulin production) was evident in only one of four patients. The result after 16 months was capsules surrounded by fibrous tissue, and which contained necrotic islet cells. Over-growth has also been observed on TAM beads to a greater extent than on PMCG capsules in a recent, as yet unpublished, study in cynomolgus monkeys [76], suggesting that the alginate bead design is at present not sufficiently optimized. Because it performs so well in the whole blood model, it might indicate that the presence of encapsulated cells plays a major role by, for instance, secreting proteins which might stimulate an immune response leading to increased over-growth. In this aspect, hollow APA capsules might be promising as they contain the permselective polycation layer, but at the same time outperform solid APA capsules in the whole blood assay as seen in this work. Hollow APA capsules with PLL did, however, elicit a greater sTCC and MCP-1 response. Hollow APA capsules with PLO, which did not elicit the same response, could therefore be of interest.

4.9 Future perspectives

The use of more complex and advanced coating layers, in an attempt to increase the stability of the alginate capsule and make them more biocompatible, are constantly being pursued. Whether it be the use of PLO instead of PLL in an attempt to decrease the immunogenicity of the capsules, the use of stabilizing PMCG (poly-methylene-co-guanidine) complexed with cellulose sulfate, or the introduction of biocompatible zwitterions in the coating layer of the capsule. These are all very interesting ideas which could further our search toward fully biocompatible alginate microcapsules. But as the procedure becomes more complex, with an increasing number of capsule parameters, it will at the same time be increasingly difficult to analyze the results gained from different labs. This has been one of the major obstacles when deciding what cap-

sules to make, because slight differences in alginate composition, capsule size, gelling conditions, and polycation, as well as different encapsulation procedures, makes it harder to compare the insulin independence achieved by the different research groups. A standardized capsule protocol should therefore be developed, in order to get the most out of the experiments performed, and minimize the time until we actually do come up with a satisfactory alginate capsule capable of curing Type 1 diabetes. This is why the TAM bead is so promising. It is simple to make, it is biocompatible as tested in the *in vitro* whole blood assay, and it appears to be stable enough for implantation into the peritoneal cavity. Further research into different alginate types should be continued, in order to minimize over-growth which limits the diffusion of nutrients and insulin in and out of the capsules.

Further studies could be performed with isolated monocytes to observe how they attach to the capsule surface. Incubating different capsules with cells, and observing capsules daily over a longer period of time, would tell us to what degree cells start attaching to the capsule surface. If the cells develop into macrophages, we might observe “frustrated phagocytosis”, a process in which the macrophages are not able to engulf the target capsule, and will release toxic chemicals [27] capable of inducing inflammation and over-growth. By co-culturing the macrophages with fibroblasts, over-growth could be studied with a higher level of precision. Cytokine expression of biomaterial adherent macrophages *in vivo* has previously been found to be dependent on the surface chemistry of the material [102]. Performing RT-PCR on macrophages incubated with capsules would therefore show the cytokine expression profile of the cells, and how it might change with different capsule parameters. Up-regulation of tissue factor on macrophages would also be interesting to look for, as this might help trigger the extrinsic pathway of coagulation.

The protein adsorption assay performed here was an initial screening of proteins present in the plasma that could possibly affect complement activation, coagulation cascade triggering, and leukocyte attachment. As the proteins screened for were mostly zymogens, it would also be possible to extend this screen to look for their activated counterparts, such as for instance plasmin instead of plasminogen and fibrin instead of fibrinogen. Screening for further coagulation components such as factor XIIIa might also present interesting results.

5 CONCLUSION

The present study has demonstrated the inflammatory potential of different parameters of alginate microcapsules and microbeads in the whole blood assay. The results showed the following:

Polycation containing solid APA microcapsules triggered complement activation, increased secretion of chemokines, inflammatory cytokines, and growth factors, as well as up-regulation of CD11b expression on leukocytes.

TAM alginate microbeads did not incite any significant complement activation or cytokine secretion. For almost all cytokines tested for, as well as the complement component sTCC, and CD11b expression, responses towards TAM beads were at or slightly below the saline control, indicating no activation beyond the auto-activation of the incubation vials themselves.

Hollow APA capsules with PLL triggered a rapid and strong sTCC response, as well as significantly increased secretion of the chemokine MCP-1. At the same time, a significant decrease in secretion of chemokines, cytokines, and growth factors pointed at a reduced inflammatory potential of these capsules. It was suggested that either the detected sTCC was the result of an assay mediated artifact, or that these capsules adsorbed the anaphylatoxins C3a and C5a, thus preventing the complement mediated activation of leukocytes and the subsequent secretion of cytokines.

No increased surface adsorption of C3 was detected for hollow APA capsules compared to solid APA capsules. Instead, the C3 adsorption was higher on solid APA capsules, thus not reflecting the increased sTCC generation seen for hollow APA capsules.

No apparent change in inflammatory potential could be observed by exchanging the polycation PLL with PLO, except for abolishing the strong sTCC response observed for hollow APA capsules with PLL as well as lowering the MCP-1 response.

Increasing PLL concentration resulted in increased sTCC production for High G alginate APA capsules. The same could not be observed for High M alginate capsules, however, the chemokine IL-8 and the inflammatory cytokines IL-1 β and TNF α increased with increasing PLL concentration, suggesting increased inflammation with increasing PLL concentration.

No change in inflammatory potential could be detected with varying alginate microbead diameter. Nor could any change in inflammatory potential be observed by the addition of HEPES in the gelling solution.

TAM microbeads appeared exceedingly inert with regard to protein adsorption on the bead

surface. No detectable protein deposition of the ones screened for after 6 hours of incubation in plasma was observed. A slight increase in adsorption was detected (especially for plasminogen) when incubating overnight. Solid APA capsules displayed heavy C3 deposition, as well as vitronectin and factor H on the capsules surface, suggesting increased complement activity on these capsules.

References

- [1] Penn, I. Post-transplant malignancy - The role of immunosuppression. *Drug saf* **23**, 101-112 (2000)
- [2] The Diabetes Control and Complications Trial Research Group. The effect of intensive insulin treatment of diabetes on the development and progression of long-term complication in insulin-dependent diabetes mellitus. *N Engl J Med* **329**, 977-986 (1993)
- [3] Type 1 Diabetes, 2010; Prime Group for JDRF, Mar. 2011
- [4] Rokstad, A. A. Alginate capsules as bioreactors for cell therapy. *Doctoral theses at NTNU*, **24** (2006)
- [5] Onsøyen, E. Commercial applications of alginates. *Carbohydrates in Europe* **14**, 26-31 (1996)
- [6] Thomas, S. Alginate dressings in surgery and wound management - Part 1. *J Wound Care* **9**, 56-60 (2000)
- [7] Rehm, B.H.A. Alginates: Biology and Applications. *Microbiology* **13** (2009).
- [8] Ertesvåg, H., Valla, S., and Skjåk-Bræk, G. Genetics and biosynthesis of alginates. *Carbohydrates in Europe* **14**, 14-18 (1996).
- [9] Draget, K. I., Smidsrød, O., Skjåk-Bræk, G. Alginates from algae. In *Biopolymers*, pp. 215-244, A. Wiley-VCH Verlag GmbH (2002)
- [10] Otterlei, M., Østgård, K., Skjåk-Bræk, G., Smidsrød, O., Soon-Shion, P., and Espevik, T. Induction of cytokine production from human monocytes stimulated with alginate. *J. Immunother.* **10**, 286-291 (1991)
- [11] Skjåk-Bræk, G., Grasdalen, H., and Larsen, B. Monomer sequence and acetylation pattern in some bacterial alginates. *Carbohydr. Res.* **154**, 239-250 (1986b)
- [12] Skjåk-Bræk, G., Zanetti, F., and Paoletti, S. Effect of acetylation on some solution and gelling properties of alginate. *Carbohydr. Res.* **185**, 131-138 (1989a)
- [13] Grant, G. T., Morris, E. R., Rees, D. A., Smith, P. J. C., and Thom, D. Biological interactions between polysaccharides and divalent cations: The egg-box model. *FEBS Lett* **32**, 195-198, (1973)
- [14] Haug, A., and Smidsrød, O. Selectivity of some anionic polymers for divalent metal ions. *Acta Chem. Scand.* **24**, 843-854 (1970)
- [15] Smidsrød, O., and Haug, A. Dependence upon uronic acid composition of some ion-exchange properties of alginates. *Acta Chem Scand B* **22**, 1989-1997 (1968)

- [16] Martinsen, A., Skjåk-Bræk, G., and Smidsrød, O. Alginate as immobilization material: I. Correlation between chemical and physical properties of alginate gel beads. *Biotechnology and Bioengineering* **33**, 79-89 (1989)
- [17] Mørch, Y. A. Novel alginate microcapsules for cell therapy - A study of the structure-function relationships in native and structurally engineered alginates. *Doctoral theses at NTNU*, **49** (2008)
- [18] Skjåk-Bræk, G., Grasdalen, H., and Smidsrød, O. Inhomogeneous polysaccharide ionic gels. *Carbohydr. Polym.* **10**, 31-54 (1989)
- [19] Lim, F. and Sun, A.M. Microencapsulated Islets as Bioartificial Endocrine Pancreas. *Science*, **210**, 908-910 (1980)
- [20] Rokstad, A.M., Brekke, O., Steinkjer, B., Ryan, L., Kollarikova, G., Strand, B.L., Skjåk-Bræk, G., Lacik, I., Espevik, T., and Mollnes, T.E. Alginate microbeads are complement compatible, in contrast to polycation containing microcapsules, as revealed in a human whole blood model. *Acta Biomaterialia*, **7**, 2566-2578 (2011)
- [21] De Vos, P., De Haan, B., and Van Schilfgaarde, R. Effect of the alginate composition on the biocompatibility of alginate-polylysine microcapsules. *Biomaterials* **18**, 273-278 (1997)
- [22] Qi, M., Strand, B.L., Mørch, Y., Lacík, I., Wang, Y., Salehi, P., Barbaro, B., Gangemi, A., Kuechle, J., Romagnoli, T., Hansen, M.A., Rodriguez, L.A., Benedetti, E., Hunkeler, D., Skjåk-Bræk, G., and Oberholzer, J. Encapsulation of Human Islets in Novel Inhomogeneous Alginate- Ca²⁺/Ba²⁺ Microbeads: In Vitro and In Vivo Function. *Artificial Cells, Blood Substitutes, and Biotechnology*, **36**, 5, 403-420 (2008)
- [23] Ratner, B.D. The Biocompatibility Manifesto: Biocompatibility for the Twenty-first Century. *J. of Cardiovasc. Trans. Res.* **4**, 523-527 (2011)
- [24] Anderson, J.M., Rodriguez, A., and Chang, D.T. Foreign body reaction to biomaterials. *Seminars in Immunology* **20**, 86-100 (2008)
- [25] Engberg, A. Biomaterials and Hemocompatibility. Dissertation, *Linnaeus University Press*, Kalmar, Växjö (2010)
- [26] Ekdahl, K.N., Lambris, J.D., Elwing, H., Ricklin, D., Nilsson, P.H., Teramura, Y., Nicholls, I.A., and Nilsson, B. Innate immunity activation on biomaterial surfaces: A mechanistic model and coping strategies. *Advanced drug delivery reviews* **63**, 1042-1050 (2011).
- [27] Murphy, K., Travers, P., Walport, M. *Janeway's immunobiology*, 7th ed. Garland Science, 61-81 (2007)

- [28] Gorbet, M. B., and Sefton, M. V. Biomaterial-associated thrombosis: roles of coagulation factors, complement, platelets and leukocytes. *Biomaterials* **25**, 26, 5681-5703 (2004)
- [29] Harboe, M., Ulvund, G., Vien, L., Fung, M., and Mollnes, T.E. The quantitative role of alternative pathway amplification in classical pathway induced terminal complement activation. *Clin. Exp. Immunol.* **138**, 439-446 (2004)
- [30] Spitzer, D., Mitchell, L.M., Atkinson, J.P., and Hourcade, D.E. Properdin can initiate complement activation by binding specific target surfaces and providing a platform for de novo convertase assembly. *J. Immunol.* **179**, 2600-2608 (2007)
- [31] Mollnes, T.E., Brekke, O.L., Fung, M., Fure, H., Christiansen, D., Bergseth, G. Essential role of the C5a receptor in E. coli-induced oxidative burst and inflammation. *Blood*, **100**, 1869-1877 (2002)
- [32] Kimberley, F.C., Sivasankar, B., and Paul Morgan, B. Alternative roles for CD59. *Mol Immunol* **118**, 127-36 (2006)
- [33] Su, H.R. S-protein/vitronectin interaction with the C5b and the C8 of the complement membrane attack complex. *Int Arch Allergy Immunol* **110**, 314-317 (1996)
- [34] Sim, R.B., and Laich, A. Serine proteases of the complement system. *Biochem Soc Trans* **28**, 545-550 (2000)
- [35] Thern, A., Stenberg, L., Dahlback, B., and Lindahl, G. Ig-binding surface proteins of *Streptococcus pyogenes* also bind human C4b-binding protein (C4BP), a regulatory component of the complement system. *J Immunol* **154**, 375-386 (1995)
- [36] Morrissey, J.H. Tissue factor: a key molecule in hemostatic and nonhemostatic systems. *Int J Hematol*, **79**, 2, 103-108 (2004)
- [37] Chou, J., Mackman, N., Merrill-Skoloff, G., Pedersen, B., Furie, B.C., and Furie, B. Hematopoietic cell-derived microparticle tissue factor contributes to fibrin formation during thrombus propagation. *Blood*, **104**, 10, 3190-3197 (2004)
- [38] Celi, A., Pellegrini, G., Lorenzet, R., De Blasi, A., Ready, N., Furie, B.C., and Furie, B. P-selectin induces the expression of tissue factor on monocytes. *Proc Natl Acad Sci USA*, **91**, 19, 8767-8771 (1994)
- [39] Schmaier, A.H. The elusive physiologic role of Factor XII. *J Clin Invest*, **118**, 9, 3208-3218 (2008)
- [40] Chatterjee, K., Vogler, E.A., and Siedlecki, C.A. Procoagulant activity of surface-immobilized Hageman factor. *Biomaterials*, **27**, 33, 5643-5650 (2006)

- [41] Chatterjee, K., Guo, Z., Vogler, E.A., and Siedlecki, C.A. Contributions of contact activation pathways of coagulation factor XII in plasma. *Journal of biomedical materials research*, **90**, 1, 27-34 (2008)
- [42] Hoffbrand, A.V., Moss, P., and Pettit, J. Essential haematology, 5th ed. Oxford: Blackwell Publishing Ltd. (2006)
- [43] Joseph, K., and Kaplan, A. P. Formation of Bradykinin: A Major Contributor to the Innate Inflammatory Response. *Advances in Immunology* **86**, 159–208 (2005)
- [44] Gros, P., Milder, F.J., and Janssen, B.J. Complement driven by conformational changes. *Nat Rev Immunol*, **8**, 1, 48-58 (2008)
- [45] Wettero, J., Bengtsson, T., and Tengvall, P. C1q-independent activation of neutrophils by immunoglobulin M-coated surfaces. *J Biomed Mater Res*, **57**, 4, 550-558 (2001)
- [46] Schousboe, I., Nyström, B.T., and Hansen, G.H. Differential binding of factor XII and activated factor XII to soluble and immobilized fibronectin-localization of the Hep-1/Fib-1 binding site for activated factor XII. *FEBS J.* **275**, 5161-5172 (2008)
- [47] Wu, Y., Simonovsky, F.I., Ratner, B.D., and Horbett, T.A. The role of adsorbed fibrinogen in platelet adhesion to polyurethane surfaces: a comparison of surface hydrophobicity, protein adsorption, monoclonal antibody binding, and platelet adhesion. *J. Biomed. Mater. Res. A*, **74**, 722-738 (2005)
- [48] Anderson, J.M., Rodriguez, A., Chang, D.T. Review: Foreign body reaction to biomaterials. *Seminars in Immunology* **20**, 86-100 (2008)
- [49] Ziats, N., Pankowsky, D.A., Tierney, B.P., Ratnoff, O.D., and Anderson, J.M. Adsorption of Hageman Factor (Factor XII) and other human plasma proteins to biomedical polymers. *J Lab Clin Med*, **116**, 687-696 (1990)
- [50] Mulzer, S.R., and Brash, J.L. Identification of plasma proteins adsorbed to hemodialyzers during clinical use. *J Biomed Mater Res*, **23**, 1483-1504 (1989)
- [51] Cornelius, R.M., and Brash, J.L. Identification of proteins adsorbed to hemodialyser membranes from heparinized plasma. *J Biomater Sci Polym Ed*, **4**, 291-304 (1993)
- [52] Burman, J.F., Chung, H.I., and Lane, D.A. Role of Factor XII in thrombin generation and fibrinolysis during cardiopulmonary bypass. *Lancet*, **344**, 1192-1193 (1994)
- [53] Hong, J., Ekdahl, N.K., Reynolds, H., Larsson, R., and Nilsson, B. A new in vitro model to study interaction between whole blood and biomaterials. Studies of platelet and coagulation activation and the effect of aspirin. *Biomaterials*, **20**, 603-611 (1999)
- [54] Martin, P., Leibovich, S.J. Inflammatory cells during wound repair: the good, the bad and the ugly. *Trends Cell Biol* **15**, 599–607 (2005)

- [55] Miller, K.M., Anderson, J.M. In vitro stimulation of fibroblast activity by factors generated from human monocytes activated by biomedical polymers. *J Biomed Mater Res* **23** 911–30 (1989)
- [56] Babensee, J.E., Anderson, J.M., McIntire, L.V., Mikos, A.G. Host response to tissue engineered devices. *Advanced Drug Delivery Reviews* **33**, 111-139 (1998)
- [57] Duvivier-Kali, V.F., Omer, A., Parent R.J., O’Neil, J.J., and Weir, G.C. Complete protection of islets against allorejection and autoimmunity by a simple barium-alginate membrane. *Diabetes* **50**, 1698 –1705 (2001)
- [58] Soon-Shiong, P., Feldman, E., Nelson, R., Heintz, R., Yao, Q., Yao, Z., Zheng, T., Merideth, N., Skjåk-Bræk, G., and Espevik, T. Long-term reversal of diabetes by the injection of immunoprotected islets. *Proc. Natl. Acad. Sci. USA*, **90**, 5843-5847 (1993)
- [59] Elliott, R.B., Escobar, L., Calafiore, R., Basta, G., Garkavenko, O., Vasconcellos, A., and Bimbra, C. Transplantation of Micro- and Macroencapsulated Piglet Islets Into Mice and Monkeys. *Transplantation Proceedings*, **37**, 466–469 (2005)
- [60] Basta, G., Montanucci, P., Luca, G., Boselli, C., Noya, G., Barbaro, B., Qi, M., Kinzer, K., Oberholzer, J., and Calafiore, R. Long-Term Metabolic and Immunological Follow-Up of Nonimmunosuppressed Patients With Type 1 Diabetes Treated With Microencapsulated Islet Allografts - Four Cases. *Diabetes Care*, **34**, 2406-2409 (2011)
- [61] Tuch, B.E., Keogh, G.W., Williams, L.J., Wu, W., Foster, J.L., Vaithilingam, V., and Philips, R. Safety and viability of microencapsulated human islets transplanted into diabetic humans. *Diabetes Care* **32**, 1887-1889 (2009)
- [62] Wang, X.Y., Robertson, J.L., Spillman, W.B., and Claus, R.O. Effects of the chemical structure and the surface properties of polymeric biomaterials on their biocompatibility. *Pharm Res*, **21**, 1362-73 (2004)
- [63] Vendra, V.K., Wu, L., and Krishnan, S. Polymer Thin Films for Biomedical Applications. *Nanomaterials for the Life Sciences Vol.5: Nanostructured Thin Films and Surfaces*, WILEY-VCH Verlag GmbH & Co. KGaA, Weinheim (2010)
- [64] Andersson, J., Larsson, R., Richter, R., Ekdahl, K.N., and Nilsson, B. Binding of a model regulator of complement activation (RCA) to a biomaterial surface: surface-bound factor H inhibits complement activation. *Biomaterials*, **22**, 2435-43 (2001)
- [65] Thorslund, S., Sanchez, J., Larsson, R., Nikolajeff, F., and Bergquist, J. Functionality and stability of heparin immobilized onto poly(dimethylsiloxane). *Colloids Surf B Biointerfaces*, **45**, 76-81 (2005)

- [66] Videm, V., Mollnes, T.E., Bergh, K., Fosse, E., Mohr, B., Hagve, T.A., Aasen, A.O., and Svennevig, J.L. Heparin-coated cardiopulmonary bypass equipment. II. Mechanisms for reduced complement activation in vivo. *J Thorac Cardiovasc Surg*, **117**, 803-809 (1999)
- [67] Kopp, R., Mottaghy, K., and Kirschfink, M. Mechanism of complement activation during extracorporeal blood-biomaterial interaction: effects of heparin coated and uncoated surfaces. *Asaio J*, **48**, 598-605 (2002)
- [68] Wendel, H.P. and Ziemer, G. Coating-techniques to improve the hemocompatibility of artificial devices used for extracorporeal circulation. *Eur J Cardiothorac Surg*, **16**, 342-350 (1999)
- [69] Seifert, B., Romaniuk, P., and Groth, T. Covalent immobilization of hirudin improves the haemocompatibility of polylactide-polyglycolide in vitro. *Biomaterials*, **18**, 1495-1502 (1997)
- [70] Paul, W. and Sharma, C.P. Acetylsalicylic acid loaded poly(vinyl alcohol) hemodialysis membranes: effect of drug release on blood compatibility and permeability. *J Biomater Sci Polym Ed*, **8**, 755-764 (1997)
- [71] Strand, B.L., Gåserød, O., Kulseng, B., Espevik, T., Skjåk-Bræk, G. Alginate-polylysine-alginate microcapsules: effect of size reduction on capsule properties. *J Microencapsul* **19**, 615-630 (2002)
- [72] Mollnes, T.E., Lea, T., and Harboe, M. Detection and quantification of the terminal C5b-9 complex of human complement by a sensitive enzyme-linked immunosorbent assay. *Scand. J. Immunol.* **20**, 157-166 (1984)
- [73] Bio-Rad Laboratories, Inc.: Bio-Plex Pro Assays - Cytokine chemokine, and Growth Factors, Instruction Manual
- [74] Ryan, L., and Steinkjer, B. : Personal communication (Alteration of human ELISA procedure and Bio-plex procedure)
- [75] Lappegård, K.T., Bergseth, G., Riesenfeld, J., Pharo, A., Magotti, P., Lambris, J.D., and Mollnes T.E. The artificial surface-induced whole blood inflammatory reaction revealed by increases in a series of chemokines and growth factors is largely complement dependent. *Inc. J Biomed Mater Res* **87A**, 129-135 (2008)
- [76] Rokstad, A.M. : Personal communication (as yet unpublished *in vivo* trials with TAM beads, and whole blood tests performed on TAM beads, APA capsules, AP capsules and PMCG capsules)
- [77] Bergseth, G., Lambris, J.D., Mollnes, T.E., and Lappegård, K.T. Artificial Surface-Induced Inflammation Relies on Complement Factor 5: Proof From a Deficient Person. *Ann. Thorac. Surg.* **91**, 527-533 (2011)

- [78] Sokolov, A., Hellerud, B.C., Johannessen, E.A., and Mollnes, T.E. Inflammatory response induced by candidate biomaterials of an implantable microfabricated sensor. *J Biomed Mater Res Part A*. **100A**, 1142–1150 (2012)
- [79] Strand, B.L., Ryan, L., In't Veld, P., Kulseng, B., Rokstad, A.M., Skjåk-Bræk, G. and Espevik, T. Poly-L-Lysine induces fibrosis on alginate microcapsules via the induction of cytokines. *Cell Transplant*. **10**, 263-275 (2001)
- [80] Mørch, Y.A., Donati, I., Strand, B.L., and Skjåk-Bræk, G. Effect of Ca^{2+} , Ba^{2+} , and Sr^{2+} on alginate microbeads. *Biomacromolecules* **7**, 1471-1480 (2006)
- [81] Thu, B., Gåserød, O., Paus, D., Mikkelsen, A., Skjåk-Bræk, G., Toffanin, R., Vittur, F., and Rizzo, R. Inhomogeneous alginate gel spheres: an assessment of the polymer gradients by synchrotron radiation-induced X-ray emission, magnetic resonance microimaging, and mathematical modeling. *Biopolymers* **53**, 60-71 (2000)
- [82] Kulseng, B., Thu, B., Espevik, T., and Skjåk-Bræk, G. Alginate polylysine capsules as an immune barrier: Permeability of cytokines and immunoglobulins over the capsule membrane. *Cell Transplant*, **6**, 387-394 (1997)
- [83] Lanza, R.P., Kuhlreiber, W.M., Ecker, D., Staruk, J.E., and Chick, W.L. Xenotransplantation of porcine and bovine islets without immunosuppression using uncoated alginate microspheres. *Transplantation*, **59**, 1377-1384 (1995)
- [84] Banerjee, I., Pangule, R.C., and Kane, R.S. Antifouling Coatings: Recent Developments in the Design of Surfaces That Prevent Fouling by Proteins, Bacteria, and Marine Organisms. *Adv. Mater.* **23**, 690–718 (2011)
- [85] Kasák, P., Kroneková, Z., Krupa, I., and Lacík, I. Zwitterionic hydrogels crosslinked with novel zwitterionic crosslinkers: Synthesis and characterization. *Polymer* **52**, 3011-3020 (2011)
- [86] Rinder, C.S., Smith, M.J., Rinder, H.M., Cortright, D.N., Brodbeck, R.M., Krause, J.E., and Smith, B.R. Leukocyte effects of C5a-receptor blockade during simulated extracorporeal circulation. *Ann. Thorac. Surg.* **83**, 146-152 (2007)
- [87] Nilsson, B., Larsson, R., Hong, J., Elgue, G., Ekdahl, K.N., Sahu, A., and Lambris, J.D. Compstatin inhibits complement and cellular activation in whole blood in two models of extracorporeal circulation. *Blood* **92**, 1661-1667 (1998)
- [88] Pan, Z.K. Anaphylatoxins C5a and C3a induce nuclear factor kappaB activation in human peripheral blood monocytes. *Biochim.Biophys.Acta* **1443**, 90-98 (1998)
- [89] Monsinjon, T., Gasque, P., Chan, P., Ischenko, A., Brady, J.J., and Fontaine, M. et al. Regulation by complement C3a and C5a anaphylatoxins of cytokine production in human umbilical vein endothelial cells. *Faseb J.* **17**, 1003-1014 (2003)

- [90] Takeda, Y., Kaneda, K., Jimma, F., Shiobara, N., Hidaka, M., Saniabadi, A. R. and Wakabayashi, I. Inhibition of CXCL10 release by monomeric C3bi and C4b. *Clinical and Experimental Immunology*, **167**, 149–157 (2011)
- [91] Calafiore, R., Basta, G., Luca, G., Boselli, C., Bufalari, A., Cassarani, M.P., Giustozzi, G.M., and Brunetti, P. Transplantation of pancreatic islets contained in minimal volume microcapsules in diabetic high mammals. *Ann NY Acad Sci*, **875**, 219–232 (1999)
- [92] Calafiore, R., Basta, G., Luca, G., Lemmi, A., Racanicchi, L., Mancuso, F., Montanucci, M.P., and Brunetti, P. Standard technical procedures for microencapsulation of human islets for graft into nonimmunosuppressed patients with type 1 diabetes mellitus. *Transplant Proc*, **38**, 1156–1157 (2006)
- [93] Bystricky, S., Malovikova, A., and Sticzay, T. Interaction of alginate and pectins with cationic polypeptides. *Carbohydr Res* **13**, 283–294 (1990)
- [94] Clayton, H.A., London, N.J.M., Colloby, P.S., Bell, P.R.F., and James, R.F.L. The effect of capsule composition on the biocompatibility of alginate- poly-L-lysine capsules. *J Microencapsul* **8**, 221–33 (1991)
- [95] King, A., Sandler, S., and Andersson, A. The effect of host factors and capsule composition on the cellular overgrowth on implanted alginate capsules. *J Biomed.Mater.Res* **57**, 374–383 (2001)
- [96] O’Sullivan, E.S., Vegas, A., Anderson, D.G., and Weir, G.C. Islets Transplanted in Immunoisolation Devices: A Review of the Progress and the Challenges that Remain. *Endocrine Reviews* **32**, 827–844 (2011)
- [97] Tam, S.K., Dusseault, J., Polizu, S., Menard, M., Halle, J.P., and Yahia, L. Impact of residual contamination on the biofunctional properties of purified alginates used for cell encapsulation. *Biomaterials* **27**, 1296–1305 (2006)
- [98] Voskerician, G., Anderson, J.M., and Ziats, N.P. High molecular weight kininogen inhibition of endothelial cell function on biomaterials. *Journal of Biomedical Materials Research* **51**, 1–9 (2000)
- [99] Schmaier, A.H. Contact activation: a revision. *Thromb Haemost* **77**, 101–107 (1997)
- [100] Wu, Y-Q., Qu, H., Sfyroera, G., Tzekou, A., Kay, B.K., Nilsson, B., Ekdahl, K.N., Ricklin, D., and Lambris, J.D. Protection of nonself Surfaces from Complement attack by factor H-binding peptides: Implications for therapeutic medicine. *J Immunol.* **186**, 4269–4277 (2011)
- [101] Safley, S.A., Cui, H., Cauffiel, S., Tucker-Burden, C., and Weber, C.J. Biocompatibility and immune acceptance of adult porcine islets transplanted intraperitoneally in diabetic

- NOD mice in calcium alginate poly-L-lysine microcapsules versus barium alginate microcapsules without poly-L-lysine. *J.Diabetes Sci.Technol.* **2**, 760-767 (2008)
- [102] Brodbeck, W.G., Voskerician, G., Ziats, N.P., Nakayama, Y., Matsuda, T., and Anderson, J.M. In vivo leukocyte cytokine mRNA responses to biomaterials are dependent on surface chemistry. *J Biomed Mater Res A* **64**, 320-329 (2003)

A Materials and instruments

A list of materials and instruments are shown in tables A.1, A.2, and A.3 below.

Table A.1: List of the reagents used in the experiments

<i>Reagent</i>	<i>Producer</i>	<i>Catalogue number</i>	<i>Additional Information</i>
UP-LVG	Pronova, NovaMatrix, Norway	Batch: FP-603-04	$F_G=0.67$, $F_{GG}=0.55$, $N_{G>1}=12$
UP-LVG*	Pronova, NovaMatrix, Norway	Batch: BP-1108-01	$F_G=0.67$, $F_{GG}=0.55$, $N_{G>1}=12$
UP-100M	Pronova, NovaMatrix, Norway	Batch: FP-209-02	$F_G=0.44$
Poly-L-Lysine Hydrochloride	Sigma-Aldrich Corp., St. Louis, MO, USA	P2658-1G	DP(vis)=127, MW(vis)=20900, DP(MALLS)=69, MW(MALLS)=11400
Poly-L-Ornithine Hydrobromide	Sigma-Aldrich Corp., St. Louis, MO, USA	P-3530	DP(vis)=118, MW(vis)=2300 DP(LALLS)=102, MW(LALLS)=19900
CaCl ₂ , BaCl ₂ , Na-citrate D-mannitol	Merck, Darmstadt, Germany BDH Anala R., VWR International Ltd, Pool, England		HPLC degree
LPS from E.coli strain 0111:B4 Zymosan	Invivogen, San Diego, USA Sigma-Aldrich Corp., St. Louis, MO, USA	t1rl-pelps Z4250	
Phosphate-buffered saline, PBS Bovine serum albumin, BSA	Oxoid, Hampshire, England Sigma-Aldrich Corp., St. Louis, MO, USA	BR0014G A7030-50G	
Dulbecco's Phosphate- Buffered Saline, DPBS	Sigma-Aldrich Corp., St. Louis, MO, USA	D8537	
Refludan (Lepirudin)	Celgene Corporation, Summit, NJ, USA	PZN-2480375	
EDTA, 510 mM Paraformaldehyde, PFA LDS-751	Sigma-Aldrich Corp., St. Louis, MO, USA Life Technologies, New York, USA	300410 P6148-1KG L7595	
Color reagent CD14 Color reagent CD11b EasyLyse	BD Biosciences, USA BD Biosciences, USA Dako Cytomation, Glostrup, Denmark	345784 333142	Erythrocyte lysis buffer

Table A.2: List of the reagents used in the experiments

<i>Reagent</i>	<i>Producer</i>	<i>Catalogue number</i>	<i>Additional Information</i>
α C3c Ab	Dako Cytomation, Glostrup, Denmark	FO210	FITC labeled rabbit anti-human C3c
α Fibrinogen Ab	Dako Cytomation, Glostrup, Denmark	FO111	FITC labeled rabbit anti-human fibrinogen
Neg. Control	Dako Cytomation, Glostrup, Denmark	FO261	FITC labeled rabbit anti-mouse IgG
α FactorH	The Binding Site Grout Ltd, Birmingham, UK	PC030	Sheep anti-human factor H
α Factor I	The Binding Site Grout Ltd, Birmingham, UK	PC031	Sheep anti-human factor I
α Plasminogen	The Binding Site Grout Ltd, Birmingham, UK	PC065	Sheep anti-human plasminogen
α Vitronectin	The Binding Site Grout Ltd, Birmingham, UK	PC111	Sheep anti-human vitronectin
α HMW Kininogen	The Binding Site Grout Ltd, Birmingham, UK	PC115	Sheep anti-human HMW Kininogen
α Fibrinogen	The Binding Site Grout Ltd, Birmingham, UK	PC056	Sheep anti-human fibrinogen
α C1 inactivator	The Binding Site Grout Ltd, Birmingham, UK	PC019	Sheep anti-human C1-i
Neg. Control	Sigma-Aldrich Corp., St. Louis, MO, USA	I5131	Sheep IgG
2 ^o Ab	Sigma-Aldrich Corp., St. Louis, MO, USA	SAB4600134	CF 633 labeled donkey anti-sheep IgG
Human CXCL8/IL-8 DuoSet ELISA kit	R&D Systems, USA	DY208	
Human TNF- α DuoSet ELISA kit	R&D Systems, USA	DY210	
Tween20			
TCC primary antibody, anti-C5b-9	AntiBodyShop, Gentofte, Denmark	DIA 011-01	
Biotinylated Monoclonal Anti-human	Quidel, San Diego, USA	A711	
SC5b-9 (TCC secondary antibody)			
Streptavidin-PE	BioLegend, San Diego, USA	405210	
Substrate reagent A	R&D Systems, Minneapolis, USA	DY999	
Substrate reagent B	R&D Systems, Minneapolis, USA	DY999	
1 M H_2SO_4	R&D Systems, Minneapolis, USA	DY994	
Bio-plex kit (17-plex)	Bio-Rad Laboratories, Inc., Hercules, California, USA	M50-0003IYV	

Table A.3: List of equipment used in the experiments

<i>Equipment</i>	<i>Producer</i>	<i>Catalogue number</i>
Centrifuge	Kubota Corporation, Tokyo, Japan	
Epics XL-MCL Flow cytometer	Beckman Coulter, Inc., Brea, California, USA	WS-EPICSXL
LSM 510 Meta	Carl Zeiss, Jena, Germany	
Confocal Microscope		
Bio-Plex Pro Wash Station	Bio-Rad Laboratories, Inc., Hercules, California, USA	300-34376
Plate shaker	Heidolph Instruments, Schwabach, Germany	
Bio-Plex 200 System	Bio-Rad Laboratories, Inc., Hercules, California, USA	
DynaMag Spin	Invitrogen, Carlsbad, California, USA	123.20D
Magnetic separator		
1.8 mL Cryo tubes	Nunc, Roskilde, Denmark	366656
24-well culture plates	Nunc, Roskilde, Denmark	145387
96-well storage plates	Nunc, Roskilde, Denmark	
1.8 mL polypropylene tubes	Nunc, Roskilde, Denmark	363401
Falcon flow tubes		
ELISA plates	R&D Systems, Minneapolis, USA	DY990
ELISA Plate Sealers	R&D Systems, Minneapolis, USA	DY992
Bio-Rad Plate reader	Bio-Rad Laboratories, Inc., Hercules, California, USA	
Microplate Manager	Bio-Rad Laboratories, Inc., Hercules, California, USA	
Software, version 6.1		

B Individual donors

A comparison of IL-8 secretion, sTCC formation, and leukocyte CD11b expression for three individual donors after 1 hour incubation in whole blood is shown in figure B.1. The comparison shows the variation present in the IL-8 data, which makes it hard to detect any trends. The sTCC data are much more stable. It appears like sTCC generation is strongest for hollow capsules with PLL, with PLO hollow capsules showing a smaller response. CD11b expression reflect the sTCC data to a certain degree. Interpreting the CD11b results may not be as straightforward, as it could be that some capsules acitvated the cells but that the cells then attached to the capsule surface, and were therefore not detected by the flow cytometer. Use of PLO in hollow capsules appeared to affect the up-regulation of the receptor to a lesser extent than when using PLL. In addition, the same decrease in up-regulation was seen when increasing the PLL content from 0.05 % to 0.10 % in the high M capsules, a trend that was also seen in sTCC formation. This effect was inverted when the alginate was changed to high G, where an increase in PLL resulted in an increased sTCC generation, as well as increased CD11b up-regulation.

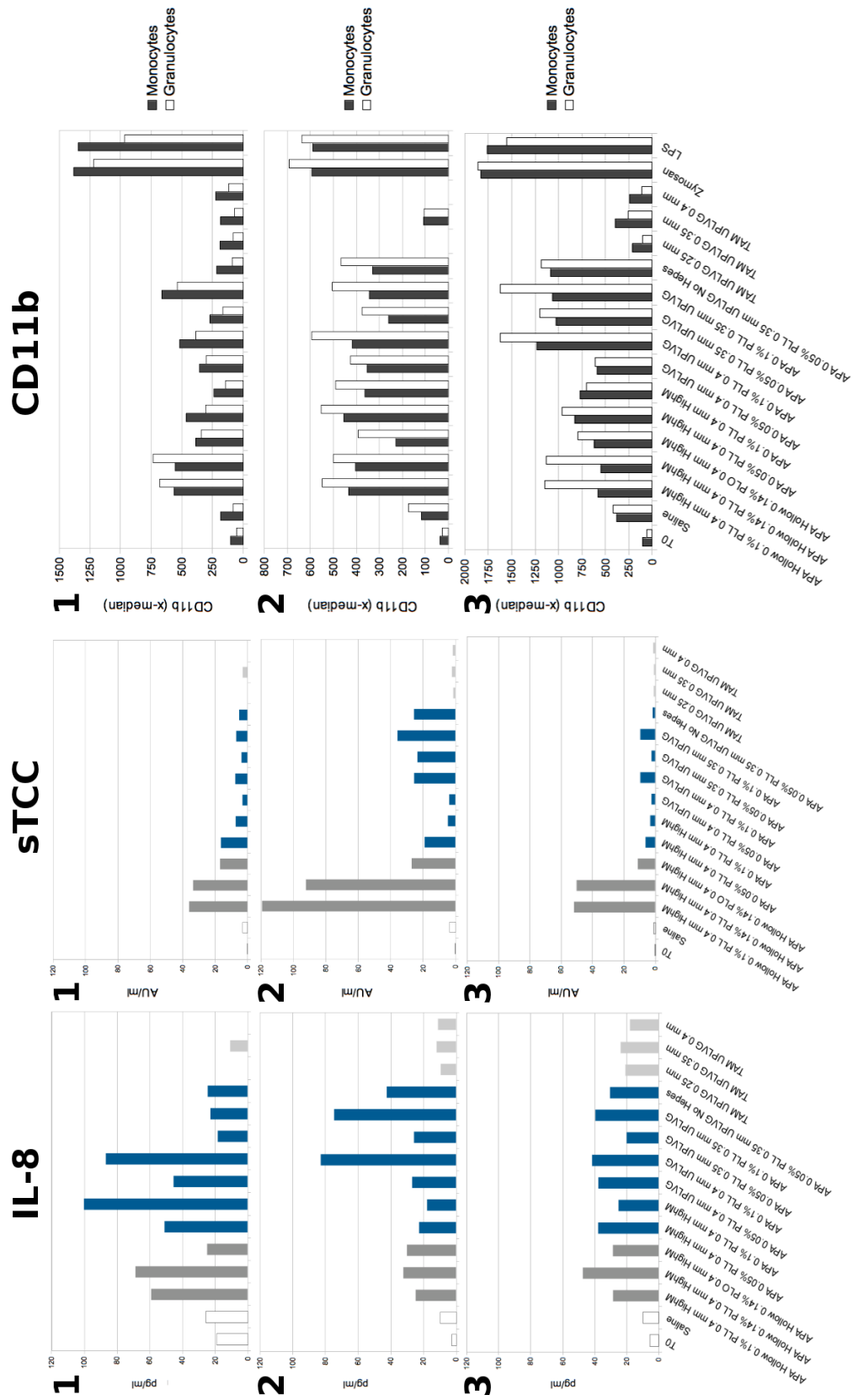


Figure B.1: IL-8 secretion, sTCC generation, and leukocyte CD11b expression for 3 donors (donor 1, 2, and 3) after 1 hour incubation in lepirudin anti-coagulated whole blood. CD11b expression was measured as median fluorescence intensity on monocytes and granulocytes.

C ELISA data

IL-8 and sTCC levels in plasma after incubating alginate microcapsules in whole blood for 1 and 4 hours are shown in tables C.1-C.4 below.

C.1 IL-8 1 h

Table C.1: IL-8 levels for 5 donors after 1 hour incubation in whole blood. Values are in pg/ml.

Sample	Donor 1	Donor 2	Donor 3	Donor 4	Donor 5
T0	18.91	2.84	2.07	2.83	5.65
Saline	25.73	14.58	4.21	9.79	10.01
Hollow, M. pyr, 0.10 % PLL, 0.4 mm	58.96	28.67	28.41	24.68	28.39
Hollow, M. pyr, 0.14 % PLL, 0.4 mm	68.55	17.90	24.69	32.20	47.27
Hollow, M. pyr, 0.14 % PLO, 0.4 mm	24.70	21.23	40.44	29.97	28.46
Solid, M. pyr, 0.05 % PLL, 0.4 mm	50.78	16.11	19.33	22.60	37.69
Solid, M. pyr, 0.10 % PLL, 0.4 mm	100.16	23.12	48.63	17.66	24.93
Solid, UP-LVG, 0.05 % PLL, 0.4 mm	45.26	36.97	44.50	26.81	37.56
Solid, UP-LVG, 0.10 % PLL, 0.4 mm	86.70	31.09	97.05	82.81	41.50
Solid, UP-LVG, 0.05 % PLL, 0.35 mm	18.23	68.02	17.81	25.71	19.92
Solid, UP-LVG, 0.10 % PLL, 0.35 mm	22.72	23.43	17.60	74.62	39.43
Solid, UP-LVG, 0.05 % PLL, 0.35 mm	24.30	17.78	19.33	42.34	30.27
No Hepes					
TAM, UP-LVG, 0.25 mm	-	9.72	8.86	9.31	20.69
TAM, UP-LVG, 0.35 mm	10.57	11.71	7.94	11.81	23.66
TAM, UP-LVG, 0.40 mm	-	8.06	13.37	10.98	17.84
Zymosan	229.28	459.83	236.57	354.70	468.72
LPS	383.06	83.98	120.65	186.44	155.64

C.2 IL-8 4 h

Table C.2: IL-8 levels for 5 donors after 4 hour incubation in whole blood. Values are in pg/ml.

Sample	Donor 1	Donor 2	Donor 3	Donor 4	Donor 5
T0	1.39	2.64	8.67	3.25	4.47
Saline	690.61	294.87	352.98	257.3	155.13
Hollow, M. pyr, 0.10 % PLL, 0.4 mm	1189.7	944.09	1208.51	403.59	1478.59
Hollow, M. pyr, 0.14 % PLL, 0.4 mm	1148.1	2467.1	1080.83	362.37	1100.26
Hollow, M. pyr, 0.14 % PLO, 0.4 mm	1869.15	185.69	868.57	659.84	977.29
Solid, M. pyr, 0.05 % PLL, 0.4 mm	3851.47	4304.11	1557.54	686.93	2168.65
Solid, M. pyr, 0.10 % PLL, 0.4 mm	5367.82	6879.56	2171.52	2790.91	4792.96
Solid, UP-LVG, 0.05 % PLL, 0.4 mm	6598.7	6802	2007.47	3117.16	2375.64
Solid, UP-LVG, 0.10 % PLL, 0.4 mm	10065.59	5344.2	1597.2	3260.5	2725.64
Solid, UP-LVG, 0.05 % PLL, 0.35 mm	6216.19	3453.91	1176.64	419.15	2221.74
Solid, UP-LVG, 0.10 % PLL, 0.35 mm	5335.63	4023.72	1225.66	1976.23	2917.54
Solid, UP-LVG, 0.05 % PLL, 0.35 mm No Hepes	3951.62	6128.61	753.95	741.17	2888.94
TAM, UP-LVG, 0.25 mm	-	127.87	160.79	295.5	171.86
TAM, UP-LVG, 0.35 mm	116.11	165.28	135.55	294.24	145.91
TAM, UP-LVG, 0.40 mm	-	208.42	93.31	266.02	377.67
Zymosan	9595.97	12191.85	8063.48	4852	11370.28

C.3 sTCC 1 h

Table C.3: sTCC levels for 5 donors after 1 hour incubation in whole blood. Values are in pg/ml.

Sample	Donor 1	Donor 2	Donor 3	Donor 4	Donor 5
T0	0.16	0.39	0.46	0.18	0.42
Saline	3.04	2.81	1.19	3.43	1.17
Hollow, M. pyr, 0.10 % PLL, 0.4 mm	35.91	46.41	61.98	119.19	51.67
Hollow, M. pyr, 0.14 % PLL, 0.4 mm	33.50	31.62	57.23	92.08	50.01
Hollow, M. pyr, 0.14 % PLO, 0.4 mm	16.83	9.06	13.53	26.85	11.03
Solid, M. pyr, 0.05 % PLL, 0.4 mm	16.30	3.40	10.03	18.99	6.09
Solid, M. pyr, 0.10 % PLL, 0.4 mm	7.16	2.70	2.19	4.56	3.06
Solid, UP-LVG, 0.05 % PLL, 0.4 mm	2.98	2.51	3.12	3.76	2.26
Solid, UP-LVG, 0.10 % PLL, 0.4 mm	7.41	3.44	12.20	25.36	9.41
Solid, UP-LVG, 0.05 % PLL, 0.35 mm	3.53	3.28	10.08	23.38	2.25
Solid, UP-LVG, 0.10 % PLL, 0.35 mm	6.86	7.53	12.04	35.67	9.41
Solid, UP-LVG, 0.05 % PLL, 0.35 mm No Hepes	5.01	3.54	11.98	25.42	1.54
TAM, UP-LVG, 0.25 mm		1.81	1.14	1.21	0.88
TAM, UP-LVG, 0.35 mm	2.80	1.60	1.41	2.11	0.80
TAM, UP-LVG, 0.40 mm		1.79	0.93	1.57	1.23
Zymosan	54.47	63.72	75.30	147.85	71.39
LSP	6.53	2.43	3.55	7.01	2.00

C.4 sTCC 4 h

Table C.4: sTCC levels for 5 donors after 4 hour incubation in whole blood. Values are in pg/ml.

Sample	Donor 1	Donor 2	Donor 3	Donor 4	Donor 5
T0	0.46	0.39	0.41	0.61	0.24
Saline	31.36	14.08	11.04	23.47	6.30
Hollow, M. pyr, 0.10 % PLL, 0.4 mm	65.19	224.98	170.40	163.98	111.70
Hollow, M. pyr, 0.14 % PLL, 0.4 mm	59.98	152.65	161.39	163.88	105.97
Hollow, M. pyr, 0.14 % PLO, 0.4 mm	38.70	35.50	32.64	72.03	35.78
Solid, M. pyr, 0.05 % PLL, 0.4 mm	37.81	47.57	81.10	82.01	38.62
Solid, M. pyr, 0.10 % PLL, 0.4 mm	33.78	73.48	127.77	92.94	50.29
Solid, UP-LVG, 0.05 % PLL, 0.4 mm	19.57	13.34	45.06	22.06	7.20
Solid, UP-LVG, 0.10 % PLL, 0.4 mm	29.58	86.13	72.31	65.59	53.09
Solid, UP-LVG, 0.05 % PLL, 0.35 mm	20.29	36.00	66.32	52.69	20.80
Solid, UP-LVG, 0.10 % PLL, 0.35 mm	29.28	118.86	96.97	122.94	42.59
Solid, UP-LVG, 0.05 % PLL, 0.35 mm	20.09	32.75	94.39	106.36	14.63
No Hepes					
TAM, UP-LVG, 0.25 mm		3.30	3.18	14.11	4.62
TAM, UP-LVG, 0.35 mm	8.53	2.96	4.30	12.37	4.47
TAM, UP-LVG, 0.40 mm		3.18	3.70	15.06	3.74
Zymosan	134.51	128.22	116.78	193.61	149.99
LPS	40.73	9.80	10.41	22.38	6.36

D Bio-plex data

Cytokine levels in plasma after incubating alginate microcapsules in whole blood for 4 hours are shown in tables D.1-D.28 below.

D.1 MIP-1 α

Table D.1: MIP-1 α levels for 5 donors. Values are in pg/ml.

Sample	Donor 1	Donor 2	Donor 3	Donor 4	Donor 5
T0	2.84	1.72	4.99	1.36	2.04
Saline	32.68	43.08	76.11	30.3	31.81
Hollow, M. pyr, 0.10 % PLL, 0.4 mm	76.23	21.34	46.64	32.51	131.08
Hollow, M. pyr, 0.14 % PLL, 0.4 mm	78.09	134.57	79.90	32.96	139.63
Hollow, M. pyr, 0.14 % PLO, 0.4 mm	91.56	34.95	74.40	65.14	95.26
Solid, M. pyr, 0.05 % PLL, 0.4 mm	439.32	722.80	231.34	121.22	239.48
Solid, M. pyr, 0.10 % PLL, 0.4 mm	611.82	365.44	345.18	330.94	558.93
Solid, UP-LVG, 0.05 % PLL, 0.4 mm	551.19	410.65	369.65	384.09	493.94
Solid, UP-LVG, 0.10 % PLL, 0.4 mm	1332.41	341.76	123.80	374.21	247.56
Solid, UP-LVG, 0.05 % PLL, 0.35 mm	532.37	483.59	161.19	67.91	444.59
Solid, UP-LVG, 0.10 % PLL, 0.35 mm	635.24	372.72	167.12	207.29	305.89
Solid, UP-LVG, 0.05 % PLL, 0.35 mm	339.16	819.67	153.68	94.2	509.65
No Hepes					
TAM, UP-LVG, 0.25 mm	-	35.09	60.68	84.13	76.29
TAM, UP-LVG, 0.35 mm	33.37	31.22	47.16	79.96	60.18
TAM, UP-LVG, 0.40 mm	-	49.84	43.34	80.14	124.39
Zymosan	3310.35	2995.8	1841.37	3107.1	3677.83

Table D.2: MIP-1 α levels for 2 donors. Values are in pg/ml. * = value extrapolated beyond standard range

Sample	Donor 1	Donor 2
T0	1.93	*0.29
Saline	234.3	120.06
Solid, UP-LVG, 0.05 % PLL, 0.4 mm	381.29	242.34
Solid, M. pyr, 0.05 % PLL, 0.4 mm	386.36	133.51
TAM, UP-LVG, 0.4 mm, No BaCl ₂	168.32	101.36
TAM, UP-LVG, 0.4 mm	147.81	76.98
TAM, M. pyr, 0.4 mm	179.65	106.5
TAM4, UP-LVG*, 0.4 mm	140.89	73.28
TAM, UP-LVG, 0.35 mm, No BaCl ₂	263.93	140.89
TAM, UP-LVG, 0.35 mm	179.07	44.28
TAM, M. pyr, 0.35 mm	151.96	95.63
TAM4, UP-LVG*, 0.35 mm	107.88	58.45
Zymosan	2426.92	2660.28

D.2 MCP-1

Table D.3: MCP-1 levels for 5 donors. Values are in pg/ml.

Sample	Donor 1	Donor 2	Donor 3	Donor 4	Donor 5
T0	66.29	69.08	49.61	63.26	94.58
Saline	151.19	114.74	73.27	86.65	81.72
Hollow, M. pyr, 0.10 % PLL, 0.4 mm	479.36	538.99	195.77	124.54	369.72
Hollow, M. pyr, 0.14 % PLL, 0.4 mm	460.32	586.26	200.39	142.37	415.07
Hollow, M. pyr, 0.14 % PLO, 0.4 mm	384.25	123.07	95.56	132.92	227.94
Solid, M. pyr, 0.05 % PLL, 0.4 mm	347.53	355.1	146.25	115.94	253.77
Solid, M. pyr, 0.10 % PLL, 0.4 mm	171.48	202.87	144.18	115.64	238.41
Solid, UP-LVG, 0.05 % PLL, 0.4 mm	221.57	386.48	155.67	120.71	218.06
Solid, UP-LVG, 0.10 % PLL, 0.4 mm	163.44	384.78	132.63	140.13	248.75
Solid, UP-LVG, 0.05 % PLL, 0.35 mm	199.39	334.26	128.32	109.88	243.24
Solid, UP-LVG, 0.10 % PLL, 0.35 mm	275.28	488.29	138.59	165.03	349.26
Solid, UP-LVG, 0.05 % PLL, 0.35 mm	286.83	451.04	110.33	110.49	217.82
No Hepes					
TAM, UP-LVG, 0.25 mm		138.31	70.37	87.15	99.25
TAM, UP-LVG, 0.35 mm	95.56	150.37	68.16	82.92	93.12
TAM, UP-LVG, 0.40 mm		162.37	68.34	86.48	114.74
Zymosan	328.36	284.91	114.74	111.4	307.64

Table D.4: MCP-1 levels for 2 donors. Values are in pg/ml.

Sample	Donor 1	Donor 2
T0	64.22	62.18
Saline	132.7	92.96
Solid, UP-LVG, 0.05 % PLL, 0.4 mm	207.24	198.12
Solid, M. pyr, 0.05 % PLL, 0.4 mm	189.07	149.86
TAM, UP-LVG, 0.4 mm, No BaCl ₂	121.28	107.4
TAM, UP-LVG, 0.4 mm	104.83	85.21
TAM, M. pyr, 0.4 mm	116.99	90.56
TAM4, UP-LVG*, 0.4 mm	80.95	73.12
TAM, UP-LVG, 0.35 mm, No BaCl ₂	120.43	102.23
TAM, UP-LVG, 0.35 mm	83.52	71.73
TAM, M. pyr, 0.35 mm	85.84	82.88
TAM4, UP-LVG*, 0.35 mm	64.22	67.68
Zymosan	118.89	178.84

D.3 MIF

Table D.5: MIF levels for 5 donors. Values are in pg/ml. OOR < = out of range below.

Sample	Donor 1	Donor 2	Donor 3	Donor 4	Donor 5
T0	164.66	1874.77	3837.06	OOR <	251.87
Saline	1855.48	2733.36	1191.63	1971.11	1903.7
Hollow, M. pyr, 0.10 % PLL, 0.4 mm	3818.51	3781.41	2229.94	1280.48	649.33
Hollow, M. pyr, 0.14 % PLL, 0.4 mm	13644.98	22329.12	4133.11	1681.27	771.5
Hollow, M. pyr, 0.14 % PLO, 0.4 mm	5742.49	10670.44	9387.1	9563.45	463.54
Solid, M. pyr, 0.05 % PLL, 0.4 mm	22110.45	15864.78	1642.42	9774.83	505.14
Solid, M. pyr, 0.10 % PLL, 0.4 mm	17496.93	16634.96	3985.24	21099.63	1496.29
Solid, UP-LVG, 0.05 % PLL, 0.4 mm	16771.67	22942.45	7040.35	13817.74	4620.9
Solid, UP-LVG, 0.10 % PLL, 0.4 mm	13212.55	11378.68	8706.4	10267.07	1720.06
Solid, UP-LVG, 0.05 % PLL, 0.35 mm	13056.69	9545.82	5197.06	5651.79	690.18
Solid, UP-LVG, 0.10 % PLL, 0.35 mm	12014.88	21672.75	2258.59	4031.48	2115.12
Solid, UP-LVG, 0.05 % PLL, 0.35 mm	12397.44	19933.86	2865.44	3632.79	3632.79
No Hepes					
TAM, UP-LVG, 0.25 mm		16540.93	10468.86	23806.31	1865.13
TAM, UP-LVG, 0.35 mm	3837.06	12883.38	14007.63	1632.7	1211.41
TAM, UP-LVG, 0.40 mm		13549.91	6789.11	2105.53	2657.73
Zymosan	7568.15	14050.77	1894.06	4831.68	3911.19

Table D.6: MIF levels for 2 donors. Values are in pg/ml.

Sample	Donor 1	Donor 2
T0	4288.47	2444.65
Saline	8234.98	19980.84
Solid, UP-LVG, 0.05 % PLL, 0.4 mm	13983.94	15591.76
Solid, M. pyr, 0.05 % PLL, 0.4 mm	12979.37	22536.01
TAM, UP-LVG, 0.4 mm, No BaCl ₂	3443.43	23459.69
TAM, UP-LVG, 0.4 mm	9336.49	12374.79
TAM, M. pyr, 0.4 mm	8024.07	17634.54
TAM4, UP-LVG*, 0.4 mm	7057.96	11684.01
TAM, UP-LVG, 0.35 mm, No BaCl ₂	9962.69	12643.37
TAM, UP-LVG, 0.35 mm	7383.26	14354.15
TAM, M. pyr, 0.35 mm	4476.9	12313.95
TAM4, UP-LVG*, 0.35 mm	7304.71	9604.72
Zymosan	6889	19193.25

D.4 IP-10

Table D.7: IP-10 levels for 5 donors. Values are in pg/ml.

Sample	Donor 1	Donor 2	Donor 3	Donor 4	Donor 5
T0	198.57	68.26	211.34	171.61	120.89
Saline	408.76	232.37	501.94	273.53	185.35
Hollow, M. pyr, 0.10 % PLL, 0.4 mm	1241.47	586.79	772.2	474.97	293.08
Hollow, M. pyr, 0.14 % PLL, 0.4 mm	505.13	343.02	392.35	319.56	228.93
Hollow, M. pyr, 0.14 % PLO, 0.4 mm	412.82	395.1	515.28	386.14	205.91
Solid, M. pyr, 0.05 % PLL, 0.4 mm	519.7	520.33	593.51	247.55	155.1
Solid, M. pyr, 0.10 % PLL, 0.4 mm	154.04	78.7	318.07	165.53	75.34
Solid, UP-LVG, 0.05 % PLL, 0.4 mm	202.26	184.39	331.37	157.22	98.5
Solid, UP-LVG, 0.10 % PLL, 0.4 mm	102.68	255.8	404.68	157.22	99.9
Solid, UP-LVG, 0.05 % PLL, 0.35 mm	218.46	520.96	1076.95	318.07	146.46
Solid, UP-LVG, 0.10 % PLL, 0.35 mm	207.73	305.31	311.34	259.88	115.88
Solid, UP-LVG, 0.05 % PLL, 0.35 mm	325.49	849.45	422.93	260.69	120.89
No Hepes					
TAM, UP-LVG, 0.25 mm		1424.81	698.47	237.48	172.61
TAM, UP-LVG, 0.35 mm	380.59	2639.3	522.22	175.59	144.25
TAM, UP-LVG, 0.40 mm		1080.32	683.08	198.57	163.47
Zymosan	1646.18	926.97	1458.41	1071.34	1001.61

Table D.8: IP-10 levels for 2 donors. Values are in pg/ml.

Sample	Donor 1	Donor 2
T0	308.77	105.08
Saline	320.65	279.62
Solid, UP-LVG, 0.05 % PLL, 0.4 mm	352.71	130.29
Solid, M. pyr, 0.05 % PLL, 0.4 mm	380.32	276.73
TAM, UP-LVG, 0.4 mm, No BaCl ₂	402.25	440.14
TAM, UP-LVG, 0.4 mm	327.88	269.94
TAM, M. pyr, 0.4 mm	335.04	313.36
TAM4, UP-LVG*, 0.4 mm	291.05	155.18
TAM, UP-LVG, 0.35 mm, No BaCl ₂	347.44	519.45
TAM, UP-LVG, 0.35 mm	724.9	325.17
TAM, M. pyr, 0.35 mm	418.86	307.84
TAM4, UP-LVG*, 0.35 mm	275.77	267.99
Zymosan	480.25	1384.57

D.5 IL-1 β

Table D.9: IL-1 β levels for 5 donors. Values are in pg/ml. OOR < = out of range below. * = value extrapolated beyond standard range

Sample	Donor 1	Donor 2	Donor 3	Donor 4	Donor 5
T0	OOOR <	*0.32	1.18	*0.14	1.01
Saline	2.5	5.55	6.49	2.5	1.84
Hollow, M. pyr, 0.10 % PLL, 0.4 mm	1.68	2.66	2.99	1.68	4.99
Hollow, M. pyr, 0.14 % PLL, 0.4 mm	2.66	14.56	4.99	1.51	4.75
Hollow, M. pyr, 0.14 % PLO, 0.4 mm	2.42	4.59	5.07	6.57	7.75
Solid, M. pyr, 0.05 % PLL, 0.4 mm	7.28	57.39	6.18	11.48	6.97
Solid, M. pyr, 0.10 % PLL, 0.4 mm	45.99	58.89	11.33	78.34	12.41
Solid, UP-LVG, 0.05 % PLL, 0.4 mm	44.04	47.87	24.31	79.32	12.87
Solid, UP-LVG, 0.10 % PLL, 0.4 mm	85.64	21.13	9.31	48.99	7.91
Solid, UP-LVG, 0.05 % PLL, 0.35 mm	30.96	27.64	6.65	2.17	13.02
Solid, UP-LVG, 0.10 % PLL, 0.35 mm	11.33	28.39	4.59	23.55	10.63
Solid, UP-LVG, 0.05 % PLL, 0.35 mm	20.29	59.42	5.23	5.23	44.19
No Hepes					
TAM, UP-LVG, 0.25 mm		2.33	4.59	8.84	3.15
TAM, UP-LVG, 0.35 mm	2.42	3.63	3.79	5.31	1.68
TAM, UP-LVG, 0.40 mm		6.18	3.15	6.49	6.81
Zymosan	2612.78	1453.3	1050.04	2223.46	2461.21

Table D.10: IL-1 β levels for 2 donors. Values are in pg/ml. OOR < = out of range below.

Sample	Donor 1	Donor 2
T0	OOOR <	OOOR <
Saline	17.11	12.88
Solid, UP-LVG, 0.05 % PLL, 0.4 mm	15.57	19.57
Solid, M. pyr, 0.05 % PLL, 0.4 mm	11.96	16.05
TAM, UP-LVG, 0.4 mm, No BaCl ₂	8.98	10.07
TAM, UP-LVG, 0.4 mm	7.06	8.2
TAM, M. pyr, 0.4 mm	11.96	11.75
TAM4, UP-LVG*, 0.4 mm	4.49	8.09
TAM, UP-LVG, 0.35 mm, No BaCl ₂	10.71	8.76
TAM, UP-LVG, 0.35 mm	6.35	6.71
TAM, M. pyr, 0.35 mm	5.75	8.31
TAM4, UP-LVG*, 0.35 mm	3.42	3.7
Zymosan	4315.38	1172.97

D.6 TNF- α

Table D.11: TNF- α levels for 5 donors. Values are in pg/ml. * = value extrapolated beyond standard range

Sample	Donor 1	Donor 2	Donor 3	Donor 4	Donor 5
T0	*0.72	*3.18	8.2	15.81	8.2
Saline	15.81	36.33	55.74	20.91	10.72
Hollow, M. pyr, 0.10 % PLL, 0.4 mm	28.6	5.68	33.75	59.64	132.97
Hollow, M. pyr, 0.14 % PLL, 0.4 mm	36.33	49.26	64.84	41.49	119.81
Hollow, M. pyr, 0.14 % PLO, 0.4 mm	20.91	31.18	33.75	44.08	59.64
Solid, M. pyr, 0.05 % PLL, 0.4 mm	90.95	375.52	143.52	111.93	256.3
Solid, M. pyr, 0.10 % PLL, 0.4 mm	388.97	409.17	188.48	117.18	515.96
Solid, UP-LVG, 0.05 % PLL, 0.4 mm	313.78	138.25	193.79	337.91	171.27
Solid, UP-LVG, 0.10 % PLL, 0.4 mm	1686.57	183.18	62.24	308.42	257.64
Solid, UP-LVG, 0.05 % PLL, 0.35 mm	383.59	265.64	125.08	33.75	375.52
Solid, UP-LVG, 0.10 % PLL, 0.35 mm	287.01	162.01	83.1	256.3	273.65
Solid, UP-LVG, 0.05 % PLL, 0.35 mm	167.3	244.31	109.3	127.71	366.1
No Hepes					
TAM, UP-LVG, 0.25 mm		41.49	28.6	33.75	57.04
TAM, UP-LVG, 0.35 mm	10.72	38.91	28.6	88.33	62.24
TAM, UP-LVG, 0.40 mm		44.08	33.75	88.33	80.49
Zymosan	21741.64	8902.01	15655.88	6429.36	10888.81

Table D.12: TNF- α levels for 2 donors. Values are in pg/ml. OOR < = out of range below.

Sample	Donor 1	Donor 2
T0	OOR <	OOR <
Saline	124.63	50.49
Solid, UP-LVG, 0.05 % PLL, 0.4 mm	366.32	245.35
Solid, M. pyr, 0.05 % PLL, 0.4 mm	264.28	105
TAM, UP-LVG, 0.4 mm, No BaCl ₂	133	85.16
TAM, UP-LVG, 0.4 mm	130.21	110.62
TAM, M. pyr, 0.4 mm	119.04	107.81
TAM4, UP-LVG*, 0.4 mm	72.28	41.62
TAM, UP-LVG, 0.35 mm, No BaCl ₂	166.21	164.84
TAM, UP-LVG, 0.35 mm	133	7.63
TAM, M. pyr, 0.35 mm	73.72	149.65
TAM4, UP-LVG*, 0.35 mm	120.44	92.27
Zymosan	31494.05	7362.18

D.7 IL-6

Table D.13: IL-6 levels for 5 donors. Values are in pg/ml.

Sample	Donor 1	Donor 2	Donor 3	Donor 4	Donor 5
T0	0.95	1.51	3.2	0.4	2.07
Saline	3.2	10.05	7.18	10.33	17.54
Hollow, M. pyr, 0.10 % PLL, 0.4 mm	6.04	12.35	6.9	26.83	50.24
Hollow, M. pyr, 0.14 % PLL, 0.4 mm	9.47	18.7	14.07	26.54	66.76
Hollow, M. pyr, 0.14 % PLO, 0.4 mm	6.61	9.47	8.9	38.5	39.09
Solid, M. pyr, 0.05 % PLL, 0.4 mm	9.47	28.87	18.12	56.43	52.6
Solid, M. pyr, 0.10 % PLL, 0.4 mm	22.47	15.23	14.07	67.35	42.9
Solid, UP-LVG, 0.05 % PLL, 0.4 mm	16.96	19.28	13.79	54.07	36.16
Solid, UP-LVG, 0.10 % PLL, 0.4 mm	149.27	18.41	11.2	68.24	41.43
Solid, UP-LVG, 0.05 % PLL, 0.35 mm	10.05	29.74	19.28	47.3	55.54
Solid, UP-LVG, 0.10 % PLL, 0.35 mm	16.38	18.7	15.23	59.08	43.78
Solid, UP-LVG, 0.05 % PLL, 0.35 mm	7.18	21.89	10.05	49.36	34.99
No Hepes					
TAM, UP-LVG, 0.25 mm		11.77	7.18	22.18	22.18
TAM, UP-LVG, 0.35 mm	3.2	13.5	6.61	23.92	21.02
TAM, UP-LVG, 0.40 mm		19.86	5.47	24.5	32.07
Zymosan	11228.55	8895.68	5039.91	7068.08	13173.34

Table D.14: IL-6 levels for 2 donors. Values are in pg/ml. OOR \leq out of range below.

Sample	Donor 1	Donor 2
T0	1.28	1.28
Saline	24.73	28.79
Solid, UP-LVG, 0.05 % PLL, 0.4 mm	44.14	26.36
Solid, M. pyr, 0.05 % PLL, 0.4 mm	44.52	42.2
TAM, UP-LVG, 0.4 mm, No BaCl ₂	51.78	41.43
TAM, UP-LVG, 0.4 mm	30.4	21.84
TAM, M. pyr, 0.4 mm	29.19	33.98
TAM4, UP-LVG*, 0.4 mm	31.6	23.08
TAM, UP-LVG, 0.35 mm, No BaCl ₂	39.48	26.36
TAM, UP-LVG, 0.35 mm	37.53	18.9
TAM, M. pyr, 0.35 mm	35.96	26.36
TAM4, UP-LVG*, 0.35 mm	26.36	15.48
Zymosan	19254.85	9975.65

D.8 IL-1RA

Table D.15: IL-1RA levels for 5 donors. Values are in pg/ml.

Sample	Donor 1	Donor 2	Donor 3	Donor 4	Donor 5
T0	38	114.35	467.88	38	153.03
Saline	289.87	1110.71	787.83	231	231
Hollow, M. pyr, 0.10 % PLL, 0.4 mm	627.41	667.44	388.54	231	507.67
Hollow, M. pyr, 0.14 % PLL, 0.4 mm	807.94	1272.96	507.67	270.21	309.55
Hollow, M. pyr, 0.14 % PLO, 0.4 mm	428.17	1557.96	667.44	467.88	309.55
Solid, M. pyr, 0.05 % PLL, 0.4 mm	1070.22	2645.93	868.32	667.44	467.88
Solid, M. pyr, 0.10 % PLL, 0.4 mm	1741.78	2254.51	908.63	787.83	388.54
Solid, UP-LVG, 0.05 % PLL, 0.4 mm	1232.35	2172.29	1232.35	828.05	547.52
Solid, UP-LVG, 0.10 % PLL, 0.4 mm	1212.06	1967.03	747.65	587.44	507.67
Solid, UP-LVG, 0.05 % PLL, 0.35 mm	1070.22	2460.35	627.41	507.67	667.44
Solid, UP-LVG, 0.10 % PLL, 0.35 mm	828.05	2254.51	587.44	787.83	507.67
Solid, UP-LVG, 0.05 % PLL, 0.35 mm	1110.71	3080.02	587.44	567.47	787.83
No Hepes					
TAM, UP-LVG, 0.25 mm		908.63	1029.77	607.42	388.54
TAM, UP-LVG, 0.35 mm	329.26	1374.6	807.94	507.67	270.21
TAM, UP-LVG, 0.40 mm		1517.17	707.52	547.52	547.52
Zymosan	1232.35	3038.61	1191.77	667.44	868.32

Table D.16: IL-1RA levels for 2 donors. Values are in pg/ml. OOR \leq out of range below.

Sample	Donor 1	Donor 2
T0	91.35	15.86
Saline	593.7	710.36
Solid, UP-LVG, 0.05 % PLL, 0.4 mm	1077.98	652.29
Solid, M. pyr, 0.05 % PLL, 0.4 mm	881.92	564.19
TAM, UP-LVG, 0.4 mm, No BaCl ₂	994.43	825.14
TAM, UP-LVG, 0.4 mm	767.97	767.97
TAM, M. pyr, 0.4 mm	825.14	767.97
TAM4, UP-LVG*, 0.4 mm	652.29	593.7
TAM, UP-LVG, 0.35 mm, No BaCl ₂	1105.69	825.14
TAM, UP-LVG, 0.35 mm	1105.69	825.14
TAM, M. pyr, 0.35 mm	994.43	652.29
TAM4, UP-LVG*, 0.35 mm	652.29	414.1
Zymosan	938.35	994.43

D.9 IL-10

Table D.17: IL-10 levels for 5 donors. Values are in pg/ml. * = value extrapolated beyond standard range

Sample	Donor 1	Donor 2	Donor 3	Donor 4	Donor 5
T0	1.49	4.02	3.16	*1.22	2.03
Saline	2.17	5.79	2.87	*1.22	*1.22
Hollow, M. pyr, 0.10 % PLL, 0.4 mm	4.31	7.14	2.45	*1.22	2.59
Hollow, M. pyr, 0.14 % PLL, 0.4 mm	3.16	7.9	1.76	1.49	2.31
Hollow, M. pyr, 0.14 % PLO, 0.4 mm	3.01	6.54	3.01	1.76	2.03
Solid, M. pyr, 0.05 % PLL, 0.4 mm	2.03	8.06	2.03	1.76	2.31
Solid, M. pyr, 0.10 % PLL, 0.4 mm	3.73	4.31	2.31	1.9	2.03
Solid, UP-LVG, 0.05 % PLL, 0.4 mm	3.16	7.29	2.03	2.03	2.03
Solid, UP-LVG, 0.10 % PLL, 0.4 mm	4.02	7.6	3.16	1.76	2.31
Solid, UP-LVG, 0.05 % PLL, 0.35 mm	3.44	7.29	3.16	1.76	2.87
Solid, UP-LVG, 0.10 % PLL, 0.35 mm	3.01	6.69	2.03	*1.22	2.59
Solid, UP-LVG, 0.05 % PLL, 0.35 mm No Hepes	5.34	8.98	2.31	1.49	3.44
TAM, UP-LVG, 0.25 mm		6.23	2.73	1.49	2.31
TAM, UP-LVG, 0.35 mm	3.16	8.21	3.44	1.76	2.31
TAM, UP-LVG, 0.40 mm		8.83	2.59	*1.22	1.9
Zymosan	11.64	9.45	6.69	5.19	10.07

Table D.18: IL-10 levels for 2 donors. Values are in pg/ml. OOR < = out of range below.

Sample	Donor 1	Donor 2
T0	0.9	0.39
Saline	1.36	0.9
Solid, UP-LVG, 0.05 % PLL, 0.4 mm	1.36	0.9
Solid, M. pyr, 0.05 % PLL, 0.4 mm	1.79	1.79
TAM, UP-LVG, 0.4 mm, No BaCl ₂	1.36	1.36
TAM, UP-LVG, 0.4 mm	2.6	0.39
TAM, M. pyr, 0.4 mm	2.6	1.36
TAM4, UP-LVG*, 0.4 mm	0.9	0.39
TAM, UP-LVG, 0.35 mm, No BaCl ₂	2	1.79
TAM, UP-LVG, 0.35 mm	1.79	1.36
TAM, M. pyr, 0.35 mm	3.38	1.36
TAM4, UP-LVG*, 0.35 mm	0.9	0.39
Zymosan	12.73	8.38

D.10 PDGF-BB

Table D.19: PDGF-BB levels for 5 donors. Values are in pg/ml.

Sample	Donor 1	Donor 2	Donor 3	Donor 4	Donor 5
T0	11.47	105.19	1050.37	62.92	298.55
Saline	579.45	1101.31	983.02	245.01	374.76
Hollow, M. pyr, 0.10 % PLL, 0.4 mm	676.96	770.08	618.6	432.79	389.98
Hollow, M. pyr, 0.14 % PLL, 0.4 mm	555.61	1696.59	1226.42	492.73	277.54
Hollow, M. pyr, 0.14 % PLO, 0.4 mm	487.02	1311.73	1172.11	710.51	337.63
Solid, M. pyr, 0.05 % PLL, 0.4 mm	741.23	2148.3	839.49	624.33	207.55
Solid, M. pyr, 0.10 % PLL, 0.4 mm	1339.6	1533.18	1586.77	595.68	355.72
Solid, UP-LVG, 0.05 % PLL, 0.4 mm	1458.66	3194.42	1662.95	546.07	433.74
Solid, UP-LVG, 0.10 % PLL, 0.4 mm	1343.59	1957.06	1674.16	553.7	382.37
Solid, UP-LVG, 0.05 % PLL, 0.35 mm	1233.35	2021.58	1469.71	500.35	746.04
Solid, UP-LVG, 0.10 % PLL, 0.35 mm	773.93	2428.51	1258.11	860.75	945.08
Solid, UP-LVG, 0.05 % PLL, 0.35 mm	1098.37	3299.27	1214.56	490.83	357.63
No Hepes					
TAM, UP-LVG, 0.25 mm		1291.85	1974.72	437.54	252.68
TAM, UP-LVG, 0.35 mm	977.18	2639.87	1027.89	296.64	166.95
TAM, UP-LVG, 0.40 mm		3654.76	1396.51	344.3	367.15
Zymosan	1011.29	2953.46	1313.72	1067.98	1048.41

Table D.20: PDGF-BB levels for 2 donors. Values are in pg/ml. OOR \leq out of range below.

Sample	Donor 1	Donor 2
T0	81.25	63.3
Saline	746.57	337.76
Solid, UP-LVG, 0.05 % PLL, 0.4 mm	1519.6	767.58
Solid, M. pyr, 0.05 % PLL, 0.4 mm	1761.99	800.62
TAM, UP-LVG, 0.4 mm, No BaCl ₂	1070.14	659.59
TAM, UP-LVG, 0.4 mm	1197.84	317.49
TAM, M. pyr, 0.4 mm	1173.46	396.27
TAM4, UP-LVG*, 0.4 mm	1240.58	225.52
TAM, UP-LVG, 0.35 mm, No BaCl ₂	983.37	622.61
TAM, UP-LVG, 0.35 mm	2365.33	599.63
TAM, M. pyr, 0.35 mm	1736.87	480.6
TAM4, UP-LVG*, 0.35 mm	1047.91	144.05
Zymosan	1900.81	785.6

D.11 HGF

Table D.21: HGF levels for 5 donors. Values are in pg/ml.

Sample	Donor 1	Donor 2	Donor 3	Donor 4	Donor 5
T0	66.59	210.08	167.76	34.56	89.24
Saline	686.53	833.95	734.93	345.18	378.29
Hollow, M. pyr, 0.10 % PLL, 0.4 mm	1487.7	673.33	462.06	334.14	963.87
Hollow, M. pyr, 0.14 % PLL, 0.4 mm	1005.74	1173.41	550.13	294.34	519.31
Hollow, M. pyr, 0.14 % PLO, 0.4 mm	899.99	732.73	748.13	267.77	462.06
Solid, M. pyr, 0.05 % PLL, 0.4 mm	1712.2	2477.07	972.68	281.06	776.73
Solid, M. pyr, 0.10 % PLL, 0.4 mm	990.31	2346.17	1127.05	435.62	1104.98
Solid, UP-LVG, 0.05 % PLL, 0.4 mm	1538.75	1779.06	886.78	387.12	919.81
Solid, UP-LVG, 0.10 % PLL, 0.4 mm	1268.43	1917.47	796.54	320.88	906.6
Solid, UP-LVG, 0.05 % PLL, 0.35 mm	1350.3	2163.93	825.14	274.42	1104.98
Solid, UP-LVG, 0.10 % PLL, 0.35 mm	1264.01	2211.12	585.33	356.22	1023.37
Solid, UP-LVG, 0.05 % PLL, 0.35 mm No Hepes	1087.33	2542.65	708.53	294.34	1027.78
TAM, UP-LVG, 0.25 mm		530.32	86.98	66.59	289.92
TAM, UP-LVG, 0.35 mm	267.77	345.18	232.29	48.34	210.08
TAM, UP-LVG, 0.40 mm		391.53	102.77	93.76	241.17
Zymosan	1412.31	2029.36	1184.45	360.64	1241.9

Table D.22: HGF levels for 2 donors. Values are in pg/ml. OOR < = out of range below. * = value extrapolated beyond standard range

Sample	Donor 1	Donor 2
T0	OOR <	OOR <
Saline	508.62	891.76
Solid, UP-LVG, 0.05 % PLL, 0.4 mm	446.73	674.46
Solid, M. pyr, 0.05 % PLL, 0.4 mm	441	1098.18
TAM, UP-LVG, 0.4 mm, No BaCl ₂	497.51	648.38
TAM, UP-LVG, 0.4 mm	259.47	199.61
TAM, M. pyr, 0.4 mm	412.02	611.48
TAM4, UP-LVG*, 0.4 mm	131.87	136.21
TAM, UP-LVG, 0.35 mm, No BaCl ₂	321.23	807.14
TAM, UP-LVG, 0.35 mm	382.47	469.47
TAM, M. pyr, 0.35 mm	199.61	627.35
TAM4, UP-LVG*, 0.35 mm	*89.42	295.74
Zymosan	346.11	913.93

D.12 VEGF

Table D.23: VEGF levels for 5 donors. Values are in pg/ml. OOR < = out of range below. * = value extrapolated beyond standard range

Sample	Donor 1	Donor 2	Donor 3	Donor 4	Donor 5
T0	OOOR <	*1.11	21.66	OOOR <	OOOR <
Saline	26.03	67.73	68.48	18.76	5.22
Hollow, M. pyr, 0.10 % PLL, 0.4 mm	51.94	29.7	42.25	20.94	23.84
Hollow, M. pyr, 0.14 % PLL, 0.4 mm	56.81	147.69	63.95	22.39	13.72
Hollow, M. pyr, 0.14 % PLO, 0.4 mm	30.43	38.91	74.54	28.23	14.44
Solid, M. pyr, 0.05 % PLL, 0.4 mm	46.71	225.09	95.11	45.97	36.69
Solid, M. pyr, 0.10 % PLL, 0.4 mm	71.51	240.29	149.25	62.45	66.97
Solid, UP-LVG, 0.05 % PLL, 0.4 mm	69.24	199.63	136.78	62.45	54.94
Solid, UP-LVG, 0.10 % PLL, 0.4 mm	88.23	257.16	88.99	55.69	44.85
Solid, UP-LVG, 0.05 % PLL, 0.35 mm	72.64	196.06	93.96	40.03	45.97
Solid, UP-LVG, 0.10 % PLL, 0.35 mm	74.54	221.1	82.89	61.32	48.95
Solid, UP-LVG, 0.05 % PLL, 0.35 mm No Hepes	48.21	281.38	100.85	43.74	57.56
TAM, UP-LVG, 0.25 mm		48.21	35.96	44.48	16.23
TAM, UP-LVG, 0.35 mm	17.32	41.51	34.11	27.5	14.44
TAM, UP-LVG, 0.40 mm		72.26	41.51	37.43	27.13
Zymosan	18.76	129.79	73.02	30.43	22.39

Table D.24: VEGF levels for 2 donors. Values are in pg/ml. OOR < = out of range below. * = value extrapolated beyond standard range

Sample	Donor 1	Donor 2
T0	12.69	13.66
Saline	68.06	91.4
Solid, UP-LVG, 0.05 % PLL, 0.4 mm	69.86	86.03
Solid, M. pyr, 0.05 % PLL, 0.4 mm	67.61	158.16
TAM, UP-LVG, 0.4 mm, No BaCl ₂	44.46	67.16
TAM, UP-LVG, 0.4 mm	56.3	56.3
TAM, M. pyr, 0.4 mm	54.94	61.28
TAM4, UP-LVG*, 0.4 mm	41.71	54.49
TAM, UP-LVG, 0.35 mm, No BaCl ₂	53.58	94.98
TAM, UP-LVG, 0.35 mm	56.3	36.2
TAM, M. pyr, 0.35 mm	32.96	64.9
TAM4, UP-LVG*, 0.35 mm	29.71	54.49
Zymosan	72.56	76.16

D.13 IFN- γ

Table D.25: IFN- γ levels for 5 donors. Values are in pg/ml. OOR < = out of range below.

Sample	Donor 1	Donor 2	Donor 3	Donor 4	Donor 5
T0	OOOR <	36.98	178.06	OOOR <	196.48
Saline	93.83	93.83	138.59	36.98	36.98
Hollow, M. pyr, 0.10 % PLL, 0.4 mm	67.92	67.92	158.82	OOOR <	178.06
Hollow, M. pyr, 0.14 % PLL, 0.4 mm	117.09	138.59	93.83	67.92	36.98
Hollow, M. pyr, 0.14 % PLO, 0.4 mm	67.92	138.59	158.82	67.92	67.92
Solid, M. pyr, 0.05 % PLL, 0.4 mm	93.83	138.59	93.83	67.92	67.92
Solid, M. pyr, 0.10 % PLL, 0.4 mm	158.82	93.83	128.02	93.83	67.92
Solid, UP-LVG, 0.05 % PLL, 0.4 mm	93.83	214.23	138.59	67.92	36.98
Solid, UP-LVG, 0.10 % PLL, 0.4 mm	117.09	138.59	138.59	67.92	67.92
Solid, UP-LVG, 0.05 % PLL, 0.35 mm	158.82	117.09	178.06	117.09	93.83
Solid, UP-LVG, 0.10 % PLL, 0.35 mm	117.09	105.72	117.09	117.09	67.92
Solid, UP-LVG, 0.05 % PLL, 0.35 mm No Hepes	67.92	158.82	128.02	36.98	67.92
TAM, UP-LVG, 0.25 mm		158.82	196.48	93.83	36.98
TAM, UP-LVG, 0.35 mm	67.92	231.4	214.23	OOOR <	36.98
TAM, UP-LVG, 0.40 mm		158.82	222.88	36.98	67.92
Zymosan	138.59	168.55	138.59	158.82	93.83

Table D.26: IFN- γ levels for 2 donors. Values are in pg/ml. OOR < = out of range below. * = value extrapolated beyond standard range

Sample	Donor 1	Donor 2
T0	OOOR <	OOOR <
Saline	OOOR <	OOOR <
Solid, UP-LVG, 0.05 % PLL, 0.4 mm	OOOR <	OOOR <
Solid, M. pyr, 0.05 % PLL, 0.4 mm	OOOR <	OOOR <
TAM, UP-LVG, 0.4 mm, No BaCl ₂	OOOR <	OOOR <
TAM, UP-LVG, 0.4 mm	OOOR <	OOOR <
TAM, M. pyr, 0.4 mm	OOOR <	OOOR <
TAM4, UP-LVG*, 0.4 mm	OOOR <	OOOR <
TAM, UP-LVG, 0.35 mm, No BaCl ₂	OOOR <	OOOR <
TAM, UP-LVG, 0.35 mm	OOOR <	OOOR <
TAM, M. pyr, 0.35 mm	OOOR <	OOOR <
TAM4, UP-LVG*, 0.35 mm	OOOR <	OOOR <
Zymosan	OOOR <	OOOR <

D.14 RANTES

Table D.27: RANTES levels for 5 donors. Values are in pg/ml. OOR \leq out of range below.

Sample	Donor 1	Donor 2	Donor 3	Donor 4	Donor 5
T0	1196.96	1950.06	8902.54	639.6	8335.7
Saline	2242.41	2563.29	3181.1	393.18	2154.91
Hollow, M. pyr, 0.10 % PLL, 0.4 mm	4201.94	1746.32	1877.78	753.29	1816.12
Hollow, M. pyr, 0.14 % PLL, 0.4 mm	3831.84	4118.89	4751.03	1158.62	1284.44
Hollow, M. pyr, 0.14 % PLO, 0.4 mm	1615.59	5088.22	4158.88	1567.19	988.39
Solid, M. pyr, 0.05 % PLL, 0.4 mm	3266.68	5005.73	1987.24	1146.22	713.71
Solid, M. pyr, 0.10 % PLL, 0.4 mm	10565.36	4464.6	4121.21	1413.63	967.24
Solid, UP-LVG, 0.05 % PLL, 0.4 mm	14514.06	13743.4	4613.39	1335.93	1156.32
Solid, UP-LVG, 0.10 % PLL, 0.4 mm	12724.58	7769.95	3574.16	1327.11	1275.43
Solid, UP-LVG, 0.05 % PLL, 0.35 mm	7798.78	5810.25	5079.67	916.81	1362.84
Solid, UP-LVG, 0.10 % PLL, 0.35 mm	3305.1	7694.54	3223.79	1906.67	2411.88
Solid, UP-LVG, 0.05 % PLL, 0.35 mm No Hepes	6901.57	15257.58	3383.33	1034.85	889.61
TAM, UP-LVG, 0.25 mm		2871.14	7177.31	1189.69	1216.97
TAM, UP-LVG, 0.35 mm	4206.67	12475.71	3842.73	929.87	840.07
TAM, UP-LVG, 0.40 mm		5222.12	4001.35	878.08	1514.03
Zymosan	7732.13	17196.74	3189.33	4140.84	3141.22

Table D.28: RANTES levels for 2 donors. Values are in pg/ml. OOR \leq out of range below.
* = value extrapolated beyond standard range

Sample	Donor 1	Donor 2
T0	2130.71	4514.63
Saline	4684.63	1112.63
Solid, UP-LVG, 0.05 % PLL, 0.4 mm	6252.28	3294.14
Solid, M. pyr, 0.05 % PLL, 0.4 mm	9087.33	4238.61
TAM, UP-LVG, 0.4 mm, No BaCl ₂	5733.86	2469.85
TAM, UP-LVG, 0.4 mm	4404.95	2436.72
TAM, M. pyr, 0.4 mm	7875.23	2703.2
TAM4, UP-LVG*, 0.4 mm	7397.35	2169.87
TAM, UP-LVG, 0.35 mm, No BaCl ₂	8177.66	2098.23
TAM, UP-LVG, 0.35 mm	10176.63	1875.89
TAM, M. pyr, 0.35 mm	8898.75	3367.28
TAM4, UP-LVG*, 0.35 mm	4848.15	1144.46
Zymosan	18800.01	14327.31

E Flow cytometer data

CD11b expression data for monocytes and granulocytes after incubation of capsules in whole blood for 1 hour are shown in table E.1. The data consist of samples from 3 blood donors.

Table E.1: CD11b expression on leukocytes, measured as median fluorescence intensity. MC = monocytes, GC = granulocytes

Sample	Donor 1		Donor 4		Donor 5	
	MC	GC	MC	GC	MC	GC
T0	35.5	26.7	99.1	59.9	101.8	54.7
Saline	116.5	171.5	378.6	414.2	184.3	79.1
Hollow, M. pyr, 0.10 % PLL, 0.4 mm	433.2	547.4	577.7	1144.4	562.3	679.3
Hollow, M. pyr, 0.14 % PLL, 0.4 mm	403.2	500.3	547.4	1134	552.3	736.5
Hollow, M. pyr, 0.14 % PLO, 0.4 mm	226.7	392.4	620.8	791.5	385.4	342.9
Solid, M. pyr, 0.05 % PLL, 0.4 mm	453.2	552.3	827.9	964.7	465.6	305.1
Solid, M. pyr, 0.10 % PLL, 0.4 mm	361.9	491.4	770.4	697.8	237.1	145.9
Solid, UP-LVG, 0.05 % PLL, 0.4 mm	352.3	425.5	588.2	609.8	355.5	302.3
Solid, UP-LVG, 0.10 % PLL, 0.4 mm	417.9	593.5	1229.8	1625.3	518.6	388.9
Solid, UP-LVG, 0.05 % PLL, 0.35 mm	259.5	375.2	1027.4	1197.1	271.4	167
Solid, UP-LVG, 0.10 % PLL, 0.35 mm	342.9	504.8	1065	1625.3	661.2	537.6
Solid, UP-LVG, 0.05 % PLL, 0.35 mm, No Hepes	327.8	465.6	1084.3	1186.4	214.8	90.6
TAM, UP-LVG, 0.25 mm			212.9	104.6	189.4	82
TAM, UP-LVG, 0.35 mm	107.5	104.6	392.4	257.1	186	71.7
TAM, UP-LVG, 0.40 mm			239.3	109.4	222.7	117.6
Zymosan	593.5	691.6	1826.9	1860.1	1382.4	1218.8
LPS	588.2	637.8	1762.4	1553.8	1345.6	964.7

F Statistical analysis

Statistical analysis was performed on the cytokine levels after incubating the different capsules in whole blood for 4 hours. The software SPSS Statistics (v. 20, IBM) was used to perform Wilcoxon signed-rank tests. Differences were considered significant at $P < 0.05$. SPSS output is shown in tables F.1-F.36 below.

F.1 IL-8 1h

Table F.1: Descriptive Statistics - IL-8 1h

Sample Abr.	Capsule parameters	N	Mean	Std. Deviation	Minimum	Maximum
T ₀		5	6.4608	7.09282	2.07	18.91
Saline		5	12.8650	8.07949	4.21	25.73
Ab	Hollow, M. pyr, 0.10 % PLL, 0.4 mm	5	33.8208	14.15141	24.68	58.96
A2b	Hollow, M. pyr, 0.14 % PLL, 0.4 mm	5	38.1197	20.21119	17.90	68.55
Db	Hollow, M. pyr, 0.14 % PLO, 0.4 mm	5	28.9627	7.26258	21.23	40.44
Eb	Solid, M. pyr, 0.05 % PLL, 0.4 mm	5	29.3043	14.57915	16.11	50.78
Fb	Solid, M. pyr, 0.10 % PLL, 0.4 mm	5	42.8985	34.14061	17.66	100.16
Gb	Solid, UP-LVG, 0.05 % PLL, 0.4 mm	5	38.2206	7.43530	26.81	45.26
Hb	Solid, UP-LVG, 0.10 % PLL, 0.4 mm	5	67.8293	29.48448	31.09	97.05
I2b	Solid, UP-LVG, 0.05 % PLL, 0.35 mm	5	29.9368	21.52463	17.81	68.02
J2b	Solid, UP-LVG, 0.10 % PLL, 0.35 mm	5	35.5620	23.32162	17.60	74.62
K2b	Solid, UP-LVG, 0.05 % PLL, 0.35 mm No Hepes	5	26.8040	9.96256	17.78	42.34
R	TAM, UP-LVG, 0.25 mm	4	12.1456	5.70644	8.86	20.69
S	TAM, UP-LVG, 0.35 mm	4	13.7830	6.82969	7.94	23.66
T	TAM, UP-LVG, 0.40 mm	4	12.5619	4.13615	8.06	17.84
Zymosan		5	349.8204	115.78078	229.28	468.72

Table F.2: Test Statistics^a - IL-8 1h

	A2b-Ab	Db-Ab	Db-A2b	Fb - Ab	Fb - Eb	Hb - Gb
Z	-.674 ^b	-.135 ^c	-.674 ^c	-.405 ^b	-.944 ^b	-1.483 ^b
Asymp. Sig. (2-tailed)	.500	.893	.500	.686	.345	.138
	J2b - I2b	K2b - I2b	Gb - Eb	Hb - Fb	I2b - Gb	J2b - Hb
Z	-.674 ^b	-.674 ^b	-.944 ^b	-1.483 ^b	-.674 ^c	-2.023 ^c
Asymp. Sig. (2-tailed)	.500	.500	.345	.138	.500	.043
	S-R	T-R	T-S	Saline-Ab	Saline-A2b	Saline-Db
Z	-1.461 ^b	.000 ^c	-.730 ^c	-2.023 ^c	-2.023 ^c	-1.753 ^c
Asymp. Sig. (2-tailed)	.144	1.000	.465	.043	.043	.080
	Saline-Eb	Saline-Fb	Saline-Gb	Saline-Hb	Saline-I2b	Saline-J2b
Z	-2.023 ^c	-2.023 ^c	-2.023 ^c	-2.023 ^c	-1.753 ^c	-1.753 ^c
Asymp. Sig. (2-tailed)	.043	.043	.043	.043	.080	.080
	Saline-K2b	Saline-R	Saline-S	Saline-T	Saline-Zymosan	
Z	-1.753 ^c	-.405 ^b	-.135 ^c	-.135 ^c	-2.023 ^c	
Asymp. Sig. (2-tailed)	.080	.686	.893	.893	.043	
a. Wilcoxon Signed Ranks Test						
b. Based on negative ranks.						
c. Based on positive ranks.						

F.2 IL-8 4h

Table F.3: Descriptive Statistics - IL-8 4h

Sample Abr.	Capsule parameters	N	Mean	Std. Deviation	Minimum	Maximum
T ₀		5	4.0840	2.79369	1.39	8.67
Saline		5	350.1780	203.48883	155.13	690.61
Ab	Hollow, M. pyr, 0.10 % PLL, 0.4 mm	5	1044.8960	405.35893	403.59	1478.59
A2b	Hollow, M. pyr, 0.14 % PLL, 0.4 mm	5	1231.7320	763.04898	362.37	2467.10
Db	Hollow, M. pyr, 0.14 % PLO, 0.4 mm	5	912.1080	615.10078	185.69	1869.15
Eb	Solid, M. pyr, 0.05 % PLL, 0.4 mm	5	2513.7400	1530.16230	686.93	4304.11
Fb	Solid, M. pyr, 0.10 % PLL, 0.4 mm	5	4400.5540	1923.18766	2171.52	6879.56
Gb	Solid, UP-LVG, 0.05 % PLL, 0.4 mm	5	4180.1940	2336.14126	2007.47	6802.00
Hb	Solid, UP-LVG, 0.10 % PLL, 0.4 mm	5	4598.6260	3344.80163	1597.20	10065.59
I2b	Solid, UP-LVG, 0.05 % PLL, 0.35 mm	5	2697.5260	2273.96003	419.15	6216.19
J2b	Solid, UP-LVG, 0.10 % PLL, 0.35 mm	5	3095.7560	1632.52191	1225.66	5335.63
K2b	Solid, UP-LVG, 0.05 % PLL, 0.35 mm No Hepes	5	2892.8580	2280.11908	741.17	6128.61
R	TAM, UP-LVG, 0.25 mm	4	189.0050	73.41369	127.87	295.50
S	TAM, UP-LVG, 0.35 mm	4	185.2450	73.70063	135.55	294.24
T	TAM, UP-LVG, 0.40 mm	4	236.3550	118.45137	93.31	377.67
Zymosan		5	9214.7160	2916.06639	4852.00	12191.85

Table F.4: Test Statistics^a - IL-8 4h

	A2b-Ab	Db-Ab	Db-A2b	Fb - Ab	Fb - Eb	Hb - Gb
Z	-.674 ^b	-.674 ^b	-.135 ^b	-2.023 ^b	-2.023 ^b	-.135 ^b
Asymp. Sig. (2-tailed)	.500	.500	.893	.043	.043	.893
	J2b - I2b	K2b - I2b	Gb - Eb	Hb - Fb	I2b - Gb	J2b - Hb
Z	-.944 ^b	-.405 ^b	-2.023 ^b	-.405 ^c	-2.023 ^c	-1.753 ^c
Asymp. Sig. (2-tailed)	.345	.686	.043	.686	.043	.080
	S-R	T-R	T-S	Saline-Ab	Saline-A2b	Saline-Db
Z	-.365 ^b	-.730 ^c	-.730 ^c	-2.023 ^c	-2.023 ^c	-1.753 ^c
Asymp. Sig. (2-tailed)	.715	.465	.465	.043	.043	.080
	Saline-Eb	Saline-Fb	Saline-Gb	Saline-Hb	Saline-I2b	Saline-J2b
Z	-2.023 ^c					
Asymp. Sig. (2-tailed)	.043	.043	.043	.043	.043	.043
	Saline-K2b	Saline-R	Saline-S	Saline-T	Saline-Zymosan	
Z	-2.023 ^c	-.730 ^b	-1.483 ^b	-.365 ^b	-2.023 ^c	
Asymp. Sig. (2-tailed)	.043	.465	.138	.715	.043	
a. Wilcoxon Signed Ranks Test						
b. Based on negative ranks.						
c. Based on positive ranks.						

F.3 sTCC 1h

Table F.5: Descriptive Statistics - sTCC 1h

Sample Abr.	Capsule parameters	N	Mean	Std. Deviation	Minimum	Maximum
T ₀		5	.3221	.14132	.16	.46
Saline		5	2.3275	1.07014	1.17	3.43
Ab	Hollow, M. pyr, 0.10 % PLL, 0.4 mm	5	63.0329	32.76967	35.91	119.19
A2b	Hollow, M. pyr, 0.14 % PLL, 0.4 mm	5	52.8888	24.44967	31.62	92.08
Db	Hollow, M. pyr, 0.14 % PLO, 0.4 mm	5	15.4614	7.00075	9.06	26.85
Eb	Solid, M. pyr, 0.05 % PLL, 0.4 mm	5	10.9616	6.60872	3.40	18.99
Fb	Solid, M. pyr, 0.10 % PLL, 0.4 mm	5	3.9328	2.00556	2.19	7.16
Gb	Solid, UP-LVG, 0.05 % PLL, 0.4 mm	5	2.9263	.58164	2.26	3.76
Hb	Solid, UP-LVG, 0.10 % PLL, 0.4 mm	5	11.5635	8.34680	3.44	25.36
I2b	Solid, UP-LVG, 0.05 % PLL, 0.35 mm	5	8.5032	8.87290	2.25	23.38
J2b	Solid, UP-LVG, 0.10 % PLL, 0.35 mm	5	14.3007	12.11173	6.86	35.67
K2b	Solid, UP-LVG, 0.05 % PLL, 0.35 mm No Hepes	5	9.4963	9.72817	1.54	25.42
R	TAM, UP-LVG, 0.25 mm	4	1.2602	.39400	.88	1.81
S	TAM, UP-LVG, 0.35 mm	4	1.4790	.54117	.80	2.11
T	TAM, UP-LVG, 0.40 mm	4	1.3814	.37764	.93	1.79
Zymosan		5	82.5438	37.36303	54.47	147.85

Table F.6: Test Statistics^a - sTCC 1h

	A2b-Ab	Db-Ab	Db-A2b	Fb - Ab	Fb - Eb	Hb - Gb
Z	-2.023 ^b	-2.023 ^c				
Asymp. Sig. (2-tailed)	.043	.043	.043	.043	.043	.043
	J2b - I2b	K2b - I2b	Gb - Eb	Hb - Fb	I2b - Gb	J2b - Hb
Z	-2.023 ^c	-1.483 ^c	-2.023 ^b	-2.023 ^c	-1.753 ^c	-.674 ^c
Asymp. Sig. (2-tailed)	.043	.138	.043	.043	.080	.500
	S-R	T-R	T-S	Saline-Ab	Saline-A2b	Saline-Db
Z	-.730 ^b	-.730 ^b	-.730 ^c	-2.023 ^c	-2.023 ^c	-2.023 ^c
Asymp. Sig. (2-tailed)	.465	.465	.465	.043	.043	.043
	Saline-Eb	Saline-Fb	Saline-Gb	Saline-Hb	Saline-I2b	Saline-J2b
Z	-2.023 ^c	-1.753 ^c	-1.214 ^c	-2.023 ^c	-2.023 ^c	-2.023 ^c
Asymp. Sig. (2-tailed)	.043	.080	.225	.043	.043	.043
	Saline-K2b	Saline-R	Saline-S	Saline-T	Saline-Zymosan	Saline-LPS
Z	-2.023 ^c	-1.826 ^b	-1.753 ^b	-1.461 ^b	-2.023 ^c	-1.753 ^c
Asymp. Sig. (2-tailed)	.043	.068	.080	.144	.043	.080
a. Wilcoxon Signed Ranks Test						
b. Based on negative ranks.						
c. Based on positive ranks.						

F.4 sTCC 4h

Table F.7: Descriptive Statistics - sTCC 4h

Sample Abr.	Capsule parameters	N	Mean	Std. Deviation	Minimum	Maximum
T ₀		5	.4213	.13422	.24	.61
Saline		5	17.2501	10.07845	6.30	31.36
Ab	Hollow, M. pyr, 0.10 % PLL, 0.4 mm	5	147.2494	60.93740	65.19	224.98
A2b	Hollow, M. pyr, 0.14 % PLL, 0.4 mm	5	128.7753	45.05308	59.98	163.88
Db	Hollow, M. pyr, 0.14 % PLO, 0.4 mm	5	42.9312	16.41020	32.64	72.03
Eb	Solid, M. pyr, 0.05 % PLL, 0.4 mm	5	57.4229	22.36119	37.81	82.01
Fb	Solid, M. pyr, 0.10 % PLL, 0.4 mm	5	75.6500	36.79900	33.78	127.77
Gb	Solid, UP-LVG, 0.05 % PLL, 0.4 mm	5	21.4456	14.40741	7.20	45.06
Hb	Solid, UP-LVG, 0.10 % PLL, 0.4 mm	5	61.3385	21.38792	29.58	86.13
I2b	Solid, UP-LVG, 0.05 % PLL, 0.35 mm	5	39.2189	20.14846	20.29	66.32
J2b	Solid, UP-LVG, 0.10 % PLL, 0.35 mm	5	82.1278	43.56215	29.28	122.94
K2b	Solid, UP-LVG, 0.05 % PLL, 0.35 mm No Hepes	5	53.6435	43.37009	14.63	106.36
R	TAM, UP-LVG, 0.25 mm	4	6.3028	5.24281	3.18	14.11
S	TAM, UP-LVG, 0.35 mm	4	6.0266	4.28397	2.96	12.37
T	TAM, UP-LVG, 0.40 mm	4	6.4188	5.76905	3.18	15.06
Zymosan		5	144.6234	29.89242	116.78	193.61

Table F.8: Test Statistics^a - sTCC 4h

	A2b-Ab	Db-Ab	Db-A2b	Fb - Ab	Fb - Eb	Hb - Gb
Z	-2.023 ^b	-2.023 ^b	-2.023 ^b	-2.023 ^b	-1.753 ^c	-2.023 ^c
Asymp. Sig. (2-tailed)	.043	.043	.043	.043	.080	.043
	J2b - I2b	K2b - I2b	Gb - Eb	Hb - Fb	I2b - Gb	J2b - Hb
Z	-2.023 ^c	-.405 ^c	-2.023 ^b	-.944 ^b	-2.023 ^c	-1.214 ^c
Asymp. Sig. (2-tailed)	.043	.686	.043	.345	.043	.225
	S-R	T-R	T-S	Saline-Ab	Saline-A2b	Saline-Db
Z	-.730 ^b	-.365 ^c	-.000 ^d	-2.023 ^c	-2.023 ^c	-2.023 ^c
Asymp. Sig. (2-tailed)	.465	.715	1.000	.043	.043	.043
	Saline-Eb	Saline-Fb	Saline-Gb	Saline-Hb	Saline-I2b	Saline-J2b
Z	-2.023 ^c	-2.023 ^c	-.135 ^b	-1.753 ^c	-1.753 ^c	-1.753 ^c
Asymp. Sig. (2-tailed)	.043	.043	.893	.080	.080	.080
	Saline-K2b	Saline-R	Saline-S	Saline-T	Saline-Zymosan	Saline-LPS
Z	-1.483 ^c	-1.826 ^b	-2.023 ^c	-1.826 ^b	-2.023 ^c	-.405 ^b
Asymp. Sig. (2-tailed)	.138	.068	.043	.068	.043	.686
a. Wilcoxon Signed Ranks Test						
b. Based on negative ranks.						
c. Based on positive ranks.						
d. The sum of negative ranks equals the sum of positive ranks.						

F.5 MIP-1 α

Table F.9: Descriptive Statistics - MIP-1 α

Sample Abr.	Capsule parameters	N	Mean	Std. Deviation	Minimum	Maximum
T ₀		5	2.5900	1.44869	1.36	4.99
Saline		5	42.7960	19.29429	30.30	76.11
Ab	Hollow, M. pyr, 0.10 % PLL, 0.4 mm	5	61.5600	43.96702	21.34	131.08
A2b	Hollow, M. pyr, 0.14 % PLL, 0.4 mm	5	93.0300	44.44417	32.96	139.63
Db	Hollow, M. pyr, 0.14 % PLO, 0.4 mm	5	72.2620	24.23221	34.95	95.26
Eb	Solid, M. pyr, 0.05 % PLL, 0.4 mm	5	350.8320	237.48137	121.22	722.80
Fb	Solid, M. pyr, 0.10 % PLL, 0.4 mm	5	442.4620	132.36338	330.94	611.82
Gb	Solid, UP-LVG, 0.05 % PLL, 0.4 mm	5	441.9040	77.76742	369.65	551.19
Hb	Solid, UP-LVG, 0.10 % PLL, 0.4 mm	5	483.9480	484.18320	123.80	1332.41
I2b	Solid, UP-LVG, 0.05 % PLL, 0.35 mm	5	337.9300	208.89467	67.91	532.37
J2b	Solid, UP-LVG, 0.10 % PLL, 0.35 mm	5	337.6520	184.98150	167.12	635.24
K2b	Solid, UP-LVG, 0.05 % PLL, 0.35 mm No Hepes	5	383.2720	293.52836	94.20	819.67
R	TAM, UP-LVG, 0.25 mm	4	64.0475	21.62608	35.09	84.13
S	TAM, UP-LVG, 0.35 mm	5	50.3780	20.23506	31.22	79.96
T	TAM, UP-LVG, 0.40 mm	4	74.4275	36.96783	43.34	124.39
Zymosan		5	2986.4900	690.79113	1841.37	3677.83

Table F.10: Test Statistics^a - MIP-1 α

	A2b-Ab	Db-Ab	Db-A2b	Fb - Ab	Fb - Eb	Hb - Gb
Z	-2.023 ^c	-.674 ^b	-.674 ^c	-2.023 ^b	-.674 ^b	-.674 ^c
Asymp. Sig. (2-tailed)	.043	.500	.500	.043	.500	.500
	J2b - I2b	K2b - I2b	Gb - Eb	Hb - Fb	I2b - Gb	J2b - Hb
Z	-.135 ^c	-.674 ^b	-.674 ^b	-.135 ^c	-1.214 ^c	-.405 ^c
Asymp. Sig. (2-tailed)	.893	.500	.500	.893	.225	.686
	S-R	T-R	T-S	Saline-Ab	Saline-A2b	Saline-Db
Z	-1.826 ^c	-.365 ^b	-1.095 ^b	-.674 ^c	-2.023 ^c	-1.214 ^c
Asymp. Sig. (2-tailed)	.068	.715	.273	.500	.043	.225
	Saline-Eb	Saline-Fb	Saline-Gb	Saline-Hb	Saline-I2b	Saline-J2b
Z	-2.023 ^c					
Asymp. Sig. (2-tailed)	.043	.043	.043	.043	.043	.043
	Saline-K2b	Saline-R	Saline-S	Saline-T	Saline-Zymosan	Saline-LPS
Z	-2.023 ^c	-.730 ^c	-.405 ^c	-1.095 ^c	-2.023 ^c	
Asymp. Sig. (2-tailed)	.043	.465	.686	.273	.043	
a. Wilcoxon Signed Ranks Test						
b. Based on negative ranks.						
c. Based on positive ranks.						

F.6 MCP-1

Table F.11: Descriptive Statistics - MCP-1

Sample Abr.	Capsule parameters	N	Mean	Std. Deviation	Minimum	Maximum
T ₀		5	68.5640	16.35280	49.61	94.58
Saline		5	101.5140	31.83197	73.27	151.19
Ab	Hollow, M. pyr, 0.10 % PLL, 0.4 mm	5	341.6760	178.26439	124.54	538.99
A2b	Hollow, M. pyr, 0.14 % PLL, 0.4 mm	5	360.8820	185.15174	142.37	586.26
Db	Hollow, M. pyr, 0.14 % PLO, 0.4 mm	5	192.7480	118.10103	95.56	384.25
Eb	Solid, M. pyr, 0.05 % PLL, 0.4 mm	5	243.7180	110.80518	115.94	355.10
Fb	Solid, M. pyr, 0.10 % PLL, 0.4 mm	5	174.5160	48.17226	115.64	238.41
Gb	Solid, UP-LVG, 0.05 % PLL, 0.4 mm	5	220.4980	102.12423	120.71	386.48
Hb	Solid, UP-LVG, 0.10 % PLL, 0.4 mm	5	213.9460	106.07488	132.63	384.78
I2b	Solid, UP-LVG, 0.05 % PLL, 0.35 mm	5	203.0180	90.98065	109.88	334.26
J2b	Solid, UP-LVG, 0.10 % PLL, 0.35 mm	5	283.2900	142.62251	138.59	488.29
K2b	Solid, UP-LVG, 0.05 % PLL, 0.35 mm No Hepes	5	235.3020	142.03844	110.33	451.04
R	TAM, UP-LVG, 0.25 mm	4	98.7700	28.89767	70.37	138.31
S	TAM, UP-LVG, 0.35 mm	5	98.0260	31.18579	68.16	150.37
T	TAM, UP-LVG, 0.40 mm	4	107.9825	40.97784	68.34	162.37
Zymosan		5	229.4100	107.31595	111.40	328.36

Table F.12: Test Statistics^a - MCP-1

	A2b-Ab	Db-Ab	Db-A2b	Fb - Ab	Fb - Eb	Hb - Gb
Z	-1.214 ^c	-1.753 ^c	-2.023 ^c	-2.023 ^c	-2.023 ^c	-.405 ^c
Asymp. Sig. (2-tailed)	.225	.080	.043	.043	.043	.686
	J2b - I2b	K2b - I2b	Gb - Eb	Hb - Fb	I2b - Gb	J2b - Hb
Z	-2.023 ^c	-.674 ^b	-.405 ^c	-.944 ^b	-1.214 ^c	-2.023 ^b
Asymp. Sig. (2-tailed)	.043	.500	.686	.345	.225	.043
	S-R	T-R	T-S	Saline-Ab	Saline-A2b	Saline-Db
Z	-.365 ^c	-.730 ^b	-1.826 ^b	-2.023 ^c	-2.023 ^c	-2.023 ^c
Asymp. Sig. (2-tailed)	.715	.465	.068	.043	.043	.043
	Saline-Eb	Saline-Fb	Saline-Gb	Saline-Hb	Saline-I2b	Saline-J2b
Z	-2.023 ^c					
Asymp. Sig. (2-tailed)	.043	.043	.043	.043	.043	.043
	Saline-K2b	Saline-R	Saline-S	Saline-T	Saline-Zymosan	Saline-LPS
Z	-2.023 ^c	-1.095 ^c	-.135 ^b	-.730 ^c	-2.023 ^c	
Asymp. Sig. (2-tailed)	.043	.273	.893	.465	.043	
a. Wilcoxon Signed Ranks Test						
b. Based on negative ranks.						
c. Based on positive ranks.						
d. The sum of negative ranks equals the sum of positive ranks.						

F.7 MIF

Table F.13: Descriptive Statistics - MIF

Sample Abr.	Capsule parameters	N	Mean	Std. Deviation	Minimum	Maximum
T ₀		4	1532.0900	1726.18504	164.66	3837.06
Saline		5	1931.0560	547.38170	1191.63	2733.36
Ab	Hollow, M. pyr, 0.10 % PLL, 0.4 mm	5	2351.9340	1436.66309	649.33	3818.51
A2b	Hollow, M. pyr, 0.14 % PLL, 0.4 mm	5	8511.9960	9260.25349	771.50	22329.12
Db	Hollow, M. pyr, 0.14 % PLO, 0.4 mm	5	7165.4040	4180.65487	463.54	10670.44
Eb	Solid, M. pyr, 0.05 % PLL, 0.4 mm	5	9979.5240	9234.56494	505.14	22110.45
Fb	Solid, M. pyr, 0.10 % PLL, 0.4 mm	5	12142.6100	8788.69975	1496.29	21099.63
Gb	Solid, UP-LVG, 0.05 % PLL, 0.4 mm	5	13038.6220	7407.18894	4620.90	22942.45
Hb	Solid, UP-LVG, 0.10 % PLL, 0.4 mm	5	9056.9520	4418.05025	1720.06	13212.55
I2b	Solid, UP-LVG, 0.05 % PLL, 0.35 mm	5	6828.3080	4687.73383	690.18	13056.69
J2b	Solid, UP-LVG, 0.10 % PLL, 0.35 mm	5	8418.5640	8448.84796	2115.12	21672.75
K2b	Solid, UP-LVG, 0.05 % PLL, 0.35 mm No Hepes	5	8492.4640	7500.84398	2865.44	19933.86
R	TAM, UP-LVG, 0.25 mm	4	13170.3075	9302.15929	1865.13	23806.31
S	TAM, UP-LVG, 0.35 mm	5	6714.4360	6237.65135	1211.41	14007.63
T	TAM, UP-LVG, 0.40 mm	4	6275.5700	5280.71162	2105.53	13549.91
Zymosan		5	6451.1700	4712.82989	1894.06	14050.77

Table F.14: Test Statistics^a - MIF

	A2b-Ab	Db-Ab	Db-A2b	Fb - Ab	Fb - Eb	Hb - Gb
Z	-2.023 ^b	-1.753 ^b	-.674 ^c	-2.023 ^b	-.944 ^b	-1.753 ^c
Asymp. Sig. (2-tailed)	.043	.080	.500	.043	.345	.080
	J2b - I2b	K2b - I2b	Gb - Eb	Hb - Fb	I2b - Gb	J2b - Hb
Z	-.135 ^b	-.405 ^b	-1.214 ^b	-.944 ^c	-2.023 ^c	-.405 ^c
Asymp. Sig. (2-tailed)	.893	.686	.225	.345	.043	.686
	S-R	T-R	T-S	Saline-Ab	Saline-A2b	Saline-Db
Z	-1.095 ^c	-1.461 ^c	-.365 ^b	-.674 ^c	-1.214 ^c	-1.753 ^c
Asymp. Sig. (2-tailed)	.273	.144	.715	.500	.225	.080
	Saline-Eb	Saline-Fb	Saline-Gb	Saline-Hb	Saline-I2b	Saline-J2b
Z	-1.483 ^c	-1.753 ^c	-2.023 ^c	-1.753 ^c	-1.753 ^c	-2.023 ^c
Asymp. Sig. (2-tailed)	.138	.080	.043	.080	.080	.043
	Saline-K2b	Saline-R	Saline-S	Saline-T	Saline-Zymosan	Saline-LPS
Z	-2.023 ^c	-1.461 ^c	-1.214 ^c	-1.826 ^c	-2.023 ^c	
Asymp. Sig. (2-tailed)	.043	.144	.225	.068	.043	
a. Wilcoxon Signed Ranks Test						
b. Based on negative ranks.						
c. Based on positive ranks.						
d. The sum of negative ranks equals the sum of positive ranks.						

F.8 IP-10

Table F.15: Descriptive Statistics - IP-10

Sample Abr.	Capsule parameters	N	Mean	Std. Deviation	Minimum	Maximum
T ₀		5	154.1340	59.22838	68.26	211.34
Saline		5	320.3900	131.29056	185.35	501.94
Ab	Hollow, M. pyr, 0.10 % PLL, 0.4 mm	5	673.7020	361.93355	293.08	1241.47
A2b	Hollow, M. pyr, 0.14 % PLL, 0.4 mm	5	357.7980	101.47420	228.93	505.13
Db	Hollow, M. pyr, 0.14 % PLO, 0.4 mm	5	383.0500	111.69641	205.91	515.28
Eb	Solid, M. pyr, 0.05 % PLL, 0.4 mm	5	407.2380	193.13764	155.10	593.51
Fb	Solid, M. pyr, 0.10 % PLL, 0.4 mm	5	158.3360	98.50811	75.34	318.07
Gb	Solid, UP-LVG, 0.05 % PLL, 0.4 mm	5	194.7480	85.87974	98.50	331.37
Hb	Solid, UP-LVG, 0.10 % PLL, 0.4 mm	5	204.0560	128.69208	99.90	404.68
I2b	Solid, UP-LVG, 0.05 % PLL, 0.35 mm	5	456.1800	374.52086	146.46	1076.95
J2b	Solid, UP-LVG, 0.10 % PLL, 0.35 mm	5	240.0280	80.92764	115.88	311.34
K2b	Solid, UP-LVG, 0.05 % PLL, 0.35 mm No Hepes	5	395.8900	276.27343	120.89	849.45
R	TAM, UP-LVG, 0.25 mm	4	633.3425	577.24748	172.61	1424.81
S	TAM, UP-LVG, 0.35 mm	5	772.3900	1055.00892	144.25	2639.30
T	TAM, UP-LVG, 0.40 mm	4	531.3600	436.06891	163.47	1080.32
Zymosan		5	1220.9020	313.89697	926.97	1646.18

Table F.16: Test Statistics^a - IP-10

	A2b-Ab	Db-Ab	Db-A2b	Fb - Ab	Fb - Eb	Hb - Gb
Z	-2.023 ^b	-2.023 ^c	-.674 ^b	-2.023 ^b	-2.023 ^b	-.365 ^c
Asymp. Sig. (2-tailed)	.043	.043	.500	.043	.043	.715
	J2b - I2b	K2b - I2b	Gb - Eb	Hb - Fb	I2b - Gb	J2b - Hb
Z	-2.023 ^b	-.135 ^b	-2.023 ^b	-.944 ^c	-2.023 ^c	-1.214 ^c
Asymp. Sig. (2-tailed)	.043	.893	.043	.345	.043	.225
	S-R	T-R	T-S	Saline-Ab	Saline-A2b	Saline-Db
Z	-.365 ^c	-1.826 ^c	-.365 ^b	-2.023 ^c	-.944 ^c	-2.023 ^c
Asymp. Sig. (2-tailed)	.715	.068	.715	.043	.345	.043
	Saline-Eb	Saline-Fb	Saline-Gb	Saline-Hb	Saline-I2b	Saline-J2b
Z	-1.214 ^c	-2.023 ^b	-2.023 ^b	-1.753 ^b	-.944 ^c	-1.214 ^b
Asymp. Sig. (2-tailed)	.225	.043	.043	.080	.345	.225
	Saline-K2b	Saline-R	Saline-S	Saline-T	Saline-Zymosan	Saline-LPS
Z	-.674 ^b	-.730 ^c	-.405 ^b	-.730 ^c	-2.023 ^c	
Asymp. Sig. (2-tailed)	.500	.465	.686	.465	.043	
a. Wilcoxon Signed Ranks Test						
b. Based on negative ranks.						
c. Based on positive ranks.						
d. The sum of negative ranks equals the sum of positive ranks.						

F.9 IL-1 β

Table F.17: Descriptive Statistics - IL-1 β

Sample Abr.	Capsule parameters	N	Mean	Std. Deviation	Minimum	Maximum
T ₀		4	.6625	.50953	.14	1.18
Saline		5	3.7760	2.09268	1.84	6.49
Ab	Hollow, M. pyr, 0.10 % PLL, 0.4 mm	5	2.8000	1.35652	1.68	4.99
A2b	Hollow, M. pyr, 0.14 % PLL, 0.4 mm	5	5.6940	5.16487	1.51	14.56
Db	Hollow, M. pyr, 0.14 % PLO, 0.4 mm	5	5.2800	2.02884	2.42	7.75
Eb	Solid, M. pyr, 0.05 % PLL, 0.4 mm	5	17.8600	22.19390	6.18	57.39
Fb	Solid, M. pyr, 0.10 % PLL, 0.4 mm	5	41.3920	29.30937	11.33	78.34
Gb	Solid, UP-LVG, 0.05 % PLL, 0.4 mm	5	41.6820	25.45775	12.87	79.32
Hb	Solid, UP-LVG, 0.10 % PLL, 0.4 mm	5	34.5960	32.96033	7.91	85.64
I2b	Solid, UP-LVG, 0.05 % PLL, 0.35 mm	5	16.0880	12.71637	2.17	30.96
J2b	Solid, UP-LVG, 0.10 % PLL, 0.35 mm	5	15.6980	9.88550	4.59	28.39
K2b	Solid, UP-LVG, 0.05 % PLL, 0.35 mm No Hepes	5	26.8720	24.18347	5.23	59.42
R	TAM, UP-LVG, 0.25 mm	4	4.7275	2.89644	2.33	8.84
S	TAM, UP-LVG, 0.35 mm	5	3.3660	1.39339	1.68	5.31
T	TAM, UP-LVG, 0.40 mm	4	5.6575	1.69134	3.15	6.81
Zymosan		5	1960.1580	676.66763	1050.04	2612.78

Table F.18: Test Statistics^a - IL-1 β

	A2b-Ab	Db-Ab	Db-A2b	Fb - Ab	Fb - Eb	Hb - Gb
Z	-1.214 ^b	-2.023 ^c	-.135 ^c	-2.023 ^b	-2.023 ^b	-.674 ^c
Asymp. Sig. (2-tailed)	.225	.043	.893	.043	.043	.500
	J2b - I2b	K2b - I2b	Gb - Eb	Hb - Fb	I2b - Gb	J2b - Hb
Z	-.405 ^c	-.944 ^b	-1.483 ^b	-.674 ^c	-1.753 ^c	-.944 ^c
Asymp. Sig. (2-tailed)	.686	.345	.138	.500	.080	.345
	S-R	T-R	T-S	Saline-Ab	Saline-A2b	Saline-Db
Z	-1.095 ^b	-.730 ^c	-1.461 ^c	-.948 ^b	-.674 ^c	-.405 ^c
Asymp. Sig. (2-tailed)	.273	.465	.144	.343	.500	.686
	Saline-Eb	Saline-Fb	Saline-Gb	Saline-Hb	Saline-I2b	Saline-J2b
Z	-1.753 ^c	-2.023 ^c	-2.023 ^c	-2.023 ^c	-1.483 ^c	-1.753 ^c
Asymp. Sig. (2-tailed)	.080	.043	.043	.043	.138	.080
	Saline-K2b	Saline-R	Saline-S	Saline-T	Saline-Zymosan	Saline-LPS
Z	-1.753 ^c	.000 ^d	-.674 ^b	-1.095 ^c	-2.023 ^c	
Asymp. Sig. (2-tailed)	.080	1.000	.500	.273	.043	
a. Wilcoxon Signed Ranks Test						
b. Based on negative ranks.						
c. Based on positive ranks.						
d. The sum of negative ranks equals the sum of positive ranks.						

F.10 TNF- α

Table F.19: Descriptive Statistics - TNF- α

Sample Abr.	Capsule parameters	N	Mean	Std. Deviation	Minimum	Maximum
T ₀		5	7.2220	5.79397	.72	15.81
Saline		5	27.9020	18.27779	10.72	55.74
Ab	Hollow, M. pyr, 0.10 % PLL, 0.4 mm	5	52.1280	49.09326	5.68	132.97
A2b	Hollow, M. pyr, 0.14 % PLL, 0.4 mm	5	62.3460	33.87986	36.33	119.81
Db	Hollow, M. pyr, 0.14 % PLO, 0.4 mm	5	37.9120	14.67873	20.91	59.64
Eb	Solid, M. pyr, 0.05 % PLL, 0.4 mm	5	195.6440	119.08012	90.95	375.52
Fb	Solid, M. pyr, 0.10 % PLL, 0.4 mm	5	323.9520	165.42660	117.18	515.96
Gb	Solid, UP-LVG, 0.05 % PLL, 0.4 mm	5	231.0000	89.21476	138.25	337.91
Hb	Solid, UP-LVG, 0.10 % PLL, 0.4 mm	5	499.6100	669.96224	62.24	1686.57
I2b	Solid, UP-LVG, 0.05 % PLL, 0.35 mm	5	236.7160	154.38014	33.75	383.59
J2b	Solid, UP-LVG, 0.10 % PLL, 0.35 mm	5	212.4140	87.32563	83.10	287.01
K2b	Solid, UP-LVG, 0.05 % PLL, 0.35 mm No Hepes	5	202.9440	104.91768	109.30	366.10
R	TAM, UP-LVG, 0.25 mm	4	40.2200	12.40176	28.60	57.04
S	TAM, UP-LVG, 0.35 mm	4	54.5200	26.57212	28.60	88.33
T	TAM, UP-LVG, 0.40 mm	4	61.6625	26.79479	33.75	88.33
Zymosan		5	12723.5400	6072.72124	6429.36	21741.64

Table F.20: Test Statistics^a - TNF- α

	A2b-Ab	Db-Ab	Db-A2b	Fb - Ab	Fb - Eb	Hb - Gb
Z	-.674 ^b	-.730 ^c	-1.753 ^c	-2.023 ^b	-2.023 ^b	-.674 ^b
Asymp. Sig. (2-tailed)	.500	.465	.080	.043	.043	.500
	J2b - I2b	K2b - I2b	Gb - Eb	Hb - Fb	I2b - Gb	J2b - Hb
Z	-.674 ^c	-.944 ^c	-.135 ^b	-.135 ^c	-.405 ^b	-1.214 ^c
Asymp. Sig. (2-tailed)	.500	.345	.893	.893	.686	.225
	S-R	T-R	T-S	Saline-Ab	Saline-A2b	Saline-Db
Z	-1.069 ^b	-1.826 ^b	-1.604 ^b	-.674 ^c	-2.023 ^c	-.674 ^c
Asymp. Sig. (2-tailed)	.285	.068	.109	.500	.043	.500
	Saline-Eb	Saline-Fb	Saline-Gb	Saline-Hb	Saline-I2b	Saline-J2b
Z	-2.023 ^c					
Asymp. Sig. (2-tailed)	.043	.043	.043	.043	.043	.043
	Saline-K2b	Saline-R	Saline-S	Saline-T	Saline-Zymosan	Saline-LPS
Z	-2.023 ^c	-.730 ^c	-.674 ^c	-1.095 ^c	-2.023 ^c	
Asymp. Sig. (2-tailed)	.043	.465	.500	.273	.043	
a. Wilcoxon Signed Ranks Test						
b. Based on negative ranks.						
c. Based on positive ranks.						
d. The sum of negative ranks equals the sum of positive ranks.						

F.11 IL-6

Table F.21: Descriptive Statistics - IL-6

Sample Abr.	Capsule parameters	N	Mean	Std. Deviation	Minimum	Maximum
T ₀		5	1.6260	1.07797	.40	3.20
Saline		5	9.6600	5.25779	3.20	17.54
Ab	Hollow, M. pyr, 0.10 % PLL, 0.4 mm	5	20.4720	18.60784	6.04	50.24
A2b	Hollow, M. pyr, 0.14 % PLL, 0.4 mm	5	27.1080	23.04553	9.47	66.76
Db	Hollow, M. pyr, 0.14 % PLO, 0.4 mm	5	20.5140	16.72379	6.61	39.09
Eb	Solid, M. pyr, 0.05 % PLL, 0.4 mm	5	33.0980	20.76782	9.47	56.43
Fb	Solid, M. pyr, 0.10 % PLL, 0.4 mm	5	32.4040	22.69997	14.07	67.35
Gb	Solid, UP-LVG, 0.05 % PLL, 0.4 mm	5	28.0520	16.92676	13.79	54.07
Hb	Solid, UP-LVG, 0.10 % PLL, 0.4 mm	5	57.7100	55.82746	11.20	149.27
I2b	Solid, UP-LVG, 0.05 % PLL, 0.35 mm	5	32.3820	18.94862	10.05	55.54
J2b	Solid, UP-LVG, 0.10 % PLL, 0.35 mm	5	30.6340	19.77923	15.23	59.08
K2b	Solid, UP-LVG, 0.05 % PLL, 0.35 mm No Hepes	5	24.6940	17.63142	7.18	49.36
R	TAM, UP-LVG, 0.25 mm	4	15.8275	7.57080	7.18	22.18
S	TAM, UP-LVG, 0.35 mm	4	13.6500	8.92435	3.20	23.92
T	TAM, UP-LVG, 0.40 mm	4	20.4750	11.19781	5.47	32.07
Zymosan		5	9081.1120	3231.71071	5039.91	13173.34

Table F.22: Test Statistics^a - IL-6

	A2b-Ab	Db-Ab	Db-A2b	Fb - Ab	Fb - Eb	Hb - Gb
Z	-1.753 ^b	-.135 ^b	-.944 ^b	-1.214 ^b	-.135 ^b	-1.214 ^c
Asymp. Sig. (2-tailed)	.080	.893	.345	.225	.893	.225
	J2b - I2b	K2b - I2b	Gb - Eb	Hb - Fb	I2b - Gb	J2b - Hb
Z	-.135 ^c	-1.753 ^b	-1.214 ^b	-.674 ^c	-.674 ^c	-.405 ^b
Asymp. Sig. (2-tailed)	.893	.080	.225	.500	.500	.686
	S-R	T-R	T-S	Saline-Ab	Saline-A2b	Saline-Db
Z	-.730 ^c	-1.461 ^c	-1.095 ^c	-1.753 ^c	-2.023 ^c	-1.753 ^c
Asymp. Sig. (2-tailed)	.465	.144	.273	.080	.043	.080
	Saline-Eb	Saline-Fb	Saline-Gb	Saline-Hb	Saline-I2b	Saline-J2b
Z	-2.023 ^c					
Asymp. Sig. (2-tailed)	.043	.043	.043	.043	.043	.043
	Saline-K2b	Saline-R	Saline-S	Saline-T	Saline-Zymosan	Saline-LPS
Z	-2.023 ^c	-1.604 ^c	-1.461 ^c	-1.461 ^c	-2.023 ^c	
Asymp. Sig. (2-tailed)	.043	.109	.144	.144	.043	
a. Wilcoxon Signed Ranks Test						
b. Based on negative ranks.						
c. Based on positive ranks.						
d. The sum of negative ranks equals the sum of positive ranks.						

F.12 IL-1RA

Table F.23: Descriptive Statistics - IL-1RA

Sample Abr.	Capsule parameters	N	Mean	Std. Deviation	Minimum	Maximum
T ₀		5	162.2520	177.95030	38.00	467.88
Saline		5	530.0820	400.05150	231.00	1110.71
Ab	Hollow, M. pyr, 0.10 % PLL, 0.4 mm	5	484.4120	178.81394	231.00	667.44
A2b	Hollow, M. pyr, 0.14 % PLL, 0.4 mm	5	633.6660	415.96114	270.21	1272.96
Db	Hollow, M. pyr, 0.14 % PLO, 0.4 mm	5	686.2000	504.08971	309.55	1557.96
Eb	Solid, M. pyr, 0.05 % PLL, 0.4 mm	5	1143.9580	869.12087	467.88	2645.93
Fb	Solid, M. pyr, 0.10 % PLL, 0.4 mm	5	1216.2580	761.15754	388.54	2254.51
Gb	Solid, UP-LVG, 0.05 % PLL, 0.4 mm	5	1202.5120	614.71259	547.52	2172.29
Hb	Solid, UP-LVG, 0.10 % PLL, 0.4 mm	5	1004.3700	603.38547	507.67	1967.03
I2b	Solid, UP-LVG, 0.05 % PLL, 0.35 mm	5	1066.6180	807.33690	507.67	2460.35
J2b	Solid, UP-LVG, 0.10 % PLL, 0.35 mm	5	993.1000	717.76298	507.67	2254.51
K2b	Solid, UP-LVG, 0.05 % PLL, 0.35 mm No Hepes	5	1226.6940	1058.78387	567.47	3080.02
R	TAM, UP-LVG, 0.25 mm	4	733.5900	290.59707	388.54	1029.77
S	TAM, UP-LVG, 0.35 mm	4	657.9360	451.95346	270.21	1374.60
T	TAM, UP-LVG, 0.40 mm	4	829.9325	464.32526	547.52	1517.17
Zymosan		5	1399.6980	945.49409	667.44	3038.61

Table F.24: Test Statistics^a - IL-1RA

	A2b-Ab	Db-Ab	Db-A2b	Fb - Ab	Fb - Eb	Hb - Gb
Z	-.944 ^b	-1.214 ^c	-.365 ^c	-1.753 ^b	-.405 ^b	-2.023 ^c
Asymp. Sig. (2-tailed)	.345	.225	.715	.080	.686	.043
	J2b - I2b	K2b - I2b	Gb - Eb	Hb - Fb	I2b - Gb	J2b - Hb
Z	-.674 ^c	-1.753 ^b	-.674 ^b	-1.753 ^c	-.944 ^c	.000 ^d
Asymp. Sig. (2-tailed)	.500	.080	.500	.080	.345	1.000
	S-R	T-R	T-S	Saline-Ab	Saline-A2b	Saline-Db
Z	-.365 ^b	-.365 ^c	-1.095 ^c	-.730 ^b	-.944 ^c	-1.483 ^c
Asymp. Sig. (2-tailed)	.715	.715	.273	.465	.345	.138
	Saline-Eb	Saline-Fb	Saline-Gb	Saline-Hb	Saline-I2b	Saline-J2b
Z	-2.023 ^c	-2.023 ^c	-2.023 ^c	-1.753 ^c	-1.753 ^c	-1.753 ^c
Asymp. Sig. (2-tailed)	.043	.043	.043	.080	.080	.080
	Saline-K2b	Saline-R	Saline-S	Saline-T	Saline-Zymosan	Saline-LPS
Z	-1.753 ^c	-1.095 ^c	-2.023 ^c	-1.473 ^c	-2.023 ^c	
Asymp. Sig. (2-tailed)	.080	.273	.043	.141	.043	
a. Wilcoxon Signed Ranks Test						
b. Based on negative ranks.						
c. Based on positive ranks.						
d. The sum of negative ranks equals the sum of positive ranks.						

F.13 IL-10

Table F.25: Descriptive Statistics - IL-10

Sample Abr.	Capsule parameters	N	Mean	Std. Deviation	Minimum	Maximum
T ₀		5	2.3840	1.17878	1.22	4.02
Saline		5	2.6540	1.88601	1.22	5.79
Ab	Hollow, M. pyr, 0.10 % PLL, 0.4 mm	5	3.5420	2.29270	1.22	7.14
A2b	Hollow, M. pyr, 0.14 % PLL, 0.4 mm	5	3.3240	2.63650	1.49	7.90
Db	Hollow, M. pyr, 0.14 % PLO, 0.4 mm	5	3.2700	1.91349	1.76	6.54
Eb	Solid, M. pyr, 0.05 % PLL, 0.4 mm	5	3.2380	2.70259	1.76	8.06
Fb	Solid, M. pyr, 0.10 % PLL, 0.4 mm	5	2.8560	1.09228	1.90	4.31
Gb	Solid, UP-LVG, 0.05 % PLL, 0.4 mm	5	3.3080	2.27915	2.03	7.29
Hb	Solid, UP-LVG, 0.10 % PLL, 0.4 mm	5	3.7700	2.30625	1.76	7.60
I2b	Solid, UP-LVG, 0.05 % PLL, 0.35 mm	5	3.7040	2.10355	1.76	7.29
J2b	Solid, UP-LVG, 0.10 % PLL, 0.35 mm	5	3.1080	2.11159	1.22	6.69
K2b	Solid, UP-LVG, 0.05 % PLL, 0.35 mm No Hepes	5	4.3120	2.98241	1.49	8.98
R	TAM, UP-LVG, 0.25 mm	4	3.1900	2.09106	1.49	6.23
S	TAM, UP-LVG, 0.35 mm	5	3.7760	2.56740	1.76	8.21
T	TAM, UP-LVG, 0.40 mm	4	3.6350	3.50820	1.22	8.83
Zymosan		5	8.6080	2.61729	5.19	11.64

Table F.26: Test Statistics^a- IL-10

	A2b-Ab	Db-Ab	Db-A2b	Fb - Ab	Fb - Eb	Hb - Gb
Z	-.674 ^b	-1.084 ^c	-.405 ^c	-.944 ^b	.000 ^d	-1.753 ^c
Asymp. Sig. (2-tailed)	.500	.279	.686	.345	1.000	.080
	J2b - I2b	K2b - I2b	Gb - Eb	Hb - Fb	I2b - Gb	J2b - Hb
Z	-2.023 ^b	-.944 ^c	.000 ^d	-1.753 ^c	-1.461 ^c	-1.753 ^b
Asymp. Sig. (2-tailed)	.043	.345	1.000	.080	.144	.080
	S-R	T-R	T-S	Saline-Ab	Saline-A2b	Saline-Db
Z	-1.604 ^b	-.365 ^c	-.730 ^c	-1.461 ^c	-.944 ^c	-2.023 ^c
Asymp. Sig. (2-tailed)	.109	.715	.465	.144	.345	.043
	Saline-Eb	Saline-Fb	Saline-Gb	Saline-Hb	Saline-I2b	Saline-J2b
Z	-.944 ^c	-.674 ^c	-1.219 ^c	-2.023 ^c	-2.023 ^c	-1.289 ^c
Asymp. Sig. (2-tailed)	.345	.500	.223	.043	.043	.197
	Saline-K2b	Saline-R	Saline-S	Saline-T	Saline-Zymosan	Saline-LPS
Z	-1.483 ^c	-1.461 ^c	-2.023 ^c	-1.069 ^c	-2.023 ^c	
Asymp. Sig. (2-tailed)	.138	.144	.043	.285	.043	
a. Wilcoxon Signed Ranks Test						
b. Based on negative ranks.						
c. Based on positive ranks.						
d. The sum of negative ranks equals the sum of positive ranks.						

F.14 PDGF

Table F.27: Descriptive Statistics - PDGF

Sample Abr.	Capsule parameters	N	Mean	Std. Deviation	Minimum	Maximum
T ₀		5	305.7000	430.20408	11.47	1050.37
Saline		5	656.7100	373.86802	245.01	1101.31
Ab	Hollow, M. pyr, 0.10 % PLL, 0.4 mm	5	577.6820	161.84339	389.98	770.08
A2b	Hollow, M. pyr, 0.14 % PLL, 0.4 mm	5	849.7780	591.69759	277.54	1696.59
Db	Hollow, M. pyr, 0.14 % PLO, 0.4 mm	5	803.8000	424.26766	337.63	1311.73
Eb	Solid, M. pyr, 0.05 % PLL, 0.4 mm	5	912.1800	731.75499	207.55	2148.30
Fb	Solid, M. pyr, 0.10 % PLL, 0.4 mm	5	1082.1900	567.60539	355.72	1586.77
Gb	Solid, UP-LVG, 0.05 % PLL, 0.4 mm	5	1459.1680	1111.06676	433.74	3194.42
Hb	Solid, UP-LVG, 0.10 % PLL, 0.4 mm	5	1182.1760	689.78614	382.37	1957.06
I2b	Solid, UP-LVG, 0.05 % PLL, 0.35 mm	5	1194.2060	600.88921	500.35	2021.58
J2b	Solid, UP-LVG, 0.10 % PLL, 0.35 mm	5	1253.2760	681.91501	773.93	2428.51
K2b	Solid, UP-LVG, 0.05 % PLL, 0.35 mm No Hepes	5	1292.1320	1181.89921	357.63	3299.27
R	TAM, UP-LVG, 0.25 mm	4	989.1975	797.83815	252.68	1974.72
S	TAM, UP-LVG, 0.35 mm	5	1021.7060	984.48007	166.95	2639.87
T	TAM, UP-LVG, 0.40 mm	4	1440.6800	1555.48674	344.30	3654.76
Zymosan		5	1478.9720	832.83366	1011.29	2953.46

Table F.28: Test Statistics^a - PDGF

	A2b-Ab	Db-Ab	Db-A2b	Fb - Ab	Fb - Eb	Hb - Gb
Z	-.674 ^c	-1.214 ^b	-.405 ^c	-1.753 ^b	-.674 ^b	-1.214 ^c
Asymp. Sig. (2-tailed)	.500	.225	.686	.080	.500	.225
	J2b - I2b	K2b - I2b	Gb - Eb	Hb - Fb	I2b - Gb	J2b - Hb
Z	-.135 ^b	-.674 ^c	-1.753 ^b	-1.214 ^b	-.944 ^c	-.135 ^b
Asymp. Sig. (2-tailed)	.893	.500	.080	.225	.345	.893
	S-R	T-R	T-S	Saline-Ab	Saline-A2b	Saline-Db
Z	-.365 ^c	-.365 ^b	-1.826 ^b	-.405 ^b	-1.214 ^c	-1.214 ^c
Asymp. Sig. (2-tailed)	.715	.715	.068	.686	.225	.225
	Saline-Eb	Saline-Fb	Saline-Gb	Saline-Hb	Saline-I2b	Saline-J2b
Z	-.944 ^c	-1.753 ^c	-2.023 ^c	-2.023 ^c	-2.023 ^c	-2.023 ^c
Asymp. Sig. (2-tailed)	.345	.080	.043	.043	.043	.043
	Saline-K2b	Saline-R	Saline-S	Saline-T	Saline-Zymosan	Saline-LPS
Z	-1.753 ^c	-1.461 ^c	-1.214 ^c	-1.461 ^c	-2.023 ^c	
Asymp. Sig. (2-tailed)	.080	.144	.225	.144	.043	
a. Wilcoxon Signed Ranks Test						
b. Based on negative ranks.						
c. Based on positive ranks.						
d. The sum of negative ranks equals the sum of positive ranks.						

F.15 HGF

Table F.29: Descriptive Statistics - HGF

Sample Abr.	Capsule parameters	N	Mean	Std. Deviation	Minimum	Maximum
T ₀		5	113.6460	72.95950	34.56	210.08
Saline		5	595.7760	220.46853	345.18	833.95
Ab	Hollow, M. pyr, 0.10 % PLL, 0.4 mm	5	784.2200	459.84071	334.14	1487.70
A2b	Hollow, M. pyr, 0.14 % PLL, 0.4 mm	5	708.5860	366.36570	294.34	1173.41
Db	Hollow, M. pyr, 0.14 % PLO, 0.4 mm	5	622.1360	253.23307	267.77	899.99
Eb	Solid, M. pyr, 0.05 % PLL, 0.4 mm	5	1243.9480	860.07007	281.06	2477.07
Fb	Solid, M. pyr, 0.10 % PLL, 0.4 mm	5	1200.8260	699.33887	435.62	2346.17
Gb	Solid, UP-LVG, 0.05 % PLL, 0.4 mm	5	1102.3040	556.71505	387.12	1779.06
Hb	Solid, UP-LVG, 0.10 % PLL, 0.4 mm	5	1041.9840	595.04540	320.88	1917.47
I2b	Solid, UP-LVG, 0.05 % PLL, 0.35 mm	5	1143.7540	696.81063	274.42	2163.93
J2b	Solid, UP-LVG, 0.10 % PLL, 0.35 mm	5	1088.0100	721.93043	356.22	2211.12
K2b	Solid, UP-LVG, 0.05 % PLL, 0.35 mm No Hepes	5	1132.1260	849.08652	294.34	2542.65
R	TAM, UP-LVG, 0.25 mm	4	243.4525	216.19141	66.59	530.32
S	TAM, UP-LVG, 0.35 mm	5	220.7320	109.16265	48.34	345.18
T	TAM, UP-LVG, 0.40 mm	4	207.3075	140.12580	93.76	391.53
Zymosan		5	1245.7320	597.69957	360.64	2029.36

Table F.30: Test Statistics^a - HGF

	A2b-Ab	Db-Ab	Db-A2b	Fb - Ab	Fb - Eb	Hb - Gb
Z	-.135 ^b	-.944 ^c	-.944 ^c	-1.214 ^b	-.405 ^b	-.944 ^c
Asymp. Sig. (2-tailed)	.893	.345	.345	.225	.684	.345
	J2b - I2b	K2b - I2b	Gb - Eb	Hb - Fb	I2b - Gb	J2b - Hb
Z	-.944 ^b	-.405 ^c	-.674 ^c	-1.214 ^c	-.135 ^b	-.674 ^b
Asymp. Sig. (2-tailed)	.345	.686	.500	.225	.893	.500
	S-R	T-R	T-S	Saline-Ab	Saline-A2b	Saline-Db
Z	-.730 ^c	-.730 ^c	-.365 ^b	-.405 ^c	-.944 ^c	-.405 ^c
Asymp. Sig. (2-tailed)	.465	.465	.715	.686	.345	.686
	Saline-Eb	Saline-Fb	Saline-Gb	Saline-Hb	Saline-I2b	Saline-J2b
Z	-1.753 ^c	-2.023 ^c	-2.023 ^c	-1.753 ^c	-1.753 ^c	-1.483 ^c
Asymp. Sig. (2-tailed)	.080	.043	.043	.080	.080	.138
	Saline-K2b	Saline-R	Saline-S	Saline-T	Saline-Zymosan	Saline-LPS
Z	-1.214 ^c	-1.826 ^b	-2.023 ^b	-1.826 ^b	-2.023 ^c	
Asymp. Sig. (2-tailed)	.225	.068	.043	.068	.043	
a. Wilcoxon Signed Ranks Test						
b. Based on negative ranks.						
c. Based on positive ranks.						
d. The sum of negative ranks equals the sum of positive ranks.						

F.16 VEGF

Table F.31: Descriptive Statistics - VEGF

Sample Abr.	Capsule parameters	N	Mean	Std. Deviation	Minimum	Maximum
T ₀		2	11.3850	14.53104	1.11	21.66
Saline		5	37.2440	29.14632	5.22	68.48
Ab	Hollow, M. pyr, 0.10 % PLL, 0.4 mm	5	33.7340	13.05595	20.94	51.94
A2b	Hollow, M. pyr, 0.14 % PLL, 0.4 mm	5	60.9120	53.07426	13.72	147.69
Db	Hollow, M. pyr, 0.14 % PLO, 0.4 mm	5	37.3100	22.59121	14.44	74.54
Eb	Solid, M. pyr, 0.05 % PLL, 0.4 mm	5	89.9140	78.94619	36.69	225.09
Fb	Solid, M. pyr, 0.10 % PLL, 0.4 mm	5	118.0940	77.10795	62.45	240.29
Gb	Solid, UP-LVG, 0.05 % PLL, 0.4 mm	5	104.6080	62.36850	54.94	199.63
Hb	Solid, UP-LVG, 0.10 % PLL, 0.4 mm	5	106.9840	86.19750	44.85	257.16
I2b	Solid, UP-LVG, 0.05 % PLL, 0.35 mm	5	89.7320	63.24764	40.03	196.06
J2b	Solid, UP-LVG, 0.10 % PLL, 0.35 mm	5	97.7600	70.14865	48.95	221.10
K2b	Solid, UP-LVG, 0.05 % PLL, 0.35 mm No Hepes	5	106.3480	100.43217	43.74	281.38
R	TAM, UP-LVG, 0.25 mm	4	36.2200	14.27884	16.23	48.21
S	TAM, UP-LVG, 0.35 mm	5	26.9760	11.32249	14.44	41.51
T	TAM, UP-LVG, 0.40 mm	4	44.5825	19.41848	27.13	72.26
Zymosan		5	54.8780	47.16626	18.76	129.79

Table F.32: Test Statistics^a - VEGF

	A2b-Ab	Db-Ab	Db-A2b	Fb - Ab	Fb - Eb	Hb - Gb
Z	-1.214 ^c	-.135 ^b	-.405 ^c	-2.023 ^b	-2.023 ^b	-.135 ^b
Asymp. Sig. (2-tailed)	.225	.893	.686	.043	.043	.893
	J2b - I2b	K2b - I2b	Gb - Eb	Hb - Fb	I2b - Gb	J2b - Hb
Z	-1.214 ^c	-.944 ^b	-.944 ^b	-.674 ^c	-1.753 ^c	-1.214 ^c
Asymp. Sig. (2-tailed)	.225	.345	.345	.500	.080	.225
	S-R	T-R	T-S	Saline-Ab	Saline-A2b	Saline-Db
Z	-1.826 ^c	-1.095 ^b	-1.826 ^b	-.405 ^b	-1.483 ^c	-.674 ^c
Asymp. Sig. (2-tailed)	.068	.273	.068	.686	.138	.498
	Saline-Eb	Saline-Fb	Saline-Gb	Saline-Hb	Saline-I2b	Saline-J2b
Z	-2.023 ^c					
Asymp. Sig. (2-tailed)	.043	.043	.043	.043	.043	.043
	Saline-K2b	Saline-R	Saline-S	Saline-T	Saline-Zymosan	Saline-LPS
Z	-2.023 ^c	-.365 ^b	-.674 ^b	-.365 ^c	-1.483 ^c	
Asymp. Sig. (2-tailed)	.043	.715	.500	.715	.138	
a. Wilcoxon Signed Ranks Test						
b. Based on negative ranks.						
c. Based on positive ranks.						
d. The sum of negative ranks equals the sum of positive ranks.						

F.17 IFN- γ

Table F.33: Descriptive Statistics - IFN- γ

Sample Abr.	Capsule parameters	N	Mean	Std. Deviation	Minimum	Maximum
T ₀		3	137.1733	87.25739	36.98	196.48
Saline		5	80.0420	43.34962	36.98	138.59
Ab	Hollow, M. pyr, 0.10 % PLL, 0.4 mm	4	118.1800	58.56438	67.92	178.06
A2b	Hollow, M. pyr, 0.14 % PLL, 0.4 mm	5	90.8820	40.01338	36.98	138.59
Db	Hollow, M. pyr, 0.14 % PLO, 0.4 mm	5	100.2340	44.82211	67.92	158.82
Eb	Solid, M. pyr, 0.05 % PLL, 0.4 mm	5	92.4180	28.87969	67.92	138.59
Fb	Solid, M. pyr, 0.10 % PLL, 0.4 mm	5	108.4840	35.32098	67.92	158.82
Gb	Solid, UP-LVG, 0.05 % PLL, 0.4 mm	5	110.3100	69.00166	36.98	214.23
Hb	Solid, UP-LVG, 0.10 % PLL, 0.4 mm	5	106.0220	35.87260	67.92	138.59
I2b	Solid, UP-LVG, 0.05 % PLL, 0.35 mm	5	132.9780	34.41518	93.83	178.06
J2b	Solid, UP-LVG, 0.10 % PLL, 0.35 mm	5	104.9820	21.29523	67.92	117.09
K2b	Solid, UP-LVG, 0.05 % PLL, 0.35 mm No Hepes	5	91.9320	49.87290	36.98	158.82
R	TAM, UP-LVG, 0.25 mm	4	121.5275	70.53141	36.98	196.48
S	TAM, UP-LVG, 0.35 mm	4	137.6325	99.41542	36.98	231.40
T	TAM, UP-LVG, 0.40 mm	4	121.6500	85.01969	36.98	222.88
Zymosan		5	139.6760	28.74202	93.83	168.55

Table F.34: Test Statistics^a - IFN- γ

	A2b-Ab	Db-Ab	Db-A2b	Fb - Ab	Fb - Eb	Hb - Gb
Z	-.365 ^b	-.447 ^c	-.535 ^b	-.365 ^b	-.730 ^c	.000 ^d
Asymp. Sig. (2-tailed)	.715	.655	.593	.715	.465	1.000
	J2b - I2b	K2b - I2b	Gb - Eb	Hb - Fb	I2b - Gb	J2b - Hb
Z	-1.826 ^b	-1.483 ^b	-1.069 ^c	.000 ^d	-.674 ^c	.000 ^d
Asymp. Sig. (2-tailed)	.068	.138	.285	1.000	.500	1.000
	S-R	T-R	T-S	Saline-Ab	Saline-A2b	Saline-Db
Z	-1.342 ^b	.000 ^d	.000 ^d	.000 ^d	-.552 ^b	-1.490 ^b
Asymp. Sig. (2-tailed)	.180	1.000	1.000	1.000	.581	.136
	Saline-Eb	Saline-Fb	Saline-Gb	Saline-Hb	Saline-I2b	Saline-J2b
Z	-.557 ^b	-1.461 ^b	-1.342 ^b	-1.841 ^b	-2.023 ^b	-1.483 ^b
Asymp. Sig. (2-tailed)	.577	.144	.180	.066	.043	.138
	Saline-K2b	Saline-R	Saline-S	Saline-T	Saline-Zymosan	Saline-LPS
Z	-.730 ^b	-1.604 ^b	-1.069 ^b	-1.604 ^b	-1.826 ^b	
Asymp. Sig. (2-tailed)	.465	.109	.285	.109	.068	
a. Wilcoxon Signed Ranks Test						
b. Based on negative ranks.						
c. Based on positive ranks.						
d. The sum of negative ranks equals the sum of positive ranks.						

F.18 RANTES

Table F.35: Descriptive Statistics - RANTES

Sample Abr.	Capsule parameters	N	Mean	Std. Deviation	Minimum	Maximum
T ₀		5	4204.9720	4061.24060	639.60	8902.54
Saline		5	2106.9780	1039.19459	393.18	3181.10
Ab	Hollow, M. pyr, 0.10 % PLL, 0.4 mm	5	2079.0900	1273.24905	753.29	4201.94
A2b	Hollow, M. pyr, 0.14 % PLL, 0.4 mm	5	3028.9640	1683.71691	1158.62	4751.03
Db	Hollow, M. pyr, 0.14 % PLO, 0.4 mm	5	2683.6540	1817.92478	988.39	5088.22
Eb	Solid, M. pyr, 0.05 % PLL, 0.4 mm	5	2423.9160	1740.97762	713.71	5005.73
Fb	Solid, M. pyr, 0.10 % PLL, 0.4 mm	5	4306.4080	3832.49301	967.24	10565.36
Gb	Solid, UP-LVG, 0.05 % PLL, 0.4 mm	5	7072.6200	6592.31304	1156.32	14514.06
Hb	Solid, UP-LVG, 0.10 % PLL, 0.4 mm	5	5334.2460	4903.53749	1275.43	12724.58
I2b	Solid, UP-LVG, 0.05 % PLL, 0.35 mm	5	4193.6700	2964.22650	916.81	7798.78
J2b	Solid, UP-LVG, 0.10 % PLL, 0.35 mm	5	3708.3960	2302.93318	1906.67	7694.54
K2b	Solid, UP-LVG, 0.05 % PLL, 0.35 mm No Hepes	5	5493.3880	5975.95389	889.61	15257.58
R	TAM, UP-LVG, 0.25 mm	4	3113.7775	2820.82498	1189.69	7177.31
S	TAM, UP-LVG, 0.35 mm	5	4459.0100	4750.32923	840.07	12475.71
T	TAM, UP-LVG, 0.40 mm	4	2903.8950	2050.54674	878.08	5222.12
Zymosan		5	7080.0520	5959.52314	3141.22	17196.74

Table F.36: Test Statistics^a - RANTES

	A2b-Ab	Db-Ab	Db-A2b	Fb - Ab	Fb - Eb	Hb - Gb
Z	-.944 ^b	-.405 ^c	-.405 ^b	-1.483 ^c	-1.214 ^c	-1.483 ^b
Asymp. Sig. (2-tailed)	.345	.686	.686	.138	.225	.138
	J2b - I2b	K2b - I2b	Gb - Eb	Hb - Fb	I2b - Gb	J2b - Hb
Z	-.135 ^c	-.405 ^b	-2.023 ^c	-.944 ^c	-.944 ^b	-.135 ^b
Asymp. Sig. (2-tailed)	.893	.686	.043	.345	.345	.893
	S-R	T-R	T-S	Saline-Ab	Saline-A2b	Saline-Db
Z	-.365 ^b	-.365 ^b	.000 ^d	-.135 ^c	-1.483 ^b	-.944 ^b
Asymp. Sig. (2-tailed)	.715	.715	1.000	.893	.138	.345
	Saline-Eb	Saline-Fb	Saline-Gb	Saline-Hb	Saline-I2b	Saline-J2b
Z	-.135 ^b	-1.214 ^b	-1.483 ^b	-1.483 ^b	-1.483 ^b	-2.023 ^b
Asymp. Sig. (2-tailed)	.893	.225	.138	.138	.138	.043
	Saline-K2b	Saline-R	Saline-S	Saline-T	Saline-Zymosan	Saline-LPS
Z	-1.214 ^b	-.730 ^b	-1.214 ^b	-1.095 ^b	-2.023 ^b	
Asymp. Sig. (2-tailed)	.225	.465	.225	.273	.043	
a. Wilcoxon Signed Ranks Test						
b. Based on negative ranks.						
c. Based on positive ranks.						
d. The sum of negative ranks equals the sum of positive ranks.						